

The Potential of Bast Natural Fibres as Reinforcement for Polymeric Composite Materials in Building Applications

A thesis submitted for the degree of

Doctor of Philosophy

by

Bartosz Tomasz Węcławski

Department of Mechanical, Aerospace and Civil Engineering

Brunel University London

Supervisors: Prof. Mizi Fan and Prof. Luiz Wrobel

September 2015

Abstract

Natural fibre composites (NFCs), which are polymers reinforced with cellulosic bast fibres, have the potential to be applied into a range of building products. They are seen as an alternative to glass fibre reinforced plastics (GFRP) in some applications, because of natural fibres (NF) relatively high strength and low density. Moreover, natural fibres have a set of beneficial traits, such as thermal insulation, thermal stability, biodegradability, and are inherently renewable. Those characteristics are of importance when NF are used as reinforcements in polymer composites, but developments in mechanical performance, reliability and economic viability are still required in order to be adopted fully by industry. The goal of this thesis was the development of a processing methodology for NFC laminate and subsequent material characterisation to assess the developed material suitability for building applications. Research objectives included materials selection, processing route development for laminates and tubes, manufacture of NFC laminates and analysis of mechanical properties in order to find an optimal composition. Hemp and flax fibres were selected as the reinforcement, because both have high mechanical properties and are important bast fibre crops in the European region with established cultivation and processing methods. As a matrix, fossil-fuel based and partially bio-derived thermoset resin systems were used. Handling and processing methodologies were developed for laminates and composite tubes based on filament winding and compression moulding techniques. The effects of the selected factors, namely material composition, volume fraction, processing parameters, reinforcement linear density, yarn twist, lamination sequence, yarn waviness and hybrid hemp-wool reinforcement were subsequently described in mechanical properties analysis of laminates. The influence of weathering conditions on the mechanical performance of the NFCs was examined. Furthermore, a study of NFC tubes under compression was performed. Results showed that the developed laminates reinforced with NF yarns have sufficient mechanical properties to be utilised in sandwich panels and/or tubes. However, a low resistance to moisture-related weathering restricts the developed NFCs for indoor applications.

Declaration

The work in this thesis is based on research carried out at the Brunel University London, United Kingdom. No part of this thesis has been submitted elsewhere for any other degree or qualification and it is all my own work unless referenced to the contrary in the text.

Copyright © 2015 by Bartosz T. Węclawski

“The copyright of this thesis rests with the author. No quotations from it should be published without the author’s prior written consent and information derived from it should be acknowledged”.

Acknowledgements

I would like to express my deepest gratitude to Professor Mizi Fan and Professor Luiz Wrobel for their supervision and invaluable help with my research project. It was great opportunity for me to work with them and their research group. Professor Mizi Fan has tirelessly assisted me with every step of my research and never been short of good advice and direction when it was needed the most in the past few years.

I would like to express my gratitude to Malcolm Austin and Paul Shadorski from Civil Engineering Department, and Keith Withers and Paul Yates from School of Engineering and Design for their help, advice, technical assistance and all the support given during my research.

I would like to extend my sincerest thank to Dr Krystian Wika for his encouragement and technical support throughout the years.

I would like to sincerely thank my family and friends for their persisting support during these last couple of years of my study.

Contents

1	Introduction	1
1.1	Research Hypothesis	1
1.2	Rationale.....	1
1.3	Aims and Objectives of the Project.....	2
1.4	Structure of the Thesis	2
2	Literature Review.....	5
2.1	Terms Used in NFC Area.....	6
2.2	Classification of Natural Fibres.....	6
2.3	Key Points in NFC History.....	7
2.4	Reinforcements	10
2.5	Bast Fibre Reinforcements	14
2.6	Resin Systems for NFCs	34
2.7	NFC in Building Applications.....	39
3	Experimental Procedures and Methodology	42
3.1	Material Selection.....	42
3.2	Production	51
3.3	Testing.....	63
3.4	Sampling.....	71
4	Influence of Reinforcements on Tensile Properties of BFRPs	83
4.1	Why Investigate Tensile Properties of BFRPs?	83
4.2	Effect of Yarn Linear Density.....	87
4.3	Effect of the Yarn Twist.....	90
4.4	Effect of Lamination	96
4.5	Effect of Impregnation	97
4.6	Effect of Yarn Arrangement in Fabric.....	98
4.7	Effect of Hybrid Hemp-Wool Reinforcement	100
4.8	Minimum and Maximum Volume Fraction	104
4.9	Effect of Volume Fraction	106
4.10	Comparison with Rule of Mixtures (ROM)	111
4.11	Summary	116
5	Flexural Properties of BFRPs	118
5.1	Effect of Yarn Linear Density.....	119
5.2	Effect of Yarn Twist.....	122

5.3	Effect of Composite Lamination.....	124
5.4	Effect of Fabric Waviness	127
5.5	Effect of Volume Fraction	128
5.6	Comparison with Other Composite Materials	136
5.7	Summary	139
6	Compressive Behaviour of NFC Tubes	141
6.1	Tube Structures	142
6.2	Yarn Properties and Resin Distribution.....	143
6.3	NFC Tubes Compressive Properties.....	146
6.4	Laminate Properties.....	149
6.5	Failure Modes.....	150
6.6	Summary	155
7	Weathering Performance of NFCs	156
7.1	Heat Ageing.....	157
7.2	Immersion in Fluids and Environmental Weathering.....	159
7.3	Water Absorption	165
7.4	Summary	169
8	Inter Laminar Shear Strength of Hemp and Flax Laminates	171
8.1	Double Notch Shear Test.....	171
8.2	Effect of Reinforcement Type	172
8.3	Flax and Hemp Unidirectional Laminates.....	173
8.4	Summary	174
9	Final Conclusions	175
10	Recommendations for Future Work.....	177
11	References	178

List of Figures

Figure 1 Diagram representing main aspects of the work flow	4
Figure 2 Classification of natural fibres according to the nature of the reinforcement [4].....	7
Figure 3 (A) Reconstruction of a Ming dynasty Kaiyuan bow by Chinese bowyer Gao Xiang, made with horn, bamboo and sinew composite, (B) The experimental Spitfire fuselage constructed by Aero Research Ltd. Apart from the main spar member and certain pick-up fittings, the fuselage was built almost entirely of Gordon Aerolite [13], (C) Flax/polypropylene underbody components have replaced glass fibre reinforced plastic components in vehicles such as the Mercedes Benz A-Class [14], (D) A close up of the ECO Elise hood shows the hemp fibre pattern in the clear-finished stripe [12].....	10
Figure 4 Typical composition of layered laminate for structural application [16].....	12
Figure 5 Flax. A, B - plant; 1 - sepal; 2 - bud without cup; 3 - lobe; 4 and 5 - the stamens from different angles; 6 - pollen grain; 7 - pestle with 5 columns (stilodiyami); 8 - a flower without calyx, corolla and staminodes; 8a - the same with staminodes; 9 - the same in a longitudinal section; 10 and 11 - unripe fruit from different angles; 12 - the same in cross section; 13 - ripe fruit; 14 - seed - normal and enlarged view; 15 - the same in a longitudinal section [47].....	16
Figure 6 A comparison of flax area harvested [48]	17
Figure 7 Comparison of production values of flax [48]	18
Figure 8 Flax yield expressed in metric tonnes per hectare [48]	18
Figure 9 Hemp plant. A flowering male and B seed-bearing female plant, actual size; 1 male flower, enlarged detail; 2 and 3 pollen sac of same from various angles; 4 pollen grain of same; 5 female flower with cover petal; 6 female flower, cover petal removed; 7 female fruit cluster, longitudinal section; 8 fruit with cover petal; 9 same without cover petal; 10 same; 11 same in cross-section; 12 same in longitudinal section; 13 seed without hull [55]	19
Figure 10 A comparison of hemp production in the World [48].....	20
Figure 11 A comparison of area harvested in hemp production	21
Figure 12 Comparison of hemp yield in the world [48]	22

Figure 13 (A) Longitudinal cross-section of hemp stem [59] and (B) cross section of industrial hemp stem microstructure [60]	23
Figure 14 Bast fibre microstructure diagram [62].....	24
Figure 15 A natural fibre processing flow-chart [89]	29
Figure 16 (A) Dry mat forming machine [96], (B) Various types of short natural fibre mats [99].....	30
Figure 17 Principal components of the hydro entanglement system [97]	30
Figure 18 Diagrams comparing ring spun yarns with the twisted fibres: (A) and wrapped yarns without twist and fibres aligned in the main yarn direction (B).....	31
Figure 19 The ring spinning element for processing yarns with twisted fibres [102]	32
Figure 20 Composite fabric reinforcements and preforms [103, 105]	33
Figure 21 Composite laminate processing steps with thermoset resin systems.....	35
Figure 22 Schematic representation of unsaturated polyester curing process [119].....	36
Figure 23 Applications of grains and legumes refinery products [4].....	38
Figure 24 (A) Various types of NFC panels [4] (B) Monolithic house roof made of NFC [135]	41
Figure 25 (A) Door elements made out of NFC (B) Exhibition door frame made out of NFC [4].....	41
Figure 26 (A) Hemp mat roll (B) Hemp mat fibres and fibre bundles	44
Figure 27 (A) Hemp-wool mat stripes (visible surface parallel lines are created by water jet nozzles during processing) (B) Impregnated hemp-wool mat in polyester resin with black and white wool fibres and light brown hemp fibres	45
Figure 28 (A) Hopsack 4x4 flax biaxial fabric with a distinctive plane wave arrangement of yarns (B) Twill 2x2 flax biaxial fabric with distinctive twill surface diagonal pattern	46
Figure 29 (A) Flax unidirectional rowing made out of aligned 240Tex twisted fibre yarns (B) Flax unidirectional rowing made out of 590Tex twisted fibre yarns.....	47
Figure 30 (A) 80g/m ² plane wave E-glass fabric (B) 380g/m ² plane wave E-glass fabric	47

Figure 31 (A) Six grades of hemp yarns on spools, (B) Bundles of hemp yarns (C) A single yarn with distinguishable surface fibre pattern.....	48
Figure 32 (A) A single hybrid hemp-wool yarn (B) Aligned hemp-wool yarns prepared for processing of unidirectionally reinforced laminate.....	49
Figure 33 (A) Flax 250Tex non-twisted fibre yarn (B) Flax yarn bundles	50
Figure 34 (A) Aluminium moulds with square and dumbbell shapes (B) Hemp, flax and jute mat samples used in feasibility study	52
Figure 35(A) Image of one of the trial samples processed to assess hot press procedure. Hemp mat reinforcing polyester resin (B) Rectangular moulds with the dimensions 25mm x 250mm during trial hot pressing of NFC laminates.....	53
Figure 36 (A) Diagram representing arrangement during compression moulding (B) Flax fabric reinforcement in a mould during impregnation and (C) Palapreg ECO laminate reinforced with flax 4x4 hopsack fabric	54
Figure 37 (A) Diagram representing setting during procedure of processing samples with vacuum impregnation (B) Picture of prepared set-up.....	55
Figure 38 (A) Unidirectionally aligned hemp yarns in the rectangular mould (B) Unidirectionally aligned yarns placed in the 2 nd type of a square mould	55
Figure 39 Diagram representing unidirectional yarn samples preparation methodology.....	56
Figure 40 Batch of various Palapreg-Eco resin laminate samples (from left: flax fabric reinforced laminates, hemp unidirectionally reinforced laminates flax and hemp-wool reinforced laminates).....	57
Figure 41 (A) Feasibility studies of the NFC tube processing by compression moulding with various types of reinforcement. (B) Set of trial stage NFC tubes, processed by compression moulding technique.....	58
Figure 42 (A) NFRP tube impregnated with applied external pressure from the thermo shrinking tape. (B) Surface of impregnated and cured NFC tube reinforced with flax unidirectional fabric (C) Impregnation of three tube samples by resin transfer moulding.....	59
Figure 43 (A) Tube mould with pinned end cups ready for filament winding. (B) Manual procedure for the hemp composite tube composite by pin winding.....	59
Figure 44 (A) Aluminium end cups with pins (B) moulds with wrapped yarns, (C) Collapsible mould with pinned end cups assembly diagram	60

Figure 45 Diagram of the natural fibre yarn tube filament winding set-up	61
Figure 46 (A) Laboratory scale natural fibre winder during sample preparation (B) Tubular mould with surface yarns winded at 90° to the sample direction	62
Figure 47 (A) Diagram of the sample rotating stand used during gelling and curing (B) Macro image of the interior part of the trial thin walled samples revealing a criss-crossed reinforcement pattern	63
Figure 48 (A) Instron 5585 universal testing machine set-up (B) Hemp unidirectional laminate sample prepared for the tensile test	66
Figure 49 Flax 250 Tex yarn reinforced laminate test pieces after the test with fractures within the gauge area	66
Figure 50 (A) Diagram of the sample loading with dimensions [141] (B) Laminate with Palapreg-Eco resin reinforced with glass fibres during flexural test	67
Figure 51 (A) Hemp twisted yarn reinforced tube during compression test (B) Two flax reinforced laminate trial tubes with progressive collapse fracture after compression test	68
Figure 52 (A) ILSS sample drawing with dimensions (B) ILSS samples made out of GFRP with Palapreg-Eco resin	69
Figure 53 (A) GFRP with Palapreg-Eco resin ILSS sample fracture surface (B) Hemp yarn reinforced Palapreg-Eco ILSS sample after the test	70
Figure 54 Dumbbell shaped tensile sample cut out from hemp mat/polyester laminate with laser plotter	72
Figure 55 (A) Hopsack flax fabric in polyester laminate machined with a band saw (B) Table top precision cutter used for machining smaller samples	72
Figure 56 Examples of a trial hemp reinforced unidirectional samples fracturing at the edge of the grip area. Stress concentration created by grips causes premature sample fracture and invalidity	73
Figure 57 (A) Four laminate test pieces with aligned hemp twisted yarn reinforcement in Palapreg-eco resin (B) A batch of NFRP test pieces with glass fibre end tabs prepared for the tensile test	73
Figure 58 (Top) unidirectional reinforced tensile sample dimensioning (Bottom) Textile and mat reinforced samples arrangement	74
Figure 59 (A) One batch of samples trimmed and prepared for the compression test (B) Macro image the 130Tex hemp twisted yarn reinforced composite tube with the fibres oriented at $\pm 45^\circ$	80
Figure 60 A batch of samples being casted prior to polishing	81

Figure 61 Yarn breaking force results for 250mm gauge length.....	88
Figure 62 Influence of the yarn linear density (Tex) on tensile modulus, tensile stress and tensile strain in NFC laminates reinforced with twisted architecture hemp yarns.....	89
Figure 63 Cross sections of 25Tex hemp yarn unidirectionally reinforced laminate: (A) transverse and (B) longitudinal	90
Figure 64 Relationship between the twist level and yarn strength [148].....	91
Figure 65 (A) Uniform yarn stacking arrangement in twisted flax yarn reinforced laminate transverse cross section with visible (B) Longitudinal cross section of flax reinforced laminate with yarns and wrapping wire.....	93
Figure 66 (A) Twisted flax F12 yarn rowing laminate (B) Non-twisted flax yarn reinforced UD sample fracture modes	94
Figure 67 Comparison of non-twisted and twisted yarns. (A) Hemp-wool 1000Tex non-twisted yarn (B) Hemp twisted 39Tex yarn (C) Flax 250Tex non-twisted yarns. (D) Hemp 130Tex twisted yarn.....	94
Figure 68 Diagram of unidirectional non-twisted yarn theoretical shape (Left) and actual shape deformation morphology (Right).....	95
Figure 69 Common weave architectures [11].....	99
Figure 70 (A) Surface of a laminate reinforced with 4x4 hopsack fabric (B) Surface of a laminate reinforced with a 2x2 twill fabric.....	99
Figure 71 Differences in tensile properties between laminates made with fabrics and unidirectional laminate.....	100
Figure 72 (A) Impregnated hemp-wool mat in polyester resin with black and white wool fibres and light brown hemp fibres (B) Fracture surface of the hemp-wool mat polyester laminate after tensile test	101
Figure 73 (A) Macro image of a single hybrid 1000Tex hemp-wool yarn (B) Fracture area after tensile test. The fracture line corresponds to the direction.....	102
Figure 74 (A) Cross section of the hemp-wool hybrid mat reinforced laminate (B) Hemp-wool hybrid yarn reinforced laminate cross section.....	104
Figure 75 Longitudinal cross section of unidirectionally reinforced laminate with 41%V _f of hemp twisted yarn.....	106
Figure 76 Effect of the volume fraction of hemp twisted fibre 39Tex yarn reinforcement on tensile properties of a unidirectionally aligned laminate with Palapreg-Eco matrix.....	107

Figure 77	Effect of the volume fraction of hemp twisted fibre 130Tex yarn reinforcement on tensile properties of a unidirectionally aligned laminate with Palapreg-Eco matrix.....	109
Figure 78	Effect of the volume fraction of flax non-twisted fibre 250Tex yarn reinforcement on tensile properties of a unidirectionally aligned laminate with Palapreg matrix.....	110
Figure 79	Flax 250Tex yarn unidirectional laminate tensile modulus compared with the rule of mixtures	114
Figure 80	Hemp 39Tex twisted yarn reinforcing Palapreg-eco results and the rule of mixtures comparison.....	114
Figure 81	Comparison between the ultimate tensile stress results calculated with rule of mixtures and experimental results for two types of hemp reinforced laminates, i.e. 39Tex yarn and 130Tex yarn.....	116
Figure 82	(A) Flax Hopsack fabric reinforced laminate during the three point bending test (B) Bottom side of the unidirectional laminate sample after the test.....	119
Figure 83	Relationship between flexural properties of twisted hemp yarn reinforced PalapregEco resin and yarn Tex value and with average volume fraction of fibres $V_f=41\%$	121
Figure 84	Comparison of flexural properties of flax twisted-fibre yarns with 240Tex and 590Tex.....	122
Figure 85	(A) Glass fibre twill fabric reinforced Palapreg-eco laminate surface (B) Cross section of the GFRP sample.....	126
Figure 86	Surface of the hemp mat (HM) reinforced Palapreg-eco resin laminate.....	126
Figure 87	Relationship between non-twisted 250Tex flax yarn reinforcement arrangement and mechanical properties of the NFC laminate. From left: 4x4 Hopsack, 2x2 Twill and parallel yarn arrangements.....	128
Figure 88	Effect of the volume fraction of hemp twisted fibre 39Tex yarn reinforcement on flexural properties of a unidirectionally aligned laminate with Palapreg-Eco matrix.....	129
Figure 89	(A) Laminate strips reinforced with 39Tex hemp twisted yarn with visible reinforcement alignment (B) Cross section of a 39Tex hemp laminate with a high 76%Vf.....	130

Figure 90	Effect of the volume fraction of hemp twisted fibre 130Tex yarn reinforcement on flexural properties of a unidirectionally aligned laminate with Palapreg-Eco matrix	131
Figure 91	250Tex non-twisted fibre flax yarn laminate strips with different volume fractions (From the top: 23.0%, 30.0%, 51.0%, 56.6%, 76.0% and 89.7% V_f).....	132
Figure 92	Effect of the volume fraction of flax non-twisted fibre 250Tex yarn reinforcement on flexural properties of a unidirectionally aligned laminate with Palapreg-Eco matrix.	133
Figure 93	Flexural properties of laminates reinforced with hemp-wool yarn as a function of volume fraction	135
Figure 94	(A) A longitudinal cross section through the hemp-wool yarn laminate (B) A transverse cross section through the hemp-wool reinforced laminate.....	135
Figure 95	Comparison of flexural modulus properties of developed NFC materials with theoretical values for natural materials plastics and composites (plotted with CES EduPack 2012)	138
Figure 96	Comparison of flexural strength of the developed NFC with theoretical values for plastics, composites and natural materials against density (plotted with CES EduPack 2012)	139
Figure 97	Examples of NFC tubes with four reinforcement arrangements: (a) T10; (b) T30; (c) T45; (d) T90.....	142
Figure 98	(A) Hemp yarn with 130Tex with visible individual technical fibres arrangement and yarn hairiness (B) A diagram with positioning of cross section images and the angle of the reinforcement	143
Figure 99	(A) Cross section of the T45 tube in the ‘A-A’ direction (B) cross section in the ‘A-A’ direction of the tube with the reinforcement oriented at 90° and 0° (C) the T90 tube in the ‘B-B’ direction and (D) the T90 tube in the ‘A-A’ direction.....	144
Figure 100	(A) Impregnation of individual technical fibres within the NFC tube (B) interface of hmp-matrix within the NFC tube wall (C) the cross section of the tube wall with porosity within the yarns visible as black areas and (D) optical image of cross section revealing delamination sites within the yarn.....	146
Figure 101	Relationship between the ultimate compression strength of the NFC tubes and the yarn wind angles.....	148

Figure 102 Relationship between the compressive modulus of the NFC tubes and the yarn wind angles.....	149
Figure 103 (A) An image of commercially pultruded NFC rods reinforced with hemp yarns (B) a fracture area of the rectangular test piece after tensile test.....	150
Figure 104 Microbuckling fracture (A) stress-strain response graph (B) Examples of T10 samples fractures in microbuckling.....	152
Figure 105 Diamond shape buckling fracture (A) A stress-strain response (dashed line represent mean post buckling load) (B) Diagonal lobes formation in diamond shape buckling collapse	153
Figure 106 Concertina shape buckling fracture (A) A Stress-strain response (B) Initial stage of concertina shape buckling collapse mode with first circumferential hinge.....	154
Figure 107 Progressive crushing (A) Examples of stress-stain responses (NFC T30 and T60 tubes with the ratio $t/D > 0.04$. Horizontal straight lines represent mean crushing loads) (B) A crushed sample during the test.....	155
Figure 108 Flexural modulus results for flax non-twisted fibre 250Tex flax yarn hopsack fabric reinforced laminates under heat ageing (compression moulded: PE- Crystic matrix and PP – Palapreg, vacuum bagged: PEV – Crystic and PPV - Palapreg).....	158
Figure 109 Flexural stress results for flax non-twisted fibre 250Tex flax yarn hopsack fabric reinforced laminates under heat ageing (compression moulded: PE- Crystic matrix and PP – Palapreg, vacuum bagged: PEV – Crystic and PPV - Palapreg)	158
Figure 110 Flexural strain results for flax non-twisted fibre 250Tex flax yarn hopsack fabric reinforced laminates under heat ageing (compression moulded: PE- Crystic matrix and PP – Palapreg, vacuum bagged: PEV – Crystic and PPV - Palapreg)	159
Figure 111 (A) Examples of flax hopsack fabric reinforced PalapregEco matrix laminate coupons. (B) Examples of samples after one month weathering exposure	160
Figure 112 Influence of environmental weathering, immersion in water and saline solution on flexural modulus for flax non-twisted fibre 250Tex flax yarn hopsack fabric reinforced laminates (compression moulded: PE- Crystic matrix and PP – Palapreg, vacuum bagged: PEV – Crystic and PPV - Palapreg).....	160

Figure 113 Influence of environmental weathering, immersion in water and saline solution on flexural stress for flax non-twisted fibre 250Tex flax yarn hopsack fabric reinforced laminates (compression moulded: PE- Crystic matrix and PP – Palapreg, vacuum bagged: PEV – Crystic and PPV - Palapreg).....	161
Figure 114 Influence of environmental weathering, immersion in water and saline solution on flexural strain for flax non-twisted fibre 250Tex flax yarn hopsack fabric reinforced laminates (compression moulded: PE- Crystic matrix and PP – Palapreg, vacuum bagged: PEV – Crystic and PPV - Palapreg).....	162
Figure 115 Influence of environmental weathering, immersion in water and saline solution on swelling for flax non-twisted fibre 250Tex flax yarn hopsack fabric reinforced laminates (compression moulded: PE- Crystic matrix and PP – Palapreg, vacuum bagged: PEV – Crystic and PPV - Palapreg).....	163
Figure 116 Mechanism of natural fibre deboning due to moisture induced swelling [188]	165
Figure 117 Relationship between time (sec) and water absorption (%) of the total mass. Data compares unsaturated polyester resin (crystic)/flax composite and Palapreg/flax composite	167
Figure 118 Comparison of flax 4x4 Hoopsack reinforcing unsaturated polyester (Crystic) laminate water absorption data with Fick’s model.....	168
Figure 119 Comparison of flax 4x4 Hoopsack reinforcing PalapregEco laminate water absorption data with Fick’s model.....	169

List of Tables

Table 1 Composition of natural fibre	25
Table 2 Properties of selected cellulosic fibres and man-made fibres.....	27
Table 3 Comparative properties of the three main synthetic thermoset resins.	37
Table 4 Samples types prepared for the tensile test.	74
Table 5 Sample types prepared for the flexural test.....	76
Table 6 Sample types prepared for the weathering test.....	78
Table 7 Tube compression samples types.	80
Table 8 Reinforcements and corresponding parameters studied	86
Table 9 Tensile properties of laminates with twisted and non-twisted yarn with Palapreg-Eco resin as a matrix	92
Table 10 Tensile test results for unsaturated polyester reinforced with fabrics weaved from twist less flax yarns.	97
Table 12 Properties of hemp mat and hemp wool hybrid mat	101
Table 13 Tensile properties of aligned non-twisted yarn reinforced hemp-wool hybrid composites with Palapreg-Eco matrix.	103
Table 14 Comparison of hemp and flax unidirectional laminates tensile properties.	111
Table 15 Flexural properties comparison of two laminates reinforced with flax yarns with twisted and non-twisted architecture.....	123
Table 16 Flexural properties of the laminates reinforced with natural fibre fabrics and mats.	125
Table 17 Comparison of three impregnation procedures used for processing of the laminates	127
Table 18 Comparison of three laminates tensile properties with $V_f=51\%$	134
Table 19 Flexural properties of the composites reinforced with aligned hemp or flax fibres.....	137
Table 20 Moisture absorption of selected NF	166
Table 21 ILSS compound test results for selected samples reinforced with NF fabrics. Only samples which fractured correctly are included.	172
Table 22 ILSS test results for the flax unidirectional laminate samples.....	173
Table 23 ILSS test results for the unidirectional hemp composites	173
Table 24 Influence of the winding angle on compression properties	147

Nomenclature

°C	Degrees Celsius
BFRP	Bast Fibre Reinforced Plastic
DNST	Double Notch Shear Test
FAO	Food and Agriculture Organization of the United Nations
GFRP	Glass Fibre Reinforced Plastic
GPa	Gigapascals
ILSS	Interlaminar Shear Strength
LCA	Life Cycle Analysis
MOR	Modulus of resilience
MPa	Megapascals
NFC	Natural Fibre Composite
NRFP	Natural Fibre Reinforced Plastic
OSB	Oriented Strand Board
PB	Particleboard
PE	Polyester
RH	Relative Humidity
TEX	Yarn linear density
V_f	Volume fraction
VOC	Volatile Organic Compound
WPC	Wood Plastic Composite

Introduction, Literature Review and Methodology

1 Introduction

1.1 Research Hypothesis

Existing natural fibre composites (NFCs) are not suitable for building applications due to their poor mechanical performance. These properties can be improved, because fibre related issues are the major influencing factor in the laminate mechanical properties. Natural fibre reinforcement type and arrangement has, similarly to synthetic reinforcements, an influence on laminate mechanical properties, which can be optimised. If reinforcement and process parameters can be optimised, this will allow for the development of NFCs with sufficient mechanical properties to be used as sandwich, panels, sandwich panels or tubes for civil engineering.

1.2 Rationale

Buildings are a major source of energy consumption and CO₂ emissions, and at the end of their life cycle 30% of construction and demolition waste goes to landfill. Plants store CO₂; therefore use of NF in construction should result in material of lowered embodied energy, renewable and sustainable. There is an increased interest in the use of NF in construction, but there are a couple of problems preventing its wide implementation. There is a perception of low mechanical properties, dimensional instability and moisture resistance related with NFCs, because of the lack of understanding of this group of materials. At present, NFCs are being used in non-structural or semi structural applications. The existing solutions are not sufficient for civil engineering, which promotes these materials to be investigated.

1.3 Aims and Objectives of the Project

The project aims and objectives were set in order to achieve an improved understanding of processing, performance and applicability of NFCs for civil engineering applications. It is composed of theoretical and experimental investigations into the subject of NFC based on hemp and flax fibres. The aim was to analyse the mechanical performance and applicability of processed NFCs. The program is divided into five objectives. In the first objective natural fibre reinforcements and suitable resin systems are selected. The second objective is to study and select a suitable processing methodology for laminate board manufacture, which allows for control over a range of factors. The third objective is to study and develop a methodology for NFC tubes processing. The fourth objective is to analyse processed laminates and tubes in terms of mechanical properties experimentally and theoretically. The fifth objective is to study the response of the material under weathering conditions. As shown in the literature review more detailed information about the processing performance and applicability of NFCs is needed.

1.4 Structure of the Thesis

This thesis is composed of three main sections, i.e. Literature Review, Experimental Procedures and Methodology and Experimental Results and Analysis. The thesis is divided into ten chapters. Chapter 1 consists of introduction to the thesis. Chapter 2 provides literature review related with the studied subject. Chapter 3 consists of experimental procedures and methodology. Chapter 4, the first chapter of the Results and Analysis discusses an influence of the reinforcement on tensile properties of Natural Fibre Composites (NFC). Chapter 5 discusses flexural properties of the NFCs. Chapter 6 provides an analysis of weathering conditions influence on flexural properties of flax reinforced composites. Chapter 8 discusses differences in interlinear shear strength of various NFCs. Chapter 6 provides analysis of compressive behaviour of the NFC tubes. Chapter 9 consists of final conclusions. Chapter 10 provides recommendations for future work. Figure 1 presents a diagram of the work flow. The work was divided into multiple

stages. The first stage of the work consisted of material selection procedures and feasibility studies. Multiple fibres, e.g. jute, sisal, flax, hemp, were assessed for their properties and availability both theoretically and experimentally. The hemp and flax fibres were selected. At the same time resin system, for use with aforementioned fibres were selected and tested. Next task was to select and develop processing procedure for a NFC laminate processing, which was followed by testing procedures development. Conclusions drawn during laminate processing were used in NFC tube feasibility studies. The next stage planned was to prepare a repeatable way for processing of NFC tubes. When procedures for processing flat laminates and tubes were developed, an experimental design was drafted, which aimed at finding influence of processing and composition factors on mechanical properties of NFCs.

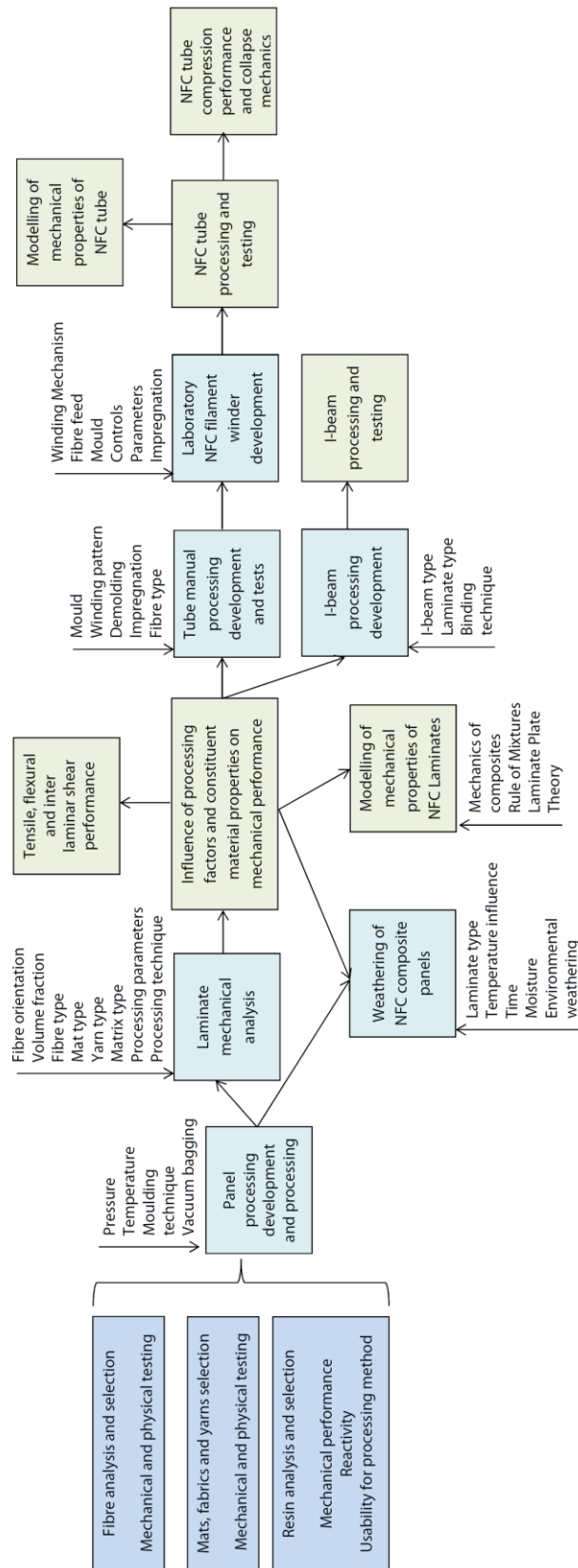


Figure 1 Diagram representing main aspects of the work flow

2 Literature Review

The goal of this literature review is to introduce the key terms and ideas relevant to the experimental analysis of natural fibre composites (NFCs) reinforced with hemp and flax fibres. NFC terminology is clarified. Hemp and flax fibre structure, properties, history of cultivation and research activities are discussed. Furthermore, constituent NFC materials are analysed, which is followed by a review of fibre production. In the final section, current and possible uses for NFCs in building applications are introduced and discussed.

Definitions of NFC, NFRP and BFRP are provided in section 2.1. Section 2.2 presents classification of natural fibres, whereas section 2.3 lists important points in NFC history. A comparison between synthetic and natural fibres is made in section 2.4. Section 2.6 focusses on natural fibres and their reinforcements. It discusses the significance of hemp and flax plants and describes production methods used for NF reinforcements. Moreover it provides information about natural fibres, i.e. structure, chemical composition and mechanical properties. Section 2.6 describes resin systems used for production of NFCs. Section 2.7 presents building applications for NFCs.

The main reasons for NFC development are renewability, specific mechanical properties and relatively low embodied energy inherent in plant based materials. The competitive reinforcement price is another trait, but it is not necessary for the NFRP to be economically viable, since ‘environmental awareness’ is an increasingly important factor considered in customer selection process. Competitive embodied energy is one of the key arguments when comparing NFCs with glass fibre reinforced plastics [1]. Additional treatments and procedure increase material cost and NFC embodied energy, therefore costs reducing continuous processing routes are considered in this thesis. Moreover, there is a need for new designs, which utilise performance and environmental benefits specific for NFCs in building applications. Tubes and panels are versatile components prevalent in many building applications.

2.1 Terms Used in NFC Area

At the beginning it is important to clarify the natural fibre composite nomenclature, which is often used imprecisely or incorrectly. NFC is a broad term, which relates to all composite materials containing fibres from natural sources. This includes organic and inorganic sources like plants, minerals and animals. Therefore, the ‘NFC’ term contains material groups, including natural fibre reinforced plastic (NFRP), particleboard (PB), oriented strand board (OSB), wood plastic composite (WPC), fibre cement (e.g. Eternit ®) or insulation materials based on shiv like Hempcrete®. In this thesis, the main focus is on polymeric matrix reinforced with hemp and flax bast fibres. Additionally, hybrid hemp-wool fibre blend reinforcement is analysed. All three composite types belong to the NFRP group. Unfortunately, this is not specific enough, because particleboards made with wood and shivs (core material) are also included. The bast fibres, also called skin fibres or phloem fibres, have the most significant reinforcing properties, surpassing that of leaf, root or core material. In order to distinguish the composites reinforced with bast fibres from the others mentioned above, a new term is proposed here – bast fibre reinforced plastics (BFRP). It is a subgroup of NFRP as well as NFC. Therefore, BFRP will be used when referring to hemp and flax bast fibre composites.

2.2 Classification of Natural Fibres

Natural fibres include plant, animal and mineral fibres. This excludes reengineered fibres, like manufactured cellulose fibres (e.g. rayon or viscose). Nevertheless, natural fibres are processed and pre-treated with mechanical and chemical ways in order to meet specific requirements of the textile or composite industry, but still are distinguished as ‘natural’. Natural fibres, which are used as the reinforcement, are summarised in Figure 2. Bast fibres include flax, hemp, jute, ramie and kenaf. They act as a structural reinforcement for the plant stem. There are also other plant fibres like leaf, seed, grass and wood fibres. In

Europe fibres from wood, flax, hemp, wheat, canary grass and wool are produced in significant quantities. The asbestos inorganic composites are banned in many countries due to its cancerogenic effect on human air passages (i.e. lung cancer, mesothelioma) related with airborne asbestos fibres from weathered material [2, 3]. Cultivation of other fibres, like silk, abaka, jute, ramie, kenaf, palm and kapok requires warmer climate and their cultivation is not typically developed in Europe.

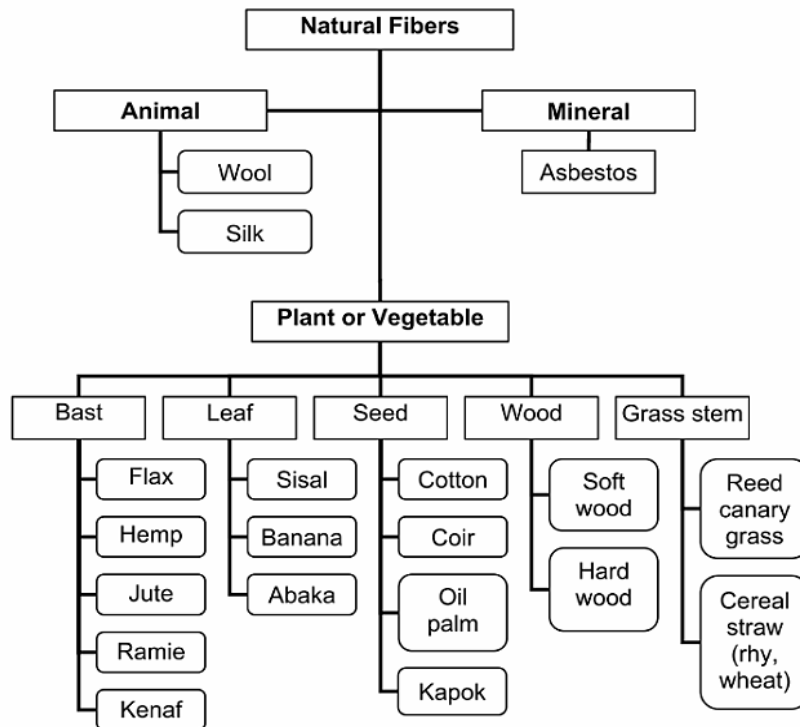


Figure 2 Classification of natural fibres according to the nature of the reinforcement [4]

2.3 Key Points in NFC History

The natural fibre composites, e.g. wood, bamboo and bone, are some of the first materials used by mankind. In these naturally occurring composites cellulose, keratine or mineral apatite plays the role of the reinforcement. Natural materials were used because of their abundance, renewability and lack of alternatives. For centuries, naturally occurring composites (i.e. wood and bast fibres) were strategic materials used in construction of houses, bridges, ships and weaponry. The first man-made composites are various form of

clay reinforced with natural fibres. Bricks reinforced with straw fibres in Ancient Egypt are considered to be the first natural fibre composites created by people. At the same time, they are the first application of NFCs in civil engineering. One of the most interesting ancient natural fibre composite was used in the composite bow (Figure 3A). It utilised compressive properties of horn and tensile properties of sinew, which were attached to the wooden core. Therefore, it incorporated three reinforcing natural fibres, namely collagen, keratin and cellulose in one laminate material. This construction allowed for production of shorter bows with higher potential energy capacity than the same size wooden bows. Use of naturally occurring composites continued until organic chemistry breakthroughs leading to creation of synthetic adhesives. In 1907 Bakelite was developed in New York, which was a thermosetting phenol formaldehyde resin with wood flour or asbestos fibres often used as filler. It found multiple applications, but was used in relatively small parts due to the brittle nature of the material. In the 1930s, Henry Ford experimented with multiple natural fibres as reinforcement for a car body [5]. The flax fibre reinforced phenolic resin composite, developed and described by Norman de Bruyne in 1937, is considered a milestone leading to the development of glass fibre composites. The composite was named Gordon Aerolite. At the time, there was a demand for light and strong materials for the automobile and aviation industries during World War II. Therefore, the scarcity of light metal alloys, created by an excessive military use and an economic warfare between countries, led to further developments and applications for BFRP. An experimental Spitfire fuselage was constructed with Gordon Aerolite (Figure 3B) [6]. From 1955 the German Democratic Republic (GDR) produced ‘Duroplast’, a natural fibre reinforced plastic. It was composed of phenol resin reinforced with recycled cotton or wool fibres. It was mainly used for body parts and interior parts of cars on a steel frame, from which the most popular was ‘Trabant’, produced until 1991. The debate about fire safety, crash safety, and end-of-life solutions are some of the reasons voiced behind stopping the production. Some engineers tried to dismiss those criticisms. However, the key factor was the fall of the Berlin Wall in 1989 and public perception of a ‘Trabant’ as a symbol of the GDR previous system. Nevertheless, the use of NFRP in the automotive industry is growing. A renewed interest in NFCs is observed over the last two decades. This is evident in the number of research papers published in the field, e.g. [7-11]. The NFRPs in the Trabant car, which was compared to ‘cardbord’ or ‘soap dish’; is now rebranded as ‘green’ and

‘environmentally friendly’. NFCs are now seen as potential materials for car internal components, civil engineering and other applications, because of their strength-to-weight properties, renewability, possible low-cost, and reduced environmental footprint. Mercedes replaced glass fibre composites for flax-polypropylene composites in the underbody components of the A-class car (Figure 3C). In 2003, Ford released a hybrid electric car with corn-based polylactic acid (PLA) materials used for interior elements. In 2008 the ECO Elise Lotus car was presented at the British International Motor Show, which has hood, roof and seats made out of hemp/polyester BFRP (Figure 3D). Bayer Polymers is producing polyurethane resin reinforced with bast fibres, which are molded into car door inner trim panels [12]. Similarly, sports goods like surfing boards, helmets or kayaks are designed with BFRPs. The renewed interest is related with a better understanding of NFRP properties, material science developments and conviction that NFRP contributes to the creation of a sustainable economy. The use of BFRP in the building industry is significantly smaller and mostly narrowed to experimental trials, therefore the analysis of applications of BFRP and the development of new materials is timely and justified. A discussion on building applications is presented in the ‘Building applications’ section at the end of this chapter.

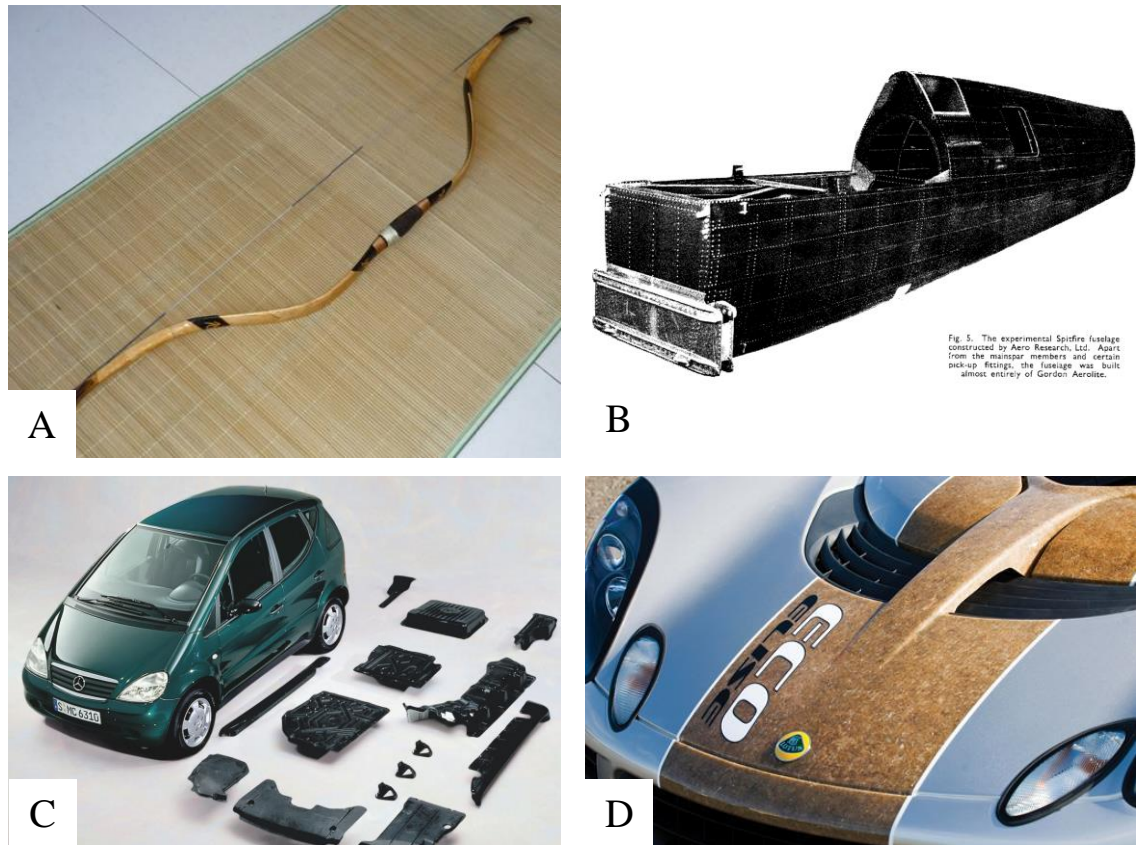


Figure 3 (A) Reconstruction of a Ming dynasty Kaiyuan bow by Chinese bowyer Gao Xiang, made with horn, bamboo and sinew composite, (B) The experimental Spitfire fuselage constructed by Aero Research Ltd. Apart from the main spar member and certain pick-up fittings, the fuselage was built almost entirely of Gordon Aerolite [13], (C) Flax/polypropylene underbody components have replaced glass fibre reinforced plastic components in vehicles such as the Mercedes Benz A-Class [14], (D) A close up of the ECO Elise hood shows the hemp fibre pattern in the clear-finished stripe [12]

2.4 Reinforcements

2.4.1 Synthetic and NF Reinforcements

There are three main composite types, namely particulate, fibrous and laminates. The synthetic or man-made reinforcements have short or continuous fibres, e.g. glass, aramid, carbon, boron, silicon carbide, steel and viscose. They are engineered to meet specific demands, therefore are produced in desired lengths and thicknesses. This is not possible

with natural fibres, which have inherently various lengths, thickness and cross section shapes. Additionally, NFs have defects along the fibre length, which present mechanical properties unlike the rest of the fibres. During consecutive processing stages natural fibres are refined and shortened. This causes irregularity in mechanical properties of individual fibres and reinforcements processed with them. Therefore, possible fibre orientations and processing techniques are limited. Composites are processed to have isotropic or anisotropic properties with control of the reinforcement orientation. The isotropic composites have the same properties in all directions, e.g. composites with randomly distributed particulate or short fibre reinforcement. The anisotropy of composites implies that material properties are directionally dependent. A special case of anisotropy is orthotropic composites with three axes of symmetry, e.g. unidirectional composite. Therefore, parts made with these composites are tailored to have the highest properties in the direction of applied load. This reduces cross section and weight of a produced part. Unidirectional composites have the highest mechanical properties, like tensile or compression, in the fibre direction. The force applied to the unidirectionally reinforced laminate in the perpendicular direction is the lowest, which creates material failure. Anisotropic layers can be stacked in the form of a laminate at various orientations, in order to fulfil design requirements in other directions [15]. The most common types of laminate layers are presented in Figure 4, namely randomly oriented mat composite with fibres without arrangement, unidirectional layer with fibres arranged in one direction, biaxial fabric with reinforcement arranged at longitudinal and transverse directions, transverse layer and a layer with reinforcement arranged at 45°. In synthetic reinforcements orienting fibres is straightforward because of the aforementioned wide control over fibre morphology. This is not the case with NFs, which have to be converted into yarns in order to control their orientation. As a custom in NFC terminology, ‘unidirectional composite’ refers to a material which has yarns or bundles arranged in one direction, e.g. individual fibres composing twisted yarns are not oriented in the same direction. The processing of natural fibres and its reinforcements is presented in the Chapter 2.5.5. The NF reinforcement orientation relationship with mechanical properties is explained in-depth in chapters 5 and 6 of this thesis.

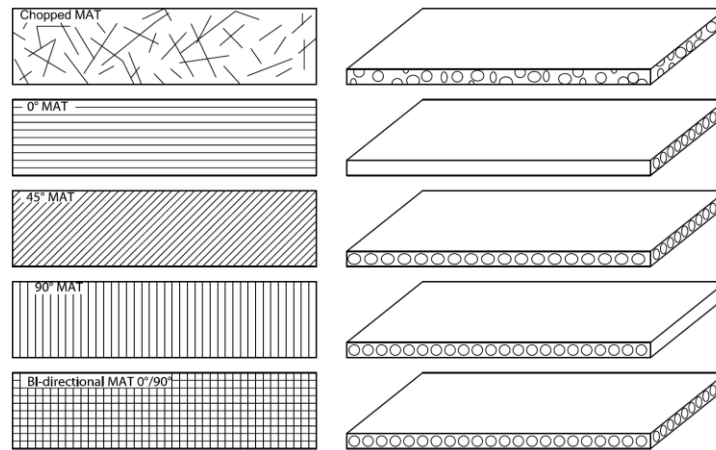


Figure 4 Typical composition of layered laminate for structural application [16]

2.4.2 Cost

Natural fibre building products are described as low-cost and lightweight with better environmental properties than glass fibre. Nevertheless, the cost of natural fibre products is higher than glass fibre products. The direct cost comparison of BFRP and GFRP is difficult because of the discrepancy between materials development levels and existence on the market, which is highly regulated and competitive. There is an established network of glass fibre manufacturers, suppliers and trained construction personnel. Natural fibres and glass fibres cannot be compared simply by unit of volume or mass. Both have different properties and there are many forms of reinforcement or insulation types. Therefore, a common comparison unit needs to be selected based on the outcome properties. For instance, composite material cost per m^2 for 100MPa tensile strength or cost per m^2 at $0.3 \text{ W/m}^2\cdot\text{K}$ in case of insulation materials. From flax and hemp fibre based products, the insulation material market is the most established, but still constitutes just a fraction of the glass wool insulation market. In the United Kingdom, the natural fibre insulation market, which includes hemp, flax and wool, is established at close to 2% of the insulation materials market. The prices for NF insulations are higher. In 2007 the cost per m^2 at $0.3 \text{ W/m}^2\cdot\text{K}$ per flax wool and hemp insulation were €14.04 and €16.30 respectively, while the cost of glass wool was €9.60 [17]. In 2013 the cost per m^3 at $0.3 \text{ W/m}^2\cdot\text{K}$ per flax wool and hemp insulation were from €17 to €19 and from €14 to €19 respectively, while the cost of glass wool was from €7 to €21 respectively [18]. Building materials are a long term

investment. Materials which are proven over 30-40 years have a clear advantage over new products. The other benefits claimed for NF building products, like health or comfort, are secondary selection criteria and only convince a special type of informed customer. Producers claim that information campaigns and improvements in regulations will be a decisive factor in the wider implementation of NF-based products

2.4.3 Life Cycle Impact

The environmental and health benefits are usually confirmed by presenting results of a material life cycle assessment (LCA). Unfortunately, conducting this analysis is not straightforward. There are detailed guidance on Life Cycle Impact Assessment, which are unifying procedures to make comparisons reliable, namely EU standard ISO14040 [19], EU Commission EUR 24586 EN [20] or UK PAS 2050 [21]. From the analysis method point of view the key aspects, which influence LCA, are the range of analysis, boundary conditions, inventory selection and data sources selection. From the process or material point of view there are different ways of handling raw material, processing methods, end-use technology and the reference material selection. Often full-range analysis is restricted by data availability on composition or process, protected by patent laws or simply the cost of such analysis [22]. There is a room for bias and special attention is necessary when making conclusions. For instance, one of the aspects inherently connected with natural fibres is whether the full biomass carbon cycle is recognised. In case of hemp there are different ways of performing fibre separation, i.e. retting and decortication or mechanical decortication [23]. Both processes produce hemp fibre, but use different processes and substrates, hence different impacts. In LCA analysis outcomes are often wide-range results and recommendations [24]. In the case of hemp and flax composites, the majority of reviews agree that materials based on natural fibres have lower environmental impact during their life cycle. As the loading of natural fibres in NFCs is higher, when compared with GFRP, this leads to a reduced matrix consumption and reduction of environmental impacts. NFCs have potential to reduce transportation emissions, due to superior specific mechanical properties. Energy recovery is also possible at the end of the materials life. Health benefits include environment control and comfort and reduction of volatile organic compounds emission in some cases [22, 25-27]. Nevertheless, natural fibre properties vary

and cannot be precisely engineered like synthetic fibres. Production and price of NFs are interconnected with weather patterns and harvesting. Simultaneously, to increase NF reinforcement production, areas dedicated for food crops are reclaimed, which might trigger socio-economic problems [28]. Weathering resistance of NFCs is inferior when compared with synthetic reinforcement and needs improvement [10, 29, 30].

2.5 Bast Fibre Reinforcements

This section presents information about hemp and flax and their reinforcements. Section 2.5.1 describes both plants with their historical significance, cultivation, use and production. Section 2.5.2 presents and discusses structure, chemical composition and mechanical properties of bast fibres. Section 2.5.3 discusses production routes of hemp and flax reinforcements. Section 2.5.4 presents mechanical properties of bast fibres. Section 2.5.5 describes types of NF reinforcements (i.e. mats, yarns and fabrics) and their processing routes.

2.5.1 Hemp and Flax – Plants with Global Significance for the NFC Industry

Flax and hemp fibre reinforcements are used in the experimental study to improve the mechanical properties of BFRP and to develop and discuss applications for this group of materials. Therefore, it is important to present and discuss information related to these natural fibres in order to better understand why those fibres were selected and which factors contribute to their performance.

Flax

Linum usitatissimum, known as flax or linseed, is a plant, which originated from the Caucasus territories. Flax has been used throughout the ages for textiles, threads, paper and nets. Flax grows up to 1.3m tall. It is an annual plant with thin stems and pale blue or bright red flowers. There was a recent discovery in the Upper Palaeolithic layers at Dzudzuana Cave,

currently Georgia, of a spun, weaved and dyed wild flax linen dating back to 30 000 B.C [31]. However, Bergfjord et al. [32] questioned the methods of fibre identification used by Kvavadze et al. [31], concluding that the unearthed 30 000 year old fibres can be identified only as bast fibres at this point, and that a further analysis is required to identify them as flax. Authors pointed out that by using Kvavadze's methodology, the ancient fibres can be equally identified as hemp. This was later refuted by Kvavadze [33] by presenting a comparison with modern micrographs of hemp, flax and nettle, but without providing further results such as DNA analysis or X-ray micro diffraction. Previously, findings from Ancient Egypt and Switzerland had been considered as the oldest. In Egypt, an almost transparent flax linen cloth was found dated at 2500 B.C with thread density of 500 per inch, which is an outstanding quality. In Swiss Neolithic lake dwellings, flax linen was found dated at 2000 B.C.[34]. Paper made out of flax was produced in China as early as 105A.D [35]. Flax is grown in temperate climate zones. In Europe, there were only a few flax cultivation and processing centres, including Russia, Denmark, England and France. Russia was producing around 90% of the flax before World War I [36]. Europe is still the leader in world flax production, due to cultivation traditions and process optimisation efforts made especially in the Western Europe, which result in the highest yields. Flax can be grown for fibres or seeds, which have nutritional value. Flax oil (linseed oil) pressed from seeds is used in cosmetics [37]. The solidified form of flax oil is the main component of linoleum [38]. Oil and seed flour are used in food products [39-41]. Moreover, it is used in resin processing like epoxy, polyester and others [42, 43]. The other applications of flax oil include paint manufacture [44] and biodiesel synthesis [45, 46].

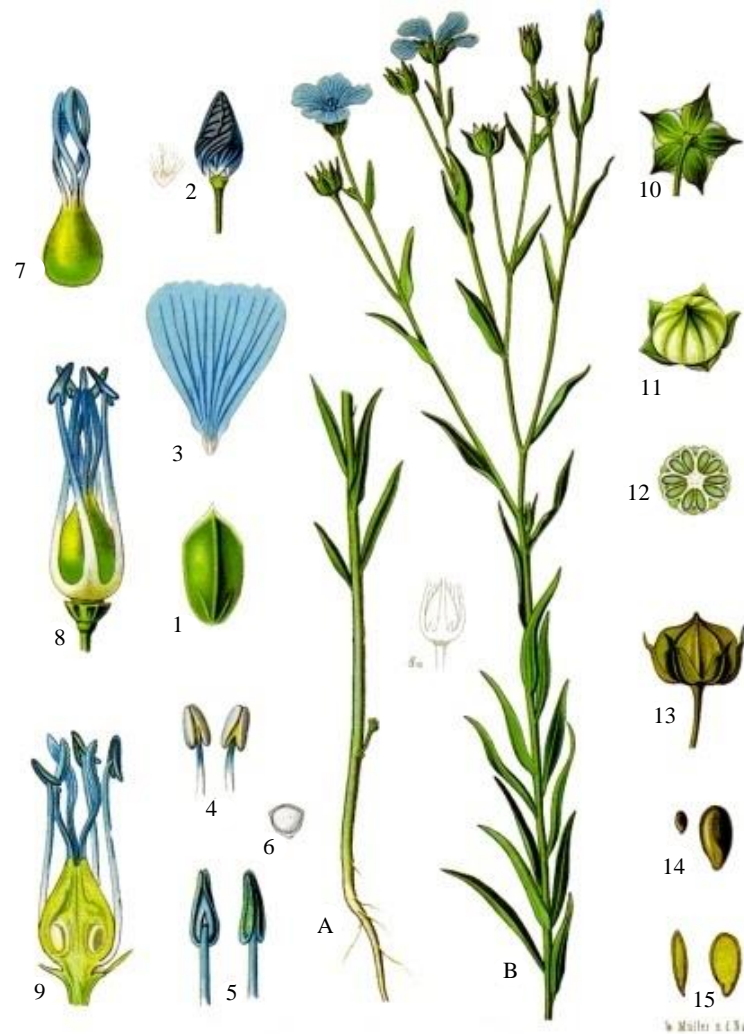


Figure 5 Flax. A, B - plant; 1 - sepal; 2 - bud without cup; 3 - lobe; 4 and 5 - the stamens from different angles; 6 - pollen grain; 7 - pestle with 5 columns (stilodiyami); 8 - a flower without calyx, corolla and staminodes; 8a - the same with staminodes; 9 - the same in a longitudinal section; 10 and 11 - unripe fruit from different angles; 12 - the same in cross section; 13 - ripe fruit; 14 – seed - normal and enlarged view; 15 - the same in a longitudinal section [47]

When analysing the production of flax fibre and tow in the World during the recent history, statistical data collected from 1961 by the Food and Agriculture Organisation of the United Nations (FAO) reveals an interesting trend, which can be correlated with changes in the market and in production techniques. There is a steady decrease of the area dedicated to flax cultivation around the World (Figure 6). This is visible from 1961, which is the start of data collection by FAO. The overall decrease sums-up to 1.8 M hectares from 1961 to 2013, which is roughly 90% of the area dedicated in 1961. One hectare (Ha) is a

measure of land used in agriculture, and is equal to 10 000 m². The biggest dedicated area was in Europe, which includes Western Europe, Eastern Europe and part of the Soviet Union, later transformed into the Russian Federation. There is a significant decrease in area dedicated for flax cultivation after 1988, which is the time of changes in Eastern Europe and Soviet Russia. There was a flax production crisis after 1990, which lasted a couple of years. This was addressed by support from the EU resulting in market stabilisation and regained interest in flax farming.

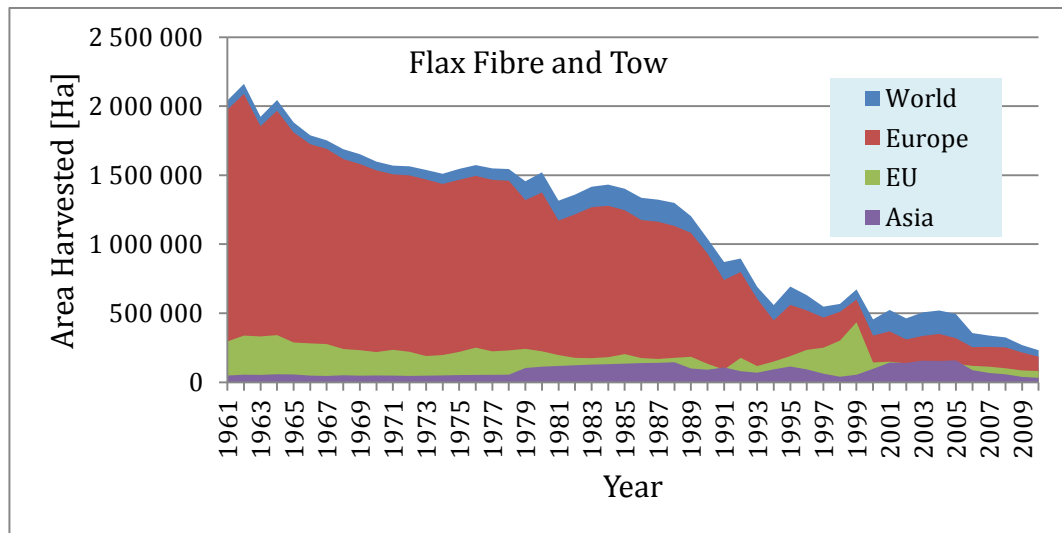


Figure 6 A comparison of flax area harvested [48]

Despite the aforementioned decrease in production area, the World production rates have fluctuated around 700k tonnes of flax fibre and tow per year (Figure 7). In the 1990s there was a crisis in flax production, which lasted for a decade. The 1990s were times of changes and improvements in global flax production techniques. The change is visible in an increase in production rates represented by yield, expressed in metric tonnes, of flax harvested from one hectare (Figure 8). A substantial improvement in the production efficiency is visible in the European Union. The mass of flax harvested from the same area increased from 1961 to 2000 by 734%. This is explained by increased production efficiency driven by developments in cultivation techniques, fertilisation, processing machinery and pest control.

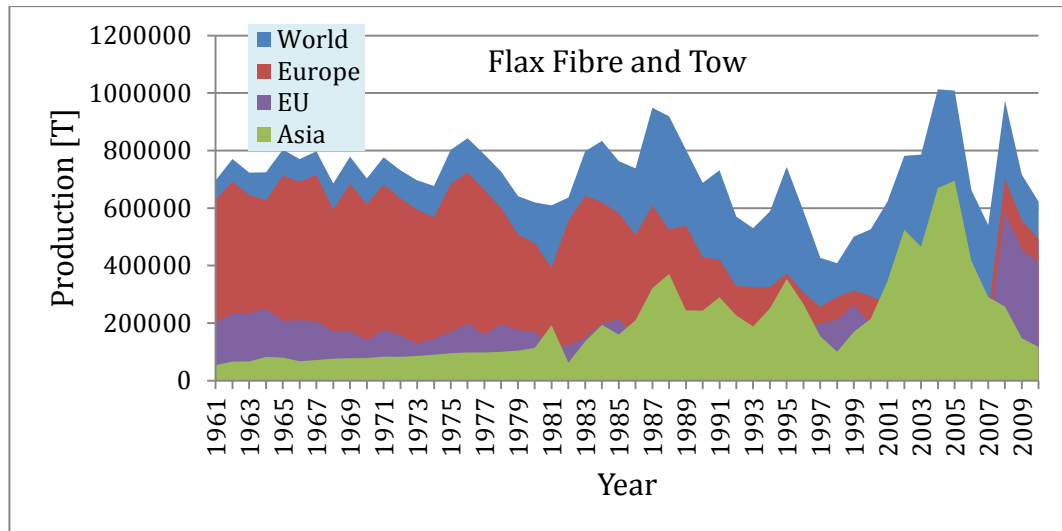


Figure 7 Comparison of production values of flax [48]

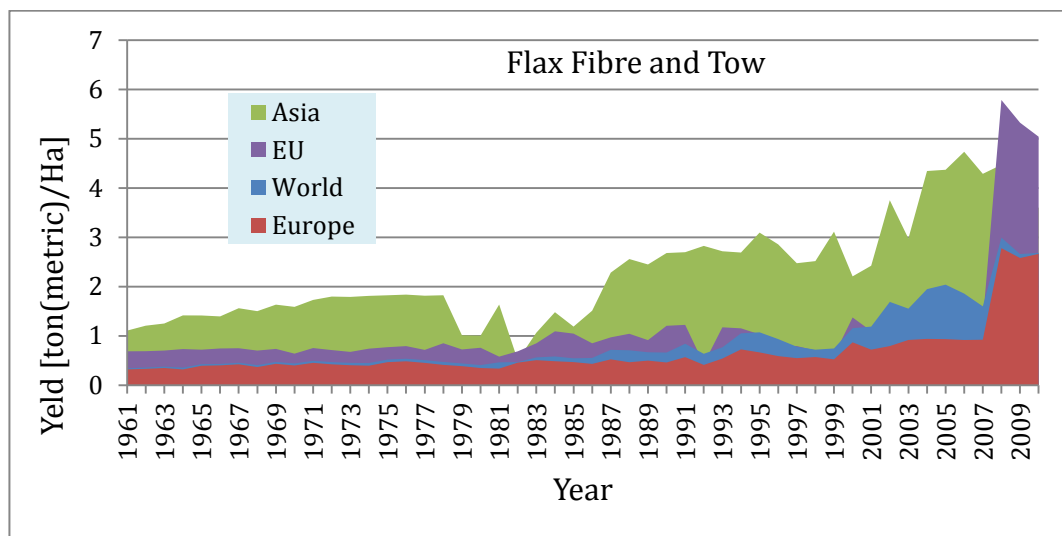


Figure 8 Flax yield expressed in metric tonnes per hectare [48]

Industrial hemp

Cannabis sativa L., known as hemp or industrial hemp, is one of the first plants to be domesticated and it is native to India and Iran. There are more than 2000 varieties of plants within that mulberry family and hemp is well known for its bast fibres [49]. Figure 9 presents a diagram depicting hemp plant flowers, seed and fruit. Industrial hemp was an important crop for millennia. Ropes were produced from hemp in China as early as 2800 BC [35]. Hemp was also used to produce the first paper in 100BC in China, during the

Western Han Dynasty [50]. It is speculated that European hemp cultivation started as early as 400BC. In UK, hemp was grown by Anglo-Saxons in 7th century [51]. In Europe, hemp was an important crop from the Middle Ages and was used for the production of ropes, sacks, threads, water hoses, sails and textiles. For centuries hemp was one of the most important and strategic crops (Renewable-Resources, 2010). In 1937 hemp was named "the most profitable and desirable crop that can be grown" [52] and "new billion dollar crop" [53]. Industrial hemp cultivation does not require herbicides, pesticides or excessive amounts of fertilisers, when compared with cotton. This makes industrial hemp a desirable crop in terms of sustainability [54]. It can take only 12 weeks for the hemp plant to grow up to 4 metres [28].



Figure 9 Hemp plant. A flowering male and B seed-bearing female plant, actual size; 1 male flower, enlarged detail; 2 and 3 pollen sac of same from various angles; 4 pollen grain of same; 5 female flower with cover petal; 6 female flower, cover petal removed; 7 female fruit cluster, longitudinal section; 8 fruit with cover petal; 9 same without cover petal; 10 same; 11 same in cross-section; 12 same in longitudinal section; 13 seed without hull [55]

The industrial hemp grows for 3-4 months and is harvested before flowering, which ensures that the fibre strength is the highest. Similar procedure, of harvesting before flowering, is used with flax. The fibres from the plants, which developed seeds, have lower mechanical properties and it takes longer to grow them. The planting is done during spring. After harvesting, it takes up to 4 tonnes of retted and dried hemp stems to produce 1 tonne of hemp fibre and over 2 tonnes of hemp shiv material as a by-product [56]. Similar to other high production crops, hemp requires fertilisation with nitrogen, phosphorus and potassium. Since it does not require herbicides or excessive pesticides, its life cycle analysis distinguishes it as a carbon negative raw material [27]. It does not require special treatments, provides high harvest yields, harvesting and fibre processing is mechanised. There are three centres for the industrial hemp cultivation, namely Canada, China and Europe. Figure 10 presents the industrial hemp production plot in the World. Europe was one of the biggest hemp producers. The world production of hemp began to fall in 1966, from almost 370 000 tonnes/year to reach a minimum in 1994 of 51 500 tonnes/year. When analysing world production in terms of total dedicated area, a significant 91% decrease is visible between 1966 and 2009 (Figure 11).

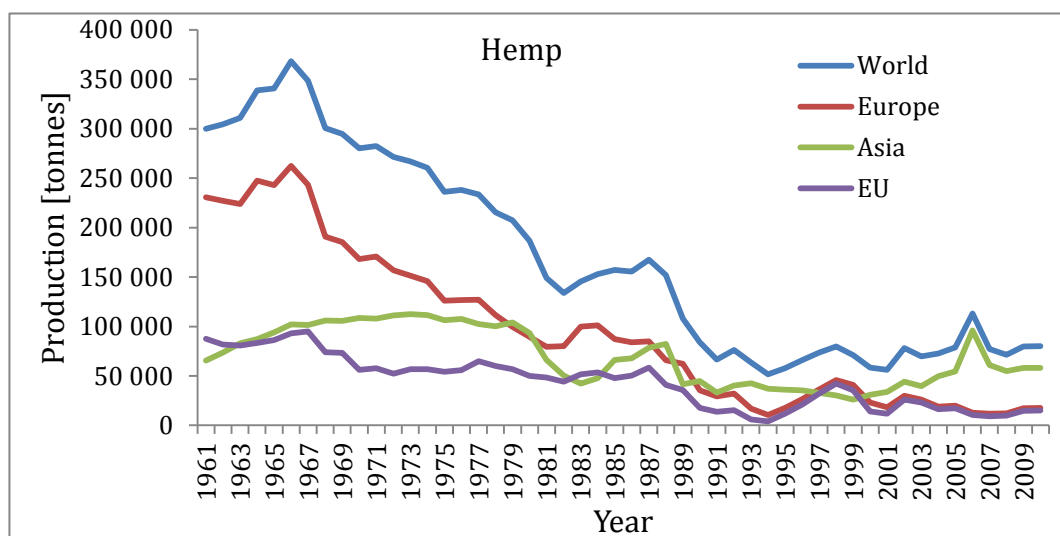


Figure 10 A comparison of hemp production in the World [48]

This decline was the outcome of the revolution in the field of synthetic fibre production and hemp regulatory laws introduced in the United States, e.g. the Marijuana Tax Act of 1937, which later influenced global industrial hemp production and trade [57]. European industrial hemp fibre is mainly used in the processing of paper and speciality paper,

technical filters, cigarette paper, NFCs, insulation material, cultivation fleeces, animal bedding and mulch. Over the last two decades the production of industrial hemp increased in Asia (Figure 10). It is possible to yield up to 25 tonnes/Ha of hemp which makes it efficient in biomass production [28].

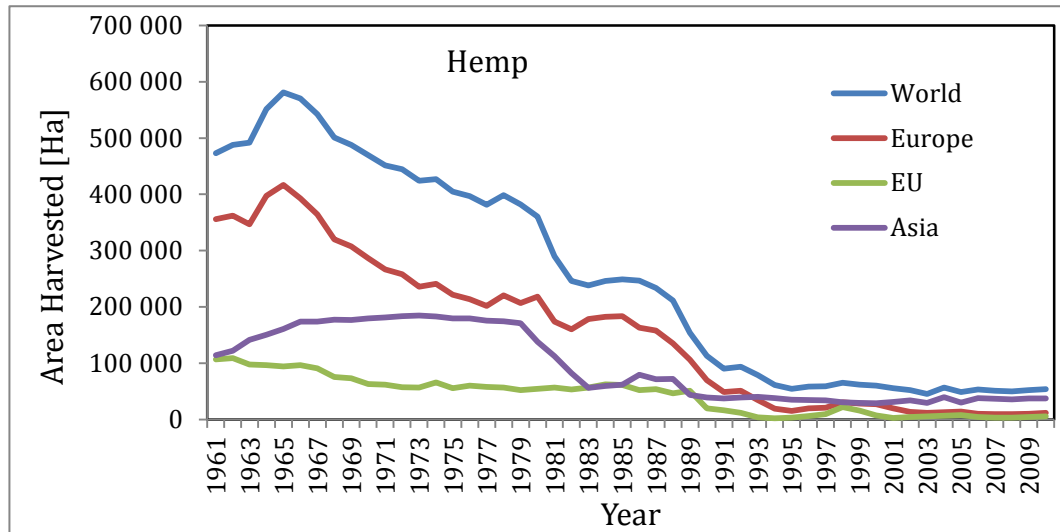


Figure 11 A comparison of area harvested in hemp production

Figure 12 presents a graph of hemp yield per hectare. The highest increase in yield happened in the early 1990s in the European Union, in which producers are some of the most efficient with pick average production yield of 5.9tonnes/Ha in 2002. The average production in the world in the past decade was at the level of 1.5tonnes/Ha, and at the same time in EU countries at the level of 3.2tonnes/Ha. The yield values increase due to improvements in processing, infrastructure development and research into optimal growth conditions. Moreover, increased yield is an outcome of factors like an easy access to farming technologies, support in obtaining specialised machines by farmers, propitious weather conditions in the temperate climate and economic drive related with land prices, which forces farmers to optimize their production.

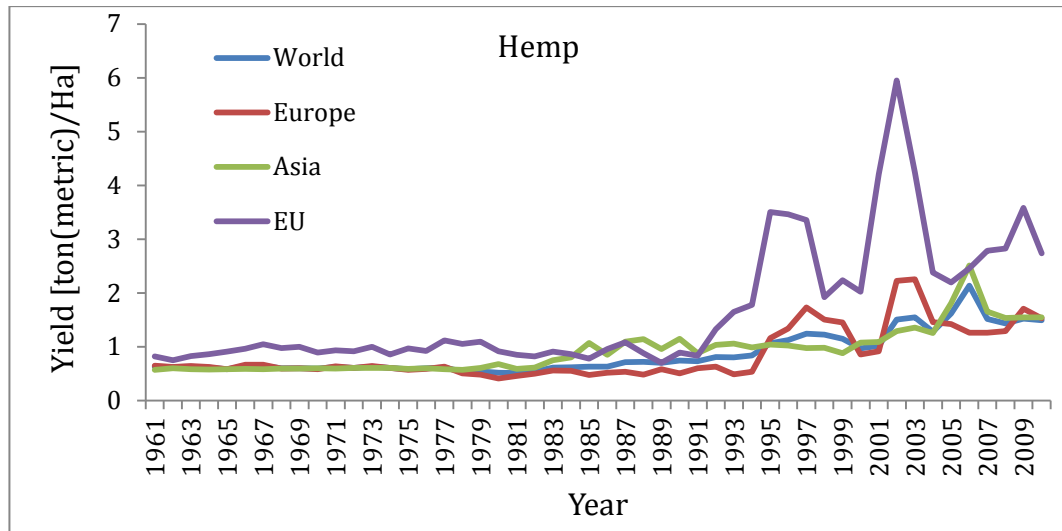


Figure 12 Comparison of hemp yield in the world [48]

2.5.2 Structure of Bast Fibre

Hemp and flax have a hierarchical structure. Plant stalk is composed of layers of fibres with different functions, e.g. providing strength, nutrient transportation, structural integrity, protection from elements and others. Figure 13A presents a longitudinal cross-section of the industrial hemp stem with distinguishable layers. Bast fibres, also called phloem fibre or skin fibre, provide structural integrity to the stem of dicotyledonous plants, and they are located close to the plant stalk surface. There are many plants, which are sources of bast fibres, including hemp, flax, ramie, nettle, linden, wisteria or mulberry [58]. Figure 13B presents a perpendicular cross-section of the industrial hemp stem with marked cell types. The bast fibres are indicated as the primary and secondary fibre cells. A tissue of the inner core and xylem has significantly lower mechanical properties, but has a porous structure allowing for water vapour permeation. This is the main reason for using this part of the plant as an insulation material in the form of shiv, i.e. Hempcrete®.

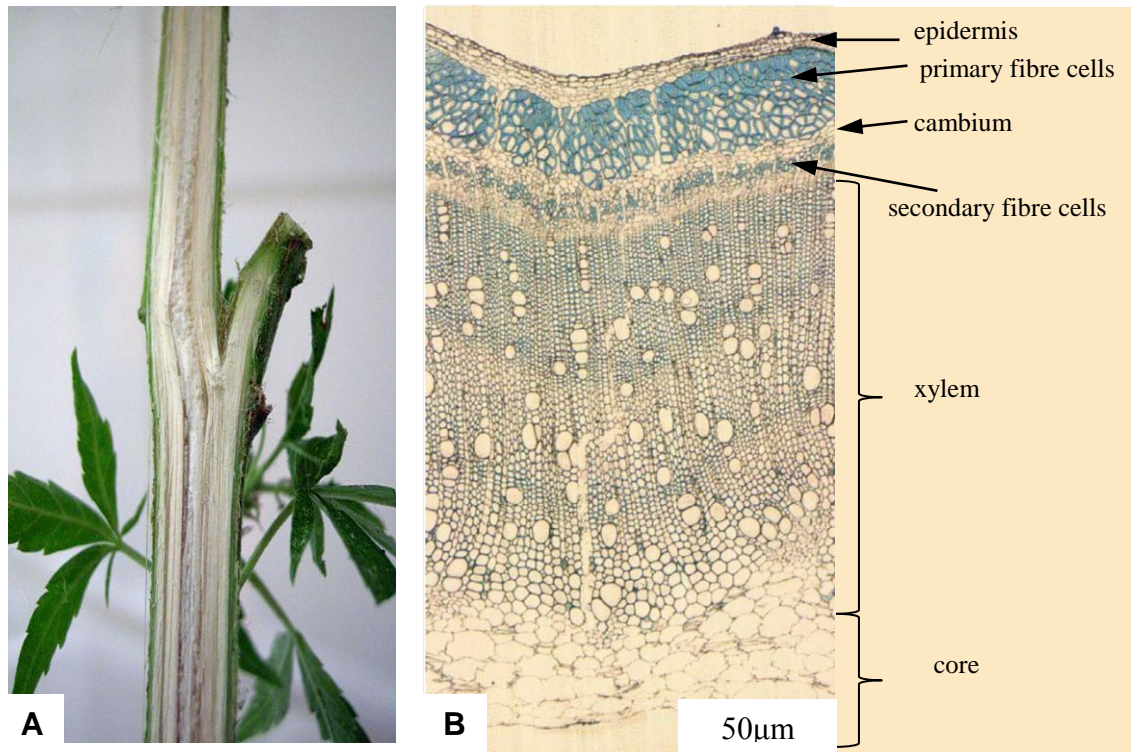


Figure 13 (A) Longitudinal cross-section of hemp stem [59] and (B) cross section of industrial hemp stem microstructure [60]

The bast fibre has a hierarchical structure. Figure 14 presents building blocks of an elementary fibre. It consists of various layers with different microfibril arrangements, namely primary wall, outer layer (S1), middle layer (S2) and inner layer (S3). Each layer has its own substructure composed of cellulose elementary fibril, hemicellulose and lignin. The layers differ in arrangement ratio between constituents. The middle lamella, composed mainly of pectin with macrofibrils, is located in the outer layer and binds the fibres together. This is followed by a thin cellulose network making up the primary wall [60]. The middle layer of the bast fibre is responsible for the plant reinforcement due to its cellulose content and arrangement. It makes up to 98% of the fibre wall. The arrangement of cellulose fibrils in the middle layer (S2) is almost longitudinal, thus is the most responsible for plant stiffness and fibre strength. The elementary cellulose fibrils of the S2 layer are bound together with hemicelluloses and amorphous lignin. The inner fibre lumen consists of proteins and pectin [16, 61].

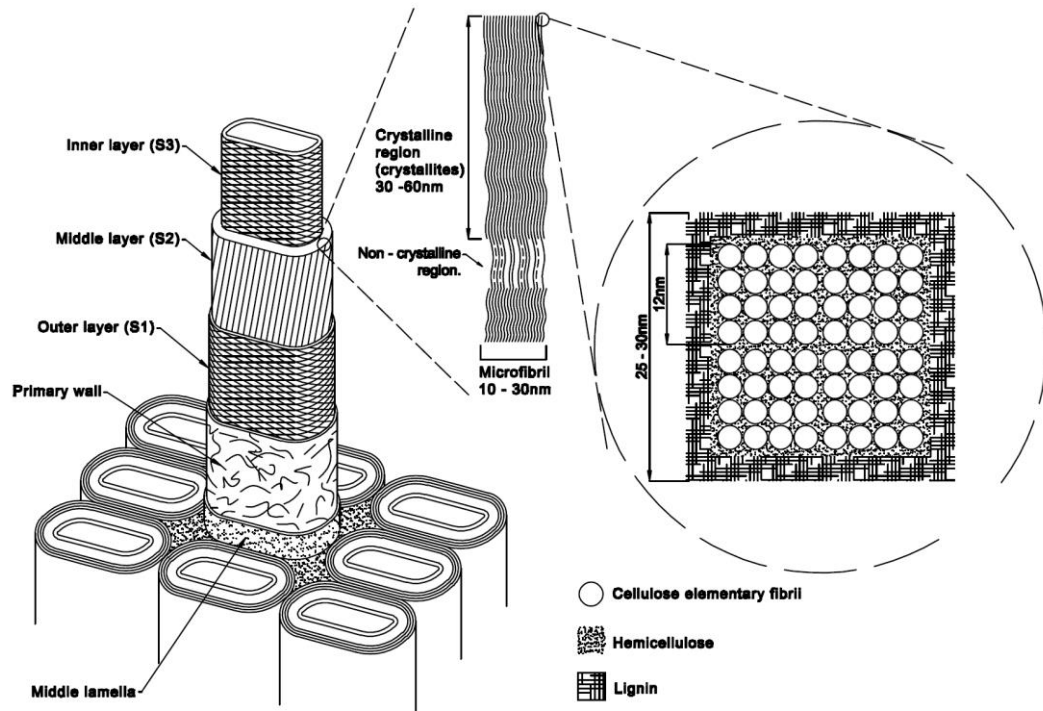


Figure 14 Bast fibre microstructure diagram [62]

2.5.3 Chemical Composition of Bast Fibre

Bast fibres, as mentioned above, are made up of similar elements as wood fibres, namely cellulose, hemicellulose, lignin and other minor elements. The ratio between constituents is not the same in each bast fibre and differs between plant species. Table 1 presents the composition of bast fibre and the microfibril angle for some fibres. All of the presented fibres except cotton have approximately 65% of cellulose content, which is the reinforcing element of the plant. The cellulose content itself is not a sole indicator of the fibre type mechanical properties since, as mentioned above, the ratio between constituents and microfibril angles contribute to the fibre strength.

Table 1 Composition of natural fibre [54, 63, 64]

	<i>Hemp</i>	<i>Flax</i>	<i>Jute</i>	<i>Sisal</i>	<i>Ramie</i>	<i>Cotton</i>
	%	%	%	%	%	%
Cellulose	67.0	62.1-64.1	64.4	65.8	68.8	82.7-92.7
Hemicellulose	16.1	16.7	12.0	12.0	13.1	5.7
Pectin	0.8	1.8	0.2	0.8	1.9	0.0
Lignin	3.3	2.0	11.8	9.9	0.6	0.0
Water soluble	2.1	3.9	1.1	1.2	5.5	1.0
Wax	0.7	1.5	0.5	0.3	0.3	0.6
Water	10	10	10	10	10	10
Microfibril angle	6.2	10.0	8.0	-	7.5	-

2.5.4 Mechanical Properties of Bast Fibres

The structure and composition of natural fibres, as mentioned above, affect their mechanical properties. It was shown that NF mechanical properties are dependent on the cellulose content, cellulose crystallinity index and microfibril angle. A natural fibre with a high cellulose content, high crystallinity index and low microfibril angle has high mechanical properties [65, 66]. Additionally, there are other factors affecting measured mechanical properties, which are related with plant structure and measurement technique. The properties of NFs vary throughout different parts of the plant. Fibres in the stem have higher mechanical properties in comparison to those of the leaf. Additionally, the position within the stem affects mechanical properties. The strongest fibres are found in the middle of the stem height and the weakest at the top. This finding led to the development of the harvesting machines which automatically alter the point at which stem is cut [67]. Moreover, the type of fibre separation from the stem has a significant influence on fibre performance [68, 69]. Table 2 summarises the tensile properties of hemp and flax single fibres. Those of other natural and conventional reinforcement fibres are also included for a comparison. The geometry of hemp fibres varies considerably, with the diameter being from 10 μ m to 67 μ m. Flax fibre diameter is reported from 10mm to 70mm. Hemp has a

wider fibre length range from 5mm to 110mm, in comparison with the flax fibre, ranging from 10mm to 70mm [70]. Short fibres can be converted into mats and used as randomly distributed reinforcement in composite production, such as compression moulding. Longer fibres are usually used in yarn spinning for textile or reinforcement purposes. The density of hemp and flax fibres is within the same range as carbon and aramid fibres and at the same time, down to half of the density of the glass reinforcement. The hemp density is similar to that of flax fibres, ranging from 1.35 g/cm³ to 1.52 g/cm³. The reported Young's modulus of flax is the highest among natural fibres, which is 100GPa and only exceeded by that of carbon fibres. The highest Young's modulus for hemp fibres is 70GPa, which is the same as that of E-glass. The difference is that E-glass stiffness is consistent and natural fibres reported stiffness starts from 5.5GPa. Both hemp and flax fibres were reported to have the highest tensile strength values above 1GPa, which is comparable with that of soft wood kraft fibres and up to three times lower than that of E-glass or aramid fibres. Strength and stiffness distributions for hemp and flax fibres differ; this might be related to the procedure with which fibres were tested, treatment of the fibres, and other aforementioned factors. The mechanical properties of natural fibres are usually measured with direct tensile test by stretching fibres or by ring test, which combines tensile and compression deformations [71, 72]. However, in many cases, bundles of technical fibres are measured instead of individual fibres, since single fibres are difficult to separate. Additionally, hemp and flax fibre bundles have a non-uniform cross-section, and accurate measurement is challenging. Therefore, a consistent way of fibre cross section measurement needs to be implemented [73]. This is usually done by testing multiple fibres and performing Weibull analysis [74, 75]. The range of presented mechanical performance data for hemp and flax is broad. There is a big difference between synthetic and natural fibres. Using it in predicting properties of a NFC part will yield a wide range of results, which is not practical. Therefore, when predicting the NFC element mechanical properties, raw materials and the processed part should be tested to predict more reliably mechanical performance. Refinement of the natural fibres is another factor, which leads to an improvement of mechanical properties. Taking wood fibres as an example, the bulk Young's modulus of wood is 10GPa. After the pulping process, single pulp fibre stiffness is 40GPa. When pulp fibres are hydrolysed and mechanically disintegrated, microfibrils are exposed which have a stiffness of 70GPa. There is no existing technology that can break

down and test microfibrils into crystallites which have a stiffness value near the level of 250GPa [76].

Table 2 Properties of selected cellulosic fibres and man-made fibres.

<i>Fibre</i>	<i>Density</i> ρ (g/cm^3)	<i>Fibre length</i> l (mm)	<i>Diameter</i> \emptyset (μm)	<i>Elong.</i> (%)	<i>Tensile</i> <i>stiffness</i> E_L (GPa)	<i>Tensile strength</i> σ_L (MPa)	<i>Ref.</i>
Hemp (<i>Cannabis sativa</i>)	1.35-1.50	5.6-110	10-67	1.6-4.2	5.5-70	690-1040	^{d f g h}
Flax (<i>Linum usitatissimum</i>)	1.38-1.52	10-70	5-38	1.5-3.2	12-100	345-1100	^{b d g e}
Wool	1.20-1.32	38-150	12-45		3.9-5.2	40-200	^a
Jute (<i>Corchorus capsularis</i>)	1.23-1.45	0.8-6.0	5-25	1.5-1.8	13.0-55.0	393-773	^{d b g}
Soft Wood Kraft	1.50				40.0	1000	^c
E-glass	2.50			2.5	70.0-72.0	2000-3500	^{d b}
Aramid	1.40			3.3-3.7	63.0-67.0	3000-3150	^c
Carbon	1.40			1.4-1.8	230-240	4000	^c

^a [77], ^b [54], ^c [63], ^d[54], ^e [78], ^f [79], ^g [80], ^h [10].

2.5.5 Production of NF Reinforcements

Reinforcement fibre can be categorised by the form. Filaments can be continuous and used directly or processed into various forms of fabrics. Discontinuous, shorter fibres can be used in the form of mats or weaved into continuous yarns. The structure and type of natural fibre reinforcement has an influence on the mechanical properties of NFCs. NFs are inherently short and in order to use them as continuous reinforcement, various forms of mats and yarns need to be prepared.

Extraction and Processing

Hemp and flax fibres are extracted from the stem by extracting other components like shiv, lignin and pectin. Fibre quality and mechanical properties depend on the retting process. This is traditional fibre separation method based on soaking hemp in water tanks, where bacteria enzymes degrade lignin and other tissues, thus freeing bast fibres [81]. During field retting procedure stalks are chopped into 30-45cm lengths, immersed and consecutively turned over in two day intervals. The procedure lasts from 14 to 21 days and its speed depends on environmental factors. Retting usually produces good quality fibre with high uniformity. The mechanical separation process called “green retting” or just decortication

has recently been used without the field retting stage. Hemp stems are driven through a series of rollers which squeeze the material separating fibres from shiv. The advantage is that there is no need for time and area consuming retting, but the decortication process induces mechanical degradation of the fibre produced [82]. Other approaches of fibre separation, aiming at improving the efficiency of the process, involve the use of bacterial enzymes or fungus [83-85], ultrasound [86], steam explosion [87], chemical retting [83, 88] or their combinations. The diagram in Figure 15 presents a natural fibre processing flow-chart with individual stages, based on the decortication process. Decortication removes non-fibrous parts of the plants by mechanical means. Hackling is done by combing the fibres, and is used to separate long fibres from short fibres and other parts of the plant. Carding produces sliver by disentanglement of the fibres between two moving surfaces. Often a combination of mechanical and chemical methods is used to create 'cottonised' short hemp fibres, which removes most of the lignin and pectin from the fibres [89, 90]. Processing of hemp and flax normally results in the loss of shives, dust and fibre about 62% - 68% of total mass. Typical hemp processing yields about 32% of the fibres, of which 23%-27% are considered as long (> 20mm). Flax processing produces about 37% of the fibres, of which 29% are long [89]. After processing, fibres can go through various treatments, namely acetylation, bleaching, grafting, mercerisation and scouring. Acetylation increases hydrophobic properties of the fibres by introduction of acetyl radical to an organic molecule. This is usually done with acetic acid [91]. To reduce lignin and pectin levels, fibres can be bleached with hydrogen peroxide, sodium hydroxide, sodium sulphite or other alkaline. The process using caustic soda is called mercerisation [92]. Grafting changes the surface property of the fibre by incorporation of monomers or oligomers [93]. Scouring removes proteins, waxes, fats, oils and impurities with treatment in aqueous or other solvents [94]. Treatments are used in the textile industry in order to create a fibre with desired properties. Moreover, they can increase wettability of the fibre and improved interface between the matrix and the reinforcement for composite production [95].

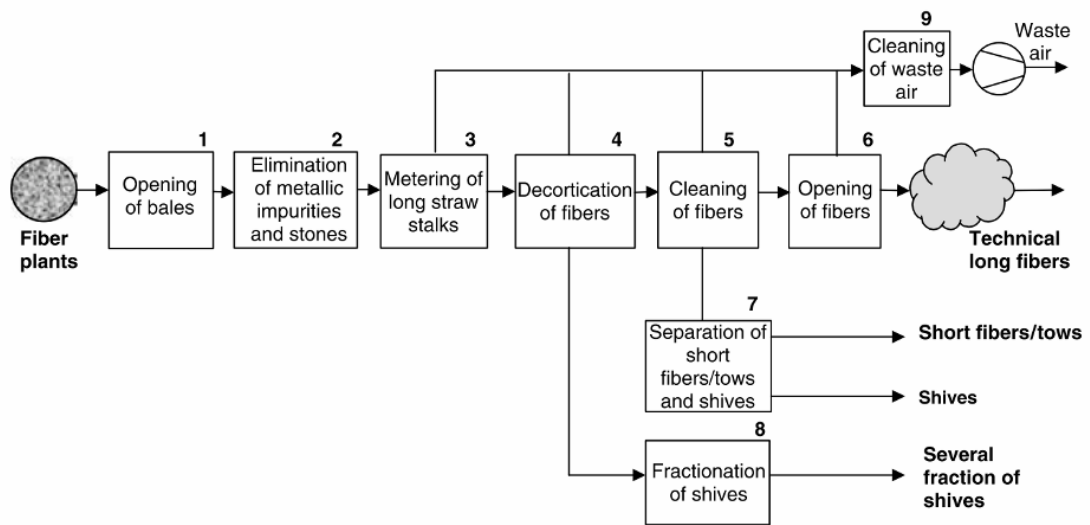


Figure 15 A natural fibre processing flow-chart [89]

Mats

The term mat is referred to a non-woven material, which is made from fibres by chemical, thermal, mechanical or other processes, but is not involved in knitting or weaving of the fibres. Examples of non-woven materials include felts, insulation mats, packaging materials, reinforcement fibre mats. Natural fibre reinforcement mats can be produced to specified forms and dimensions. The mat is defined by an average fibre length and level of processing. Mats are prepared with a whole range of fibre lengths. Short fibres are usually not incorporated into composite reinforcement mats, but can be used to produce mats for other applications, with the use of binders or technique like hydro-entanglement. Processes involving combing or water jets can create the preferred direction of the majority of fibre lengths [96]. The processing of mats usually includes chopping the fibres and separating them into specific lengths. Then, fibres with the selected lengths are used to create mats with various properties. This is done by flat or a continuous process with forming machines (Figure 16A). Most of the mats have randomly oriented fibres, which are mainly within the x-y plane of the mat. Fibres are spread over the moving belt and pressed on the continuous forming belt. The processes involve the use of mechanical force, chemical pre-treatments, heat or binders to create fibre-fibre bonds. In order to increase the mechanical interlocking between fibres, the hydro entanglement process can be used (Figure 17). It is a

continuous process which uses high pressure water jets to induce interlocking of the fibres. A web of fibres is entering the jet area and the water passes through it. The outcome is a thinner layer of non-woven mat with increased mechanical properties. Similarly to the pressed mats, hydro entangled mats can be used for composite laminate impregnation, since they do not include binders [97, 98].

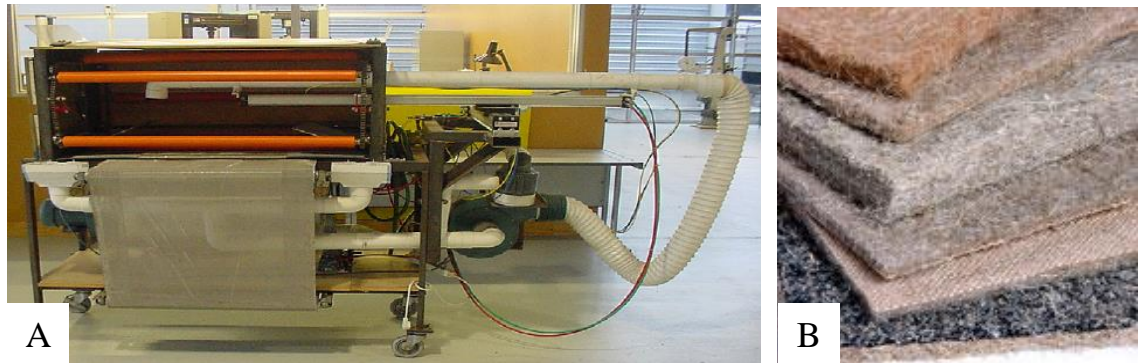


Figure 16 (A) Dry mat forming machine [96], (B) Various types of short natural fibre mats [99]

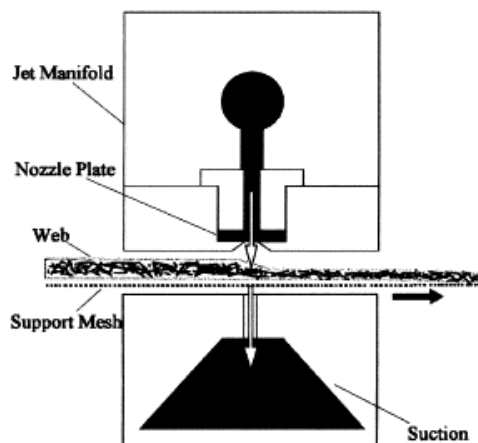


Figure 17 Principal components of the hydro entanglement system [97]

Yarns

A yarn is composed of short or long fibres, which are held together by means of mechanical interlocking [100]. Main uses of yarns include fabric processing, weaving and rope processing. Natural fibre yarns can be used as composite reinforcement. Using the yarn, instead of the mat to reinforce the composites, allows a better control fibre orientation, an increase in fibre loading, and continuous production process [101]. There

are two types of natural fibre yarns which can be used as composite reinforcement, namely twisted fibres and non-twisted fibres. Figure 18 presents diagrams of the two types of yarn.

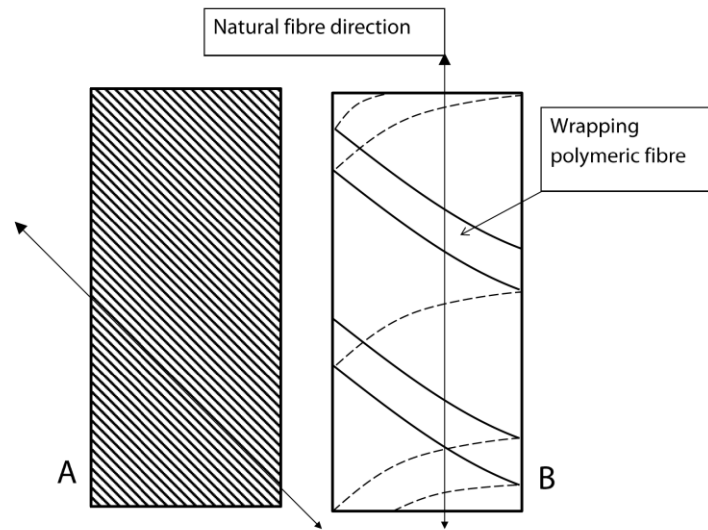


Figure 18 Diagrams comparing ring spun yarns with the twisted fibres: (A) and wrapped yarns without twist and fibres aligned in the main yarn direction (B)

Twisted yarn fibres are held together by shear forces created by fibre twisting, such as those in conventional textile yarn or rope. The fibres are aligned at an angle to the main direction of the yarn. This type of yarn is produced in the spinning process (Figure 19), and is mainly used in the textile industry [100]. The bales of technical fibres are opened mechanically or manually and transferred to a picker, which loosens and cleans the fibres. The fibres are then aligned and passed through a funnel to generate the parallel strand of fibres called sliver. Then, sets of rollers elongate and slightly twist the sliver, which is then transferred to a container. Spinning of hemp fibres differs from the spinning processes of other fibres, due to the mechanical properties of hemp. Spinning machines which are used to process cotton yarns can be used for the processing of short fibre hemp yarn, when hems go through the “cottonising” process [102]. Slivers are spun into yarns composed of one or multiple twisted slivers. The ring spinning element diagram is presented in Figure 19. Yarns can be produced continuously in S or Z arrangements, which correspond to two opposite twist directions.

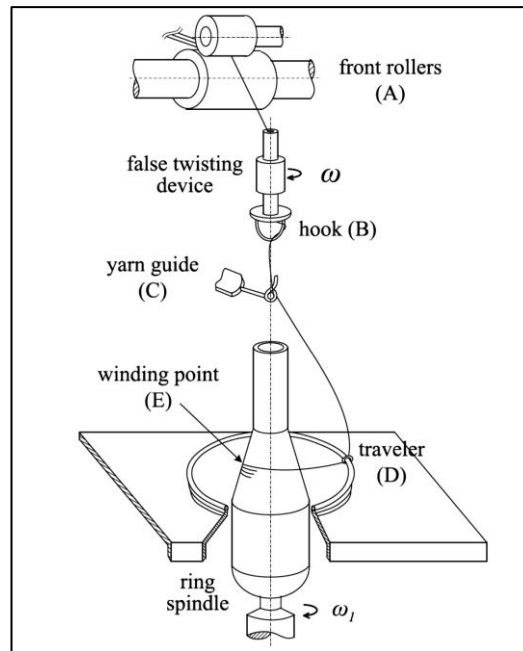


Figure 19 The ring spinning element for processing yarns with twisted fibres [102]

Non-twisted yarns (Figure 18B) were designed as composite reinforcement. The fibres are without twist and aligned in the main direction of the yarn. They are held together with friction forces created with the polymeric wrapping wire, which is made out of a continuous synthetic polymer fibre. The first stage of processing of this type of yarn is the same as processing of the twisted yarn. After the creation of the sliver, fibres are not twisted. The sliver is divided into multiple strands of slivers with the required linear density. The slivers are then wrapped with a polymeric filament, which gives rise to a pressure on the fibres creating friction forces and hold fibres together. This type of yarn has no application in the textile industry, due to its dry tenacity and low load bearing capacities. It is possible to produce yarns with various linear densities from 200Tex to over 2000Tex. Lower values of the linear densities (Tex) are usually not practical, since the ratio of artificial yarn and natural fibres becomes too high. Higher Tex values are more practical, but the compaction of the fibres in the high linear density yarn may obstruct the impregnation with resin [100].

Fabrics

Yarns may be further processed to form fabrics after spinning or wrapping, followed by weaving. There are various types of fabrics which vary in the type of wave, as well as the reinforcement direction (Figure 20). Fabrics can have yarns aligned in two, three and even four directions. 2D preforms normally include weaved, braided knitted fabrics, and 3D preforms include weaved, braided, stitched and knitted fabrics [103]. The most commonly used fabrics for composite reinforcement are the ones with two dimensional biaxial patterns [104]. Fabrics with plane and twill arrangements are some of the examples, and this fabric type with natural yarns is actually used in this research programme.

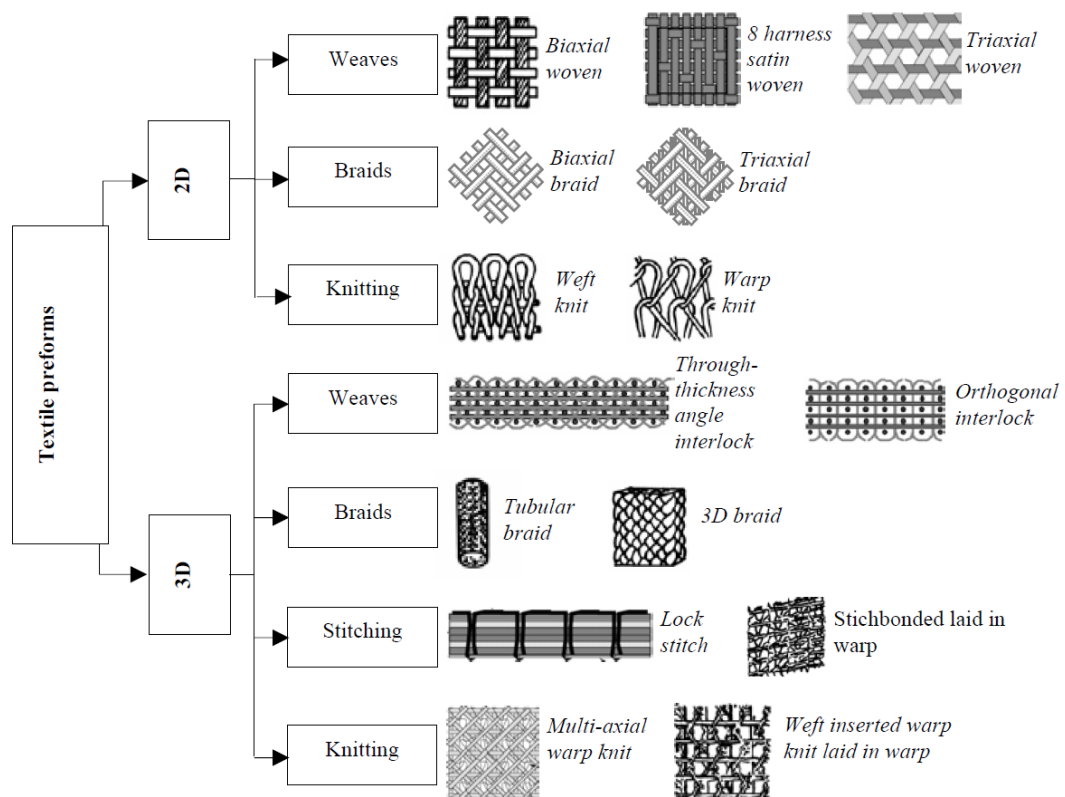


Figure 20 Composite fabric reinforcements and preforms [103, 105]

2.6 Resin Systems for NFCs

2.6.1 Synthetic Resin Systems

The prediction regarding decreasing fossil fuel resources is one of the driving forces for investigation into alternative renewable material and energy sources. At the moment, composites are mainly processed out of petroleum based resins, which are widely available on the market. Most bio-based matrices available on the market have relatively low mechanical properties and a high price; therefore, they are used mainly in the packaging industry [4]. With recent developments in thermoset biopolymers, such as phenolics, epoxy, polyester and polyurethane resins, their use as a composite matrix is possible [106, 107]. Thermoset biopolymers reinforced with natural fibres are a fully bio-sourced composite. Studies on NFC with bio-sourced matrix are being conducted [108-110].

NFCs based on bast fibres mainly use thermoset and thermoplastic polymeric matrices, which are classified by the curing mechanism. The curing mechanism influences the use of the processing techniques and is related to the mechanical performance of the cured composites. Thermoset matrix type is of interest in this thesis. Thermoset resins mainly include phenolics, polyesters, melamines, silicones, epoxies and polyurethanes. During the curing process, the resin undergoes cross-linking reactions until almost all of the molecules are cross linked to form three dimensional networks. After setting, thermoset resins cannot be melted again but the shape cannot be changed. The thermoset resins are usually supplied in partially polymerised or monomer–polymer mixtures. The cross-linking reaction can be started by the application of heat, oxidisers or UV radiation. The most frequently used thermosetting resins in composite processing are: epoxy [111-114] and polyester [115-118]. Some of thermoset resins can also be cured at room temperature, which makes it popular. Figure 21 presents a diagram of thermoset matrix laminate production. Appropriate mould, reinforcement and reinforcement lay-up sequence and the exact volumes of the matrix are prepared. Depending on the impregnation techniques selected, the following process may be different. For example, for the lay-up processing, the reinforcement layers are firstly placed one after another and impregnated with resin by using brushes or rollers. Resin mix is prepared by mixing resin with the catalyst, which

starts an exothermic curing reaction. Additionally, other substances may also be added such as accelerators, fillers, pigments and solvents. The required pressure and heat can then be applied to create the desired shape and accelerate the curing reaction. Pressure can be applied by mechanical means (hot-press), atmospheric pressure (vacuum bagging technique) or elevated pressure (autoclave). Heat can be applied to the mould by conduction or by use of microwaves.

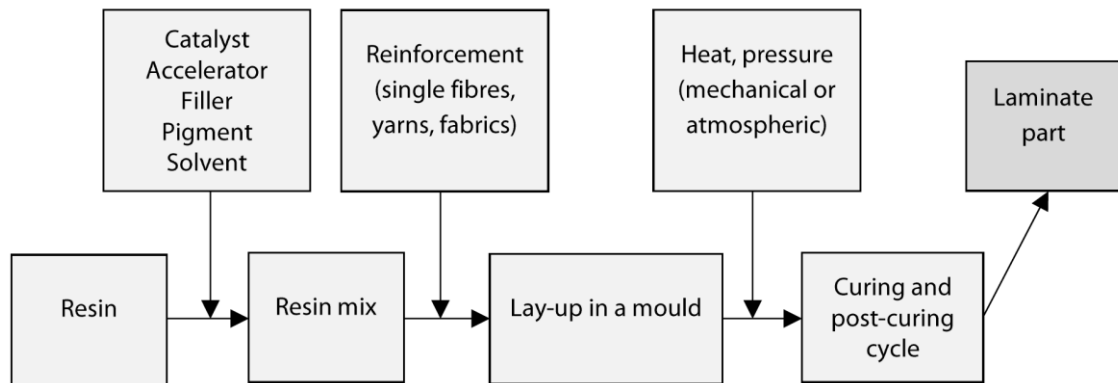


Figure 21 Composite laminate processing steps with thermoset resin systems

The degree of wetting during the production process is important for good adhesion between the fibre and the matrix. Low viscosity facilitates better wetting and penetration of the resin into the reinforcement during the impregnation process. Figure 22 presents the schematics of unsaturated polyester cross-linking reaction. Unsaturated polymers may have several carbon-carbon double bond sites. Reaction may start by a peroxide catalyst in the presence of a styrene. Peroxide initiates the reaction by combining with the carbon-carbon double bond, which forms a free-radical. The free radical is very reactive, and can create bridges between two polyester chains by reacting with styrene. When the bridge is formed, the free radical is created on the other polyester chain. Reaction continues as long as there are free radicals, styrene and unsaturation sites present. The chain reaction may stop when the free radical reacts with something else rather than styrene, such as oxygen, contaminants or peroxide molecules. Therefore, the reaction may stop prematurely, in which case an insufficient number of crosslinks will be created. It is an exothermic reaction and as such the released heat may accelerate the process, but at the same time may lead to material overheating [119].

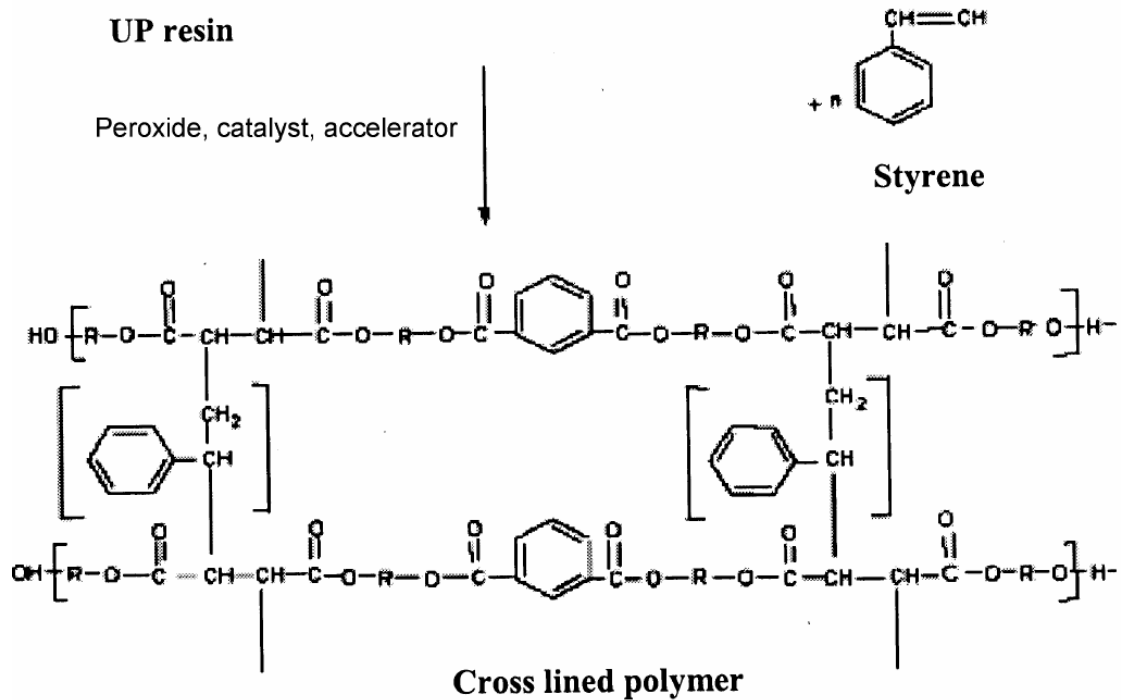


Figure 22 Schematic representation of unsaturated polyester curing process [119]

Additives affect the cross linking process. Additives, which can slow down the reaction, may include inhibitors absorbing free radicals, styrene, fillers, oxygen, flame retardants, and reinforcement. Additives, which can accelerate the process, may include initiator content, external heat, UV radiation, accelerators content, waxes and films preventing the access of oxygen. An increase in the thickness of the format composites indirectly accelerates the process by reducing heat dissipation. Factors like resin grade and type, water, pigments and contaminants, can affect the cross linking process speed in either way [120, 121]. The advantages of using a thermoset matrix system include the availability of lamination techniques, possibility of room curing or low curing temperature, relatively low cost, superior mechanical properties in comparison with thermoplastic matrices and higher temperature stability in comparison with thermoplastic matrices. However, the volatile organic compounds (VOCs) emissions, difficult recycling or reclaiming procedures, short pot and shelf life may become challenging parameters in some cases. Moreover, it is more difficult to achieve a good surface finish, compared to thermoplastics [122]. Table 3 presents a comparison of physical and mechanical properties between three of the most popular thermoset resins used in the lamination of composites, namely polyester, epoxy and vinylester. The highest stiffness and strength are achieved for the epoxy resin

composites, with up to 6GPa and 100MPa, respectively. Most of the thermoset resins are inherently brittle, but modifications are possible to elevate elongation at break. The polyester resin has the highest cure shrinkage with up to 8% [123, 124].

Table 3 Comparative properties of the three main synthetic thermoset resins [123, 124]

<i>Properties</i>	<i>Polyester Resin</i>	<i>Vinylester Resin</i>	<i>Epoxy Resin</i>
Density (g/cm ³)	1.1-1.5	1.1-1.4	1.2-1.4
Young's modulus (GPa)	2-4.5	3-6	3.1-3.8
Tensile strength (MPa)	40-90	35-100	69-83
Compressive strength (MPa)	90-250	100-200	-
Barcol hardness	20-60	35-40	
Tensile elongation to break (%)	2-6	1-6	4-7
Cure shrinkage (%)	4-8	1-2	-
Water absorption 24h at 20°C	0.1-0.3	0.1-0.4	-
Fracture energy (kJ/m ²)	-	-	2.5

2.6.2 Bio-Based Resin Systems

Bio-based polymers or bio-based plastics are a group of materials derived from bio resources, as opposed to fossil fuel based polymers. Source materials for bio-based plastics production can come from food industrial waste [125]. Bio-based plastics can be biodegradable under weathering conditions and degraded by microorganisms [126]. Bio-based origin may not be equivalent with biodegradability. Therefore, NFC fibre reinforcement is intrinsically biodegradable, but the bio-based resin may not be [107]. Bioplastics can be synthesised by microorganisms and have increased biocompatibility [127, 128]. Existing biobased polymer systems have relatively poor mechanical properties, such as polylactic acid (PLA), polyhydroxyaldehyde (PHA), polyhydroxybutyrate (PHB), polyester TP, furan resin and wood based epoxy resins [4]. The main applications of bio-

based polymers are in the packaging industry and insulation, which are mainly thermoplastic polymers. Figure 23 presents biomass sources such as grains and legumes for the production of bio-polymers, together with their main applications.

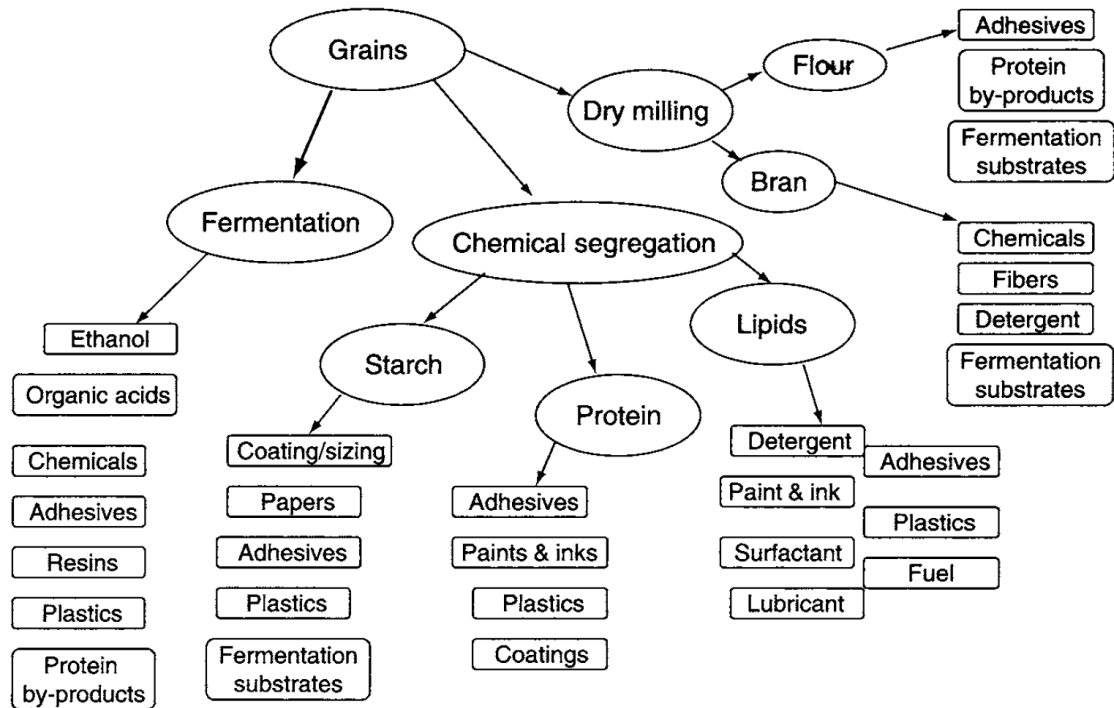


Figure 23 Applications of grains and legumes refinery products [4]

The development of new thermoset biopolymers with enhanced mechanical properties such as phenolics, epoxy, polyester and polyurethane resins, makes other applications possible [106]. Thermoset biopolymers can be reinforced with natural fibres to create a fully bio-resourced composite [129]. Plant based polymers including proteins [126], oils, carbohydrates, starch [130] and cellulose, have all been attempted. In order to improve mechanical properties, partially bio-based resin systems were developed. They combine two or more resin systems where at least one is bio-based, such as triglyceride acrylate (Cogins, Tribest S531), epoxidised pine oil waste (Amroy, EPOBIOX™), unsaturated polyester resins from renewable and recycled resources (DSM Palapreg® ECO P55-01, Ashland Envirez®), soy oil unsaturated polyester (Reichhold, POLYLITE 31325-00) [131]. Processing techniques used for biopolymers are usually similar to those for synthetic polymers. It is worth to note that DSM Palapreg® ECO resin is used in this research to process hemp and flax reinforced laminates, more details are given in the experimental

chapter. A recent increase in global fossil fuel prices led to an increased interest in bio-sources of polymers. Nevertheless, the cost of bio-based resin systems is still relatively high. In some cultivation areas production of plant oils for industrial applications can compete with food production. Cultivation area shortages, together with increasing global population, led to increased research in sea plant and microorganism sources for bio-polymers [132, 133].

2.7 NFC in Building Applications

The main goal of this investigation, as stated in the rationale and hypothesis, is the development and assessment of NFC for use in building applications and construction. Discussion of applications is important in order to show the potential of this group of materials. All elements bear loads, including stresses induced by the element own mass and external forces. Therefore, what classifies the element as 'load bearing' in building construction applications? In general, the element needs to be capable of carrying a significant imposed load. Standards provide the minimum property requirements for materials in defined conditions. For instance, according to the Association for Specialist Fire Protection (ASFP), the 'load bearing concrete wall' is "an element that is intended for use in supporting an external (applied) load in a building and maintaining this support in the event of a fire". At the moment, there are no specific guidelines on NFCs. Capabilities of NFCs as load bearing elements for building applications are discussed by comparison with requirements for competitive materials. Hemp and flax NFCs used for building elements can be divided into four types depending on their compositions, namely, long fibre structural biocomposites, inorganic shiv composites, organic shiv composites and non-structural insulation materials. Shiv is a woody inner-part of a plant stem core. It is a by-product during the fibre extraction process and for every kilogram of fibres, 1.7kg of shiv is produced [134]. Mechanical properties of shiv are low, but their use is justified by hydrothermal characteristics of high water absorption and thermal insulation. Uses of hemp shiv include: animal and other bedding (mainly for horses and chickens), which accounts for 62% of all applications, inorganic shiv composite insulation (e.g. Hemcrete®), which accounts for 15% of all applications and the rest accounts for other applications

including particleboard processing and energy production through incineration [134]. Building materials based on shiv were divided into two groups, namely inorganic shiv composites (e.g. shiv-lime mortar) and organic shiv composites (e.g. polymer matrix shiv based particleboard). Those groups differ in matrix type and applications. Inorganic matrices mainly include hydraulic lime (calcium oxide, calcium hydroxide), hydraulic cements and mixes thereof. The focus of this research is on the use of long fibre structural biocomposites for building constructions. As of today, such applications are not commercially available and in the experimental phase. Most existing research has been focused mainly on non-load bearing applications. Examples are various types of panels produced from NFC, such as roof panels or cladding (Figure 24A). Hybrid composition panels with sisal and glass fibres can also be processed by compression moulding with epoxy resin, however, the tensile properties of these panels, with 57MPa and 2.6GPa being reported for the strength and modulus respectively, are relatively low [135]. Various sandwich structures have been proposed to compensate the insufficiencies of NFCs for structural applications, for example, Dweib et al. [136] presented an idea for NFC sandwich roof construction (Figure 24B). It is supposed to be light and low cost solution for the roofing in the hurricane affected areas. The whole roof can be processed with resin transfer moulding technique. The recycled paper sheets, layered with chicken feathers, corrugated paper or glass fibre were used as reinforcements. The reported flexural rigidity and flexural strength were 12-20GPa and 24-26GPa respectively, which are similar to the flexural stiffness and two time the flexural strength of wood beams. Experimental door elements can be made of NFC sandwich panels, e.g. hybrid NFC with GFRP (Figure 25). A composite can be reinforced with short NF mats or fabrics and surface can be covered with glass fibre composite layer. A C-shape frame of the door is filled with foam. Such experimental frames passed minimum requirements in accordance with Indian standards [4].

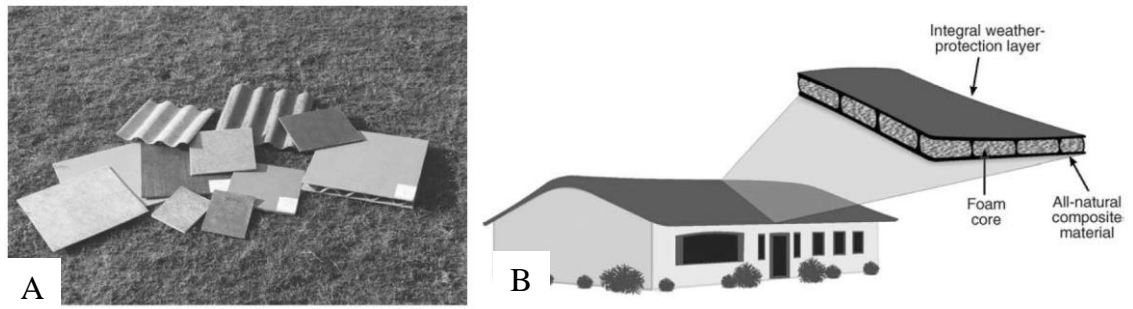


Figure 24 (A) Various types of NFC panels [4] (B) Monolithic house roof made of NFC [136]

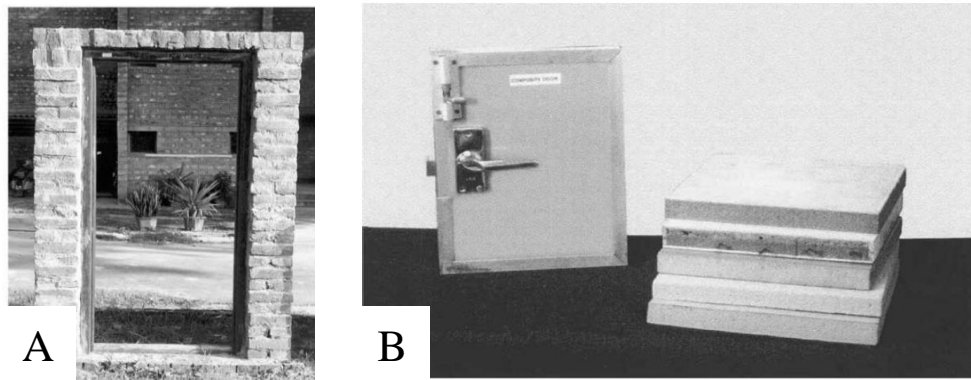


Figure 25 (A) Door elements made out of NFC (B) Exhibition door frame made out of NFC [4]

3 Experimental Procedures and Methodology

This section describes materials and methods, i.e. selection of materials, development of BFRP manufacturing procedures, sampling and testing. The theoretical material selection and preliminary experiments with natural fibres, like jute, sisal, hemp, flax and wool, lead to further works with hemp, flax and hemp-wool reinforcements. Fibres were selected based on their mechanical properties and market significance. As the matrix material both bio-derived and petroleum-derived polyesters were used. Section 3.1 provides information about materials selection used before NFC processing. It includes detailed information about of NF reinforcement types and matrix materials. Section 3.2 describes processing procedures. It provides description of feasibility studies and details of techniques used to process laminates and tubes. Section 3.3 describes testing techniques used for in experimental studies. Section 3.4 includes sampling procedures and describes samples, which were used in the experimental studies.

3.1 Material Selection

3.1.1 NF Reinforcement Selection

There are factors related with a composite reinforcement, which can be analysed during an assessment of a new composite. Those factors include type, shape, orientation, volume fraction, mechanical performance, thermal and electrical conductivity, interface properties and others. 14 different types of natural fibre reinforcements were selected for the production of natural fibre composites (NFRP) in order to gain a better understanding of the mechanisms of their reinforcing roles. The group was comprised of seven hemp fibres, five flax fibres and two hemp-wool fibres hybrid reinforcements. Moreover, the

reinforcements can be divided into three types, namely mats, yarns and fabrics. Mats are assemblies of loose, randomly oriented fibres, which are compressed together in order to gain cohesion by mechanical interlocking. Yarns are composed of aligned fibre slivers and are kept together by friction induced either by twist or by wrapping with additional yarn. Fabrics are composed of intertwined yarns in the ‘Hopsack’ or ‘Twill’ arrangements. The main restricting factor for material selection is availability since there are only few processors which supply NF reinforcement material. For instance, one of the types of hemp fibres had to be supplied from China, due to the lack of European processors able to produce the required types of hemp yarns. In following sections, the hemp and flax reinforcements used are presented. They are divided into three groups depending on the morphology of the reinforcement, namely mats, fabrics and single yarns.

Mats and Fabrics - Hemp Mat

Industrial hemp mat with randomly oriented fibres was used. The hemp variety of fibres is prepared by the field retting technique which allows separation of the cellulose fibres from the plant stem. After retting, fibres are separated from other constituents, graded, and pressed to process mat. Supplied hemp mat has 780g/m² area density. It is supplied on a roll with 1000mm width and approximately 5mm uncompressed thickness. Figure 26 presents a hemp mat roll and a close-up image of the mat. Fibres are oriented in multiple directions, have varying fibre lengths and shapes. The mat has a light-brown colour. In order to process samples, this material is cut with a steel guillotine. Supplied mat has between 7% - 10% moisture content in standard conditions. Fibres in this mat are held together by mechanical interlocking and there is no bonding additive included during processing. Therefore, single fibres can be pulled apart manually and separated from the mat. This mat is usually compacted down to 25% of its thickness.



Figure 26 (A) Hemp mat roll (B) Hemp mat fibres and fibre bundles

Mats and Fabrics - Hemp-Wool Mat

Hemp-wool mats were also studied and kindly supplied by the Innovation and Research Institute at the University of Leeds. Hemp fibres are processed from Green Hemp and Dry Hemp varieties by field retting and consecutive mechanical separation of fibres. Wool fibres in the mat are clipped and washed with a mixture of water and detergent under pressure. This type of mat is processed with hydro-entanglement process. The hemp and wool fibres are mixed together in desired ratio and spread over a conveyor belt which transports them under water jets. Pressure from small nozzles is used to interlock the fibres together, compact and process a uniform mat. The supplied mats have 80% of hemp and 20% of wool fibres. There were two types of mats supplied, with area densities of 210 g/cm³ and 280 g/cm³ with 0.5mm and 0.7mm thicknesses, respectively. The supplied roll is 500 mm wide. Figure 27A presents wool-hemp paper mat stripes and a close up of the mat surface impregnated with polyester resin. The colour of the mat is white with visible light brown fibres on the surface and a distinctive parallel line pattern in the form of water jet nozzles. Additionally, wool dark fibres are visible on the surface (Figure 27B). The hemp-wool mat is compact and due to the fibre entanglement, single fibres cannot be easily separated as in the hemp mat.

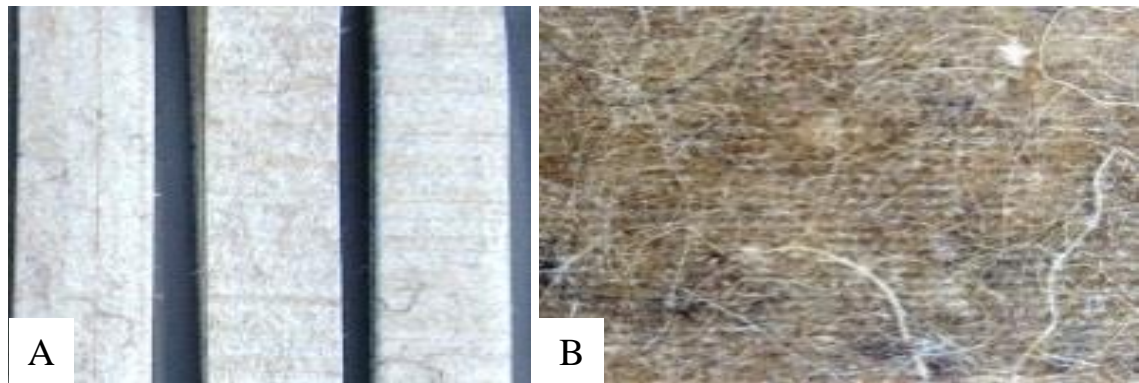


Figure 27 (A) Hemp-wool mat stripes (visible surface parallel lines are created by water jet nozzles during processing) (B) Impregnated hemp-wool mat in polyester resin with black and white wool fibres and light brown hemp fibres

Mats and Fabrics - Flax Biaxial Fabrics

Two types of fabrics, namely hopsack 4x4 and twill 2x2, were supplied by Biotex. Biaxial fabrics have the reinforcement aligned in two directions. Fabrics are composed of the same 250Tex flax yarns, which are processed without twist. Tex is a measure of yarn linear density. Further description of this type of yarn can be found in section 0. Yarns are interwoven to compose fabric with two distinctive patterns. The hopsack 4x4 fabric is composed of bundles of four yarns interweaved in a plane pattern, and has an area density of 510g/m² (Figure 28A). The twill 2x2 fabric type is processed by interweaving single yarns, and has areal density of 420 g/m² (Figure 28B). Both fabrics have two distinctive weaving patterns; therefore, they differ in the waviness of individual yarns. Both fabrics have light-brown colour. Yarns in both fabrics are not strongly compacted, this allows for easy single yarn pull-out. Both fabrics can be cut to the desired length with a steel guillotine. These fabrics were selected because both have popular weaving patterns used in glass fibre reinforcements.

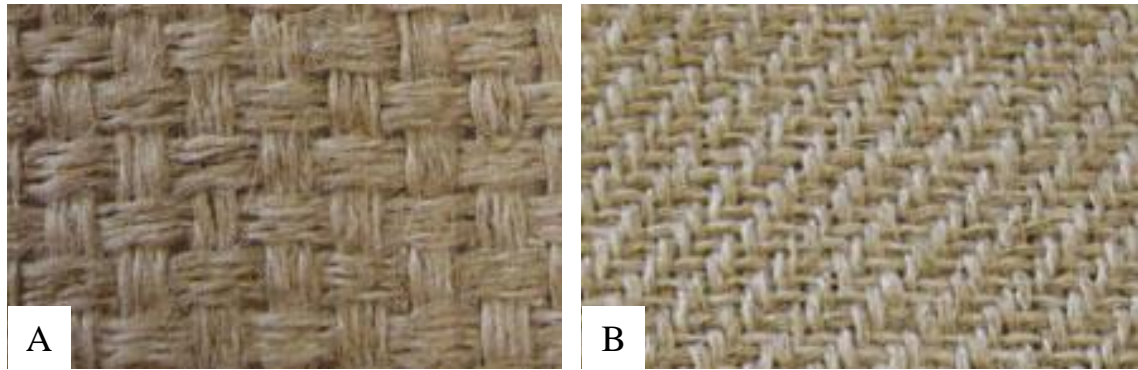


Figure 28 (A) Hopsack 4x4 flax biaxial fabric with a distinctive plane wave arrangement of yarns (B) Twill 2x2 flax biaxial fabric with distinctive twill surface diagonal pattern

Mats and Fabrics - Flax Unidirectional

Two flax unidirectional rowing types were used. The first fabric is processed with 240Tex yarns and is interwoven with a straight transverse pattern, which is compact. Single yarns can be separated from the fabric without inflicting damage. The second flax fabric is processed with 590Tex yarns and is interwoven with a criss-cross pattern. Both yarns hold fibres together with a twist. A polyester interweaving yarn is used as fill yarn, which holds NF yarns in place. Figure 29A presents a 240Tex yarn fabric, and a 590Tex fabric is depicted in Figure 29B. They have different colours, with the 590Tex fabric being light brown and the 240Tex being dark brown. This type of unidirectional fabric allows for easy processing of a NFC laminate by the lay-up technique, compression moulding or vacuum bagging. Desired quantities of fibres can be easily selected. Moreover, this type of fabric allows for processing of laminates with a high volume fraction of the reinforcement oriented in one direction. Since distances between parallel yarns are fixed, fabrics can be aligned and arranged in hexagonal packing arrangement, thus increasing volume fraction of the reinforcement.

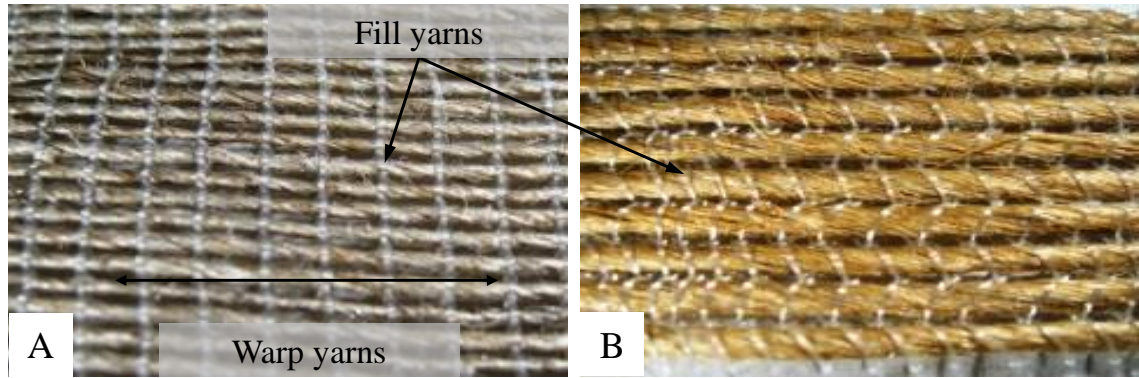


Figure 29 (A) Flax unidirectional rowing made out of aligned 240Tex twisted fibre yarns (B) Flax unidirectional rowing made out of 590Tex twisted fibre yarns

Mats and Fabrics - Glass Fibre Fabric

Two grades of a woven E-glass roving are used. Figure 30 presents two types of E-glass fabrics used. Both fabrics have plane wave patterns as aforementioned flax fabrics. Glass fibre can be produced in any length; therefore single fibres in yarns are continuous and parallel. Two types of glass reinforcement fabrics are used, namely with 380 g/m^2 and 80 g/m^2 areal densities. Material is supplied on 1m wide rolls. Both fabrics are selected to process composite laminates used as reference material.

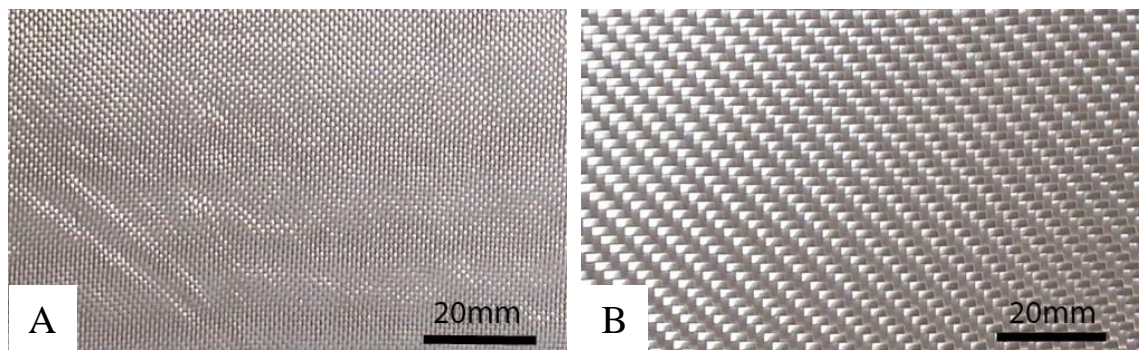


Figure 30 (A) 80 g/m^2 plane wave E-glass fabric (B) 380 g/m^2 plane wave E-glass fabric

Yarns – Hemp Yarn with a Twist

Six grades, namely 25Tex, 39Tex, 51Tex, 60Tex, 86Tex and 130Tex of hemp twisted yarns were supplied by Cyarn Ltd. Yarns differ in linear density. Hemp fibres used to process the yarns were water retted, bleached and ring spun to create yarns. Processing follows a

standard textile yarn spinning procedure. In this type of yarns, single short fibres are held together with a twist. Yarns have light brown colour and were supplied on spools (Figure 31). Six yarn grades were selected in order to produce a wide range of laminates, and to investigate if there is a correlation between yarn linear density and mechanical properties of the prepared composite.

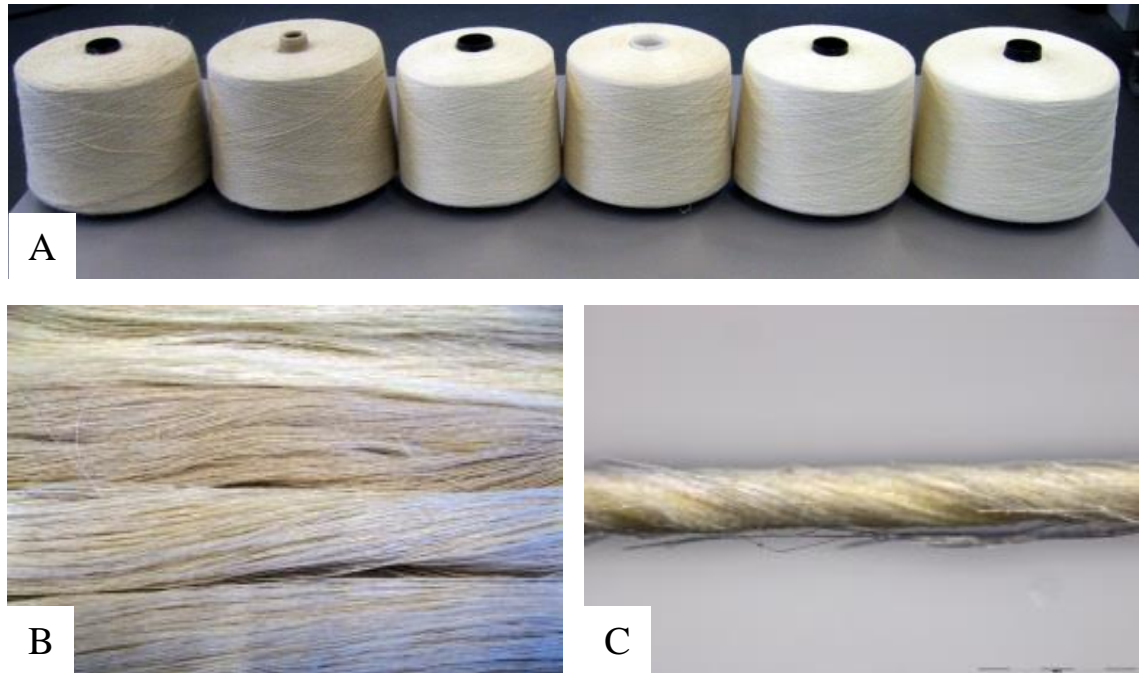


Figure 31 (A) Six grades of hemp yarns on spools, (B) Bundles of hemp yarns (C) A single yarn with distinguishable surface fibre pattern

Yarns - Non-Twisted Hemp-Wool Yarns

Samples of hemp-wool, non-twisted 1000Tex yarns were kindly supplied by the NatCom project. This hybrid yarn has significantly higher linear density in comparison with aforementioned hemp yarns. It is composed of 80% of hemp fibres and 20% of wool fibres, if a polyester wrapping yarn is not included. Figure 32A presents a hemp wool yarn with a distinguishable black wrapping yarn. Figure 32B presents a layer of aligned hybrid yarns in preparation to impregnation. Fibres within the yarn are parallel and are held together with wrapping polymeric wire. Yarns with twisted and non-twisted fibres are selected in order to investigate the architecture influence on mechanical properties of the laminate. The hemp included in the yarn was mechanically decorticated, by passing hemp

stalks through a series of gearwheels. This procedure crumbles up a shiv material from the plant and releases the fibres. The wool used for the processing of the yarn is clipped and washed under pressure with a mixture of water and detergent. In the next step hemp and wool fibres are mixed together, and aligned by brushing them on the rotating drum. The yarn with no twist is processed by separating narrow slivers of aligned fibres and subsequent wrapping with continuous synthetic fibre. Hemp-wool yarn is the second hybrid material used in this investigation. Inclusion of wool fibres into the NFC laminate can enhance vibration reducing properties as well as sound attenuation of the laminate, due to their elastic properties and thermal insulation. Moreover, inclusion of wool fibres gives the possibility to increase bio content (animal protein) from alternative sources in the composite. From another point of view, wool presents lower tensile stiffness and strength, which was presented in the review of fibre mechanical properties. Additionally, there might be interface compatibility issues between a polyester matrix and the wool fibres. Wool fibre surface has hydrophobic properties and hydrophilic interior if treated with lanoline, which is a waxy blend (wax, esters, alcohols, acids and hydrocarbons) created by animal glands.

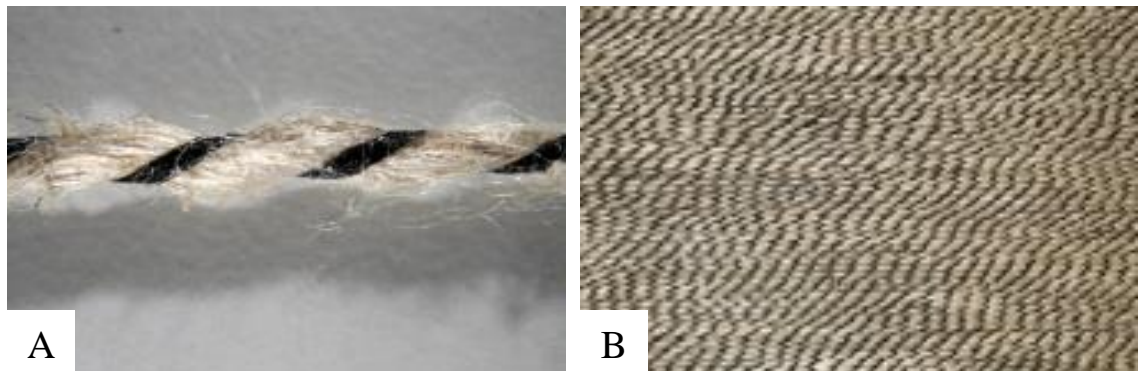


Figure 32 (A) A single hybrid hemp-wool yarn (B) Aligned hemp-wool yarns prepared for processing of unidirectionally reinforced laminate

Yarns - Non-Twisted Flax

The flax yarn was supplied by Biotex. Figure 33A presents the flax 250Tex yarn with visible white wrapping polymeric fibre. Figure 33B presents yarn bundles trimmed for use with compression moulding. This type of yarn has 250Tex value and is composed of parallel long flax fibres held together with a polymeric fibre. The yarn was tensioned for the picture, which caused clearly visible waviness. This is the same type of yarn which is used

to process flax hopsack and the twill fabrics described in the previous section. A single yarn allows for processing of unidirectionally reinforced samples, which can be used for comparison with the fabric reinforcement. The flax fibre has brown colour and single fibres are easily separated from the yarn after the wrapping yarn is removed.

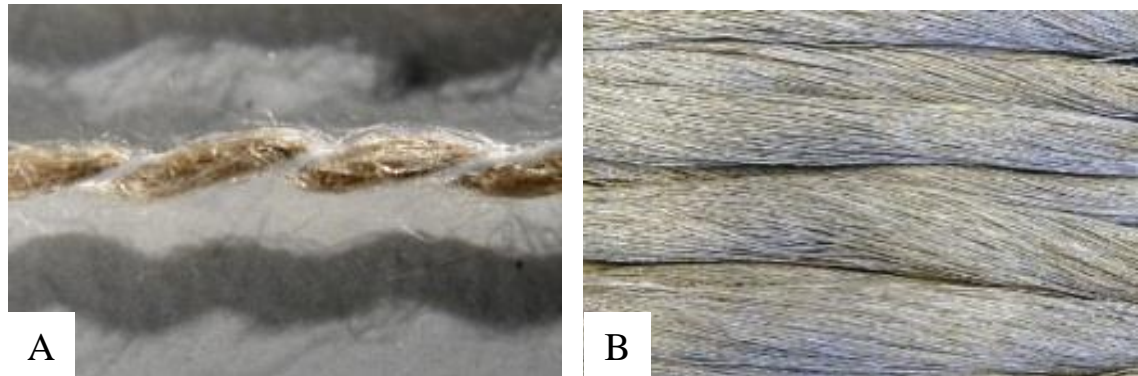


Figure 33 (A) Flax 250Tex non-twisted fibre yarn (B) Flax yarn bundles

3.1.2 Matrix

Two types of an unsaturated polyester resin are used. The first is processed from fossil fuel source and the second is partially derived mainly from renewable sources. A bio-resin, Palapreg ECO® P 55-01, was kindly supplied by Koninkilijke DSM N.V. It is partially (55%) derived from raw renewable resources. It is a low viscosity resin (0.550 - 0.850 Pa s at 23°C) with a density of 1.12 g/cm³. Palapreg ECO® has a medium reactivity and was designed for sheet moulding compound processing (SMC). It has 65MPa tested tensile strength and 3.3GPa tensile modulus. One of the applications for the resin is glass fibre reinforced composite street furniture, which requires good weathering resistance. Reported tensile properties for this resin are 65MPa and 3.3GPa for tensile strength and tensile modulus, respectively, tested in accordance with the standard BS ISO 527. The resin has a clear yellow colour and when cured has a dark yellow or light brown colours, which depends on the additives used. The second resin used is a commercial orthophthalic polyester resin Crystic 2-8500PA. It is a general purpose grade resin for industrial and other applications, with a low styrene emission. It is supplied pre-accelerated. It has the cured density of 1.12g/cm³ at 25°C. Its tensile strength and modulus are 50MPa and 3.5GPa, respectively. It has a viscosity of 2.5 – 4.6 Pa s at 23°C. Styrene can be used to reduce

viscosity if required. The resin mixes were accelerated with 1% of cobalt in aliphatic ester accelerator, i.e. Cobalt (II) 2-ethylhexanoate, and reaction was initiated with 1% of methyl ethyl ketone peroxide at room temperature or with heat. It has a greenish blue colour when liquid and light to yellowish brown when cured. Fully cured resin without reinforcement has a tensile strength of 50MPa and a tensile modulus of 3800MPa tested in accordance with BS ISO 527. The thermoset polyester resin type was selected as a matrix due to liquid form. This type of resin is used for selected processing techniques, like filament winding, compression moulding or hand lay-up. Moreover, the liquid form of the resin allows for easier fibre impregnation, lower processing heat and pressure, if compared with thermoplastic matrices.

3.2 Production

This section describes the BFRP processing route development for laminates reinforced with mats, fabrics and yarns. Laminates were processed in two shapes, i.e. flat and tube. Three main processing routes were used, namely compression moulding with use of a hot press, filament winding with use of a laboratory scale filament winder and vacuum bagging. The main goals in the processing route selection were to find the most convenient technique for use with NF reinforcement, which allows manufacturing of the desired shape.

3.2.1 Laminates Reinforced with Mats and Fabrics

Procedure Development – Feasibility Studies

At first, during the feasibility studies, in order to validate the composite processing procedure and compatibility between matrix and reinforcements, various types of reinforcements were used, i.e. hemp, jute, flax and sisal (Figure 34B). There is no official test standard specific for NFCs, and usually standards for other composites are used. Here, we based our sample preparation procedure on glass fibre composite standards, e.g. BS EN ISO 527. The procedure was developed and tested by processing a series of NF reinforced laminates. Moulds with controllable thicknesses were used with a nominal thickness of

3mm. Due to the restricted volumes of reinforcement available, small laminates were processed during procedure feasibility studies. Two sample shapes were used, i.e. rectangular and dumbbell (Figure 34A). Dumbbell shape aluminium moulds were used to process tensile samples with unreinforced matrix and reinforced with short fibre mat. Moulds were processed from aluminium. Dumbbell shape moulds are convenient for casting and testing of a pure resin, but preparing reinforced composite samples in this way introduces inconsistencies, which highly affect test procedure. It is convenient only for feasibility studies. Dumbbell shape samples are reliable when they are cut out of a laminate sheet by machining, e.g. water jet cutting or laser jet cutting. Finally, rectangular 25mm x 250mm moulds were selected to process samples during feasibility studies with all types of fibres for tensile and flexural tests. Moreover, a third type of mould was prepared with a square shape and 320x320mm dimensions (Figure 35A). The negative side of aluminium, used for preparation of moulds, is that the surfaces are prone to scratching. Prepared moulds have a fixed depth, which means that the hot press stops at the aluminium edge bars. This allows for preparation of samples with the same thicknesses.

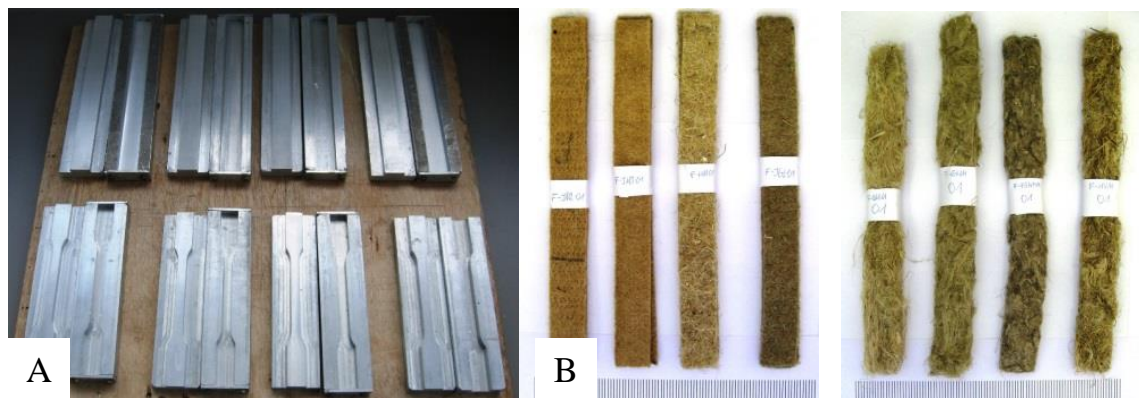


Figure 34 (A) Aluminium moulds with square and dumbbell shapes (B) Hemp, flax and jute mat samples used in feasibility study

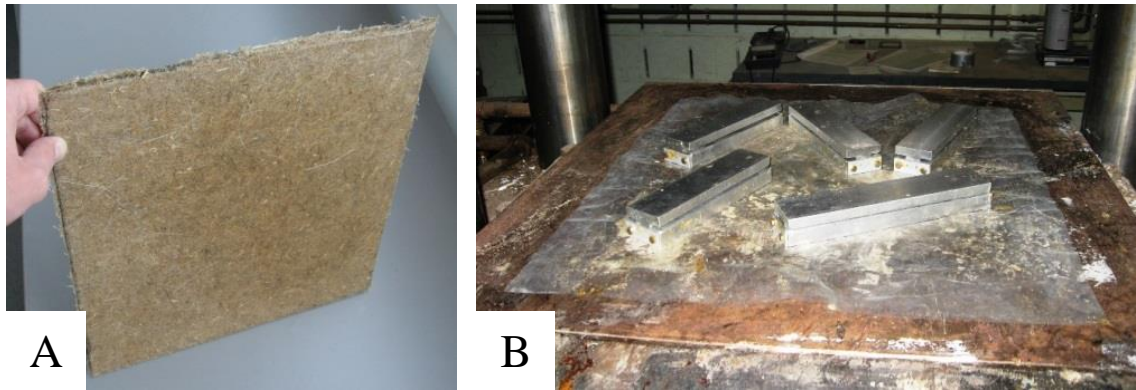


Figure 35(A) Image of one of the trial samples processed to assess hot press procedure. **Hemp mat reinforcing polyester resin (B)** Rectangular moulds with the dimensions 25mm x 250mm during trial hot pressing of NFC laminates

Selected Processing Route – Compression Moulding Procedure

Square flat laminates were processed by compression moulding. The technique requires pressure and heat to shape the laminate. A programmable hot press with 150 tonnes capacity were used. Flat aluminium moulds, with dimensions 320x320x3mm were prepared. First, textiles or mats were cut to size and dried in an air-circulating oven. Resin was mixed with an accelerator, catalyst and degassed in the vacuum chamber. Reinforcement was placed in the mould and subsequently wetted out with resin mix. Mould with wetted reinforcement was covered with polystyrene release film. Samples were cured in the hot press cycle for 15 min at 100°C with pressure of 10MPa and cooled under pressure for 20 min down to 30°C. Samples were removed from the mould and post cured for 16 h at 80°C in accordance with BS ISO 3597-1:2003[137]. Figure 36A presents a diagram of the laminate manufacturing methodology, where layers of reinforcement are stacked between aluminium mould plates.

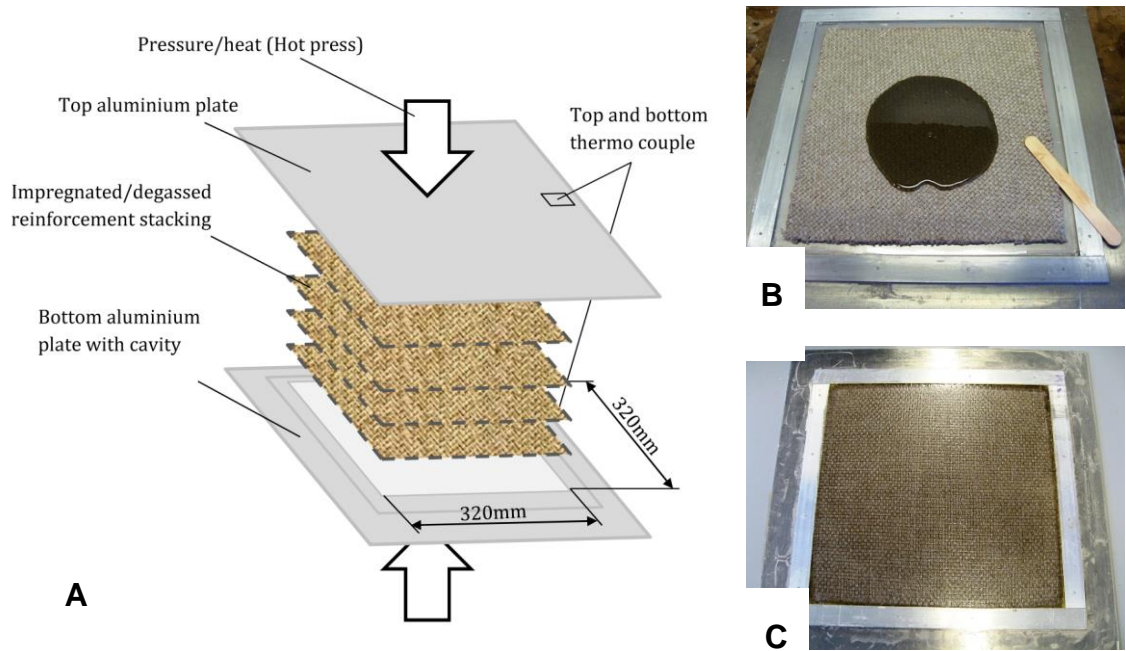


Figure 36 (A) Diagram representing arrangement during compression moulding (B) Flax fabric reinforcement in a mould during impregnation and (C) Palapreg ECO laminate reinforced with flax 4x4 hopsack fabric

Another set of laminates was processed with vacuum bagging. Figure 37 presents a schematic and image of the vacuum impregnation set-up. Laminate layers were impregnated one by one in resin using the lay-up technique. Next, the impregnated stacking was covered with perforated release and bleed out film (RF-242RP) and medium weight breather and absorption fabric (NW153). This was covered with bagging nylon film (NBF-200BT) and connected to the bottom plate with sealant tape (AT-200Y). The sample was connected with the resin trap chamber (RB-451) through a nylon bag with quick release connector (Tygavac-440) and polyethylene tubing. Pressure was controlled with a pressure gauge installed on the resin trap, which was connected to the vacuum pump. After the pumping stage all samples were checked for leaks in the vacuum bag with an ultrasonic leak detector (LEQ-70).

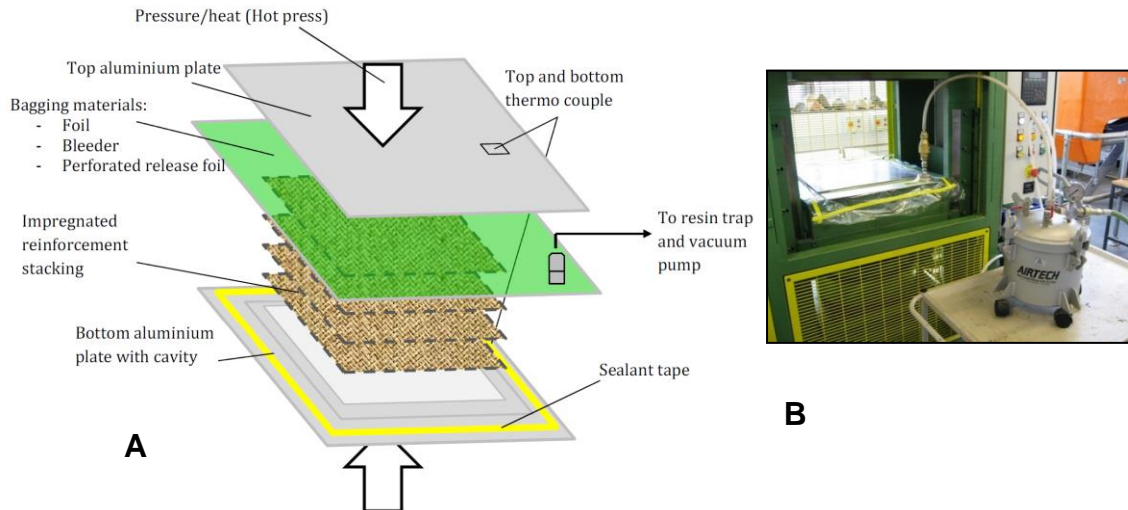


Figure 37 (A) Diagram representing setting during procedure of processing samples with vacuum impregnation (B) Picture of prepared set-up

3.2.2 Unidirectionally Reinforced NFCs

In order to find the tensile properties of the NFCs, unidirectional composite laminates were prepared. Tools were prepared and tested to select the most convenient way to align NF reinforcement in the laboratory. Selected technique involves parallel winding onto 25mm x 250mm U-shaped aluminium mould (Figure 38A) or 310mm x 310mm square frame (Figure 38B). Both allow for precise alignment of the yarns and subsequent impregnation by compression moulding or vacuum assisted process.

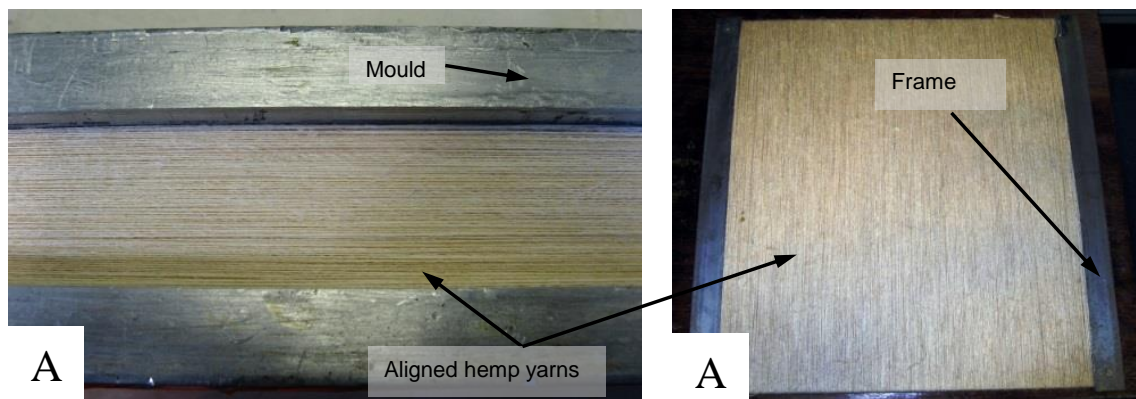


Figure 38 (A) Unidirectionally aligned hemp yarns in the rectangular mould (B) Unidirectionally aligned yarns placed in the 2nd type of a square mould

Composites with parallel yarns are wound onto mandrels. The procedure allows for control over reinforcement content and orientation. Volume fraction is controlled by changing an amount of yarns in the mould cavity. Figure 39 presents a diagram of the unidirectional composite preparation. U-shape aluminium moulds with ‘male’ and ‘female’ parts were prepared in house. Samples are prepared in three steps. In the first step, a selected number of yarns is wound onto a cavity of the mould. Fibres are clamped at the end in order to maintain tension and then dried with the mould and cooled down in a decorticator. In the next step, resin mix was introduced and the mould was exposed to negative pressure of 1atm for duration of 5 minutes in a vacuum chamber. Samples are then cured with the same hot press cycle which is used for square laminates.

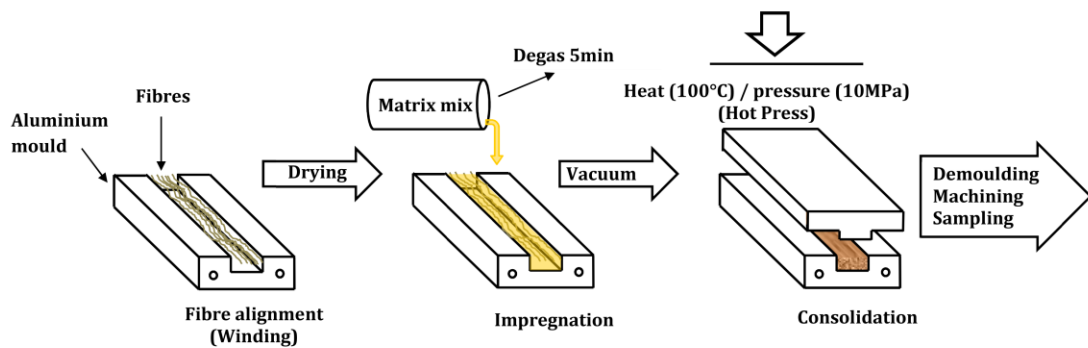


Figure 39 Diagram representing unidirectional yarn samples preparation methodology

Panel samples with dimensions $310 \times 290 \times 3 \text{mm}^3$ are processed using a similar procedure, but using a square frame mandrel. Filament winder, described in the next section, is used to wind the yarns onto the frame. This type of sample preparation allows for uniform distribution of the reinforcement throughout the panel. In the next step, samples were impregnated and cured with a procedures described in the previous section.

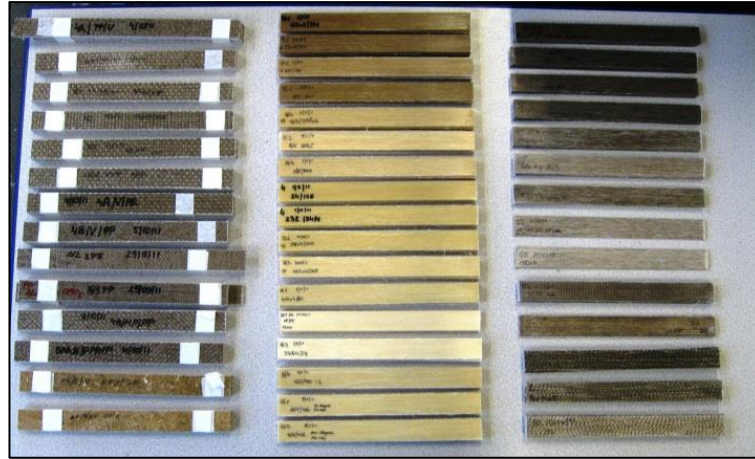


Figure 40 Batch of various Palapreg-Eco resin laminate samples (from left: flax fabric reinforced laminates, hemp unidirectionally reinforced laminates flax and hemp-wool reinforced laminates)

3.2.3 NFC Tubes

Feasibility Studies

Based on the previous work, the first technique assessed for processing of the NFC tubes was compression moulding. Aluminium tubular and half shell tube moulds were used (Figure 41A). This type of sample was processed by wrapping a mould tubular core with a pre-impregnated fibre mat. Pressure was applied through outer tube shells and samples were left for room temperature curing. It is possible to process NFC tubes with this procedure, but it is difficult to precisely control the shape and resin distribution. The procedure restricts the possibility of the samples processing to thick walled tubes. Moreover, the method is labour intensive and produces shells with inconsistent shape.

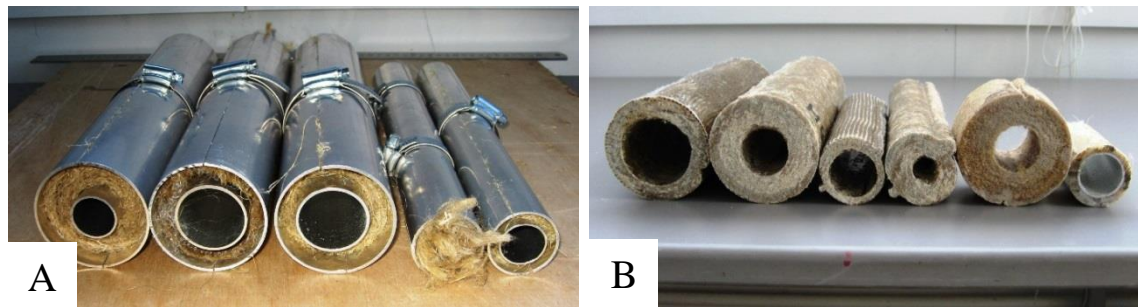


Figure 41 (A) Feasibility studies of the NFC tube processing by compression moulding with various types of reinforcement. (B) Set of trial stage NFC tubes, processed by compression moulding technique.

The aforementioned flaws led to work for the development of a procedure which would allow repetitive manufacturing of NFC tubes with control over length, wall thickness and reinforcement orientation. Goals were set up to achieve improvements in fibre orientation control, shape consistency and impregnation quality. In the first stage, other impregnation and moulding techniques were tested and adjusted for natural fibre use. In a second stage, the fibre orientation control was tackled. Natural fibre plain wave fabric was wrapped onto an aluminium tube mould and impregnation procedures were assessed. In order to improve the uniformity of the tubular laminate, pressure is applied evenly along the sample. There were a few of techniques investigated, namely lay-up impregnation with a brush, vacuum bagging, resin transfer moulding and compression moulding with use of a shrink tape. Two techniques were found to be the most useful and convenient for laboratory studies. Those were impregnation with a shrink tape, because it allowed for application of a uniform pressure around the whole tube circumference, and vacuum bagging, which as well allowed for the application of a uniform atmospheric pressure. This is achieved by the use of atmospheric pressure in vacuum assisted processes (Figure 42 B) or by the use of heat activated, thermo-shrinking tapes (Figure 42 A).

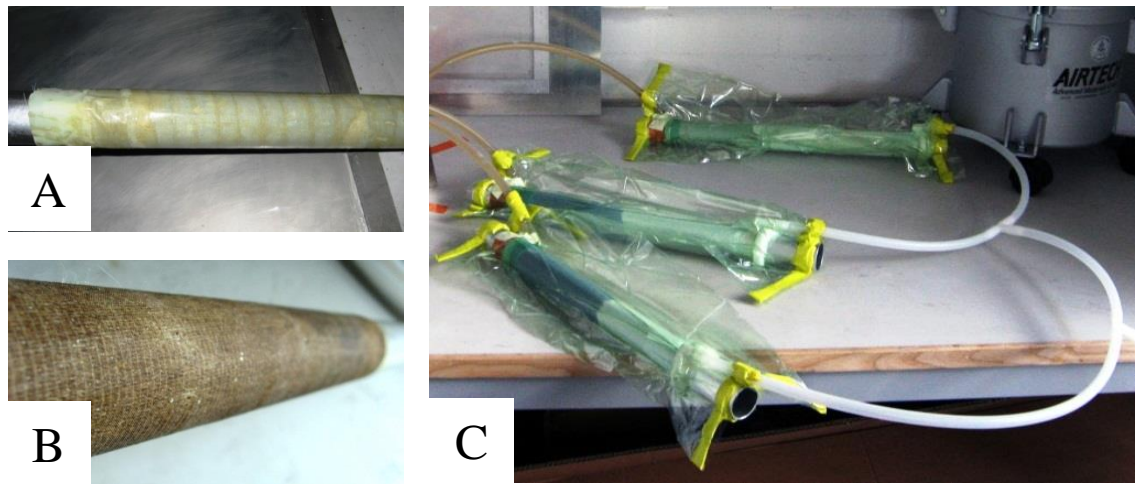


Figure 42 (A) NFRP tube impregnated with applied external pressure from the thermo shrinking tape. (B) Surface of impregnated and cured NFC tube reinforced with flax unidirectional fabric (C) Impregnation of three tube samples by resin transfer moulding

The next step was to find a way to control the reinforcement arrangement in the processed tube. This led to the preparation of the pin winding set up for a manual yarn winding (Figure 43A). Tube core mould with pinned end cups was used to manually wind hemp and other yarns at the desired wind angle (Figure 43B). Both techniques were tested and adjusted for tubular samples processing.

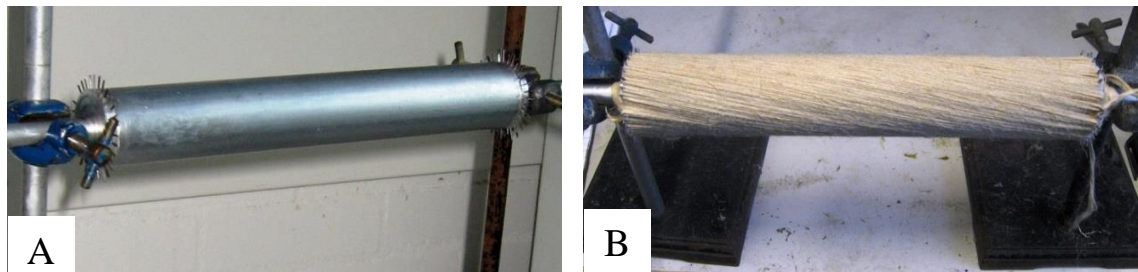


Figure 43 (A) Tube mould with pinned end cups ready for filament winding. (B) Manual procedure for the hemp composite tube composite by pin winding

Tube Processing

The manual procedure of yarn reinforcement arrangement in tube processing was labour intensive and required additional improvements. This led to the development of a laboratory scale filament winder in order to speed up the process and increase repeatability and control over yarn direction. The pin winding technique was selected as the most

applicable to control processing parameters during tube preparation. It allows for control over a whole range of fibre orientations, from 0° to 90° in relation to the mould length. First, aluminium collapsible tubular moulds (Figure 44C) and pinned end cups (Figure 44A) were prepared. Yarns or filaments are wound onto the core tube and subsequently impregnated. During curing, resin shrinks applying pressure onto the internal tube mould. This causes the NFC laminate to adhere to the aluminium mould, despite the presence of release agents; therefore, it prevents the laminate from removal without inducing damage. In order to assure easy sample removal, the tube mould core was cut diagonally (Figure 44 C). Pins attached to the end cups (Figure 44 A) allow winding yarns at the 0° direction, parallel to the tube length, which differentiates this technique from conventional filament winding of a tube. Winding of the reinforcement at specific angles and interweaving patterns is possible (Figure 44 B).

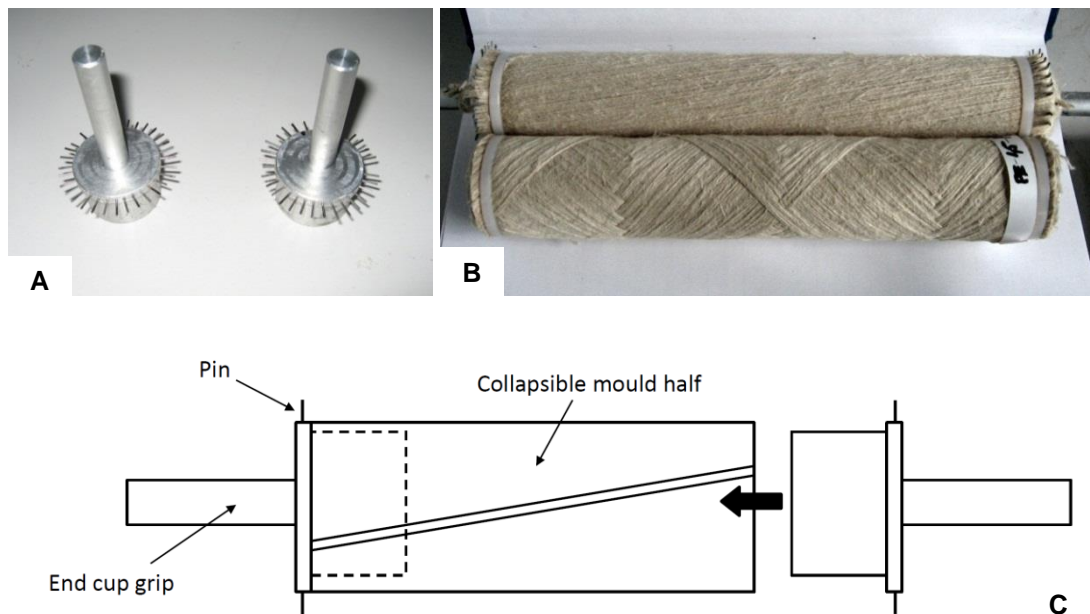


Figure 44 (A) Aluminium end cups with pins (B) moulds with wrapped yarns, (C) Collapsible mould with pinned end cups assembly diagram

Figure 45 presents a diagram with the filament winding set-up, which was prepared in order to facilitate faster and precise NFC tube processing. The mould is attached to the end cups, which are connected to the step motor with the end cup grips. This step motor rotates the mould, which pulls the yarn onto it. The rotation speed is altered with a controller, which is run by a program from a connected computer. The carriage, which is

placed on the rails, is connected to a step motor with a belt. The carriage has a set of three plastic pulleys, which redirect the yarn from the tensioning tool to the resin reservoir. A delivery loop is connected to the carriage. It allows for more precise control over the yarn placement onto the rotating mould. The step motor responsible for the carriage movement and the step motor responsible for the rotation of the tube mould are synchronised together with a Q Drive, which was supplied by ‘Applied Motion Products’. Multiple yarns are wound at the same time. Yarns are secured in their position and fed through the combining and tensioning tool. Yarn tension is facilitated by a friction loop. The software used allows for writing a simple command-based program to create the desired tube design in one procedure. Adjusting parameters in the program allows for control over winding angle, pattern and processing speed. After preparation of the winding set-up, the equipment was calibrated through multiple trials.

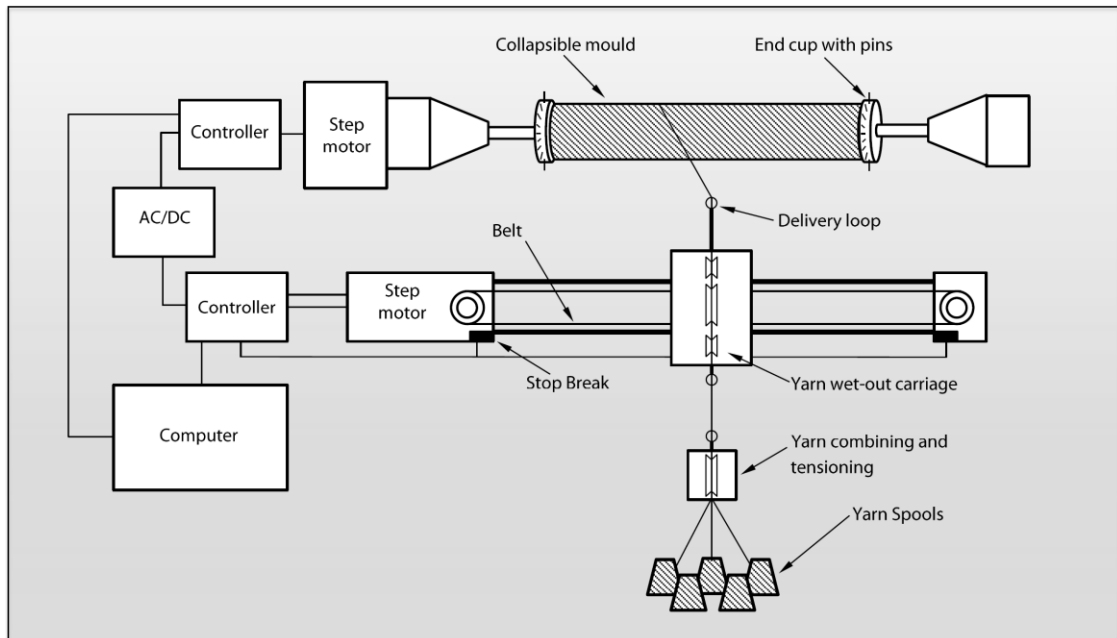


Figure 45 Diagram of the natural fibre yarn tube filament winding set-up

3.2.4 Composite Tube Fabrication

The developed NFC tube preparation procedure consists of the following steps. At first, yarns are dried at 80°C for 24 hours. This is to remove moisture from natural fibres, which is present in the hydrophilic fibres in standard conditions at about 7% to 10%. Next, yarns

are fed through a series of loops and are attached to the tube mould. Hemp yarns are wound according to the selected program (Figure 46). The rotational speed of the mould and the feeding speed of the fibre carriage are altered, in order to accommodate a change in the thickness, which was measured experimentally. In order to maintain the same wind angle, changes in speed were designed in accordance with Equation 1.

$$\frac{N}{V} = \frac{\theta}{2\pi r} \quad (1.)$$

where N denotes the constant rotational speed of the mandrel in revolutions per minute, V is the constant carriage feed, θ is wind angle in relation to the tube main axis and r represents the radius of the mandrel (Mazumdar, 2001). After the winding procedure of designated number of layers, yarns are impregnated with resin mix. Two procedures were used for the impregnation, namely compression moulding or vacuum bagging.

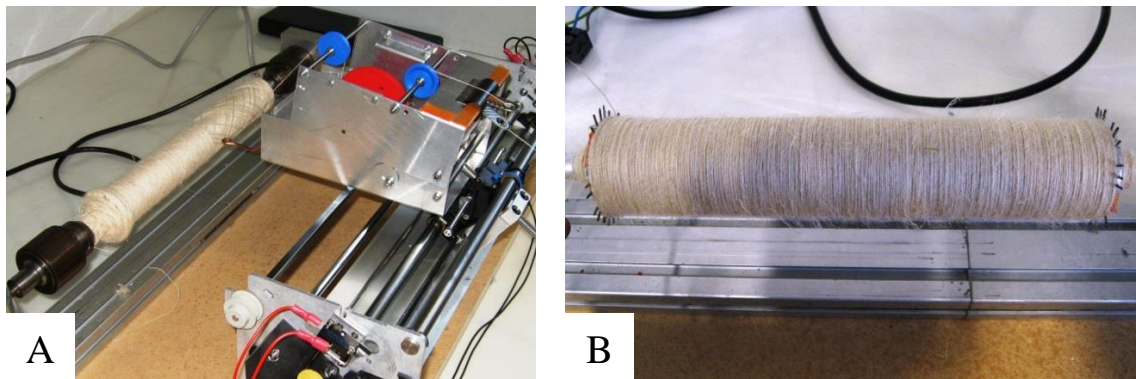


Figure 46 (A) Laboratory scale natural fibre winder during sample preparation (B) Tubular mould with surface yarns wound at 90° to the sample direction

Compression moulded samples are first impregnated with resin manually after the winding procedure. Next, the mould is covered with NV153 perforated release fabric, and wrapped with HST400 thermo-shrinking tape. Then, samples are placed on a prepared stand, which constantly rotates the prepared sample throughout the gelling and curing processes (Figure 47). Rotation is used to prevent resin agglomeration due to gravity. After placing the sample in the oven, pressure is applied by shrinkage of the tape, which is induced by heat. Samples stay in the oven for 15 minutes. Tubes are post-cured at 100°C for 24h in a

vacuum oven. Samples are removed by collapsing of the tubular mould. This prevents from inflicting damage to the thin walled tubes prepared.

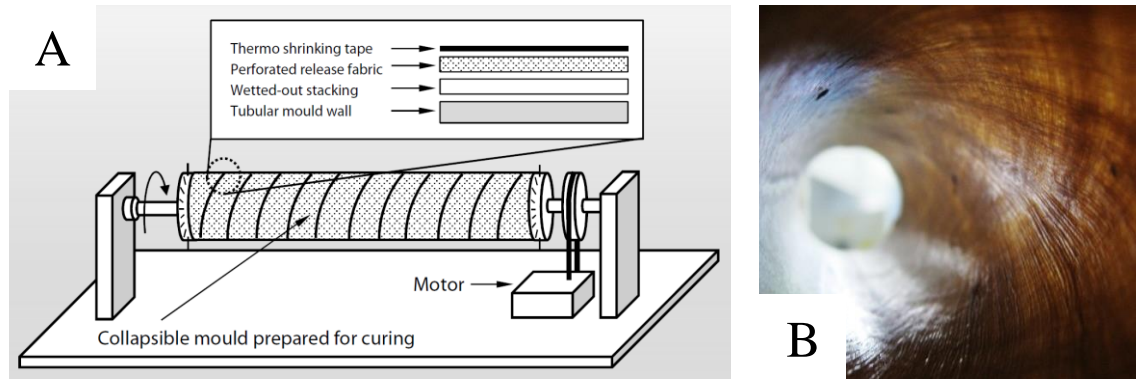


Figure 47 (A) Diagram of the sample rotating stand used during gelling and curing (B) Macro image of the interior part of the trial thin walled samples revealing a criss-crossed reinforcement pattern

3.3 Testing

This section describes test types used to analyse selected properties of the developed BFRPs and gives the rationale behind tests. This investigation was used to assess and optimise the mechanical performance. Therefore, it is focused on tests revealing the relationships between processing factors, material composition and outcome material properties. Laminates were analysed for their tensile, flexural, compression and inter-laminar shear mechanical properties. BFRPs are susceptible to weather and moisture degradation. The influence of weathering conditions on mechanical properties was analysed with accelerated thermal degradation, fluid immersion and outdoor weathering

3.3.1 Density Measurements

Density is one of the key composite material properties. It is used to calculate strength-to-weight-ratio; i.e. material strength divided by its density. Measurement methods depend on the type of investigated materials. In order to determine densities of fibres, resins or composites, techniques such as immersion in liquid, pycnometer method or titration are used. Method for plastics is described in the standard EN ISO 1183-1:2004 [138]. Bulk

material density is measured with the use of an inert liquid. For measurements of the NF and NFCs, deionized water is used as a displacement agent. Measurement is done by measuring a sample suspended on a wire before and after immersion. Displacement calculation is done with a following equation

$$\rho_{LD} = \frac{m_1 \times \rho_{IL}}{m_1 - m_2} \quad (2.)$$

where m_1 is the apparent mass of the specimen in air, expressed in grams, m_2 is the apparent mass of the specimen in the immersion liquid, expressed in grams, ρ_{IL} is the density of the immersion liquid in grams per cubic centimetre. Smaller samples are measured with pycnometer method, which uses a pycnometer flask, a glass dish with a narrow neck and calibrated volume. First, the pycnometer weight is measured with fixed volume of displacement liquid. It is useful for measuring yarn density. Air is evacuated from the liquid before weighting by the use of a vacuum chamber. In the next step, a yarn sample is measured by filling the glass up to the limit of its capacity, subsequent air evacuation and topping up of the liquid. For yarn measurements, 10m long samples were used. Results are calculated with the following equation

$$\rho_{PY} = \frac{m_s \times \rho_{IL}}{m_1 - m_2} \quad (3.)$$

where m_s is the apparent mass of the specimen expressed in grams, m_1 is the apparent mass of the liquid required to fill the empty pycnometer and m_2 is the apparent mass of the liquid required to fill the pycnometer containing the specimen.

3.3.2 Moisture Absorption Test

The moisture absorption test measures the speed of material absorption, and material capacity for absorbing liquid. There are two types of absorption measured, i.e. absorption from air humidity or absorption from immersion in liquid. Moisture absorption was measured in accordance with standard BS EN ISO 62:2008 [139]. Tested laminate pieces have 90x90mm dimensions, and were machined from 310x310 mm flat laminate plates.

Sample edges are covered with aluminium foil to prevent absorption through the edges. This is especially important in composites and NFC, since exposed fibres and fibre-matrix interface tend to conduct water at a different rate than the laminate surface. First, specimens are oven dried at 50°C for 24hrs, subsequently cooled in a desiccator and weighted. Next, samples are immersed in distilled water and their weight is monitored in scheduled intervals, until equilibrium is achieved and no more water is absorbed. Results were used to identify moisture absorption of NFC and to compare it against Fickian absorption law.

3.3.3 Yarn Tenacity Test

There are two types of yarns, namely with twisted and non-twisted fibres. The type of yarn processing directly influences its load bearing capacity when it is dry, i.e. not impregnated with resin. Tenacity provides information on maximum load which can be applied on the yarn, which is important information for processing method like filament winding. It is especially crucial for NF reinforcement, because yarns are composed out of multiple short fibres. Yarns were tested in tension using 250mm gauge length and 250mm/min crosshead speed in accordance with ISO/DIS 2062 [140]. Tests were conducted at a temperature of 20°C and moisture 51RH. Prior to the test, yarns were loaded with 0.5cN/Tex. Additionally, samples were also tested with 4mm gauge length. This reduces influence of fibre slipping.

3.3.4 Static Tensile Test

Tensile strength is one of the most important and common ways of assessing laminate strength. Moreover, it is one of the key properties of fibre reinforced composites. It is used to determine influences of factors related with reinforcement type, reinforcement arrangement or laminate processing conditions. It is a significant part of BFRP assessment in this thesis. During the test, a sample with a constant cross section is stretched. Jaws clamping the sample move at a constant displacement rate. The sample resistance to stretching is measured in newtons until material failure. Only results from test pieces which fracture in the gauge area, i.e. the narrowest part of the test piece of a constant and known

cross-section, are valid. Test samples were conditioned in the standard conditions, i.e. 55%RH humidity and temperature of 23°C before the test. A universal testing machine Instron 5585 was used (Figure 48A). It has a tensile load capacity up to 150kN and Self-locking clamps. Test pieces were statically loaded in tension with the crosshead movement of 2mm/min until fracture. Test results were recorded with the use of the Bluehill software. Figure 49 presents examples of flax fabric reinforced laminate test pieces after the tensile test. Test pieces have the dumbbell shape and all break within the gauge area.

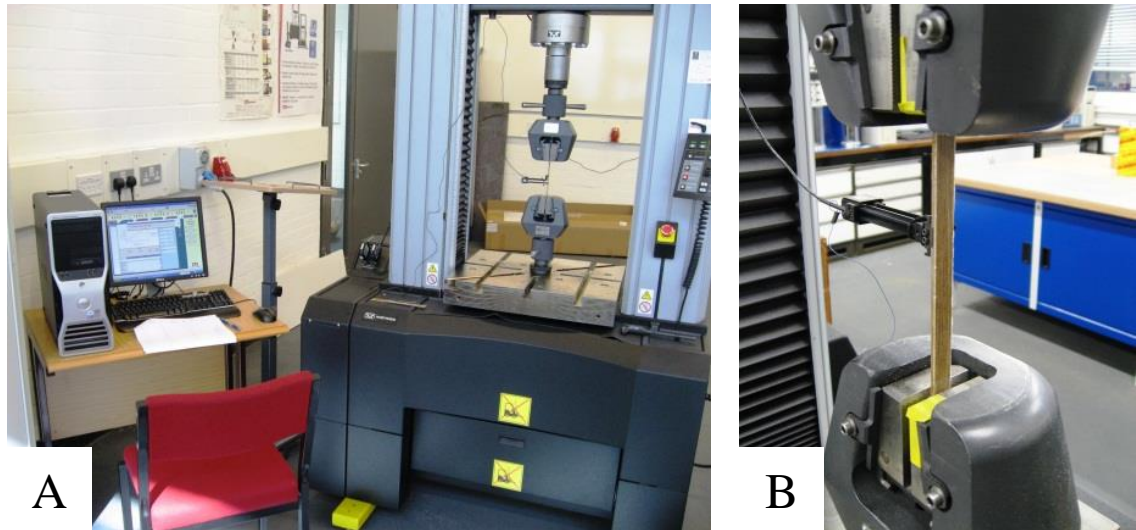


Figure 48 (A) Instron 5585 universal testing machine set-up (B) Hemp unidirectional laminate sample prepared for the tensile test

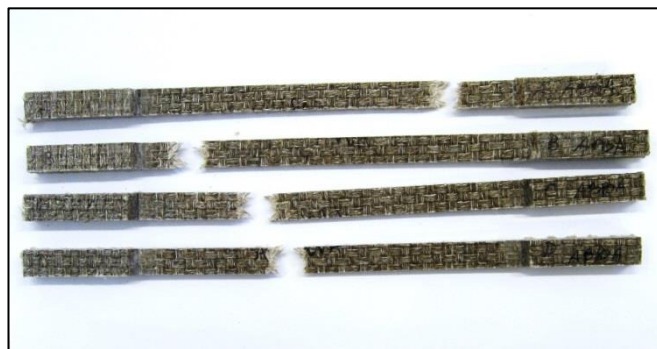


Figure 49 Flax 250 Tex yarn reinforced laminate test pieces after the test with fractures within the gauge area

3.3.5 Flexural Test

The flexural properties are measured during a three or four point bending test. The test in essence is a compound measure of three types of deformations, namely tension, compression and shear. The sample has a rectangular, square or circular cross section. During a three or four point flexural test, the sample is compressed on the top plane, stretched at the bottom plane, and shear forces act in the middle plane. Therefore, it is often used as a benchmark for an overall laminate performance. It is used to find the influence of exposure or changes in processing parameters. The flexural test for BFRPs was conducted in accordance with EN ISO 14125:1998 on Class 2 samples with dimensions 80x15x3mm [141]. It is a standard dedicated for use with GFRP. Span length between the rollers was equal to $l=64\text{mm}$, and rollers size was $R1 = 5\text{mm}$. Figure 50 illustrates the test set up and sample dimensions. Coupons were tested with an Instron 5584 universal testing machine and an in-house processed three-point bending test jig. Sample coupons were loaded at a constant rate of 2mm/min, and the test was continued until sample failure. Results were recorded with the use of the Bluehill software.

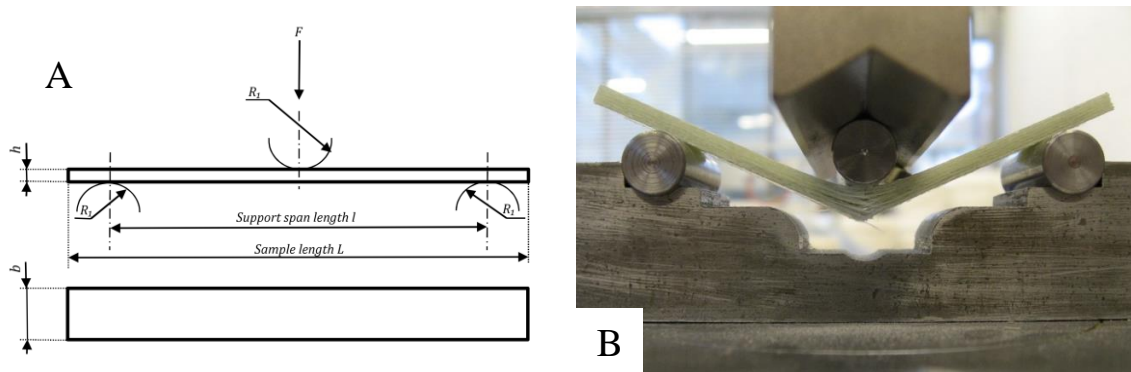


Figure 50 (A) Diagram of the sample loading with dimensions [142] (B) Laminate with Palapreg-Eco resin reinforced with glass fibres during flexural test

3.3.6 Tube Compression Test

The compression tests were conducted on BFRP tube-shaped samples. Tube is an important shape in all aspects of engineering. BFRP are not foreseen to be used in applications bearing compression loads. This is due to relatively low compression

properties of fibre reinforced composite, which primarily withstand tensile loads [143]. Nevertheless, BFRPs compression properties were analysed in order to assess their compressive performance. A tubular shape allows for a straightforward compression test. Compression in the direction parallel to the main direction of the tube was selected. Alternatively, tubes can be compressed in the perpendicular direction, but it results in a flexural deformation of the tube wall. The flexural and tensile tests were conducted on flat laminate panels. Due to labour intensive laminate preparation, the test was restricted to compression along the tube main direction. Reinforcement orientation was one of the investigated factors, analysed with tubes with different yarn orientation angles. Therefore, the goal was to find if there is a link between winding angle and compressive properties. Additionally, observations onto tube compression fracture behaviour were made by fracture analysis. The tube test pieces were squared polished and covered with polytetrafluoroethylene (PTFE) lubricant gel, which reduces the possibility of lateral stress concentration caused by friction between sample and compression plates. Sample ends were not restrained during tests. Tubes were compressed with Instron 5584 at the constant rate of 0.5mm/min. The compressive stiffness, ultimate strength and modulus of resilience were calculated. Additionally, modes of fracture were observed and recorded during compression and after the test. Figure 51A presents a BFRP tube test piece during compression. Figure 51B presents two flax reinforced tubes partially compressed.

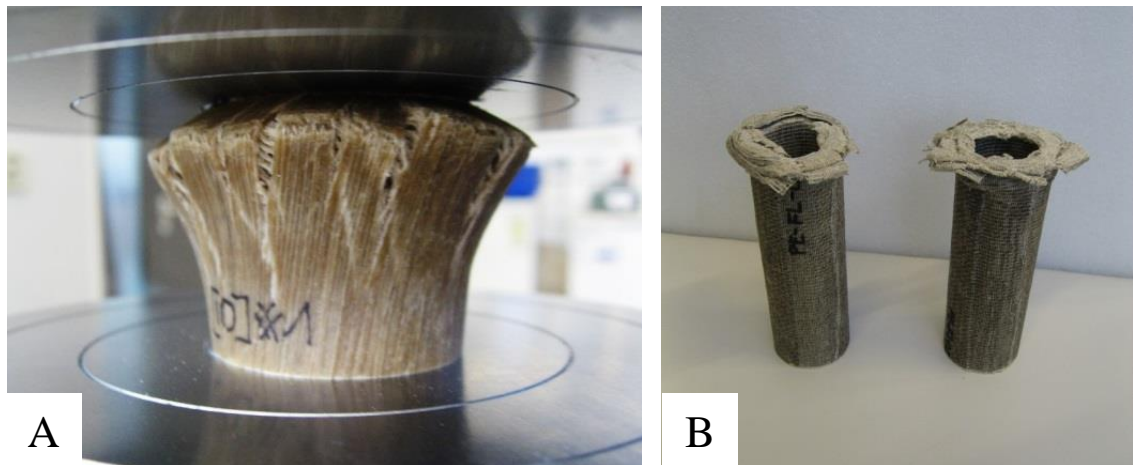


Figure 51 (A) Hemp twisted yarn reinforced tube during compression test (B) Two flax reinforced laminate trial tubes with progressive collapse fracture after compression test

3.3.7 Inter-laminar Shear Strength Test

Inter-laminar shear strength for NFC laminates can be evaluated with the use of a double notch shear test (DNST). Rectangular samples with dimensions of $80 \times 15 \times 3 \text{ mm}^3$ are used. A tensile load is applied in the longitudinal direction of the test piece until the area between the notches breaks. The sample is processed in a way that, when the load is applied, the area between notches fractures in the shear mode. Two slots perpendicular to the sample main direction are milled in opposite sides of the test piece. Figure 52 presents a diagram of the test piece and Figure 52B presents two test pieces prepared with glass fibre laminate. Slots control the size of test area (length x width). The depth of the milled slots is determined with the sample thickness and is equal to the mid plane of the sample. It is possible that the sample will fracture in a non-expected manner, i.e. some fibres break in tension. This increases the load sustained by the sample, therefore results from such samples are not taken into account. Each test piece is assessed to determine the fracture mode. Samples were mounted in the jig and loaded in the tensile mode at 2mm/min crosshead speed. The applicability of the double notch shear test (DNST) for the assessment of natural fibre composite shear values was evaluated. Figure 53A presents fracture surface of the ILSS test piece made with GFRP. Figure 53B presents an ILSS test piece, made with hemp yarn reinforced laminate, after the test.

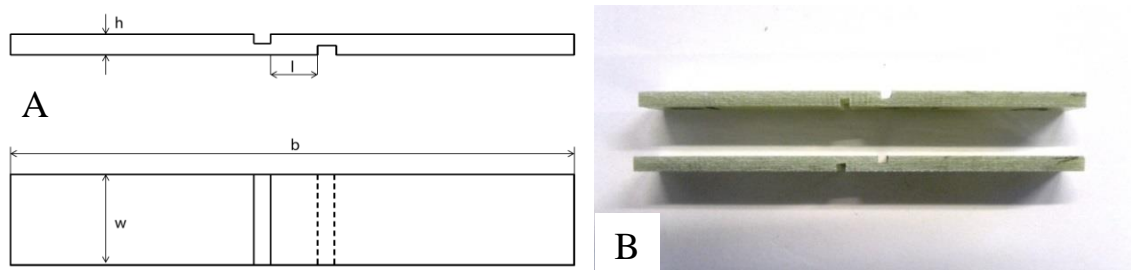


Figure 52 (A) ILSS sample drawing with dimensions (B) ILSS samples made out of GFRP with Palapreg-Eco resin

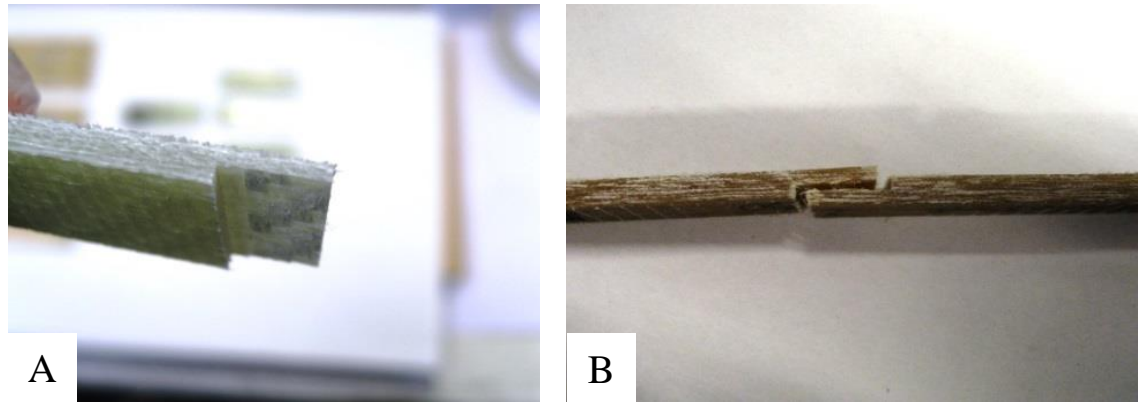


Figure 53 (A) GFRP with Palapreg-Eco resin ILSS sample fracture surface (B) Hemp yarn reinforced Palapreg-Eco ILSS sample after the test

3.3.8 Weathering Test

Heat Ageing

Polymer matrix composite properties deteriorate at elevated temperatures. Natural fibres are more susceptible to thermal degradation than glass fibres. For instance, hemicellulose is less resistant to heat than other NF constituents, i.e. lignin and cellulose. Therefore, a standard assessment of heat ageing resistance was conducted. Heat ageing was performed on BFRP test coupons, by keeping them at elevated temperatures in an air-circulated oven. There were three batches of samples. The first batch of samples was exposed for 30 min and the second for 120 hours at 110°C. Next, samples were taken out from the oven and conditioned to the standard humidity and temperature for 24hrs. Test coupons were cut into flexural coupons and tested.

Immersion in Fluids

BFRPs have hydrophilic fibres and a hydrophobic matrix. NFs absorb moisture and swell, which induces internal stresses. Moreover, when a composite is immersed in a fluid other deteriorative effects take place, such as leaching of constituents or microorganism attack thriving in a humid environment. Sets of sample coupons 100x100 mm were immersed in distilled water and a sodium chloride solution of 36g/l. Edges of samples were sealed with aluminium foil, which reduces exposed fibre sorption on the edges. Only a face area of

known size is exposed. Samples were monitored for weight and size change (swelling) in specified time intervals. Additionally, the influence of the immersion on the flexural properties was measured in one month intervals. Three point bending tests were performed in accordance with EN ISO 14125: 1998 [141] on Class 2 samples 80x15x3mm (with $L=64\text{mm}$), which were machined from the immersed coupons. Rollers used were $R_1=5\text{mm}$ and $R_2=2\text{ mm}$ for top and bottom, respectively. There were five pieces tested per sample. Prior to the test, samples were conditioned at the standard temperature and humidity for 24 hours.

Atmospheric Weathering

Another way of assessing the influence of weathering conditions is exposure to a combined environmental effect of the sunlight and moisture, i.e. environmental weathering. Sets of sample coupons with dimensions of 90x90mm were subjected to the UK climate. Coupons were placed on testing racks at a 45° angle facing south. In fifteen day intervals samples were flipped, and in 30 day intervals samples were exposed to elevated temperature of 110°C for 30min using an air circulated oven. Flexural tests were conducted in one month intervals. This test procedure is based on a standard BS PL 4:2005 [144], which is dedicated to glass fibre reinforced polyester composites.

3.4 Sampling

3.4.1 Machining of NFCs

In order to prepare samples for mechanical tests, the most suitable route to cut the samples had to be selected. NFCs can be cut with conventional saw, laser cutter or water jet cutter. Most techniques used for cutting wood are suitable for cutting of NFC material. Laser cutting trials were conducted, which gave good edge quality and precision and repeatable test results. The laser power and traverse speed are adjusted to avoid burning of the fibres. This raised concerns about the influence of the heat affected zone especially for samples with higher fibre volume fraction and thickness (Figure 54). Therefore, mechanical saw cutting was selected with a 240V table top-cutter (Figure 55). The blade used had

dimensions 80x0.5x10 with 80 teeth. Cutting at lower speeds with blades below 24 teeth gives low quality edge with pulled-out fibres.

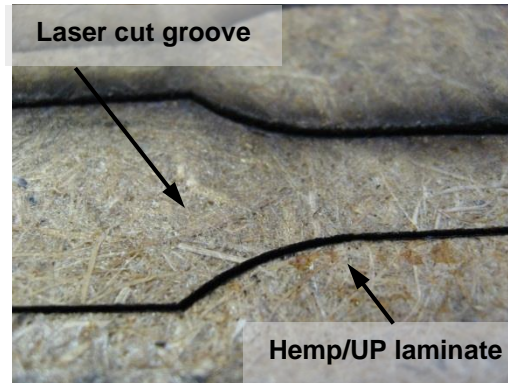


Figure 54 Dumbbell shaped tensile sample cut out from hemp mat/polyester laminate with laser plotter

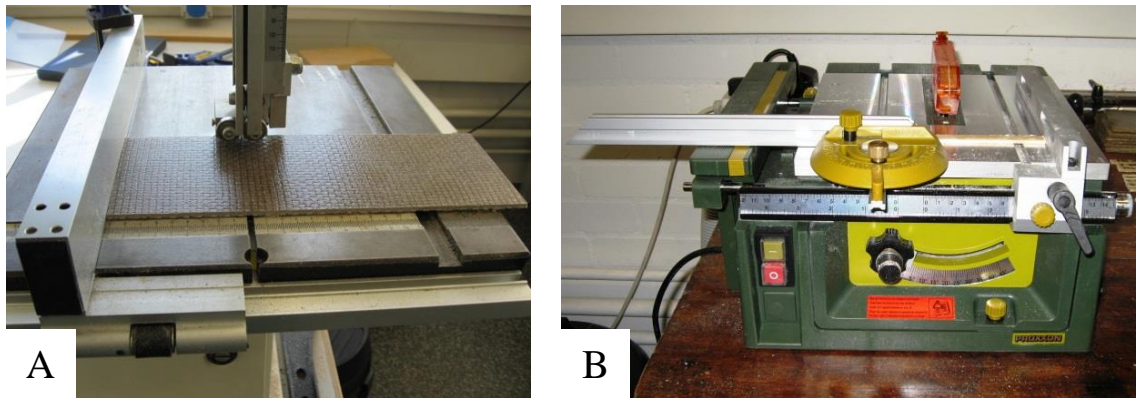


Figure 55 (A) Hopsack flax fabric in polyester laminate machined with a band saw (B) Table top precision cutter used for machining smaller samples

3.4.2 Tensile Test Coupons

Tensile samples were prepared from processed laminates. Because of the fibre unidirectional arrangement in some of the samples, a rectangular test piece shape was selected from a standard for GFRP laminates, i.e. BS EN 527 [145]. Two sizes for unidirectional and fabric composites were used. Testing of the unidirectional composite coupons is sensitive to the coupon shape and flaws. It results in sample fracturing outside the gauge area; usually within the part compressed by the grip (Figure 56). Another form of undesirable sample fracture are cracks parallel to the fibres. There are two main reasons

causing this type of fracture, namely inconsistent tensioning during winding procedure and non-parallel fibre arrangement. A yarn parallelism is ensured with filament winding and precise sample cutting. The excessive stress concentration from the test equipment grip is minimised by tapered sample end-tabs made out of NFC or GFRP (Figure 57). Therefore, sample ends were secured with glass fibre tapered tabs and glued with epoxy adhesive under pressure. Unidirectional samples were cut into 250mm x 12mm with 150mm gauge lengths. Randomly reinforced and fabric reinforced samples were cut into 250mm by 25mm with 150mm gauge length (Figure 58).



Figure 56 Examples of a trial hemp reinforced unidirectional samples fracturing at the edge of the grip area. Stress concentration created by grips causes premature sample fracture and invalidity

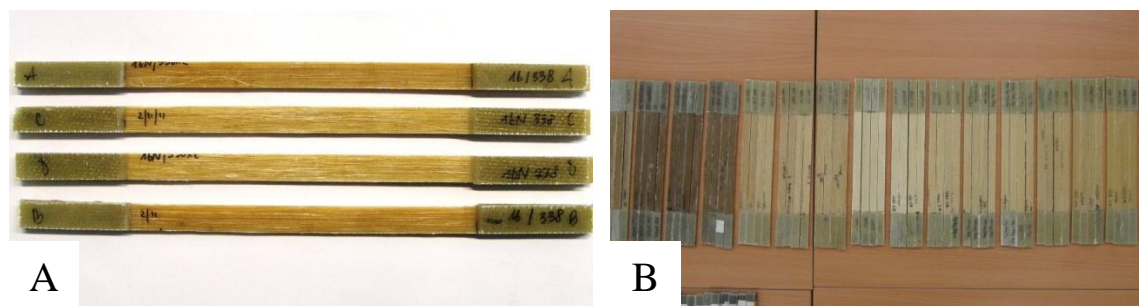


Figure 57 (A) Four laminate test pieces with aligned hemp twisted yarn reinforcement in Palapreg-eco resin (B) A batch of NFRP test pieces with glass fibre end tabs prepared for the tensile test

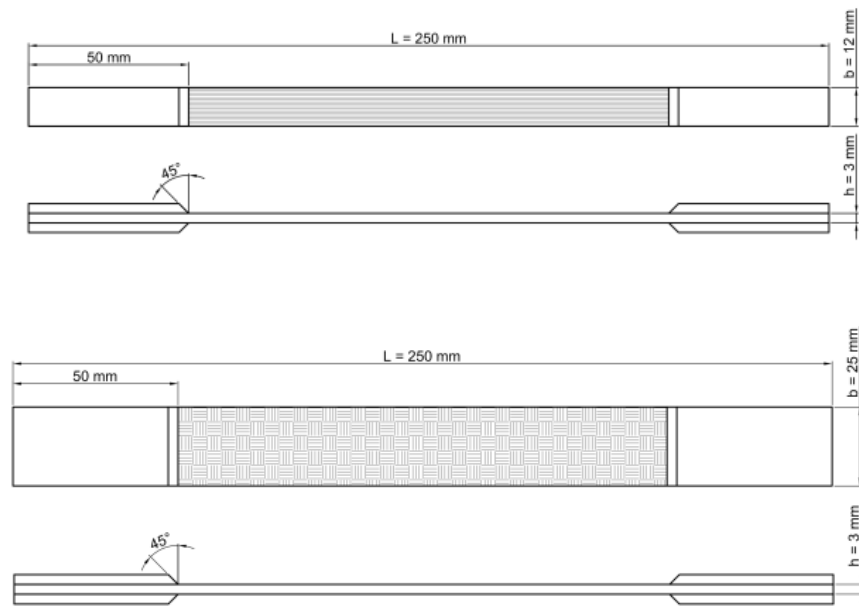


Figure 58 (Top) unidirectional reinforced tensile sample dimensioning (Bottom) Textile and mat reinforced samples arrangement

Table 4 presents a list of the sample types prepared for the tensile tests. It depicts the type of reinforcement, arrangement, processing method and matrix used. All test pieces were prepared with the aforementioned procedures. For each sample, at least three repetitions with four test pieces were prepared. There are two main types of samples, namely prepared with unidirectional reinforcement and with biaxial fabric. The laminate sequence is presented in the reinforcement specification column.

Table 4 Samples types prepared for the tensile test

<i>Fibre</i>	<i>Reinf. type</i>	<i>Reinforcement specification</i>	<i>Resin type</i>	<i>Reinforcement arrangement</i>	<i>Vf %</i>	<i>Processing Route</i>
Flax	Yarn	250Tex non-twisted	Palapreg-Eco	Unidirectional	23	Compression
Flax	Yarn	250Tex non-twisted	Palapreg-Eco	Unidirectional	30	Compression
Flax	Yarn	250Tex non-twisted	Palapreg-Eco	Unidirectional	51	Compression
Flax	Yarn	250Tex non-twisted	Palapreg-Eco	Unidirectional	56	Compression
Flax	Yarn	250Tex non-twisted	Palapreg-Eco	Unidirectional	76	Compression
Flax	Yarn	250Tex non-twisted	Palapreg-Eco	Unidirectional	89	Compression
Flax	Yarn	F12 twisted	Palapreg-Eco	Unidirectional	50	Compression
Flax	Yarn	F18 twisted	Palapreg-Eco	Unidirectional	49	Compression

Hemp Wool	Yarn	1000 non-twisted	Palapreg-Eco	Unidirectional	23	Compression
Hemp Wool	Yarn	1000 non-twisted	Palapreg-Eco	Unidirectional	42	Compression
Hemp Wool	Yarn	1000 non-twisted	Palapreg-Eco	Unidirectional	50	Compression
Hemp Wool	Yarn	1000 non-twisted	Palapreg-Eco	Unidirectional	73	Compression
Hemp	Yarn	130Tex twisted	Palapreg-Eco	Unidirectional	41	Compression
Hemp	Yarn	130Tex twisted	Palapreg-Eco	Unidirectional	50	Compression
Hemp	Yarn	130Tex twisted	Palapreg-Eco	Unidirectional	76	Compression
Hemp	Yarn	86Tex twisted	Palapreg-Eco	Unidirectional	41	Compression
Hemp	Yarn	60Tex twisted	Palapreg-Eco	Unidirectional	34	Compression
Hemp	Yarn	60Tex twisted	Palapreg-Eco	Unidirectional	41	Compression
Hemp	Yarn	51Tex twisted	Palapreg-Eco	Unidirectional	41	Compression
Hemp	Yarn	39Tex twisted	Palapreg-Eco	Unidirectional	23	Compression
Hemp	Yarn	39Tex twisted	Palapreg-Eco	Unidirectional	32	Compression
Hemp	Yarn	39Tex twisted	Palapreg-Eco	Unidirectional	41	Compression
Hemp	Yarn	39Tex twisted	Palapreg-Eco	Unidirectional	50	Compression
Hemp	Yarn	39Tex twisted	Palapreg-Eco	Unidirectional	76	Compression
Hemp	Yarn	25Tex (no vac, no degas)	Palapreg-Eco	Unidirectional	41	Compression
Hemp	Yarn	25Tex (no vac)	Palapreg-Eco	Unidirectional	41	Compression
Hemp	Yarn	25Tex twisted	Palapreg-Eco	Unidirectional	41	Compression
Flax	Fabric	4x4Hopsack [0/90] ₄	Palapreg-Eco	Biaxial Long	44	Compression
Flax	Fabric	4x4Hopsack [0/90] ₄	Crystic	Biaxial Long	44	Compression
Flax	Fabric	1x1Twill [0/90] ₅	Crystic	Biaxial Long	43	Compression
Flax	Fabric	1x1Twill [0/90] ₅	Palapreg-Eco	Biaxial Long	44	Compression
Flax/Hemp	Fabric/Mat	4x4Hop(0/90),HM,4x4(0/90)	Palapreg-Eco	Biaxial Long	43	Compression
Flax	Fabric	4x4Hop(45/45) ₄	Palapreg-Eco	Biaxial @45	44	Compression
Flax	Fabric	4x4Hop(45/45) ₄	Palapreg-Eco	Biaxial @45	44	Vacuum
Flax	Fabric	4x4Hopsack [0/90] ₄	Crystic	Biaxial Long	44	Vacuum
Flax	Fabric	4x4Hopsack [0/90] ₄	Palapreg-Eco	Biaxial Long	44	Vacuum
Flax	Fabric	4x4Hop[(0/90),(45/45)] ₅	Palapreg-Eco	Biaxial long/45	44	Compression
Hemp	Mat	Hemp mat	Palapreg-Eco	Random	29	Compression
Glass	Fabric	Glass 1x1Twill[0/90] ₂₀	Palapreg-Eco	Biaxial	43	Compression

3.4.3 Flexural Samples

Flexural test samples were prepared in accordance with the standard EN ISO 14125:1998. Samples were cut to Class 2 with size 80x15x3mm. Table 5 presents a list of sample types prepared for the flexural tests. For each sample, at least three repetitions with four test pieces were prepared.

Table 5 Sample types prepared for the flexural test

<i>Fibre</i>	<i>Reinf. type</i>	<i>Reinforcement specification</i>	<i>Resin</i>	<i>Reinforcement arrangement</i>	<i>Vf %</i>	<i>Processing Route</i>
Flax	Yarn	250Tex non-twisted	Palapreg-Eco	Unidirectional	23	Compression
Flax	Yarn	250Tex non-twisted	Palapreg-Eco	Unidirectional	30	Compression
Flax	Yarn	250Tex non-twisted	Palapreg-Eco	Unidirectional	51	Compression
Flax	Yarn	250Tex non-twisted	Palapreg-Eco	Unidirectional	56	Compression
Flax	Yarn	250Tex non-twisted	Palapreg-Eco	Unidirectional	76	Compression
Flax	Yarn	250Tex non-twisted	Palapreg-Eco	Unidirectional	89	Compression
Flax	Yarn	F12 twisted	Palapreg-Eco	Unidirectional	50	Compression
Flax	Yarn	F18 twisted	Palapreg-Eco	Unidirectional	49	Compression
Hemp Wool	Yarn	1000 non-twisted	Palapreg-Eco	Unidirectional	23	Compression
Hemp Wool	Yarn	1000 non-twisted	Palapreg-Eco	Unidirectional	42	Compression
Hemp Wool	Yarn	1000 non-twisted	Palapreg-Eco	Unidirectional	50	Compression
Hemp Wool	Yarn	1000 non-twisted	Palapreg-Eco	Unidirectional	73	Compression
Hemp	Yarn	130Tex twisted	Palapreg-Eco	Unidirectional	41	Compression
Hemp	Yarn	130Tex twisted	Palapreg-Eco	Unidirectional	50	Compression
Hemp	Yarn	130Tex twisted	Palapreg-Eco	Unidirectional	76	Compression
Hemp	Yarn	86Tex twisted	Palapreg-Eco	Unidirectional	41	Compression
Hemp	Yarn	60Tex twisted	Palapreg-Eco	Unidirectional	34	Compression
Hemp	Yarn	60Tex twisted	Palapreg-Eco	Unidirectional	41	Compression
Hemp	Yarn	51Tex twisted	Palapreg-Eco	Unidirectional	41	Compression
Hemp	Yarn	39Tex twisted	Palapreg-Eco	Unidirectional	23	Compression
Hemp	Yarn	39Tex twisted	Palapreg-Eco	Unidirectional	32	Compression
Hemp	Yarn	39Tex twisted	Palapreg-Eco	Unidirectional	41	Compression
Hemp	Yarn	39Tex twisted	Palapreg-Eco	Unidirectional	50	Compression
Hemnp	Yarn	39Tex twisted	Palapreg-Eco	Unidirectional	76	Compression

Hemp	Yarn	25Tex (no vac, no degas)	Palapreg-Eco	Unidirectional	41	Compression
Hemp	Yarn	25Tex (no vac)	Palapreg-Eco	Unidirectional	41	Compression
Hemp	Yarn	25Tex twisted	Palapreg-Eco	Unidirectional	41	Compression
Flax	Fabric	4x4Hopsack [0/90] ₄	Palapreg-Eco	Biaxial Long	44	Compression
Flax	Fabric	4x4Hopsack [0/90] ₄	Crystic	Biaxial Long	44	Compression
Flax	Fabric	1x1Twill [0/90] ₅	Crystic	Biaxial Long	43	Compression
Flax	Fabric	1x1Twill [0/90] ₅	Palapreg-Eco	Biaxial Long	44	Compression
Flax/Hemp	Fabric/Mat	4x4Hop(0/90),HM,4x4(0/90)	Palapreg-Eco	Biaxial Long	43	Compression
Flax	Fabric	4x4Hop(45/45) ₄	Palapreg-Eco	Biaxial @45	44	Compression
Flax	Fabric	4x4Hop(45/45) ₄	Palapreg-Eco	Biaxial @45	44	Vacuum
Flax	Fabric	4x4Hopsack [0/90] ₄	Crystic	Biaxial Long	44	Vacuum
Flax	Fabric	4x4Hopsack [0/90] ₄	Palapreg-Eco	Biaxial Long	44	Vacuum
Flax	Fabric	4x4Hop[(0/90),(45/45)] ₅	Palapreg-Eco	Biaxial long/45	44	Compression
Hemp	Mat	Hemp mat	Palapreg-Eco	Random	29	Compression
Glass	Fabric	Glass 1x1Twill[0/90] ₂₀	Palapreg-Eco	Biaxial	43	Compression

3.4.4 Weathering Samples

Samples for the weathering test, the heat ageing test and the water absorption test were processed with two types of reinforcements, namely natural fibre composite reinforced with a flax 4x4 hopsack fabric (area density 510g/m²) and synthetic fibre composite reinforced with a glass twill type fabric (area density of 81g/m²). One batch of samples was processed in square 320 mm x 320 mm x 3 mm moulds by the hot pressing technique and a second batch with a vacuum assisted technique. Flax reinforced laminates were composed of four 4x4 hopsack plies and glass fibre samples were composed of 12 plies. The difference in the number of plies was necessary to prepare laminates with similar volume fractions. The first batch of samples was processed to the exact size with a pressure of 1.8 MPa during hot press cycle. The size of the samples was controlled with the use of metal stoppers. The second batch of samples was consolidated using vacuum bagging. Samples processed by hot pressing had 3mm size, and samples processed by vacuum bagging had average thickness of ~4mm due to lower pressure, which is approximately 0.1 MPa. Samples were cured in the thermal cycle. First, they were heated up to 90°C, kept at this

temperature for 15min and subsequently cooled in 5min steps to the temperatures 60°C, 40°C, and 20°C. Next, plates were post-cured in a ventilated oven at 55°C for 24hours. Volume fraction of the laminates processed was equal to 45% Vf for four ply Flax fabric reinforcing Palapreg-ego resin. Square coupons were machined to 90x90mm size for weathering exposition. After exposition, coupons were machined down to 80x15mm test pieces for three point flexural test. Table 6 presents a list with the main details of the various samples processed and their test type designation.

Table 6 Sample types prepared for the weathering test

<i>Fibre</i>	<i>Reinforcement specification</i>	<i>Resin</i>	<i>Test</i>	<i>Vf</i>	<i>Processing Route</i>
				%	
Flax	4x4Hopsack [0/90] ₄	Palapreg-Eco	Reference	49	Compression
Flax	4x4Hopsack [0/90] ₄	Palapreg-Eco	Water absorption (distilled water @1m)	49	Compression
Flax	4x4Hopsack [0/90] ₄	Palapreg-Eco	Water absorption (saline solution @1m)	49	Compression
Flax	4x4Hopsack [0/90] ₄	Palapreg-Eco	Thermal ageing @110°C (30min)	49	Compression
Flax	4x4Hopsack [0/90] ₄	Palapreg-Eco	Thermal ageing @110°C (120h)	49	Compression
Flax	4x4Hopsack [0/90] ₄	Palapreg-Eco	Environmental Weathering (@1m)	49	Compression
Flax	4x4Hopsack [0/90] ₄	Palapreg-Eco	Environmental Weathering (@2m)	49	Compression
Flax	4x4Hopsack [0/90] ₄	Palapreg-Eco	Reference	44	Vacuum
Flax	4x4Hopsack [0/90] ₄	Palapreg-Eco	Water absorption (distilled water @1m)	44	Vacuum
Flax	4x4Hopsack [0/90] ₄	Palapreg-Eco	Water absorption (saline solution @1m)	44	Vacuum
Flax	4x4Hopsack [0/90] ₄	Palapreg-Eco	Thermal ageing @110°C (30min)	44	Vacuum
Flax	4x4Hopsack [0/90] ₄	Palapreg-Eco	Thermal ageing @110°C (120h)	44	Vacuum
Flax	4x4Hopsack [0/90] ₄	Palapreg-Eco	Environmental Weathering (@1m)	44	Vacuum
Flax	4x4Hopsack [0/90] ₄	Palapreg-Eco	Environmental Weathering (@2m)	44	Vacuum
Flax	4x4Hopsack [0/90] ₄	Crystic	Reference	49	Compression
Flax	4x4Hopsack [0/90] ₄	Crystic	Water absorption (distilled water @1m)	49	Compression
Flax	4x4Hopsack [0/90] ₄	Crystic	Water absorption (saline solution @1m)	49	Compression
Flax	4x4Hopsack [0/90] ₄	Crystic	Thermal ageing @110°C (30min)	49	Compression
Flax	4x4Hopsack [0/90] ₄	Crystic	Thermal ageing @110°C (120h)	49	Compression
Flax	4x4Hopsack [0/90] ₄	Crystic	Environmental Weathering (@1m)	49	Compression
Flax	4x4Hopsack [0/90] ₄	Crystic	Environmental Weathering (@2m)	49	Compression

Flax	4x4Hopsack [0/90] ₄	Crystic	Reference	49	Vacuum
Flax	4x4Hopsack [0/90] ₄	Crystic	Water absorption (distilled water @1m)	49	Vacuum
Flax	4x4Hopsack [0/90] ₄	Crystic	Water absorption (saline solution @1m)	49	Vacuum
Flax	4x4Hopsack [0/90] ₄	Crystic	Thermal ageing @110°C (30min)	49	Vacuum
Flax	4x4Hopsack [0/90] ₄	Crystic	Thermal ageing @110°C (120h)	49	Vacuum
Flax	4x4Hopsack [0/90] ₄	Crystic	Environmental Weathering (@1m)	49	Vacuum
Flax	4x4Hopsack [0/90] ₄	Crystic	Environmental Weathering (@2m)	49	Vacuum
<hr/>					
Glass	Glass 1x1Twill[0/90] ₂₀	Palapreg-Eco	Reference	43	Compression
Glass	Glass 1x1Twill[0/90] ₂₀	Palapreg-Eco	Water absorption (distilled water @1m)	43	Compression
Glass	Glass 1x1Twill[0/90] ₂₀	Palapreg-Eco	Water absorption (saline solution @1m)	43	Compression
Glass	Glass 1x1Twill[0/90] ₂₀	Palapreg-Eco	Thermal ageing @110°C (30min)	43	Compression
Glass	Glass 1x1Twill[0/90] ₂₀	Palapreg-Eco	Thermal ageing @110°C (120h)	43	Compression
Glass	Glass 1x1Twill[0/90] ₂₀	Palapreg-Eco	Environmental Weathering (@1m)	43	Compression
Glass	Glass 1x1Twill[0/90] ₂₀	Palapreg-Eco	Environmental Weathering (@2m)	43	Compression

3.4.5 Tube Compression Samples

Tubes were prepared with filament winding and subsequent compression moulding or vacuum bagging. Length of processed tubes was 150mm or 300mm. Flax fabrics were used for lay-up techniques and mostly hemp yarns for filament winding techniques. Figure 59 presents a batch of samples cut to size for the compression test. Filament wound samples were prepared with yarn arranged at angles to the main tube direction, namely 10 °; 30 °; 45 °; 60 ° and 90 °. The ratio of wall thickness to diameter was set up to $t/D < 0.04$. Prepared tubes had 45mm diameter and were machined to 45mm height test pieces. Short samples, where the diameter corresponds to the test piece length, were selected in order to prevent global off-axis buckling of the tube (Harte et al. 2000). At least three repetitions of the each winding arrangement were prepared with three samples each.

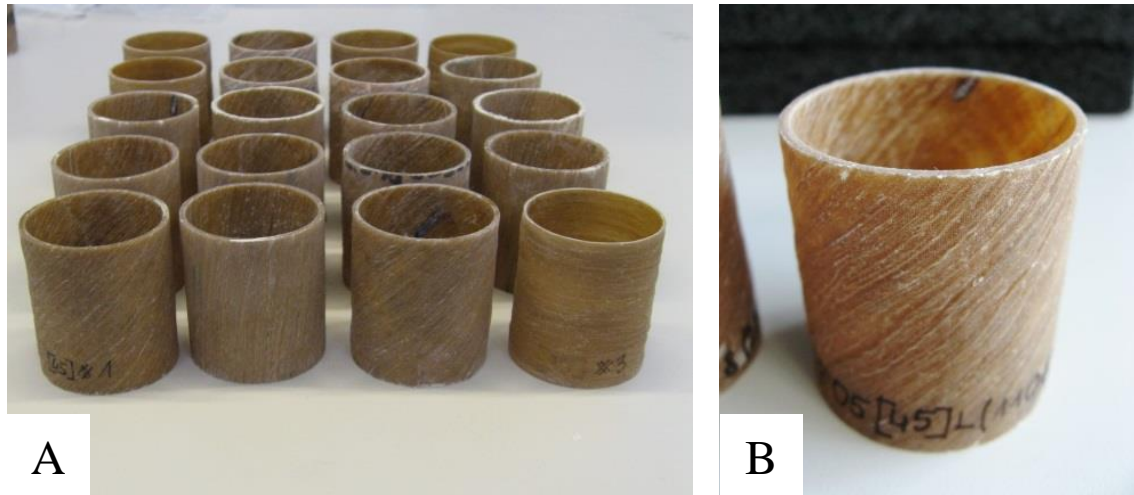


Figure 59 (A) One batch of samples trimmed and prepared for the compression test (B) Macro image the 130Tex hemp twisted yarn reinforced composite tube with the fibres oriented at $\pm 45^\circ$

Table 7 Tube compression samples types

<i>Fibre</i>	<i>Resin</i>	<i>Winding angle</i>	<i>V_f</i> %	<i>Processing Route</i>
Flax 240Tex twisted	Crystic	0	41	Lay-up + resin transfer moulding
Flax 240Tex twisted	Crystic	0	41	Lay-up + resin transfer moulding
Hemp yarn 130Tex twisted	Crystic	10	30	Filament winding + Compression
Hemp yarn 130Tex twisted	Crystic	30	30	Filament winding + Compression
Hemp yarn 130Tex twisted	Crystic	45	30	Filament winding + Compression
Hemp yarn 130Tex twisted	Crystic	60	30	Filament winding + Compression
Hemp yarn 130Tex twisted	Crystic	90	30	Filament winding + Compression

3.4.6 Moulding for Optical Microscopy and SEM

Natural fibre composite microstructure is observed with the use of optical or SEM microscopy. A cross section is finely polished in order to reveal the morphology of the individual fibre cells. In the first step, samples are casted into cylinders with Buhler acrylic resin. Then, samples are polished with sand papers starting with 100grit and ending on 2400grit. Water is used as lubricant. Additionally, the surface is polished with a diamond paste. The sample is washed between steps with distilled water in an ultrasound cleaner in

order to remove SiC particles and milling products. The cleaning prevents coarser grit particles from migrating. Between polishing stages, polishing progress is monitored with an optical microscope. SEM uses a focused electron beam, which is aimed at the observed surface, and a detector to visualise interactions between observed material atoms and electrons. It provides information about composition and topography. A conductive surface, like a metallic cross section, is the most convenient for SEM microscopy. Non-conductive surfaces cause electron agglomeration and impair the quality of the image. This is tackled by using a conductive gas atmosphere inside the SEM chamber instead of a vacuum. A second solution is coating of the sample surface with a thin layer of gold by a plasma deposition technique. Both solutions ensure electron discharge from the observed surface. The SEM technique has a deep field of view; therefore, there is no need for polishing. Observations with both methods were made to analyse processed samples for fibre distribution and agglomeration, impurities and porosities and interface morphology.



Figure 60 A batch of samples being casted prior to polishing

Experimental Results and Analyses

4 Influence of Reinforcements on Tensile Properties of BFRPs

Chapter 4 analyses results of the tensile test of various BFRPs and discusses factors influencing tensile properties of these laminates. It is composed of eleven sections. Section 4.1 presents rationale for investigating tensile properties of BFRP. Sections 4.2 and 4.3 discuss influences of the yarn traits on tensile properties of BFRP, i.e. effect of yarn linear density and an effect of the yarn twist, respectively. Section 4.4 discusses an effect of laminate reinforcement sequence. Section 4.5 analyses differences between types of impregnation techniques used. Section 4.6 discusses influence of yarn arrangement based on two types of flax fabric reinforcement. Section 4.7 analyses an influence wool fibre addition to the hemp fibre reinforcement. A subject of the volume fraction influence is discussed in sections 4.8 and 4.9. Moreover, volume fraction influence on the tensile properties of BFRP is compared with theoretical values in section 4.10. Section 4.11 provides the summary of findings for the Chapter 3.

4.1 Why Investigate Tensile Properties of BFRPs?

This chapter characterises the tensile properties of NFC for building applications. It is focused on analysing the influence of reinforcement-related factors on the tensile properties of hemp, flax and hybrid hemp-wool laminates. Both, bio and fossil fuel derived thermoset polyester matrices are used. The chapter is divided into six sections, which subsequently describe the effects of the selected factors, namely yarn linear density (T_{ex}), yarn twist, lamination, yarn waviness within the fabric, hybrid hemp-wool reinforcement and volume fraction. Tensile together with flexural properties are key factors in synthetic as well as natural fibre composites. The tensile stiffness or Young's modulus is a measure of rigidity of the object. It is defined as a ratio of stress to strain of materials. The ultimate

tensile stress is the maximum stress that a material can tolerate while being stretched. It is defined as the maximum force per unit area. The unit used to describe tensile stiffness and stress is the Pascal (Pa), which is Newton per square metre (N/m^2) in the SI unit system. An analysis of the material response subjected to tensile loading and fracture analysis provides important information about the material microstructure.

The extracted NFs have the highest tensile strength lengthwise and have inherently finite length. This hinders the stress transfer between matrix and fibres, in a case when the fibre length is shorter than the critical length for a particular assembly [146]. Moreover, the reported tensile properties of single fibres vary considerably (Table 2). This discrepancy is caused by multiple factors, namely the inherent defects of nodes and/or growing stresses, variation of plant species, region of growth, position of the fibre within the plant and extraction-related defects.




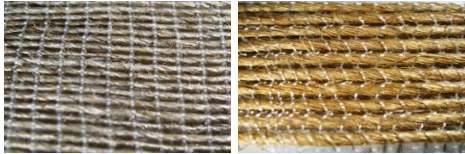



There is a need in composite manufacture for orientation control and process continuity; therefore, various forms of NF continuous reinforcement were developed; amongst them, mats or yarns are used most commonly in structural NFRPs. Mats are composed of selected fibre lengths, do not have specific fibre orientation and are held together by friction and interlocking between fibres. Yarns are processed by twisting of the slivers, as in typical textile yarns, or by wrapping aligned slivers of fibres with a polymeric yarn. The use of matrices from renewable resources is a step forward in sustainable building material economy. NFRPs mechanical properties were studied for synthetic matrices, but there are few studies on thermoset matrices from renewable resources. At the moment, it is common that renewable-based resins have disadvantage of lower mechanical properties and higher price in comparison with synthetic systems; therefore, partially bio-sourced resin blends were developed. A need to analyse the compatibility of such blends with natural fibres and analyse their influence on mechanical properties was identified. Further information on thermoset and thermoplastic green composites can be found in section 2.6.

Wool fibres were identified as potential reinforcement for the NFC for non-structural applications, due to thermal and mechanical properties combination and availability of protein-based wool fibres due to their reduced use in the textile industry [115, 147]. Thermal properties of wool fibres can potentially be beneficial for reduction of the thermal bridge effect in buildings applications like door or window frames. The thermal bridge is an

area or object in building with significantly higher heat transfer than the surrounding materials [148]. Hemp-wool hybrid yarn reinforcement with unidirectionally oriented fibres and synthetic resins was developed and investigated [116]. Later work on wool fibre mat reinforcing synthetic polyester and hybrid jute-wool mat and fabric reinforcing synthetic epoxy has confirmed the advantages of the hemp-wool reinforcement, which had higher mechanical properties [112, 115]. It was concluded that the selected processing methodology resulted in poor mechanical performance. It was identified that an analysis of compatibility of the hybrid hemp-wool reinforcement with a resin system from renewable resources should be performed

14 different types of natural fibre reinforcements were used for the production of natural fibre composites (NFRP) in order to gain a better understanding of the mechanisms of their reinforcing roles during the tensile loading. The group was comprised of seven hemp fibres, five flax fibres and two hemp-wool fibres hybrid reinforcements. Moreover, the reinforcements can be divided into three types, namely mats, yarns and fabrics. Table 8 summarises all reinforcement types used, corresponding to the specific influencing factors to be studied for the understanding of the tensile behaviour of NFRPs. A detailed description of each type of reinforcement and selection rationale is provided in the section 3.1.1.

Table 8 Reinforcements and corresponding parameters studied

Reinforcement type	Image	Description	Used to study effects*:
Hemp mat		100% hemp mat with randomly oriented short fibres, processed by field retting and subsequent mat pressing. Area density 780g/m ² .	A
Hemp-wool mat		It is composed of 80% hemp and 20% wool fibres. Processed by hydro entanglement. Kindly supplied by Innovation & Research Institute, University of Leeds.	A, F
Flax biaxial fabrics		Flax Hopsack 4x4 (left) and Twill 1x1 (right) fabrics. Processed with 250 Tex non-twisted yarns. Supplied by Biotex.	A, B, C
Flax twisted yarn		Flax yarns with twisted fibres in unidirectional roving, with 240Tex (left) and 590Tex (right) linear yarn densities respectively.	B, D, E
Flax non-twisted yarn		Non-twisted 250Tex flax yarns. Aligned fibre slivers are held together by wrapped polyester yarn. Supplied by Biotex.	A, C, D, E, G
Hybrid hemp-wool non-twisted yarn		1000 Tex non-twisted yarn with 9/1 hemp to wool fibre ratio, wrapped in polyester yarn. Kindly supplied by NatCom project.	D, E, F, G
Hemp twisted yarn		Six types of hemp yarns (130, 86, 60, 51, 39 and 25Tex). Fibres were retted and bleached with standard textile process and ring spun. Supplied by Cyarn ltd.	D, G

* A – Effect of orientation, B – Effect of lamination, C – Effect of yarn waviness, D – Effect of yarn linear density (Tex), E – Effect of yarn structure and twist, F – Combined effect of hybrid reinforcement, G – Effect of volume fraction.

4.2 Effect of Yarn Linear Density

The ‘thickness’ of a yarn is expressed in Tex, which is a yarn’s linear density. From a composite processing point of view, the yarn should be relatively thick in comparison with textile yarns. This reduces the number of yarn reels. In contrast, NF yarns with high Tex may not fill-out the moulds with fine shape details or resin penetration into the yarn might be obstructed. It influences techniques like winding, pultrusion or pulwinding, which are used in building application composites, like window frames or door frames. Therefore, the relationship between yarn linear density and mechanical properties was analysed. In the textile industry, the term breaking tenacity is the tensile stress at rupture of a fibre, yarn, filament or cord. The tenacity is expressed in Newtons per tex, grams force per tex or gram force per denier [5]. The test procedure for determination of the Tex values and tenacities of a yarn is described in standards ISO/DIS 2062 and ISO 2060:1994 . The Tex value is measured by weighting 10m yarn fragments. The result is expressed in grams per 1000 meters. The tenacity is measured by tensile testing 250mm yarn fragments. A load is applied at a constant speed of 250mm/min. Therefore, this test measures the strength of the weakest link along the 250mm gauge length. The tenacity (z) is a yarn breaking load expressed in cN and is calculated with following equation:

$$z = \frac{1000 \times F_b}{s}, \quad (4.)$$

where F_b is a yarn breaking force in Newton, and s is a linear density expressed in grams per 1000m. For instance in pultrusion a composite part is processed by dragging a multiple number of yarns through a mould. An increase of the desired volume of fraction of reinforcement in pultruded section, directly relates to an increase in applied pulling force. This is to counter the increased frictional forces created while compressing more fibres in the same mould. Therefore, individual yarns bear higher pulling forces and break if their tenacity is exceeded. Continuous fibre reinforcement, e.g. glass fibre rowing, withstands significantly higher pulling forces than those required during processing. Since natural NF reinforcements are composed of short fibre yarns, the pulling force which can be applied is

significantly lower than the strength of the individual fibres. It depends on the structure of the yarn and frictional forces keeping fibres together.

Figure 61 presents cumulative results of dry yarn tensile tests with 250mm gauge length. The highest average breaking force was measured in yarns with 86Tex and 130Tex values. As an example, hemp twisted yarn with 130Tex had mean diameter of $d = 269.3 \pm 39.8\mu\text{m}$. Constituent technical fibre composing hemp yarn has $d_f = 14.4 \pm 3.6\mu\text{m}$. The mean load carrying capacity of a 130Tex yarn at 250mm gauge length was $P_{av}=16.8\text{N}$. The same yarn measured with 4mm gauge length had an average breaking load of $P_{av}=22.45\text{N}$. The average tenacity of a 130Tex yarn was equal to $13.6\text{cN}/\text{Tex}$. High standard deviation values are a result of variation in: fibre diameter, fibre length distribution and loading uniformity on all constituent fibres during the test. Yarns without twist and with parallel fibres have significantly lower tenacity than twisted fibre yarns. The wrapping wire does not create sufficient pressure, which results in a low friction force between individual fibres. During tensile loading, single fibres may start to slide against one another instead of fracturing.

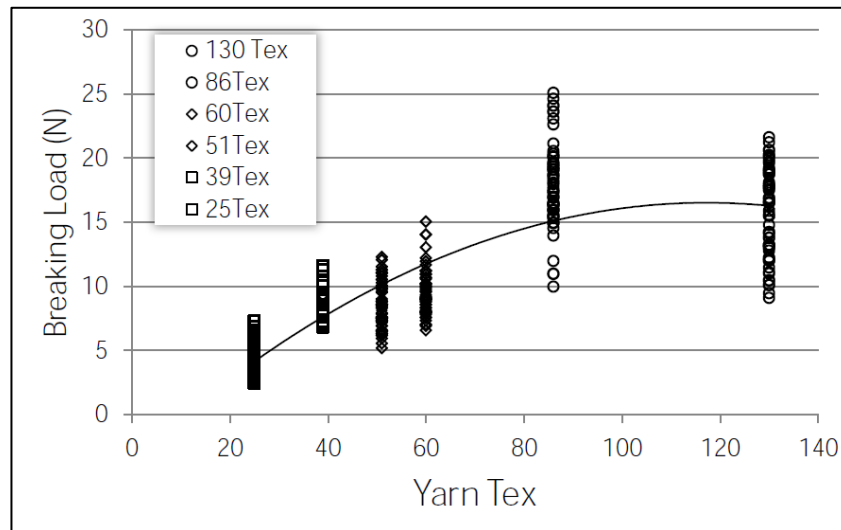


Figure 61 Yarn breaking force results for 250mm gauge length

The aforementioned tenacity results, due to their high variation, are not significant when comparing twisted fibre yarns. Nevertheless, the tenacity test indicates a significant difference in tenacity between twisted fibre and non-twisted fibre yarns. Therefore, yarns with non-twisted fibres will be difficult to use in processing techniques, which require yarn tensioning, i.e. pultrusion or winding.

In order to observe if the yarn linear density has an influence on the NFRP tensile properties, laminates made with six grades of hemp yarns were tested. Figure 62 presents a graph of tensile modulus, engineering tensile strength and tensile strain of those laminates. Hemp yarns with six Tex values, namely 25Tex, 39Tex, 51Tex, 60Tex, 86Tex to 130Tex were tested. Laminates were processed with 41% volume fraction of unidirectionally aligned yarns, which were impregnated in a PalapregECO matrix with the procedure illustrated in Figure 39.

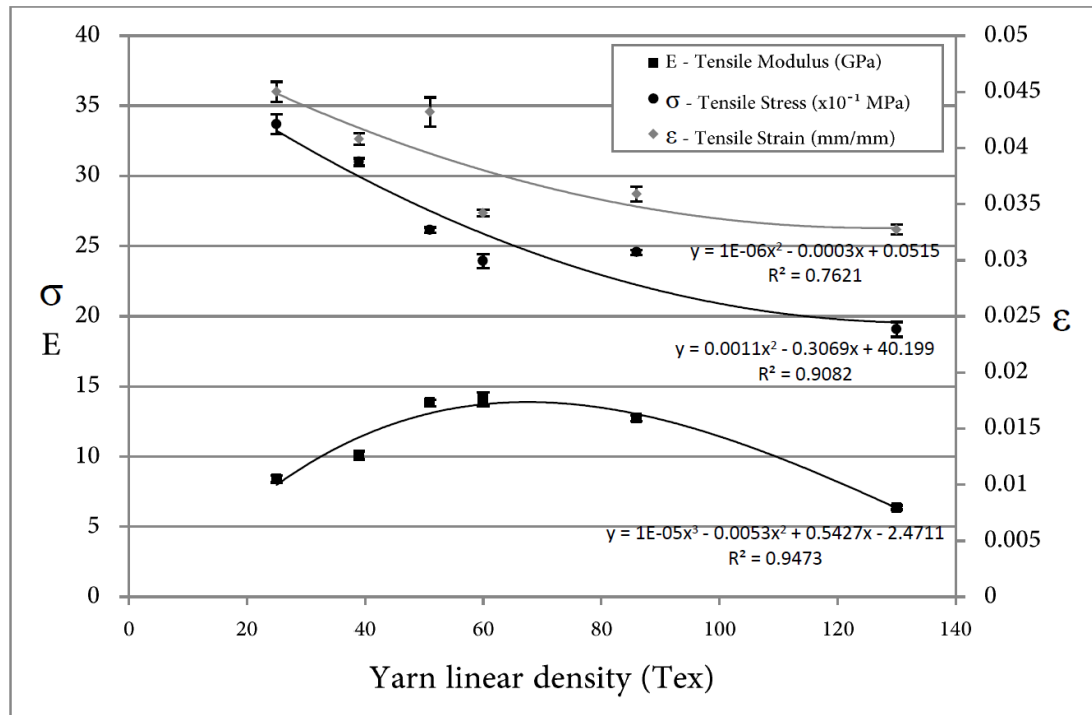


Figure 62 Influence of the yarn linear density (Tex) on tensile modulus, tensile stress and tensile strain in NFC laminates reinforced with twisted architecture hemp yarns

It is evident that the tensile modulus of the composites increased and then decreased with the increase of yarn Tex values. The optimal yarn Tex grades for the tensile modulus were 60Tex and 51Tex, which resulted in a tensile stiffness of 14.1GPa and 13.8GPa respectively. The lowest tensile modulus of 6.37GPa was obtained for the composites with 130Tex yarn. However, the relationship between yarn linear density and engineering tensile strength is different from the relationship of the tensile modulus with Tex values. It seems that there is a close to linear relationship between Tex value and tensile strength when the Tex values range from 25Tex value (337MPa) up to 60Tex (239MPa). After that, the values

deviate from a linear decrease in the ultimate tensile stress. There is about 70% difference between laminates reinforced with the 130Tex yarn and 25Tex yarn, i.e. from 190MPa to 337MPa, respectively. The highest tensile strength was achieved for yarns with the medium linear density, which might be explained by an improved wetting and resin penetration into the fine yarns. There might be dry spots and delamination present between single fibres in the inner part of too high Tex yarns due to the reduced resin penetration. It must be noted that the cross-section images do not give an unambiguous answer, because visible delamination between fibre and matrix could be present due to the polishing process during cross-section preparation. The tensile strain to failure follows the trend of the tensile strength. The highest strain to break was measured for the 25Tex reinforced laminate (0.045mm/mm) and the lowest strain to break was achieved for laminates reinforced with 130Tex yarns (0.032mm/mm). Figure 63 illustrates longitudinal and transverse cross sections of the hemp yarn unidirectionally reinforced laminate. Uniform distribution of yarns is visible with small pockets of matrix. Processing allowed for individual yarn coating and resin penetrated into the yarns. It is apparent that each individual yarn creates a separate entity and is composed out of individual fibres.

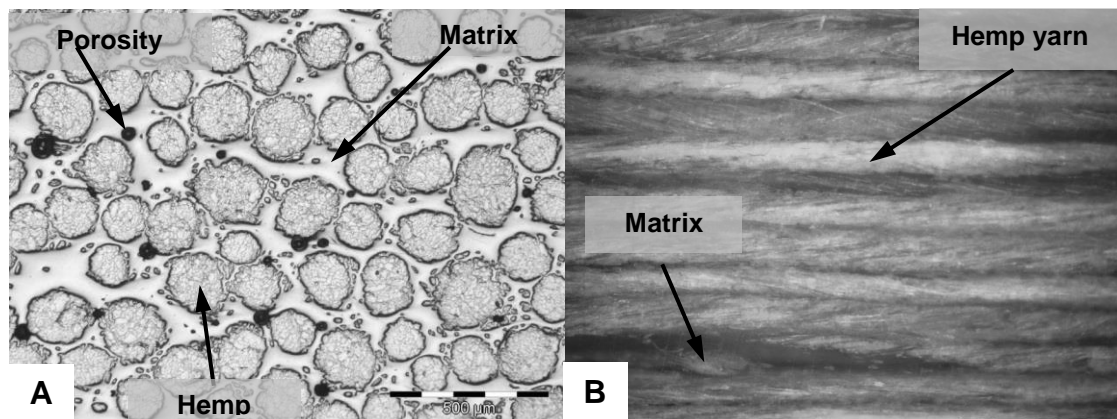


Figure 63 Cross sections of 25Tex hemp yarn unidirectionally reinforced laminate: (A) transverse and (B) longitudinal

4.3 Effect of the Yarn Twist

The highest potential for the orthotropic fibrous laminates is in their tensile properties parallel to the direction of the fibres. NFCs are not an exception. NF yarns are composted

out of multiple inherently finite in length fibres, which are combined into a coherent assembly. Yarns used as reinforcement can be classified by structure, namely twisted or parallel fibre arrangement. The twisted fibres yarns are used in the textile industry since times immemorial. The twist induces a friction force between the fibres, keeping them together. Figure 64 presents a relationship between the twist of the yarn and dry yarn strength. Increasing fibre twist increases strength of the yarn because a higher percentage of individual fibres will break, rather than slip, when the yarn is loaded. After exceeding the optimum level of the twist, fibres start to deform and yarn strength is reduced [149]. There are a couple of factors to be taken into account when analysing twisted fibre yarns, namely fibres are not evenly distributed across yarn diameter, the core of the yarn is densely packed, fibres are migrating across the diameter and individual fibres have variable mechanical and physical properties; therefore, they do not break at the same time when the yarn is loaded [150].

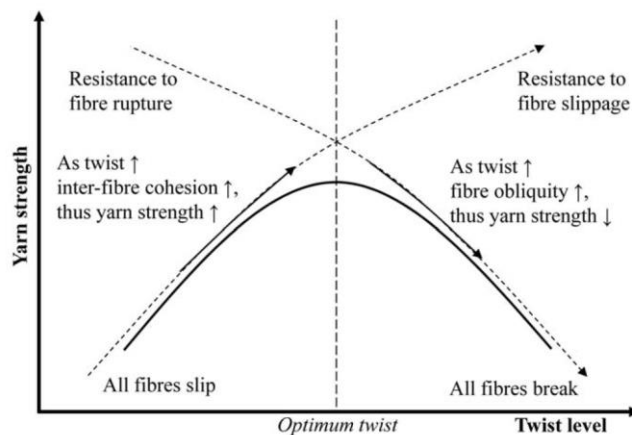


Figure 64 Relationship between the twist level and yarn strength [149]

Individual fibres within a yarn are positioned at an angle to the yarn length. This angle is dependent on the twists per unit of length, fibre and yarn dimensions. Moreover, it is not uniform, since it changes throughout the diameter of the yarn, which is an outcome of the processing procedure used. The average fibre orientation angle can be calculated [151] and works have been conducted to correlate yarn twist with composite strength [152]. Non-twisted fibre yarns are a new invention, which was specifically developed to use as a composite reinforcement. Individual fibres are aligned in sliver and wrapped with a polymeric yarn to hold fibres together. In order to compare the performances of twisted

and untwisted yarn architectures, three types of flax yarns were used i.e. two with twisted (240Tex and 390Tex twisted flax yarns) and one with non-twisted fibres (250Tex non-twisted Biotex flax yarns) (Table 9). Samples were processed by winding and compression moulding (Figure 38).

Table 9 Tensile properties of laminates with twisted and non-twisted yarn with Palapreg-Eco resin as a matrix

<i>Sample</i>	<i>Tensile Modulus (GPa)</i>	<i>RSD (%)</i>	<i>Tensile Stress (MPa)</i>	<i>RSD (%)</i>	<i>Tensile strain (mm/mm)</i>	<i>RSD (%)</i>	<i>Poissons ratio</i>	<i>RSD (%)</i>	<i>Vf (%)</i>	<i>Density (kg/m³)</i>
Non-twist 250Tex	10.3	3.5	197	3.2	0.032	1.8	0.33	9.6	50.9	1290
Twisted 240Tex	9.4	4.3	267	4.5	0.031	2.4	0.17	10.1	48.9	1310
Twisted 390Tex	7.6	9.5	244	3.7	0.035	2.1	0.20	18.3	50.3	1320

In order to compare the performances of twisted and ‘parallel fibre’ yarn architectures, three types of flax yarns were used to process laminates with PalapregEco polyester matrix. Figure 29A, Figure 29B and Figure 33 present three yarn reinforcements used, namely flax 250Tex non-twisted fibres wrapped with polymeric wire, flax unidirectional rowing made out of 240Tex yarns with the twist and flax unidirectional rowing made out of 390Tex yarns with the twist. Laminates were processed with volume fractions ranging from 50.9 to 48.9% volume fraction (Vf). It is evident that the laminate reinforced with non-twisted 250Tex yarns and laminate with twisted 240Tex yarns had a similar tensile stiffness (10.3GPa and 9.4GPa), especially when the lower Vf of the latter laminate is considered. The laminate reinforced with 390Tex yarns had the lowest stiffness (7.64GPa). Contrary to the tensile stiffness results, non-twisted yarn reinforced laminates had the lowest tensile stress (196.7MPa), while the twisted yarn 240Tex and 390Tex reinforced laminates performed at 267.3MPa and 243.7MPa, respectively. It is apparent that the yarn twist influenced the laminate tensile properties. The twisted-fibre yarn architecture has an angular arrangement of individual fibres and fibres in the non-twisted yarn architecture are parallel in relation to the yarn main axis. When analysing dry fibre tenacity, increasing fibre twist increases the strength of the yarn because a higher percentage of individual fibres may break rather than slip. However, exceeding the optimum level of the twist may result in

severe fibre deformation and hence reduction in strength [10]. This partly explains why the tensile stiffness of 250 Tex non-twisted flax laminate is higher than that of the 240 Tex twisted flax laminate, which is also higher than that of laminate reinforced with 390 Tex flax yarns. Another part of the explanation is the adhesion between fibres and matrix, which directly influences tensile stiffness, and the bond between untreated cellulosic fibres and the polyester matrix. The interface between reinforcement and matrix transfers the loads from the matrix onto fibres and from fibres onto matrix. If the interface bond between fibre and matrix is sufficient, the composite fractures by fibre break as opposed to fibre pull-out mode [153, 154]. Figure 65 presents a cross section of the flax twisted yarn reinforced laminate. There is a visible stacking arrangement of the yarns, which ensures sufficient compaction. This is one of the conditions for achieving the desired volume fraction. Polyester wire, which wraps the yarns together in a roving of parallel yarns, is visible as white areas. Nevertheless, an agglomeration of the wrapping wires in the same plane can create a site, within the laminate, with reduced matrix strength due to reduced adhesion between polymeric wire and matrix. It is the same for non-twisted flax yarns, but polymeric wires are wrapping individual yarns and travel along their lengths.

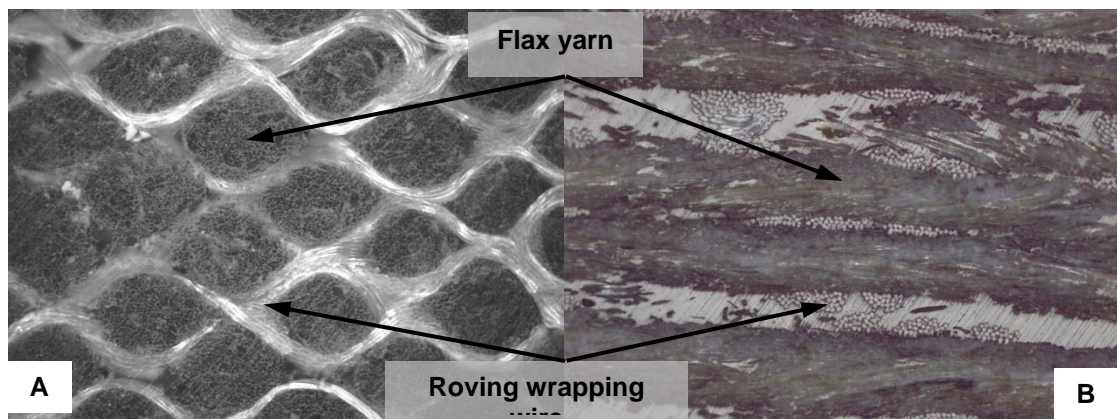


Figure 65 (A) Uniform yarn stacking arrangement in twisted flax yarn reinforced laminate transverse cross section with visible (B) Longitudinal cross section of flax reinforced laminate with yarns and wrapping wire

Fracture patterns of test pieces with two yarn types were compared. The influence of wrapping wire may explain the perpendicular fracture pattern in laminates reinforced with roving of yarns held together by a perpendicular polymeric wire (Figure 66A), and the angular fracture pattern observed for laminates with non-twisted yarns (Figure 66B). As

fractures occur at a sample's weakest point, this pattern suggests that the weakest points are at the positions where wrapping wires connect with fibres.

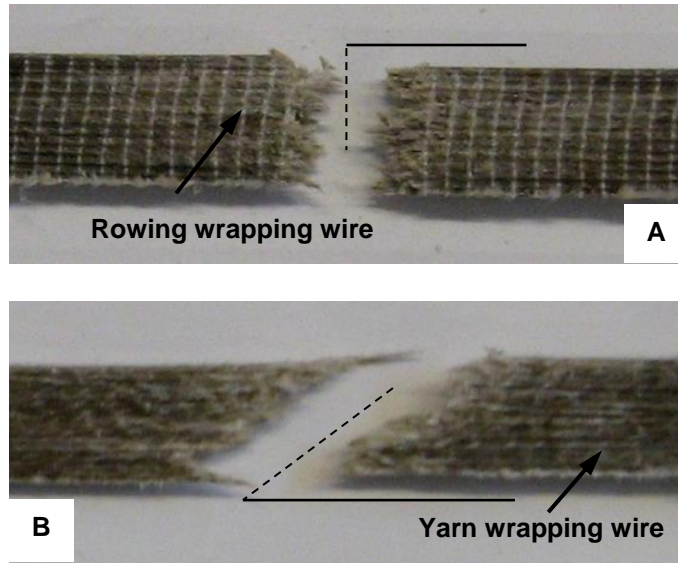


Figure 66 (A) Twisted flax F12 yarn rowing laminate (B) Non-twisted flax yarn reinforced UD sample fracture modes

Figure 67 presents examples of four yarns with twisted and non-twisted yarns, namely hemp-wool hybrid non-twisted yarn (A), flax 250Tex non-twisted yarn (C), and two hemp yarn types with twisted architecture, i.e. 39Tex (B) and 130Tex (D).

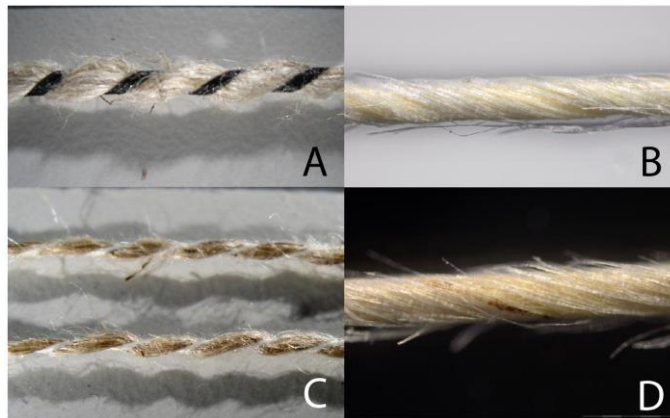


Figure 67 Comparison of non-twisted and twisted yarns. (A) Hemp-wool 1000Tex non-twisted yarn (B) Hemp twisted 39Tex yarn (C) Flax 250Tex non-twisted yarns. (D) Hemp 130Tex twisted yarn

In yarns with parallel fibres (A and C) a sinusoidal fibre pattern is clearly visible. This yarn shape is not uniform across the whole yarn length, but it is increased when the yarn is

tensioned. This suggests that the processing techniques, which use tension for reinforcement alignment, e.g. pultrusion, winding, would deform the yarn and change the orientation of the individual fibres. Figure 68 illustrates the proposed deformation diagram of the yarn wrapped with polymeric wire, where A is the non-deformed yarn with parallel fibres and B is the yarn with misalignment build-up. The reasons for the misalignment may include tensioning, stresses induced during wrapping, wire shrinkage or stretching during processing. When the wrapping wire is axially tensioned, it induces stress on fibres causing them to slide against one another and bend to accommodate. This results in misalignments of the individual fibres within the laminate. Moreover, points where the wrapping wire connects with fibres, indicated with arrows, may impair resin penetration during processing, which creates dry spots and delamination.

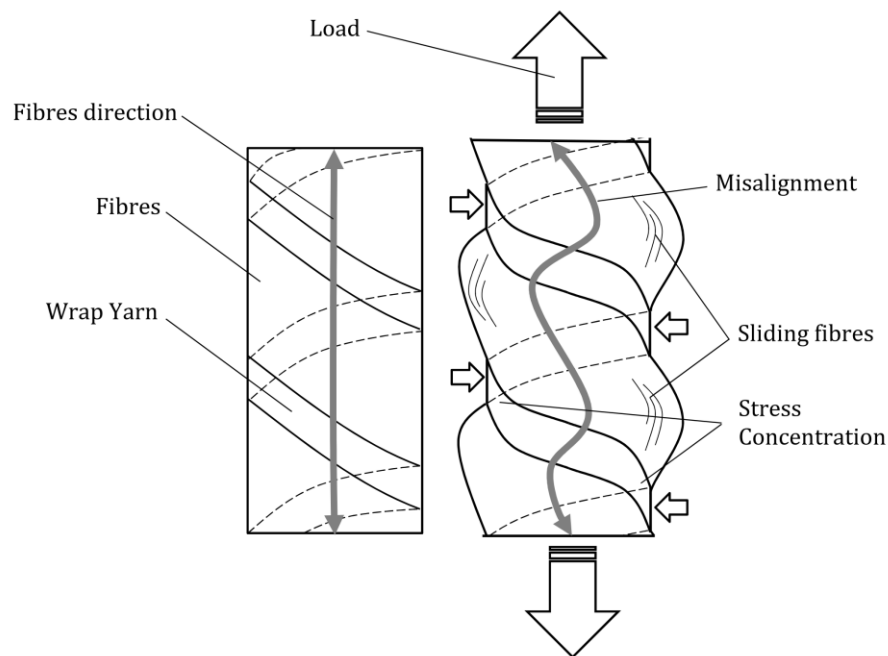


Figure 68 Diagram of unidirectional non-twisted yarn theoretical shape (Left) and actual shape deformation morphology (Right)

In summary, when comparing twisted yarns and non-twisted yarns, the higher tensile strength of the tested flax laminates made with twisted yarns may be explained by interlocking mechanism. The twisted yarns, unlike non-twisted yarn, even in the presence of a weak interface, will continue to transfer load through the friction forces between individual fibres. In contrast, flax laminates with non-twisted yarns, exhibited slightly

higher tensile stiffness, which is explained by individual fibre orientation in the yarn length direction.

4.4 Effect of Lamination

Arranging natural fibres into yarns and then into fabrics facilitate easier handling and stacking of laminate layers. The arrangement of the fabric layers within a laminate has an influence on the tensile properties (Table 10). The first four laminates in Table 4 were reinforced with four layers of 4x4hopsack fabric in $[0/90]_4$ arrangement, where $[0/90]_4$ means that four layers of hopsack fabric are arranged in the same direction ($0/90^\circ$). Among these, two laminates were processed with vacuum bagging technique and the other two with compression moulding. Both Cistic and Palapreg-Eco resins were used for compression and bagging techniques. The seventh laminate was processed with a symmetric $(4 \times 4[(0/90), (45/45)]_5)$ stacking sequence, where $[45/45]$ means that layers of hopsack fabric are arranged at 45° to the main laminate direction. The eighth laminate was composed of hemp mat between two layers of flax 4x4hopsack fabric. The last two laminates were processed with five layers of 2x2 twill fabric arranged in the same direction ($0/90^\circ$). It is apparent that, overall, the highest tensile strength was achieved for the composites with weft and wrap yarns arranged at $0/90^\circ$ to the testing direction, with tensile strength and stiffness at the level of 71MPa and 7.48GPa, respectively. This is an expected outcome, since a higher percentage of the reinforcement is aligned with the loading axis. Hybrid laminate samples composed of flax fabric outer surfaces and hemp core with 45/55 hemp to flax ratio had the lowest strain to failure, at the level of samples reinforced with randomly oriented fibres described in the previous section.

Table 10 Tensile test results for unsaturated polyester reinforced with fabrics weaved from twist less flax yarns

<i>Laminate stacking sequence</i>	<i>Process</i>	<i>Resin</i>	<i>Tensile Modulus (GPa)</i>	<i>RSD (%)</i>	<i>Tensile Stress (MPa)</i>	<i>RSD (%)</i>	<i>Tensile strain (mm/mm)</i>	<i>RSD (%)</i>	<i>V_f (%)</i>	<i>Density (kg/m³)</i>
4x4hopsack [0/90] ₄	Vac	Palapreg	4.34	6.0	41.35	7.7	0.037	6.4	32.3	1250
4x4hopsack [0/90] ₄	Vac	Crystic	5.28	5.0	54.51	3.5	0.032	6.6	33.0	1210
4x4hopsack [0/90] ₄	CM	Crystic	7.48	3.8	70.91	7.5	0.026	1.6	45.2	1340
4x4hopsack [0/90] ₄	CM	Palapreg	6.66	4.3	63.31	6.4	0.034	9.3	45.1	1320
2x2twill [0/90] ₅	CM	Crystic	5.61	6.6	66.33	8.2	0.047	9.2	43.1	1320
2x2twill [0/90] ₅	CM	Palapreg	5.98	1.8	61.13	1.6	0.035	2.8	44.1	1300
4x4[(0/90),(45/45)] ₅	CM	Palapreg	5.88	3.1	51.43	4.2	0.028	4.5	44.1	1300
4x4(0/90),HM,4x4(0/90)	CM	Palapreg	6.48	2.2	47.90	4.2	0.018	7.7	42.7	1290

Vac – Vacuum bagging processing, CM – Compression moulding with Hot Press., HM-Hemp mat., 4x4 – Hoopsack 4x4 fabric,

4.5 Effect of Impregnation

It seems that there is a direct reflection of compression to the density of the composites. The apparent density of composites ranges between 1.21 and 1.24 g/cm³ for vacuum bagged and 1.29 to 1.34 g/cm³ for hot pressed curing processes (Table 10) due to less compaction of composite mats by vacuum bagging process than by compression moulding. Naturally, the samples processed with the vacuum bagging process had low properties, e.g. 4GPa and 41MPa for tensile modulus and strength respectively in laminates reinforced with 4x4 hopsack flax fabrics. The vacuum pressure acting on the impregnated fabric stacking during processing may also be insufficient to compact the sample to achieve volume fraction above 40%V_f. The maximum achievable volume fraction of the reinforcement, for 4x4 Hopsack fabric, was at the level of 33%V_f in comparison to compression moulded laminates of 44±1.5%V_f. The difference is a direct outcome of a processing pressure used between atmospheric pressure (101kPa) in vacuum bagging and 2.4MPa applied by the hot press. The low pressure of vacuum bagging may also result in a low penetration of resin into the yarn and hence the interface quality and bonding strength of matrix and fibre reinforcement. The resin system has an influence on the penetration

into the yarn. When both resin systems are compared for 4x4hopsack $[0/90]_4$ and 2x2twill $[0/90]_5$ laminates, it is visible that the laminates with Crystic resin had slightly higher tensile properties than PalapregEco. When comparing 4x4hopsack $[0/90]_4$ laminates impregnated with the hot press procedure, the tensile properties for both strength and stiffness are 12% higher for Crystic. When compared with unreinforced Crystic resin, the tensile stiffness was doubled (i.e. increased by approx. 4GPa), and when compared with unreinforced PalapregEco resin by 3GPa. There is almost no increase in engineering tensile strength for laminates with PalapregEco matrix (i.e. from 60MPa to 63MPa), but an increase of 40% (i.e. from 50MPa to 70MPa) for laminates with Crystic matrix. The difference comes from two reasons. Firstly, the strength of cured Crystic resin itself is lower. Secondly, Crystic resin may have slightly better compatibility with the flax reinforcement.

4.6 Effect of Yarn Arrangement in Fabric

Using reinforcements in the form of fabric allows for close packing and simultaneous biaxial reinforcement. The fabric is easy to handle and arrange. Processing techniques like laying-up use woven reinforcement. The drawback in fabric is the waviness, which changes the axial filament arrangement, thus influencing the mechanical properties of the composite. Mechanical properties of laminates vary with the change in the forms of waved fabrics [155, 156]. This subject is investigated here using the example of flax fabric reinforced laminates. Figure 69 presents six most common biaxial fabric architectures, namely plain, twill, satin, basket, leno and mock leno. The differences are in how weft yarns are drawn through the wrap yarns.

Two types of fabrics with different waving levels, i.e. hopsack and twill were used to produce NFCs, compared with a laminate reinforced with a flax 250Tex yarn rowing. All three samples were made with the same flax 250Tex yarn with non-twisted fibres. Figure 70 presents laminate surfaces with both fabrics.

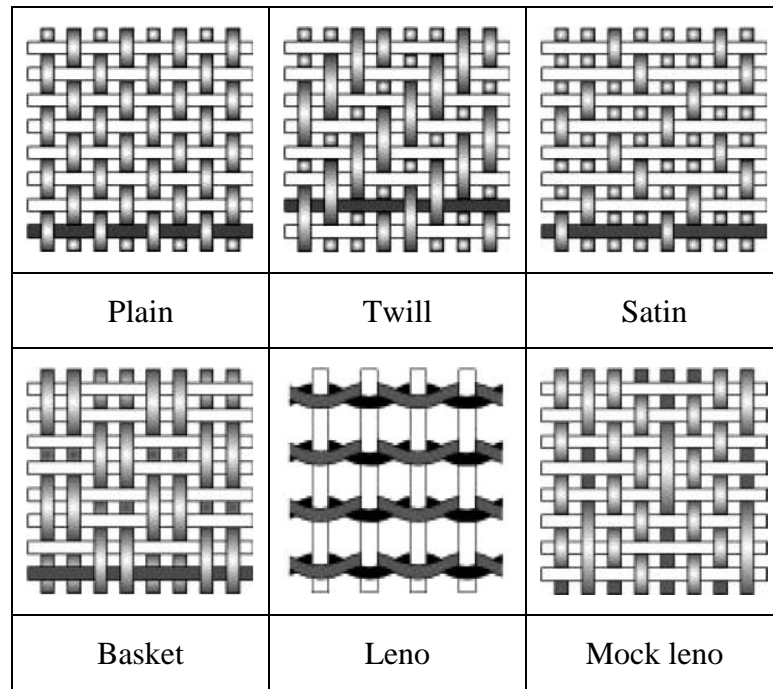


Figure 69 Common weave architectures [11]

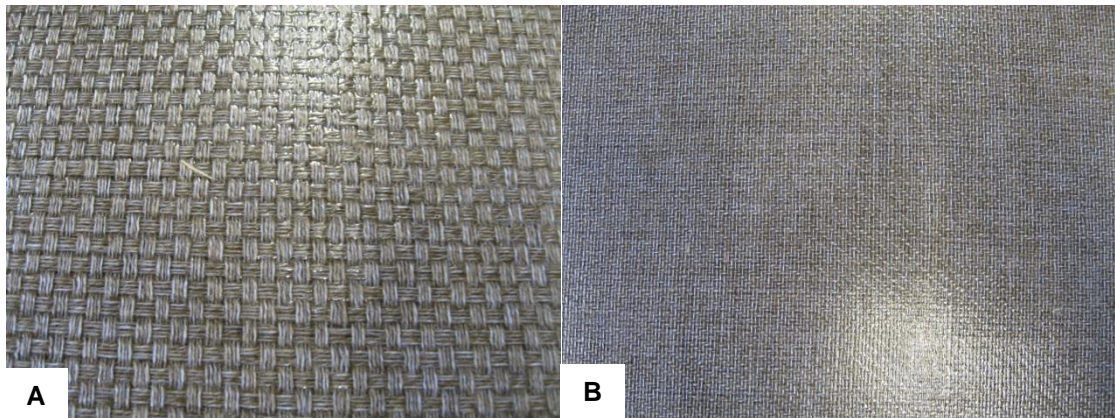


Figure 70 (A) Surface of a laminate reinforced with 4x4 hopsack fabric (B) Surface of a laminate reinforced with a 2x2 twill fabric

Weaving of yarns within a fabric may deteriorate the laminate in-plane tensile properties. It is apparent that the tensile strength and modulus of elasticity of the laminates decrease significantly between unidirectional and fabric reinforced laminates (Figure 71). There is a slight decrease of those properties with an increase in waviness (i.e. hopsack and twill fabrics), which dislocates the fibres from the axial direction and creates stress concentrations at weft and wrap crossovers. Hopsack 4x4 fabric is weaved with strands of four 250Tex yarns in a plane wave arrangement and twill 2x2 is weaved with single yarns,

where diagonal stripes are revealed. Both types of yarns are arranged at 90° lengthwise to each other, but in the twill 2x2 fabric the yarn goes through a double amount of alterations across the length when compared with 4x4 hopsack fabric[157]. This difference resulted in a decrease of 20% and 18% in modulus and tensile strength for 2x2 twill and 4x4 hopsack reinforced composites, respectively, when compared to UD composites. An increase in concentration of crossovers of twill fabrics compared to hopsack results in a decrease of tensile modulus and tensile strength of 10% and 4%, respectively. Consequently, the tensile strain to failure increases by 50% for 4x4 hopsack composites and 60% compared to 2x2 twill composites, compared to UD composites. This means that the weaving may have resulted in strain concentration and/or distortion of yarns, which could hence result in an increase or decrease of strength in a certain direction because of the anisotropic nature of natural fibres.

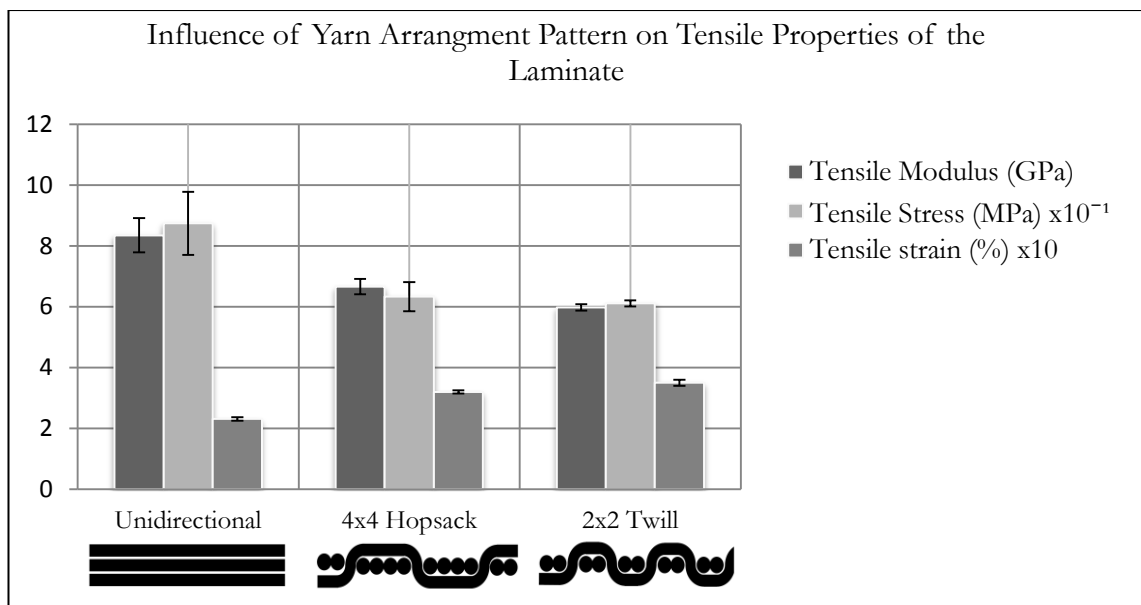


Figure 71 Differences in tensile properties between laminates made with fabrics and unidirectional laminate

4.7 Effect of Hybrid Hemp-Wool Reinforcement

Hemp-wool mat and hemp-wool yarn laminates were developed and characterised to investigate the influence of hemp fibre reinforcement hybridisation with wool fibres on tensile properties of NFRPs. Randomly oriented hemp and hemp-wool hybrid mats were

composed of 20% of wool fibres and 80% of hemp fibres, combined together by a process called hydro-entanglement. A second type of mat with 100% hemp fibres was processed by a conventional process, which uses press in order to consolidate fibres into a mat. Hemp-wool mats were laminated with Crystic polyester resin and 100% hemp mats were laminated with both Crystic and Palapreg-Eco resins. Figure 72 illustrates the surface of the processed laminate reinforced with hemp-wool mat and a fracture area of the test piece after a tensile test. It is evident that the fibres have random arrangements and the wool fibres have wavy shapes. The fracture area reveals a clear fracture with a composite fracture by fibre fracture.

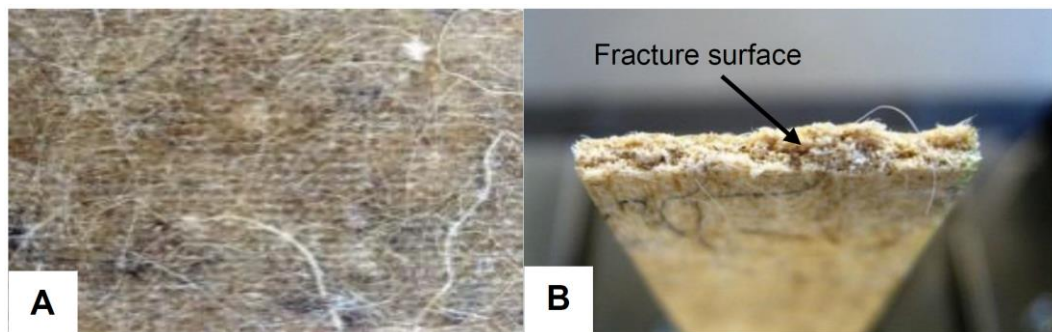


Figure 72 (A) Impregnated hemp-wool mat in polyester resin with black and white wool fibres and light brown hemp fibres (B) Fracture surface of the hemp-wool mat polyester laminate after tensile test

Table 11 presents tensile test results for three types of composites tested, namely two types of hemp mat laminates with Crystic and Palapreg-Eco resins and a hemp-wool mat laminate reinforced with Crystic resin.

Table 11 Properties of hemp mat and hemp wool hybrid mat

<i>Reinforcement</i>	<i>Matrix</i>	<i>Ultimate tensile stress (MPa)</i>	<i>RSD (%)</i>	<i>Tensile Modulus (GPa)</i>	<i>RSD (%)</i>	<i>Tensile strain (%)</i>	<i>RSD (%)</i>	<i>Fibre volume fraction (%)</i>	<i>RSD (%)</i>
Hemp-Wool mat	Crystic	38.53	3.04	2.90	3.36	1.63	8.06	26.1	2.34
Hemp mat	Crystic	50.31	3.89	6.80	2.07	1.83	6.28	29.8	3.26
Hemp mat	Palapreg-Eco	37.76	6.90	5.64	4.95	1.68	4.53	29.2	3.46

The average tensile modulus for hemp-wool composite was 2.9GPa compared to 6.8GPa for hemp mat laminate with the same resin system. The stiffness of wool fibre oscillates around 4GPa [77], which is up to 20 times lower than the stiffness of hemp or flax fibres. It must be noted that the resin systems also had an influence on tensile properties. Hemp composites with Crystic resin system achieved a higher tensile strength (50.3MPa) and stiffness (6.8GPa), compared to tensile strength (37.8MPa) and tensile stiffness (5.6GPa) of the hemp palapreg-Eco laminate. It is evident that the inclusion of wool fibres results in a reduction of both tensile strength and stiffness. This may be attributed to several factors, i.e. low self-strength of wool fibre, compatibility of wool with resin and inconsistent distribution of wool fibres in the mat. Hemp-wool yarn laminates have also been investigated. As mentioned in the previous section, composites reinforced with yarns allow for a higher volume fraction and increase in the accuracy of fibre orientation. Hemp yarns with inclusion of 10% of wool fibres were wrapped into 1000Tex linear density twist-less assembly (Figure 73). The results of the hybrid laminates reinforced with aligned yarns are given in Table 12. There were three types of composites processed with 73.5%, 50.6% and 41.4% volume fraction of the hybrid hemp-wool twist-less 1000Tex yarn.

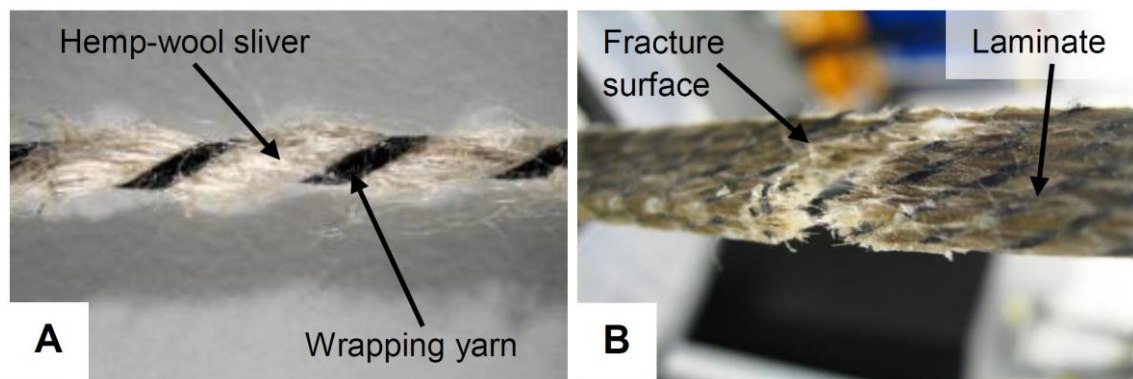


Figure 73 (A) Macro image of a single hybrid 1000Tex hemp-wool yarn (B) Fracture area after tensile test. The fracture line corresponds to the direction

The tensile properties of hemp-wool yarn laminates are influenced by the reinforcement volume fraction. The ultimate tensile stress increased by 30%, from 166MPa to 202MPa, when the volume fraction was increased by 32%. Contrary to the ultimate tensile stress, the tensile stiffness was not significantly influenced by the change in yarn volume fraction.

Tensile stiffness for these laminates ranged between 9.7GPa and 10.5GPa. The tensile strain slightly increases from 0.027mm/mm to 0.030mm/mm with the increase in volume fraction.

Table 12 Tensile properties of aligned non-twisted yarn reinforced hemp-wool hybrid composites with Palapreg-Eco matrix.

<i>Sample</i>	<i>Tensile modulus (GPa)</i>	<i>RSD (%)</i>	<i>Ultimate tensile stress (MPa)</i>	<i>RSD (%)</i>	<i>Tensile strain (mm/mm)</i>	<i>RSD (%)</i>	<i>V_f (%)</i>	<i>Density (kg/m³)</i>
Hemp Wool A	9.66	8.97	201.9	2.93	0.0298	1.76	73.56	1330
Hemp Wool B	8.98	6.85	190.2	4.16	0.0295	2.32	50.57	1310
Hemp Wool C	10.52	7.20	166.1	4.02	0.0274	3.03	41.38	1310

Yarns with unidirectional fibres were designed to enhance the control over the alignment of the fibres; thus improving the tensile properties. This is evident in the aforementioned test results. The increase in fibre loading improved ultimate tensile stress, but did not increase the tensile modulus of hybrid hemp-wool laminates. Figure 74 A presents cross sections of the hemp-wool reinforced hybrid laminates. Wool fibres are round and equally distributed throughout the hemp-wool mat. Hemp fibres are present in bundles and single fibres. Hemp fibre bundles are present because of the mechanical decortication process used for hemp fibre separation, which left some of the fibres bonded. The hemp-wool yarn (Figure 74B) is composed of wool and mechanically decorticated hemp. There are equally distributed hemp fibre bundles and wool fibres. The yarn constitutes a coherent entity, when compared with randomly distributed mat fibres. Nevertheless, it is clear that the matrix penetrated into the yarn.

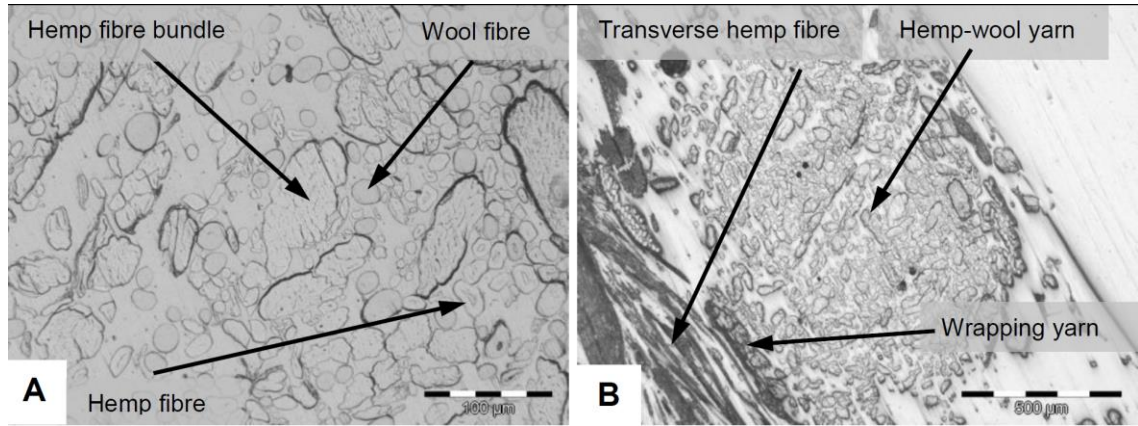


Figure 74 (A) Cross section of the hemp-wool hybrid mat reinforced laminate (B) Hemp-wool hybrid yarn reinforced laminate cross section

4.8 Minimum and Maximum Volume Fraction

The volume fraction of the reinforcement is an important factor, which influences the mechanical properties of the composites. There are two arrangements which give the highest packing of fibres with circular cross sections, i.e. hexagonal and square packing [158]. It can be shown that the maximum volume fraction for the hexagonal packing is

$$V_{fmh} = \frac{\pi}{2\sqrt{3}} \left(\frac{r}{R_{min}} \right)^2 \quad (5.)$$

and in case of the closest fibre packing it becomes

$$V_{fms} = \frac{\pi}{2\sqrt{3}} \quad (6.)$$

The maximum volume fraction for the square packing arrangement is

$$V_{fms} = \frac{\pi}{4} \left(\frac{r}{R_{min}} \right)^2 \quad (7.)$$

and for the case of closest fibre packing it becomes

$$V_{fms} = \frac{\pi}{4} \quad (8.)$$

There are minimum (V_{min}) and maximum (V_{max}) critical fibre volume fractions. Below V_{min} and above V_{max} , the properties of the composite do not follow the rule of mixtures, and do not reinforce the composite efficiently. In the case when long fibres reinforce a laminate unidirectionally, Kelly (1965) derived an expression for the minimum critical volume fraction

$$V_{min} = \frac{\sigma_{bm} - \sigma_{fm}}{\sigma_{bf} + \sigma_{bm} - \sigma_{fm}} \quad (9.)$$

where σ_{bf} is the fibre ultimate tensile stress, σ_{bm} is the matrix ultimate tensile stress, and σ_{fm} is the stress acting on the matrix while the laminate is loaded up to the fibre maximum tensile stress. The maximum critical volume fraction V_{max} provides information about the maximum fibre loading for a particular matrix and fibre reinforcement combination. The fibre geometry, resin mechanical properties, interphase properties, reinforcement arrangement and the processing technique influence this value [159]. Pan (1993) presented an expression for fibres above the critical length, linking the fibre spacing ratio and the fibre-matrix properties,

$$\frac{R_{min}}{r} = e^{\left(\frac{\sigma_{bf}}{\tau_s}\right)^2 \frac{G_m}{2E_f}} \quad (10.)$$

where R_{min} is the fibre spacing, r is the fibre radius, τ_s is the shear stress of the matrix, G_m is the shear modulus of the matrix and E_f is the fibre modulus. It was shown that with an increase of matrix shear properties, it is possible to increase efficiency of the fibre packing. For instance, a maximum fibre volume fraction of laminates, which fibres have 50% higher tensile strength than the matrix shear strength, is close to 75%. A matrix shear modulus to fibre modulus ratio (G_m/E_f) equal to 0.02 and 0.25 yields $V_{max}=70\%$ and $V_{min}=20\%$, respectively. This was compared with NF reinforced laminates. The shear modulus of Palapreg bio-polyester resin used is $G=1.28\text{GPa}$. The tensile modulus reported is from 23.5GPa to 90GPa for hemp fibres and from 27.6GPa to 103GPa for flax fibres (Table 2).

Therefore, the ratio between matrix shear modulus and fibre tensile modulus is in the range from 0.054 to 0.015 for hemp fibres, and in the range from 0.046 to 0.012 for flax fibres. It suggests that the maximum theoretical volume fraction of 75% is achievable. Nevertheless, this theoretical discussion about NFRP maximum fibre loading has small significance and an experimental analysis is conducted.

4.9 Effect of Volume Fraction

The influence of the volume fraction on laminate tensile properties was examined experimentally for three types of BFRPs reinforced with hemp and flax yarns. For each laminate type a range of fibre volume fractions was tested. All investigated laminates were processed with Plapreg-eco matrix. Yarns used included non-twisted 250Tex flax yarn, twisted 39Tex hemp yarn and twisted 130Tex hemp yarn. Each result is an average of at least four successfully tested samples. The influence of volume fraction on tensile modulus, tensile strain and tensile stress was of interest. Figure 75 presents an example of a transverse cross section through the hemp yarn unidirectionally reinforced NFC laminate with a 41% V_f . Parallel yarns stretch from left to right and are visible as packed entities. Brighter regions between yarns correspond to matrix material. Microscopic examinations revealed that the resin penetrated the yarns and that processing technique allowed for parallel yarn arrangement.

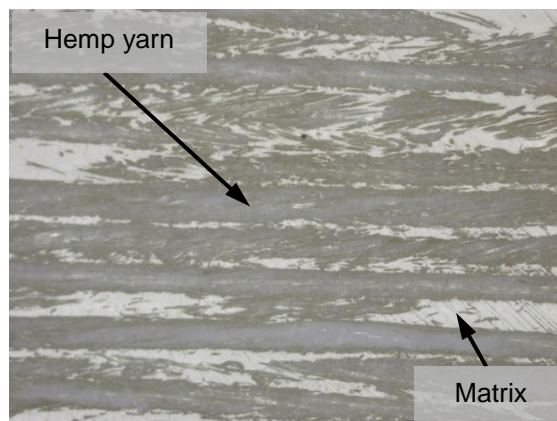


Figure 75 Longitudinal cross section of unidirectionally reinforced laminate with 41% V_f of hemp twisted yarn

4.9.1 39Tex Hemp Yarn Laminate

Figure 76 illustrates the effect of the volume fraction on a laminate with 39Tex hemp twisted fibre yarn. There were five volume fractions tested, namely 23%, 32%, 41%, 51% and 76%. The tensile modulus increases from 7.8GPa to 12.1GPa with an increasing volume fraction up to 51%. A further increase in volume fraction resulted in reduction of tensile modulus down to 10.7GPa at 76% V_f . This suggests that the optimal fibre content is between 51% $V_f < V_{max} < 76\%V_f$ for this laminate type. The tensile strain to break is rising with yarn volume fraction from 0.032 to 0.047 mm/mm in a logarithmic relationship. The tensile stress to break is increasing with the volume fraction from 180.3MPa to 411.1MPa in a logarithmic relationship. Since the maximum modulus was achieved for $V_f=51\%$, the optimally performing laminate selected from this assembly would have 12.1GPa stiffness, 354.1MPa tensile strength at 0.041mm/mm strain. Nevertheless, volume fractions between 51% and 76% could be analysed in order to find the optimal volume fraction for this assembly.

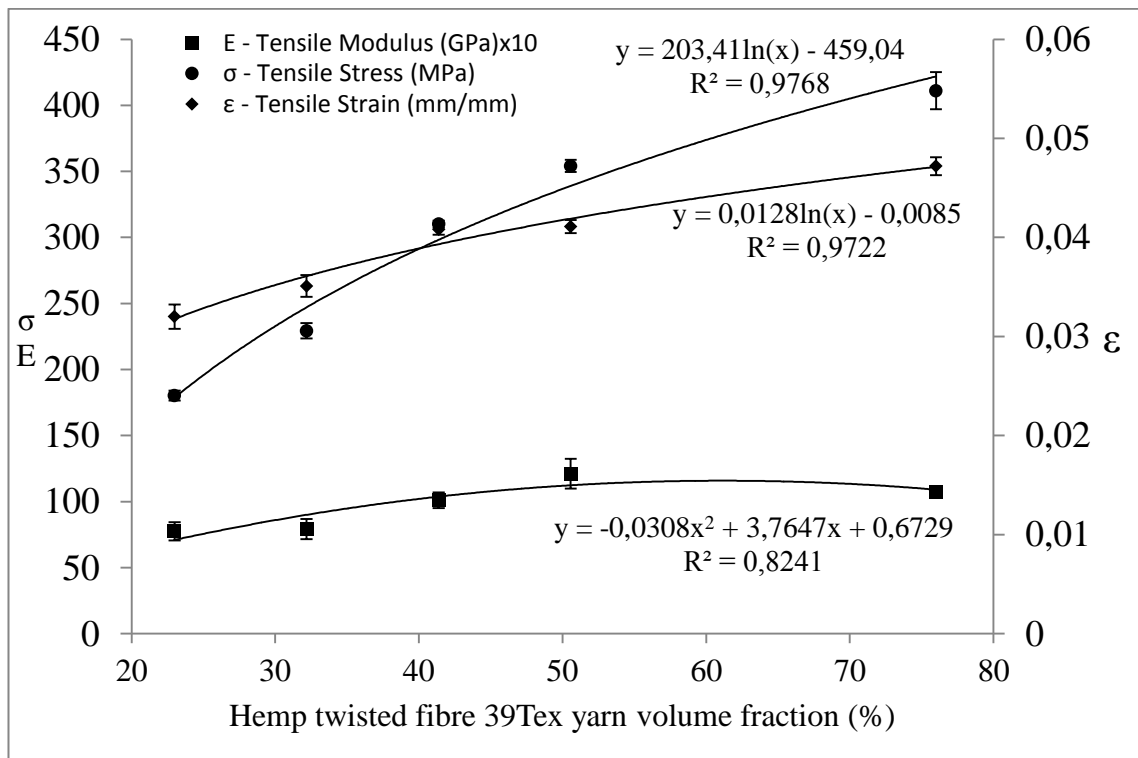


Figure 76 Effect of the volume fraction of hemp twisted fibre 39Tex yarn reinforcement on tensile properties of a unidirectionally aligned laminate with Palapreg-Eco matrix

4.9.2 130Tex Hemp Yarn Laminate

Figure 77 illustrates the effect of the 130Tex hemp twisted fibre yarn volume fraction on a laminate tensile properties. There are three volume fractions tested for this laminate, namely 41%, 51% and 76%. The tensile modulus increases from 6.4GPa to 14.2GPa together with an increase of volume fraction up to the 76%. There is no modulus deterioration visible for $V_f=76\%$, as in the case of the 39Tex yarn, but the influence of volume fraction decreases above 51%. However, the gap between 51% V_f and 76% V_f is broad. The graph suggests that the optimal fibre content, which maximises the tensile modulus, is between 51% $V_f < V_{max} < 76\%V_f$. The tensile strain increases from 0.033mm/mm to 0.036mm/mm, together with volume fraction in a linear relationship. The strain to break for the 130Tex laminate is lower than for the 39Tex hemp yarn, which is consistent with the findings described in the previous section regarding yarn linear density (Tex) influence. The tensile stress to break increases from 190.7MPa to 282.2MPa, with the volume fraction increase, which is significantly lower than results achieved for the hemp 39Tex reinforcement.

The maximum modulus was achieved for $V_f=76\%$. Results suggest that the laminate with an optimal volume fraction has 14.2GPa tensile modulus, 282MPa ultimate tensile stress and 0.036mm/mm tensile strain. However, as mentioned before, there is a wide gap between 51% and 76% volume fractions, and further analysis with finer volume fraction increments could be processed.

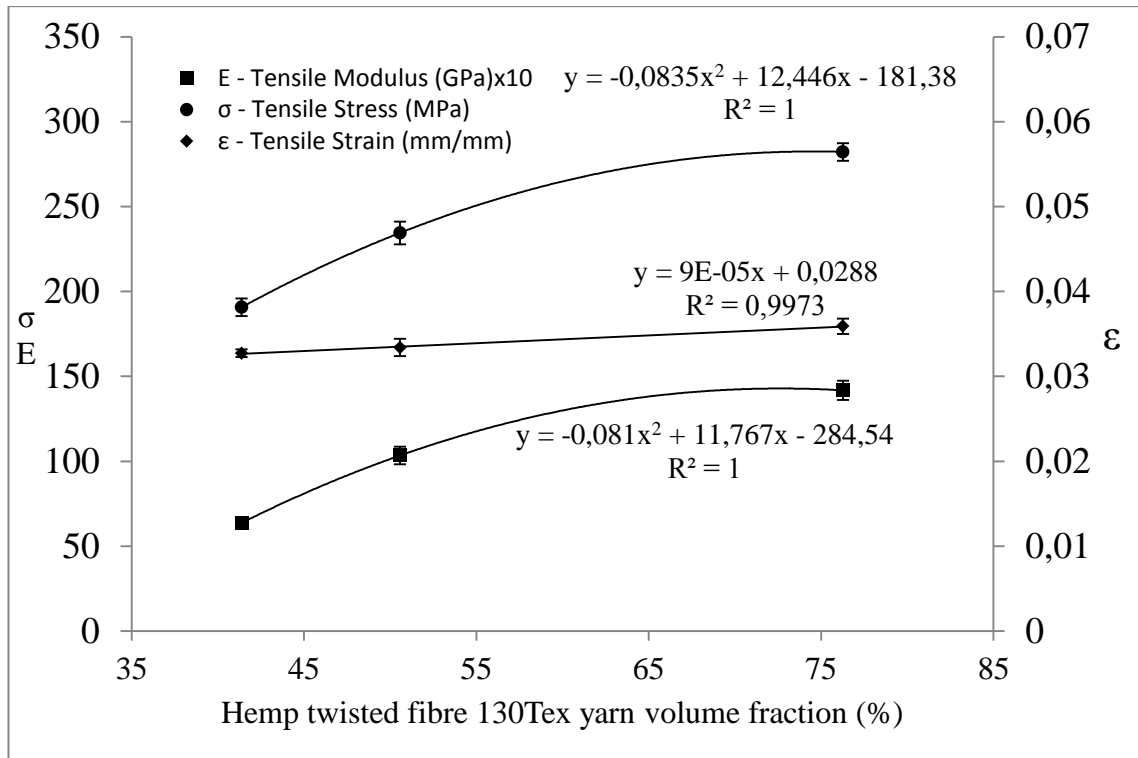


Figure 77 Effect of the volume fraction of hemp twisted fibre 130Tex yarn reinforcement on tensile properties of a unidirectionally aligned laminate with Palapreg-Eco matrix

4.9.3 250Tex Flax Yarn Laminate

Figure 78 illustrates the effect of a change in volume fraction on a laminate with non-twisted 250Tex flax fibre yarn. There were four volume fractions tested, namely 24%, 30%, 51% and 56%. The non-twisted flax yarn is a significantly different reinforcement, when compared with the previous two laminates, since the fibres are aligned and held together with a wrapping wire. The tensile modulus rises from 8.6GPa to 11.3GPa with an increase of volume fraction. The tensile modulus increases with volume fraction up to $V_f=56\%$. This suggests that the optimal fibre volume fraction, which maximises the modulus for this type of laminate, is above 56%. The tensile strain to break grows linearly from 0.023mm/mm to 0.034 mm/mm with increasing volume fraction.

The tensile stress to break increases from 87.4MPa to 196.7MPa between $24\%V_f$ and $51\%V_f$. There is a significant reduction in tensile stress for samples with $56\%V_f$, which achieved 175.3MPa. The maximum modulus was achieved for $V_f=56\%$ but the optimally

performing laminate selected from this assembly has $V_f=51\%$. This results in a laminate with 10.3GPa tensile stiffness, 196.7MPa ultimate tensile stress and 0.032mm/mm tensile strain. The tensile stress and tensile stiffness of flax yarn reinforced laminates are lower when compared to both hemp reinforcements.

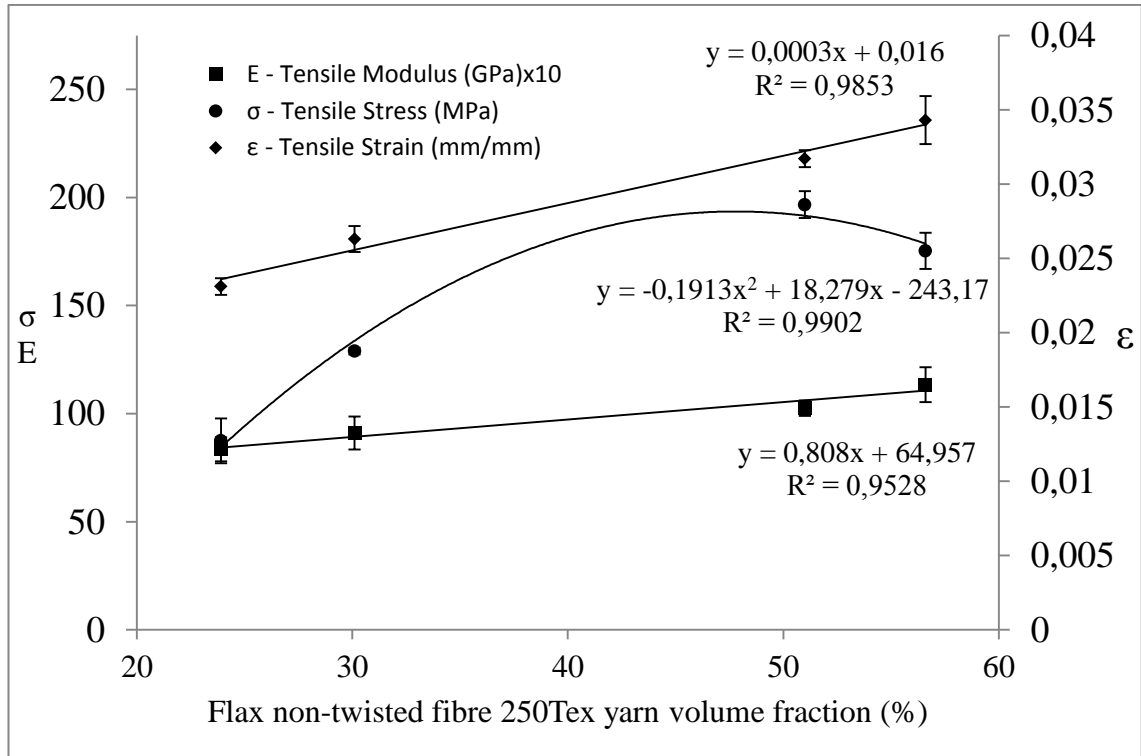


Figure 78 Effect of the volume fraction of flax non-twisted fibre 250Tex yarn reinforcement on tensile properties of a unidirectionally aligned laminate with Palapreg matrix

From the above-mentioned results for the three laminates, the highest tensile modulus, i.e. 14.2GPa, was observed for laminates reinforced with 76% V_f of hemp 130Tex twisted yarn. The highest ultimate tensile stress, i.e. 411MPa, was observed for laminates with thinner 39Tex yarn laminate reinforced as well with 76% V_f . Therefore, reinforcing with hemp twisted yarn produced laminates with higher tensile properties than flax reinforced laminates. The results for flax reinforced laminates present a range only up to 57% V_f , and the tensile modulus slowly increases to this point. However, the ultimate tensile stress declines after 51% V_f .

To summarise, tensile properties of three unidirectional laminates with the same volume fraction of 51% V_f are compared in Table 13. The increase of the fibre volume fraction up to 51% increases the tensile modulus and ultimate tensile stress for all three laminates. It is

apparent that hemp with twisted fibre yarn reinforcement produced a laminate with significantly higher tensile stress and slightly higher tensile modulus. The neat Palapreg-Eco resin system has 3.5GPa tensile modulus and 0.017mm/mm strain-to-break. Inclusion of 51% V_f of a yarn reinforcement increases the tensile modulus above 10GPa, and increases the strain to break above 0.03mm/mm. It was expected that the flax non-twisted yarn would yield a laminate with a high tensile modulus, because of the fibre parallel orientation, but it produced lower results than the twisted hemp yarn. It is assumed that the influence of the combined orientation effect, yarn architecture and interphase between fibre and matrix effect, have significantly higher influence than flax and hemp fibre strength (Table 2). The higher ultimate tensile stress, i.e. 354MPa, and approx. 20% higher tensile modulus, i.e. 12GPa indicate this laminate for use as reinforcement.

Table 13 Comparison of hemp and flax unidirectional laminates tensile properties

<i>Sample</i>	<i>Tensile</i>		<i>SD</i>		<i>Tensile</i>		<i>SD</i>		<i>Tensile</i>	<i>RSD</i>	<i>Vf</i>
	<i>Modulus</i>		<i>Stress</i>		<i>strain</i>		<i>(%)</i>				
	<i>(GPa)</i>		<i>(MPa)</i>		<i>(mm/mm)</i>		<i>(%)</i>				
Hemp 39Tex (twist)	12.1	0.8	354.1	4.6	0.041	3.2	51				
Hemp 130Tex (twist)	10.3	0.5	234.5	6.7	0.033	6.2	51				
Flax 250Tex (non-twist)	10.2	0.4	196.7	6.3	0.032	1.8	51				
Palapreg matrix	3.5	0.1	50.7	1.9	0.017	3.2	0				

4.10 Comparison with Rule of Mixtures (ROM)

The rule of mixtures (ROM) uses a weighted mean to predict the properties of a composite material in the longitudinal and transverse directions. Exploring the usefulness of this method for NFRP is of interest in the context of conducted experiments. The ROM is used for prediction of elastic modulus and ultimate tensile strength, as well as other properties like thermal or electrical conductivity. It allows for prediction of axial and

transverse properties. A case of axially loaded viscoelastic material was first described by Lord Kelvin and Woldemar Voigt; hence it is often called the Kelvin-Voight model. A case of transverse elasticity was first described by Reuss (1929); hence the name – Reuss model. The Kelvin-Voight model for axial deformation of the viscoelastic material is composed of a viscous part and an elastic spring arranged in parallel. Identical strains of the material result in

$$\varepsilon_{Total} = \varepsilon_v + \varepsilon_e \quad (11.)$$

Therefore, the stress is calculated as a sum of each component

$$\sigma_{Total} = \sigma_v + \sigma_e \quad (12.)$$

Later works improved upon Voight and Reuss models to be more specific for the analysed composite material by the addition of various factors. A basic form of the ROM method, used for predicting mechanical properties of composites, assumes conditions like fibres are uniformly distributed, there is a perfect bonding between matrix and fibres, matrix is free of voids, applied loads are either parallel or normal to the fibre direction, there are no residual stresses in lamina and matrix, and fibres behave as linearly elastic materials.

The ROM for predicting of fibre composite stiffness presented by Cox [160] was later improved by Krenchel [161] to finally include both fibre length and fibre orientation efficiency factors. Kelly [158] proposed four situations for modelling composite materials, namely elastic deformation for both the fibre and the matrix, plastic deformation of the matrix while the fibres deform elastically, plastic deformation of both the fibre and the matrix and fracturing of the fibres with consecutive fractures in the composite. This method is widely employed in predicting mechanical properties of synthetic matrix composites.

The ROM equation for the stiffness of randomly oriented short fibre reinforced composites, improved with both fibre efficiency factors, i.e. orientation and length, is

$$E_c = \eta_0 \eta_L V_f E_f + (1 - V_f) E_m \quad (13.)$$

where η_0 is the fibre orientation factor, η_L is the fibre length factor, V_f is the volume fraction of fibres, E_f is the fibre modulus of elasticity and E_m is the matrix modulus of elasticity. The fibre length efficiency factor is presented as

$$\eta_L = \left(1 - \frac{\tanh(\beta L/2)}{\beta L/2}\right) \quad (14.)$$

where

$$\beta = \frac{2}{d} \left(\frac{2G_m}{E_f \ln(\sqrt{\pi/X_i V_f})} \right)^{1/2} \quad (15.)$$

where G_m is the shear stiffness of the matrix, X_i is related to the type of packing arrangement of the fibre. A square arrangement is assumed. The fibre orientation factor derived by Krenchel (1964) can be calculated

$$\eta_o = \sum_n a_n \cos^4 \theta_n \quad (16.)$$

where a_n is the fraction of the fibres oriented at the angle θ_n to the loading axis. It is assumed that the strain is uniform, the interface is constant and there are no transverse deformations. For hemp mat compression moulded composites, it was shown that for two-dimensional random orientation the factor $\eta_0 = 3/8$, and for three-dimensional random orientation $\eta_0 = 1/5$ [162]. The ROM was used to calculate the stiffness and strength properties of NFCs, such as flax reinforcing polypropylene [163], but the results were found to be significantly overestimated.

Figure 79 presents a relationship between tensile modulus and flax reinforcement volume fraction for a 250Tex non-twisted flax yarn reinforcement. There are two dotted lines indicating results calculated with the aforementioned ROM. The finer-dotted line corresponds to the model with both fibre efficiency factors included. The coarser-dotted line corresponds to a model with only fibre length efficiency factor. Figure 80 presents a relationship between tensile modulus and hemp reinforcement volume fraction, namely 39Tex hemp twisted yarn. Two dotted lines correspond, as in the previous figure, to the model with length efficiency factor, and to a model with both length and orientation

factors. The rule of mixture, used with these factors, overestimates the predicted results for both composites. There are a number of reasons, which are related with the aforementioned assumptions for the ROM. The model fit can be improved by adding another factor, for instance, processing deterioration, which would give a numerical value for the discrepancy between theoretical and experimental values.

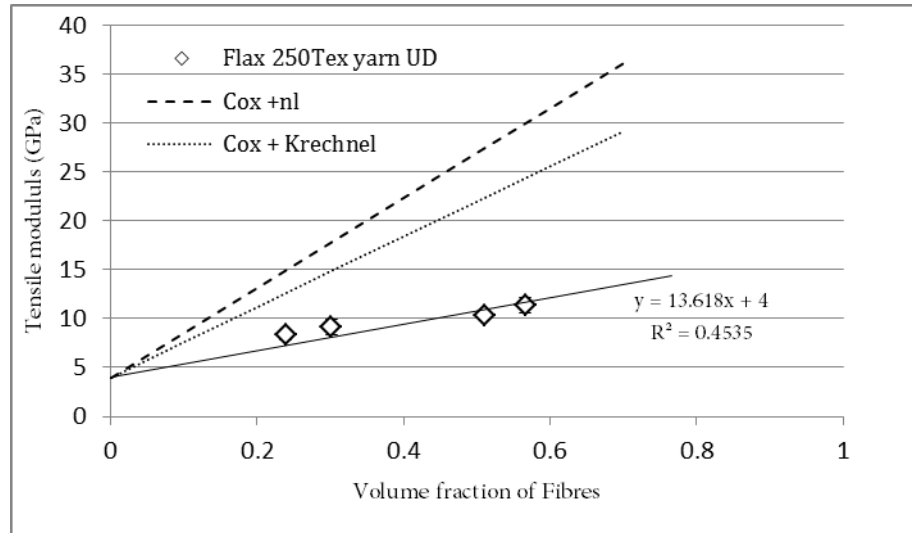


Figure 79 Flax 250Tex yarn unidirectional laminate tensile modulus compared with the rule of mixtures

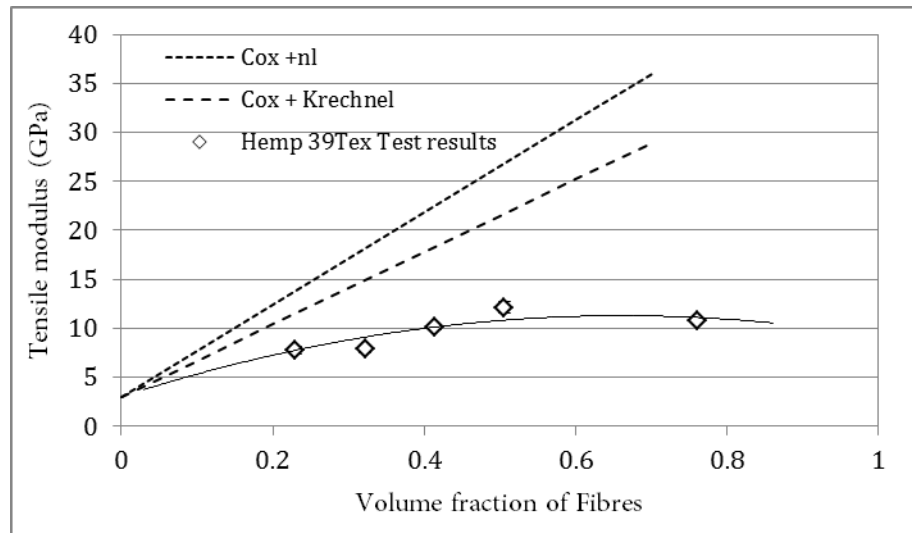


Figure 80 Hemp 39Tex twisted yarn reinforcing Palapreg-eco results and the rule of mixtures comparison

The rule of mixtures presented by Cox [160] was improved by the introduction of a fibre length efficiency factor, in cases when fibres are aligned with the loading direction [158].

Below is a ROM equation for ultimate tensile stress prediction with the fibre length efficiency factor:

$$\sigma_c = \eta_L V_f \sigma_f + (1 - V_f) \sigma_{um} \quad (17.)$$

where V_f is the fibre volume fraction, σ_f is the fibre strength, and σ_{um} is the strength of the matrix at the point of fibre failure. The fibre length efficiency factor (η_L) [164] is

$$\eta_L = \frac{1}{V_f} \left[\sum \frac{L_i V_i}{2L_c} + \sum V_j \left(1 - \frac{L_c}{2L_j} \right) \right] \quad (18.)$$

where V_i is the volume fraction of the fibres with length L_i , which are shorter than the critical length, and V_j is the volume fraction of the fibres with length L_j that are longer than the critical length, the shear stress of the fibre-matrix interface is represented by τ and d is the fibre diameter. The critical fibre length (L_c) is calculated using

$$L_c = \frac{\sigma_f d}{2\tau} \quad (19.)$$

The basis of equation 17 is a summation of the ultimate tensile stress components in the form of the fibre fracture and the fibre-matrix interface fracture of super-critical and sub-critical fibre lengths respectively. The interfacial shear strength between hemp fibre and polyester resin matrix can range between 10-20MPa, which depends mainly on the fibre treatment [95]. Figure 81 presents a comparison between the ultimate tensile stress results, calculated with the aforementioned model, and experimental results for two types of hemp reinforced laminates, i.e. 39Tex yarn and 130Tex yarn. The solid line indicates the calculated values. Similarly to the stiffness results, the model overestimates values for the ultimate tensile stress. The results for the finer yarn, i.e. 39Tex are closer to the predicted values. There is a discrepancy between results for hemp yarns with two linear densities. As shown in the experimental results, there is a difference between the two yarn types. Nevertheless, the model accounts only for the type of fibre, but not the type of yarn; hence, the results calculated for both yarns are the same.

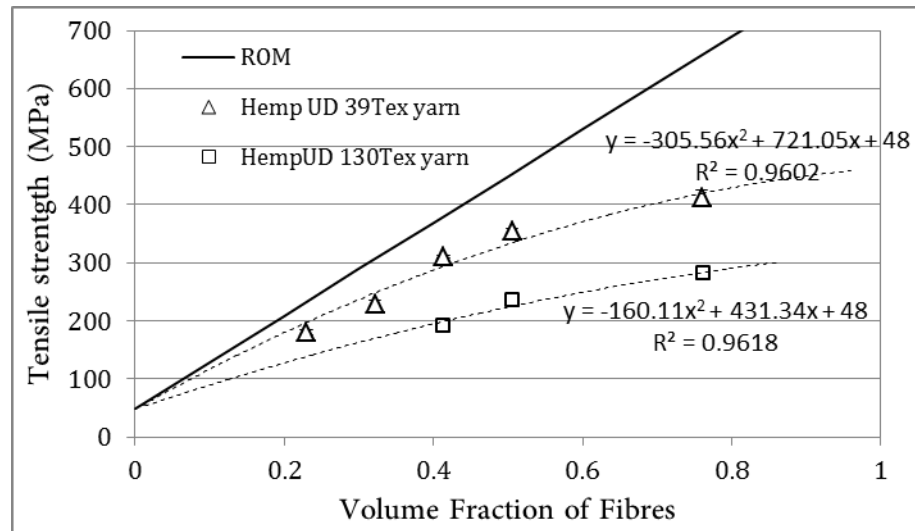


Figure 81 Comparison between the ultimate tensile stress results calculated with rule of mixtures and experimental results for two types of hemp reinforced laminates, i.e. 39Tex yarn and 130Tex yarn

4.11 Summary

The tensile behaviour of NFRP has been investigated by subsequent analyses of processing method, matrix type, fabric waviness, yarn properties like linear density and yarn twist, hybrid effect of the hemp-wool reinforcement. The main findings related with tensile properties can be summarised as follows:

- 1) Laminates of six different hemp yarns of 51%Vf achieved tensile stiffness between 6.4 and 14.1GPa and tensile strength of between 190 and 337MPa.
- 2) Yarns without twist had low tenacity and the wrapping wire did not create sufficient pressure, resulting in a low friction force between individual fibres. The linear density of the yarn influenced laminate processing and resulting properties. Laminates reinforced with 39Tex twisted yarns had the lowest stiffness (7.64GPa). Non-twisted yarn reinforced laminates exhibited the lowest tensile strength (196.7MPa), but twisted yarns 240Tex and 39Tex reinforced laminates performed at 267.3MPa and 243.7MPa, respectively.

- 3) The highest tensile properties achieved for the composite reinforced with flax fabric reinforcement, were 70MPa and 7.48GPa for ultimate tensile strength and tensile modulus respectively.
- 4) Comparison of tensile modulus and ultimate tensile stress results with rule of mixtures revealed that the model overestimates values for both tensile properties.

5 Flexural Properties of BFRPs

Chapter 5 presents findings of the investigation into flexural properties of BFRP. It is composed of seven sections. Sections 5.1 and 5.2 discuss influence of yarn related properties, i.e. yarn linear density and yarn twist, respectively. Section 5.3 discusses an influence of the composite lamination. Section 5.4 analyses an influence of fabric reinforcement type on flexural properties. Section 5.5 presents an influence of volume fraction for three types of BFRPs. Section 5.6 compares flexural properties of developed BFRPs with other NFCs. Section 5.7 includes a summary of findings for the Chapter 5.

The aim of this chapter was to find relationships between flexural properties and reinforcement-related factors, like fibre type, reinforcement type or volume fraction. Flexural properties of BFRP were analysed as a function of fibre type, i.e. hemp, flax and wool, fibre arrangement and fibre volume fraction. The main focus is on laminates with bio-derived polyester matrix, i.e. Palapreg-Eco, and some laminates with fossil-fuel-derived matrix, i.e. Crystic. This is a continuation of the previous analysis and a prerequisite for the following chapter discussing laminate weathering resistance. The flexural properties combine three types of deformations, namely tension, compression and shear. Therefore, they provide overall information about a laminate performance. It was of interest to investigate the factors influencing this compound property in BFRP. The flexural test is relatively easy to conduct; and it is often used as a screening tool to assess the influence of processing or weathering agents. The mechanical tests for this experimental programme have been adapted from EN ISO 14125, 'Flexural Properties of Fibre-Reinforced Plastic Composites' [141]. This standard is dedicated to GFRP. In order to use it for BFRP, a 'class 2' sample type with nominal dimensions of 80x15x3mm³ was selected. The three-point bending method was used with a span between rollers equal to $l=64\text{mm}$. Further explanations of the procedures for flexural testing and weathering of the samples are described in section 3.3.5. For the three point bending test, the flexural modulus is calculated with the equation

$$E_f = \frac{L^3}{4bh^3} \left(\frac{\Delta F}{\Delta s} \right) \quad (20.)$$

where L is the length between the bottom rollers, b is the width of the sample, h is the height of the sample, E_f is the flexural modulus of elasticity, Δs is the difference in deflection between two points on the linear portion of the deformation, ΔF is the difference in load corresponding to the two deflection points. The flexural stress is calculated in the form

$$\sigma_f = \frac{3FL}{2bh^2} \quad (21.)$$

where σ_f is the ultimate flexural stress in megapascals, F is the load in Newtons. Figure 82A presents a three point bending setup during the test with a fractured flax hopsack fabric reinforced laminate sample. Figure 82B presents the bottom side of the unidirectional 250Tex yarn laminate sample after the test.

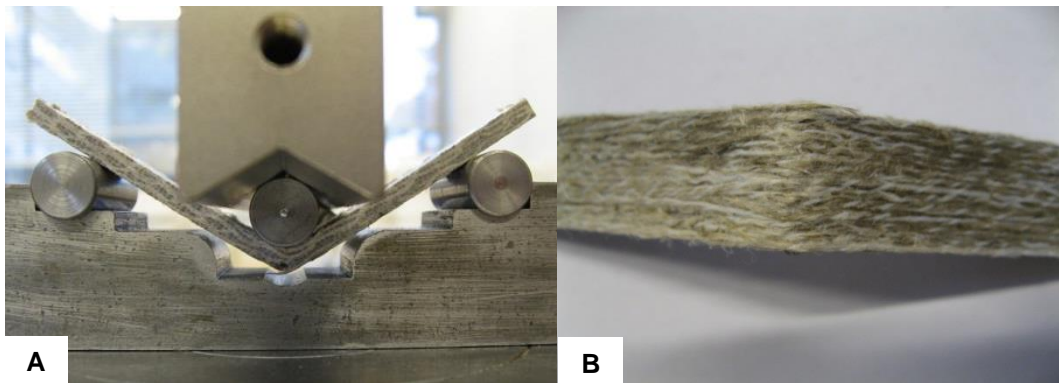


Figure 82 (A) Flax Hopsack fabric reinforced laminate during the three point bending test (B) Bottom side of the unidirectional laminate sample after the test

5.1 Effect of Yarn Linear Density

The flexural test results, i.e. flexural modulus, ultimate flexural stress and flexural strain in this section are presented as a function of the hemp yarn linear density (Figure 83). Single

fibre orientation changes between yarns is concealed within the yarn linear density change. Hemp twisted yarn reinforced laminates were processed with a volume fraction of $V_f = 41\%$. Laminates were processed by winding a pre-set number of yarns in an open-end mould based on their measured average linear density (Figure 39). There were six types of hemp twisted yarns used in the test, namely 25Tex, 39Tex, 51Tex, 60Tex, 86Tex and 130Tex. The left vertical axis correspond to the flexural modulus and ultimate flexural stress. The right vertical axis correspond to the flexural strain. The values of the flexural modulus are multiplied by a factor of 10 in order to be conveniently displayed in one graph.

5.1.1 Effect of Hemp Twisted Yarn Tex

It is evident that the relationship between flexural modulus, flexural stress and flexural strain and yarn linear density is close to linear, and is inversely proportional to the yarn linear density. Hemp laminate flexural modulus decreases from 23.2 GPa for the 25Tex yarn reinforcement to 16.0GPa for the 130Tex yarn reinforcement, which is a significant decline of 0.069GPa/Tex. This trend is different from the tensile modulus relationship with yarn linear density for the same group of laminates. There, a reverse parabolic shape, with the highest modulus value for the laminate reinforced with 60Tex hemp yarns, was observed. The laminate flexural stress decreases from 304.5MPa for the 25Tex yarn reinforcement to 226.8MPa for the 130Tex yarn reinforcement, which is a significant decrease of 0.74MPa/Tex. This trend is in line with the tensile stress relationship, where the highest values were achieved for the fine 25Tex laminate and the lowest for the 130Tex laminate. The laminate flexural strain decreases from 0.034mm/mm for the 25Tex yarn reinforcement to 0.027 for the 130Tex yarn reinforcement. This is a similar trend observed for the tensile strain relationship with yarn linear density for the same laminates. A decline in tensile properties between hemp/PET laminates reinforced with low linear density yarns was observed by Madsen et al [165], where a decrease in tensile properties between 47Tex and 53Tex hemp twisted yarns was reported. A similar discrepancy was observed between the tensile strength of dry yarns tested in tension.

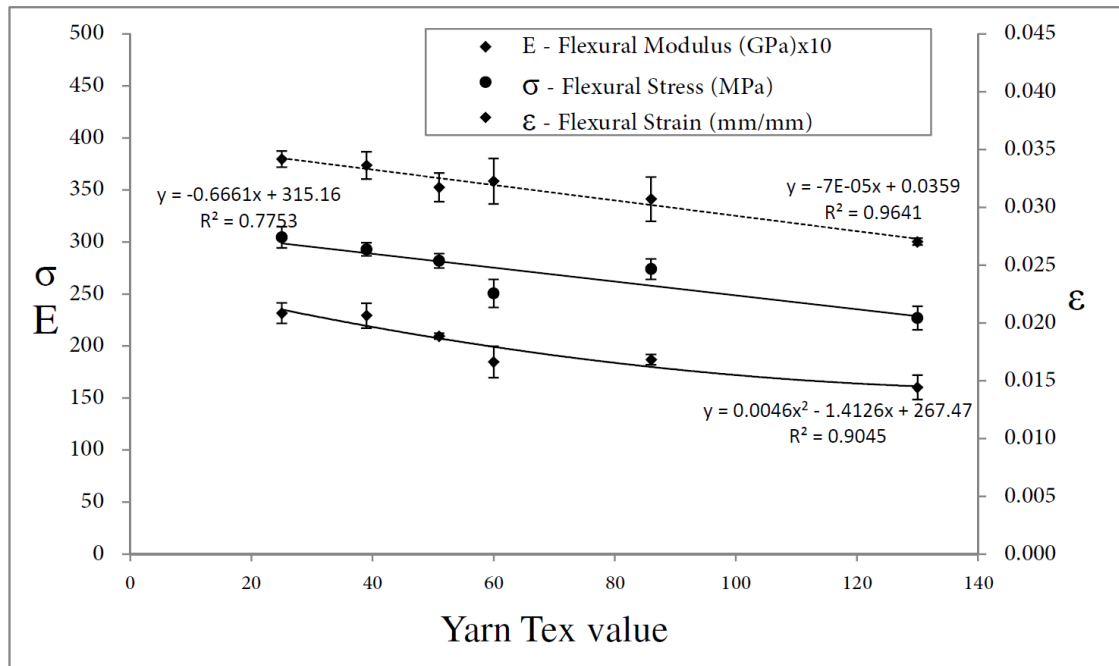


Figure 83 Relationship between flexural properties of twisted hemp yarn reinforced PalapregEco resin and yarn Tex value and with average volume fraction of fibres $V_f=41\%$

Samples were processed in a consistent manner; therefore, any processing related discrepancy would be present throughout all samples. Individual fibres average orientation between the yarns may be significant enough to influence the relationship.

Yarns were spun in the commercial textile yarn process and there might be differences in the fibre treatment as well as an average single fibre length distribution between yarn grades; hence, interphase properties differ between fibre and matrix in the tested laminates. This can be assessed with an interphase related test, e.g. single fibre fragmentation test (SFFT), but was not conducted in this investigation due to time limitations. A contribution of combined compression and shear portions of the flexural deformation can be the reason of the difference between trends of laminates flexural modulus and tensile modulus.

5.1.2 Effect of Flax Twisted Yarn Tex

The aforementioned relationship was not observed for the flax twisted yarns (Figure 84). Laminates reinforced with two high Tex values of flax yarns were compared, namely 240Tex and 590Tex, with volume fractions equal to $V_f = 50.7\%$ and $V_f = 49.9\%$

respectively. The flexural stiffness was equal to 18.0GPa and 20.2GPa for 240Tex and 590Tex laminates respectively. The tensile stress was equal to 233.0MPa and 246.5MPa for 240Tex and 590Tex flax yarn reinforced laminates. Those are increases of 0.006GPa/Tex and 0.039MPa/Tex in flexural modulus and flexural strength respectively. This can be attributed to the aforementioned processing or fibre orientation characteristics on top of change in yarn linear density. Nevertheless, this trend differs in comparison with the one observed for the hemp twisted yarns, where flexural properties decreased with the increase of yarn linear density.

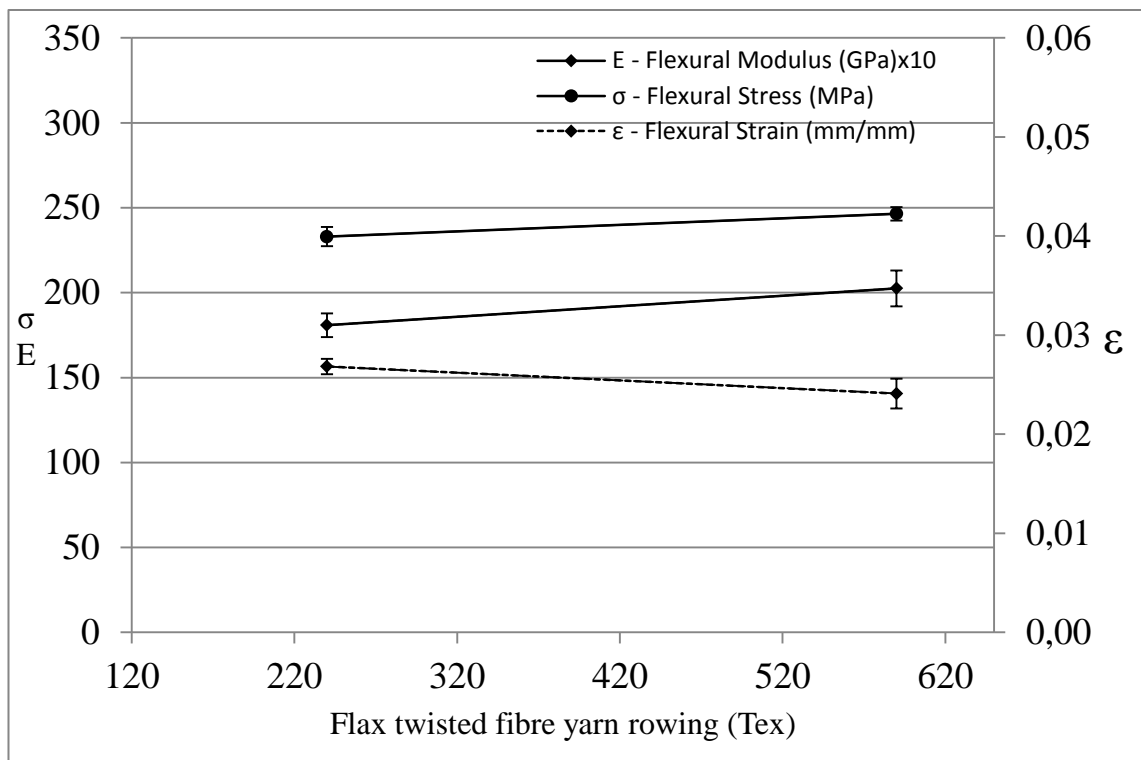


Figure 84 Comparison of flexural properties of flax twisted-fibre yarns with 240Tex and 590Tex

5.2 Effect of Yarn Twist

There are two main types of NF reinforcement yarns used in NFC, when structure is taken into account, namely with twisted filaments and with parallel filaments. Similarly to the tensile properties investigation, those reinforcement types were compared in order to find the difference in flexural properties. Two types of flax yarns dedicated as composite

reinforcements were compared. The first yarn type had twisted filament 240Tex linear density. It was supplied in the form of unidirectional rowing, where yarns are sown together with transverse polyester filaments. This assures yarns to be parallel and uniformly spaced. The second type of flax yarn was with non-twisted architecture and 250Tex linear density. It is made with parallel slivers of individual filaments, which are bonded together by a wrapping polyester yarn. The volume fraction was controlled by use of a specified number of yarns. The twisted flax fibre yarn laminate properties were compared with a non-twisted fibre yarn laminate. The flexural modulus and flexural strength are higher by 3GPa and 50MPa, respectively, when compared with non-twisted flax yarn. Nevertheless, there is a small, i.e. 10Tex difference between the yarns, in accordance to the previous tendencies. The flexural modulus decreases from 23.2 GPa for the 25Tex yarn to 16.0GPa for the 130Tex yarn. It is a decline of 0.069GPa/Tex. This trend is different from the tensile modulus relationship with yarn linear density for the same group of laminates, which had a reverse parabolic shape with a higher modulus value for the laminate reinforced with 60Tex hemp yarns. The laminate flexural stress decreases from 304.5MPa for 25Tex to 226.8MPa for 130Tex. This is a significant decrease of 0.74MPa/Tex. The trend is in line with the tensile stress relationship where the highest values were achieved for the fine 25Tex laminate and the lowest for the 130Tex laminate. The laminate flexural strain decreases from 0.034mm/mm for 25Tex to 0.027 for 130Tex. This is a similar trend observed for the tensile strain relationship with yarn linear density for the same laminates.

Table 14 Flexural properties comparison of two laminates reinforced with flax yarns with twisted and non-twisted architecture.

<i>Laminate</i>	<i>Flexural Modulus (GPa)</i>	<i>RSD (%)</i>	<i>Flexural strain (mm/mm)</i>	<i>RSD (%)</i>	<i>Flexural stress (MPa)</i>	<i>RSD (%)</i>	<i>Density (kg/m³)</i>	<i>Volume Fraction (%)</i>
Flax NT 250Tex	15.1	3.9	0.029	5.3	182.2	1.8	1290	51.0
Flax T 240Tex	18.1	3.8	0.027	2.9	233.0	2.4	1320	50.7

NT – non twisted fibre yarn, T – twisted fibre yarn

5.3 Effect of Composite Lamination

A series of NFC laminates reinforced with flax fabric and hemp mats were processed in order to assess the lamination influence on the flexural properties. Moreover, the processing parameters used were compared. Flexural test results for eight laminate types are presented in Table 15. There are five flax fabric reinforced laminates with both hopsack and twill fabrics weaved from 250Tex yarn, one flax-hemp laminate with flax fabric outer layers and hemp mat core, one hemp mat reinforced laminate and one glass twill fabric reinforced laminate. The flexural modulus of 6GPa was measured for a laminate stacking sequence ([4x4Hop(0/90),HM,4x4(0/90)]), which has core composed of hemp mat and flax fabric outer layers and 4x4 [(0/90),(45/45)]s, which is composed of four flax fabric layers, i.e. two outer layers are aligned with the longitudinal laminate direction and two inner layers are turned 45° in relation to the outer layers. The measured flexural strength of this assembly is also the same 109.7MPa and 108.6MPa, respectively. This is because the outer layers of material deformed under flexural load endure the highest strain. The stiffness of the laminate, which has outer reinforcement layers at 45° to the testing direction and two inner layers aligned with the test direction (4x4 [(45/45), (0/90)]s), was reduced to 3.9GPa. These results suggest that even in a relatively thin laminate the costly yarn reinforcement layers in the core can be replaced with mat reinforcement. Laminates with 2x2 twill fabric were processed with both Crystic polyester and Palapreg-eco resins. The volume fractions were 43% V_f and 44% V_f . Both laminate types achieved 5GPa flexural modulus but the laminate with Palapreg-eco matrix had a higher ultimate flexural stress of 106MPa in comparison with the Crystic matrix laminate ultimate flexural stress - 93MPa.

Table 15 Flexural properties of the laminates reinforced with natural fibre fabrics and mats

Laminate reinforcement and arrangement	Proc	Resin	Flexural Modulus		Flexural Stress		Flexural strain		Vf (%)	Density (kg/m ³)
			(GPa)	(%)	(MPa)	(%)	(mm/mm)	(%)		
4x4 [0/90] ₄	CM	Palapreg	3.4	6.6	72.8	3.7	0.059	6.9	45.1	1320
4x4 [(0/90),(45/45)] _s	CM	Palapreg	5.9	6.6	109.7	5.1	0.038	6.4	44.1	1300
4x4 [(45/45) ,(0/90)] _s	CM	Palapreg	3.9	7.1	82.5	1.8	0.060	1.9	44.2	1300
4x4(0/90), HM, 4x4(0/90)	CM	Palapreg	6.1	6.5	108.6	1.0	0.043	5.2	42.7	1290
2x2Twill [0/90] ₅	CM	Crystic	5.2	4.8	93.6	6.8	0.052	3.8	43.1	1320
2x2Twill [0/90] ₅	CM	Palapreg	5.0	8.1	106.1	6.0	0.039	3.8	44.1	1300
Hemp mat	CM	Palapreg	4.2	3.9	67.2	4.4	0.026	9.8	29.2	1230
Glass 1x1Twill[0/90] ₂₀	CM	Palapreg	19.6	1.1	444.9	1.7	0.028	1.9	43.1	1800

4x4 – Flax Hopsack fabric, 2x2 – flax twill fabric, [0/90]₄ – four layers of a fabric with a weft direction aligned longitudinally, 45/45 – yarns in fabric aligned at 45 degrees to the test direction, HM – hemp mat with random fibre alignment.

The glass fibre reinforced plastic (GFRP) with 43% V_f reinforcing Palapreg-eco matrix was processed using the same procedure as for flax fabric laminates. Figure 85A shows the surface of the laminate with distinct Twill pattern from the glass fibre fabric. Figure 85 B presents a cross section of the GFRP with visible glass fibre slivers in the weft and wrap directions of the fabric. The glass fibre composite had a 19.6GPa flexural modulus, 445MPa flexural strength and 0.028mm/mm flexural strain. Those are significantly higher properties when compared with flax hopsack or twill laminates, even if 30% higher density of the glass laminate is taken into account.

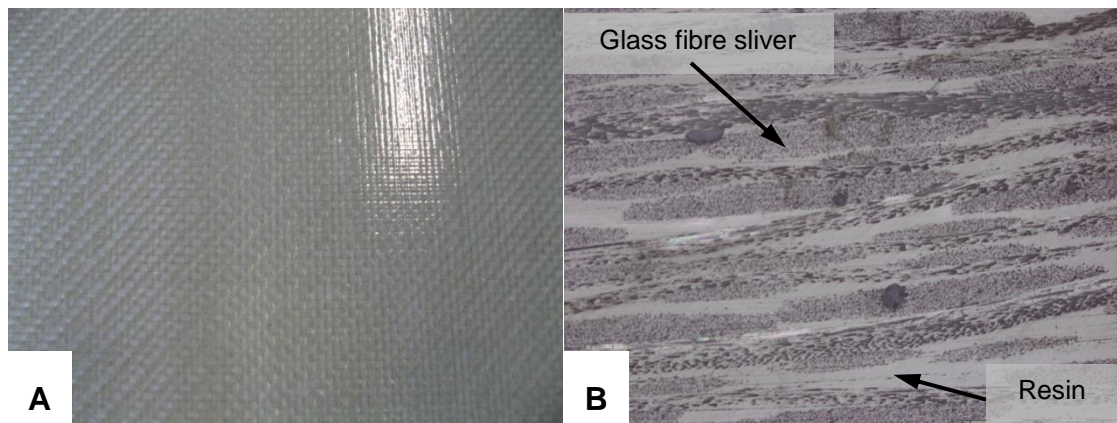


Figure 85 (A) Glass fibre twill fabric reinforced Palapreg-eco laminate surface (B) Cross section of the GFRP sample



Figure 86 Surface of the hemp mat (HM) reinforced Palapreg-eco resin laminate

In order to compare processing procedures, three impregnation procedures for the hemp laminate reinforced with 41% V_f of hemp 25Tex twist fibre yarns were compared. Each procedure differed with the degassing level of the resin embedded impregnate before compression moulding. There is a slight improvement in flexural modulus and strength for the P1 procedure which consisted of the longest degassing period, and this procedure was adopted for processing of the rest of the laminates.

Table 16 Comparison of three impregnation procedures used for processing of the laminates

	<i>Modulus</i> (GPa)	<i>RSD</i> (%)	<i>Flexure</i> <i>strain</i> (mm/mm)	<i>RSD</i> (%)	<i>Flexure</i> <i>stress</i> (MPa)	<i>RSD</i> (%)	<i>Density</i> g/cm ³	<i>Volume</i> <i>fraction</i>
Hemp 25Tex P1	23.2	4.2	0.034	2.0	304.5	3.3	1.32	41.3
Hemp 25Tex P2	21.7	5.2	0.035	1.6	293.7	6.0	1.31	41.4
Hemp 25Tex P3	22.7	3.1	0.034	4.0	293.4	2.1	1.31	41.2

5.4 Effect of Fabric Waviness

Two types of fabrics with different waving levels, i.e. hopsack and twill, were used to produce NFCs which were then compared with laminates processed without yarn waviness. All three samples were made with the same flax 250Tex yarn with non-twisted fibres. Figure 87 presents a comparison between flexural properties of composites made with Palapreg-Eco resin. Laminates were processed with square moulds. Tests were made with the same volume fraction of reinforcement in the test direction, i.e. the number of yarns in the longitudinal direction is the same. The flexural stiffness for hopsack, twill and unidirectional reinforcements are 3.4GPa, 5.0GPa and 7.4GPa respectively. When compared with 3.2GPa of neat matrix flexural strength, only twill and unidirectional reinforcements improved laminate stiffness. The flexural strengths for hopsack, twill and unidirectional reinforcements are 73MPa, 106MPa and 123MPa respectively. Similarly to the stiffness results, only twill and unidirectional reinforcements improve flexural strength when compared with neat resin. The flexural strains for hopsack, twill and unidirectional reinforcements are 0.059mm/mm, 0.039mm/mm and 0.026mm/mm respectively. A comparison of reinforcements shows that the waviness of the fabrics decreases the flexural properties of the laminate.

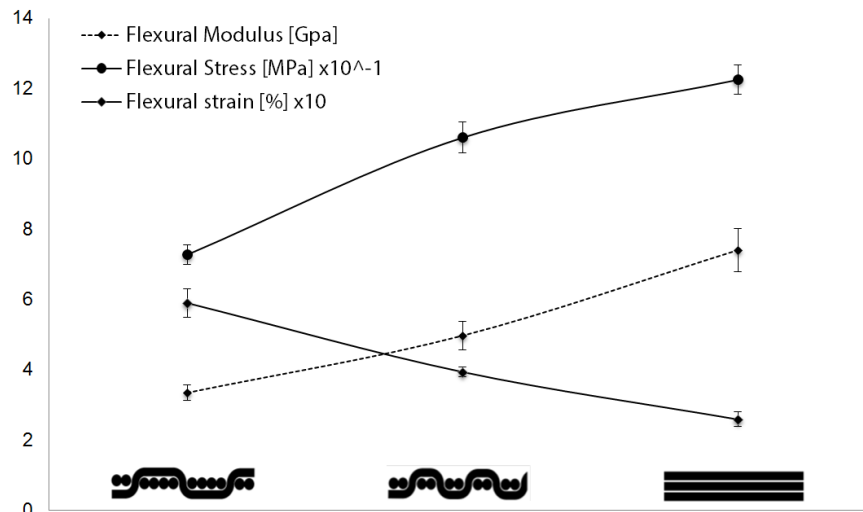


Figure 87 Relationship between non-twisted 250Tex flax yarn reinforcement arrangement and mechanical properties of the NFC laminate. From left: 4x4 Hopsack, 2x2 Twill and parallel yarn arrangements

5.5 Effect of Volume Fraction

In the previous chapter discussing tensile properties, optimal volume fractions were found for each tested laminate. This section will analyse if similar relationships are present for laminates under flexural deformation. The influence of the volume fraction of yarns on the flexural properties was examined experimentally for the hemp and flax yarn reinforcements in palapreg matrix. Yarns used included 250Tex flax non-twisted fibre yarn, 39Tex and 130Tex hemp twisted fibre yarns. Each result is an average of at least four successfully tested samples. The influence of fibre volume fraction on the flexural modulus, flexural strain, and flexural stress is presented.

5.5.1 Hemp Yarn Laminate

Figure 88 illustrates the effect of the volume fraction on a laminate with 39Tex hemp twisted fibre yarn. For this laminate, there were five volume fractions tested, namely 23.0%, 32.2%, 41.4%, 50.6% and 76.0%. The flexural modulus rises with an increasing volume fraction up to 76% from 13.4GPa to 34.5GPa, and closely follows a logarithmic shape relationship. The flexural strain to break increases slightly with volume fraction from

0.031mm/mm for 23% V_f to 0.034mm/mm for 41% V_f , after which it decreases to 0.018mm/mm for 76% V_f . The standard deviation of the strain for the laminate with 76% V_f is high, which could be attributed to a high fibre packing. The flexural stress to break increases linearly from 23% with 202MPa up to 51% V_f with 324MPa. A further increase of the laminate fibre loading does not increase the flexural stress to break, and a 76% V_f laminate has 326MPa flexural stress. Since the maximum modulus and flexural stress were achieved for the volume fraction of $V_f=76\%$, the optimally performing laminate selected from this assembly would have 34.5GPa stiffness, 326.5MPa flexural strength and 0.018mm/mm strain. This confirms the findings from the tensile properties studies of high mechanical performance for the same type of reinforcement

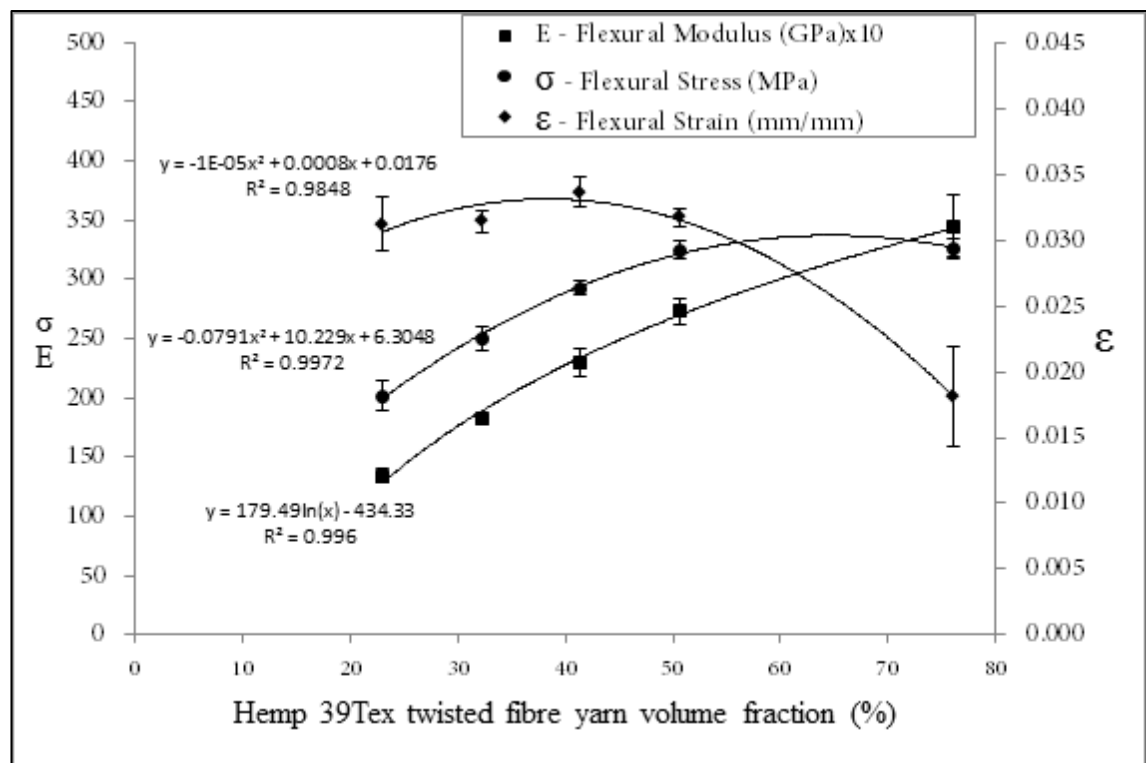


Figure 88 Effect of the volume fraction of hemp twisted fibre 39Tex yarn reinforcement on flexural properties of a unidirectionally aligned laminate with Palapreg-Eco matrix

Figure 89 presents the surface and cross section of the 39Tex laminate. Parallel aligned yarns of the unidirectional sample are visible in Figure 89A. Figure 89B presents a cross section of the highly reinforced sample with 76% V_f , which shows how densely yarns are compacted, leading to fibre-fibre contact and properties reduction.

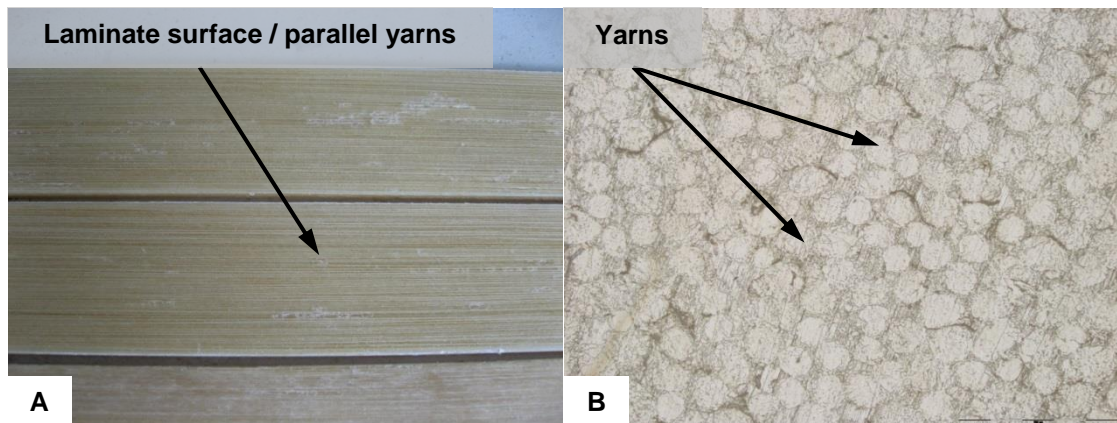


Figure 89 (A) Laminated strips reinforced with 39Tex hemp twisted yarn with visible reinforcement alignment (B) Cross section of a 39Tex hemp laminate with a high 76% V_f .

Figure 90 illustrates the effect of the volume fraction on a laminate with 130Tex hemp twisted fibre yarn. There were three volume fractions tested, namely 41%, 51% and 76%. The flexural modulus rises with an increasing volume fraction linearly up to 76%, from 16.0GPa to 28.4GPa. There is no modulus deterioration visible up to $V_f=76\%$, the same as in the case of 39Tex yarn. The flexural strain to break is almost constant across all samples ranging from 0.027mm/mm to 0.028mm/mm, which is within the range of standard deviation. The flexural stress increases linearly with the volume fraction, from 226.8MPa to 320.3MPa, which is in the same range when compared with results achieved for the hemp 39Tex reinforcement. Since the maximum modulus was achieved for $V_f=76\%$, the optimally performing laminate selected from this assembly would have 28.4GPa stiffness, 320.3MPa tensile strength and 0.027mm/mm strain.

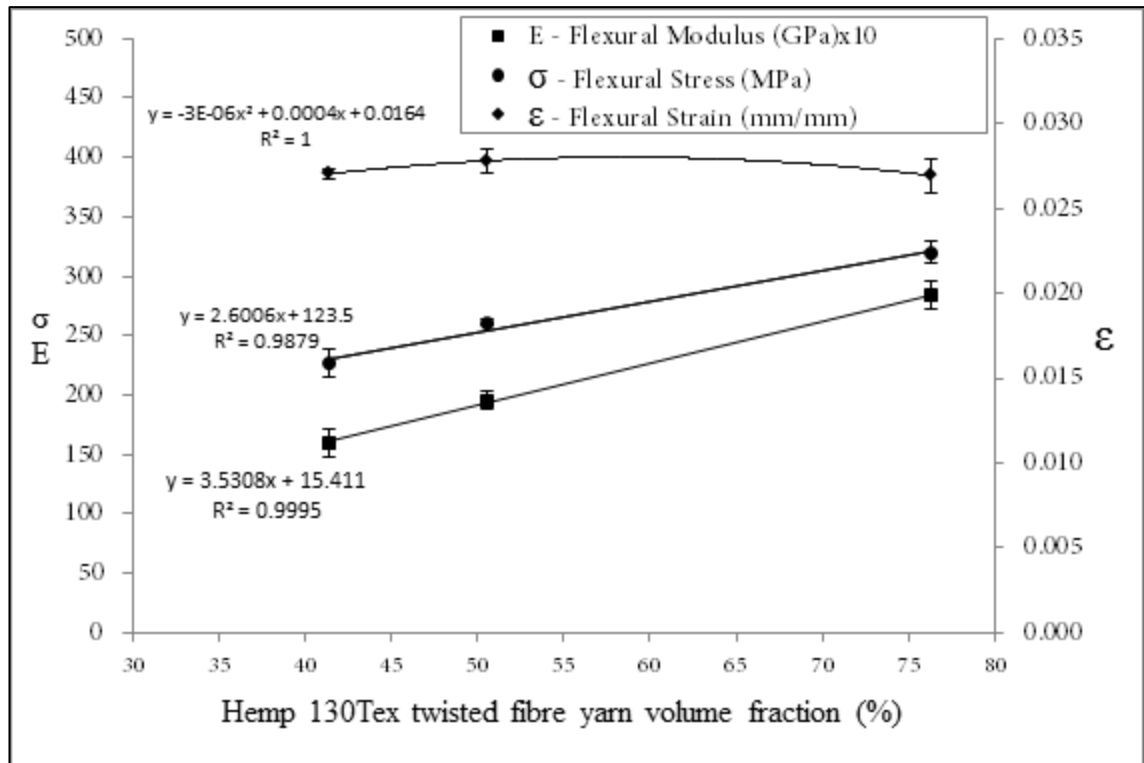


Figure 90 Effect of the volume fraction of hemp twisted fibre 130Tex yarn reinforcement on flexural properties of a unidirectionally aligned laminate with Palapreg-Eco matrix

5.5.2 Flax Yarn Laminate

The next reinforcement type was 250Tex non-twisted fibre flax yarn. Examples of processed laminates are presented in Figure 91. There is a visible difference between laminates, namely the change of the laminate colour, which indicates an increase in reinforcement content. The darkest colour indicates the lowest volume fraction of the reinforcement.



Figure 91 250Tex non-twisted fibre flax yarn laminate strips with different volume fractions (From the top: 23.0%, 30.0%, 51.0%, 56.6%, 76.0% and 89.7% V_f .)

Figure 92 illustrates the effect of the volume fraction on the laminate with 250Tex flax non-twisted fibre yarn. There were six volume fractions tested, namely 23.0%, 30.0%, 51.0%, 56.6%, 76.0% and 89.7%. The flexural modulus rises linearly with an increasing volume fraction up to 89.7% from 7.4GPa to 22.4GPa. There is no modulus deterioration visible up to $V_f=89.7\%$. The flexural strain to break grows with volume fraction, from 23% V_f up to 51% V_f ; from 0.027mm/mm to 0.029 mm/mm. Then, a sharp reduction of flexural strain is visible, from 0.026mm/mm for 56% V_f down to 0.013 for 89.6%. Such a low flexural strain suggests that interface properties are deteriorating. The flexural stress to break increases with the volume fraction up to 56.5% V_f ; from 122.5MPa to 224.3MPa. Then, when the fibre volume fraction is increased, the flexural stress is reduced to 188MPa for 76% V_f and 185.6 for 89.6% V_f . The optimal laminate selected from this assembly would have 76% V_f with 20.7GPa flexural stiffness, 188.1MPa flexural strength and 0.017mm/mm flexural strain.

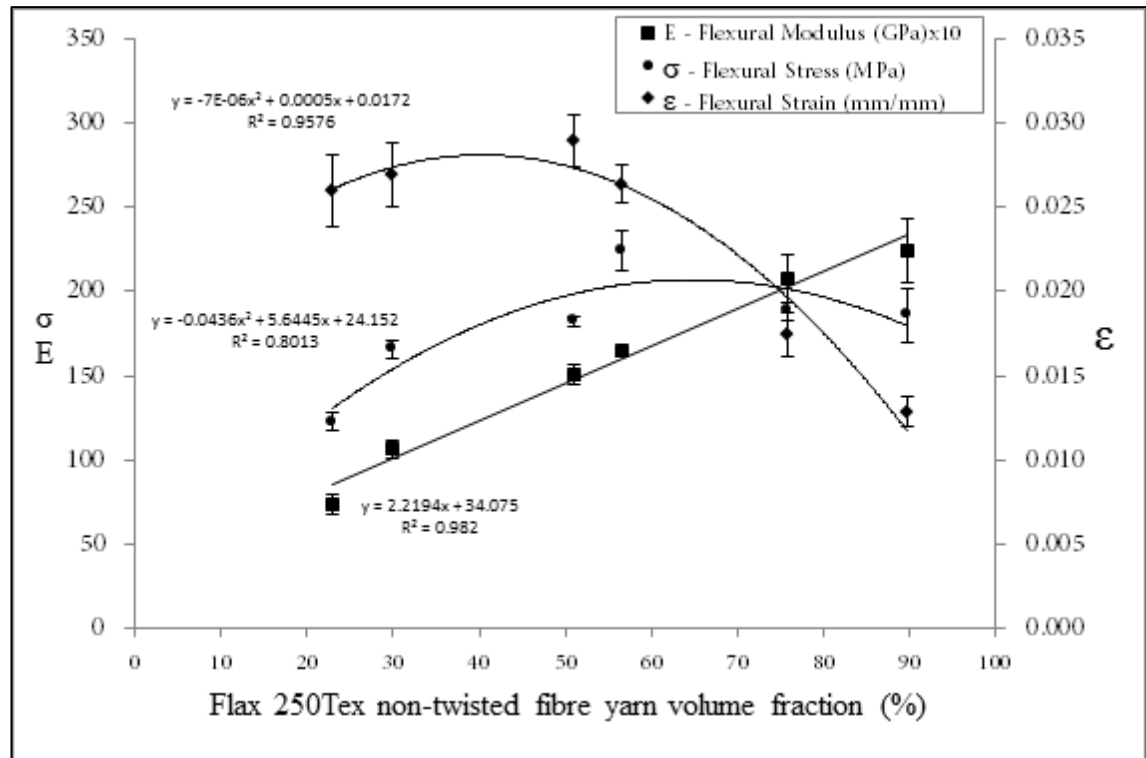


Figure 92 Effect of the volume fraction of flax non-twisted fibre 250Tex yarn reinforcement on flexural properties of a unidirectionally aligned laminate with Palapreg-Eco matrix.

Increasing the fibre loading up to 76% V_f resulted in an increase of flexural properties in all three cases. This finding is different in comparison with the tensile investigation, which concluded that 51% V_f was optimal for all laminates and only 130Tex hemp yarn improved properties up to 76% V_f . Table 17 presents flexural properties of previously analysed laminates with 76% V_f . The hemp 39Tex yarn produced the laminate with the highest flexural stiffness and strength. Results are combined with Palapreg-eco matrix flexural stiffness, which was increased 10 times with inclusion of 76% V_f of hemp fibres, and flexural stress, which was tripled.

Table 17 Comparison of three laminates tensile properties with $V_f=51\%$

<i>Sample</i>	<i>Flexural SD</i>		<i>Flexural RSD</i>		<i>Flexural RSD</i>		<i>V_f</i>
	<i>Modulus</i>	<i>Stress</i>	<i>(%)</i>	<i>strain</i>	<i>(%)</i>	<i>(%)</i>	
	<i>(GPa)</i>	<i>(MPa)</i>		<i>(mm/mm)</i>			
Hemp 39Tex (twist)	34.5	2.6	326.5	7.9	0.018	7.5	76
Hemp 130Tex (twist)	28.4	4.3	320.3	8.1	0.027	3.8	76
Flax 250Tex (non-twist)	20.7	1.3	188.1	5.4	0.017	6.3	76
Palapreg-eco matrix	3.2	0.1	108.8	14.4	0.047	1.2	0
Glass 1x1will	19.6	0.2	444.9	1.7	0.028	1.9	43

5.5.3 Influence of Volume Fraction of Hybrid Hemp-wool Reinforcement

Figure 93 presents flexural properties of hybrid laminates reinforced with aligned hemp-wool yarns. There were three types of composites processed with 41.4%, 50.6% and 73.6% volume fractions of the hybrid hemp-wool twist-less 1000Tex yarn. The flexural modulus rises with an increasing volume fraction up to 73.6%, from 12.2GPa to 16.5GPa. There is no modulus deterioration visible up to $V_f=73.6\%$. The flexural strain is reduced with increasing fibre volume fraction, from 0.032mm/mm to 0.016mm/mm. There is an interesting relationship between volume fraction and flexural stress for this reinforcement. The flexural stress is decreasing together with an increase of fibre loading above 41.4% V_f ; from 181.8MPa to 144.7MPa for 73.6%. Therefore, the flexural modulus is being improved with increased reinforcement loading, but the flexural strength decreases. The optimal laminate selected from this assembly would have 50.6% V_f with 14.8GPa flexural stiffness, 178.5MPa flexural strength and 0.029mm/mm flexural strain.

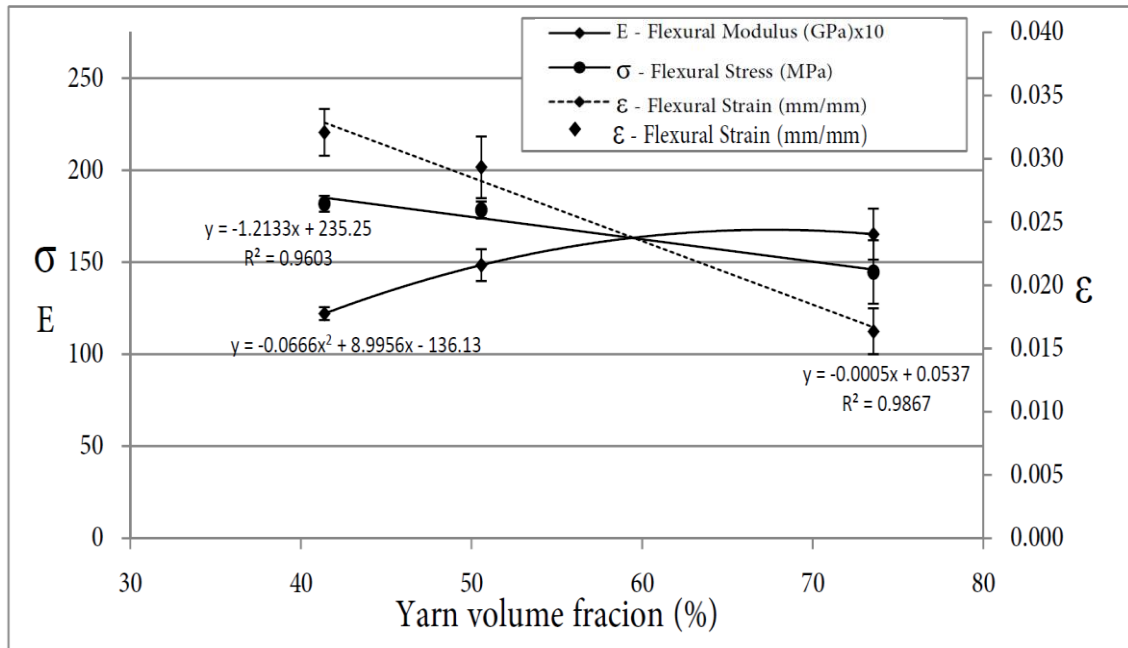


Figure 93 Flexural properties of laminates reinforced with hemp-wool yarn as a function of volume fraction

Figure 94 presents longitudinal (A) and transverse (B) cross sections through the hemp-wool laminate. There are visible aligned longitudinal hemp fibres. The transverse cross section reveals the close resin encapsulation of the hemp and wool fibres.

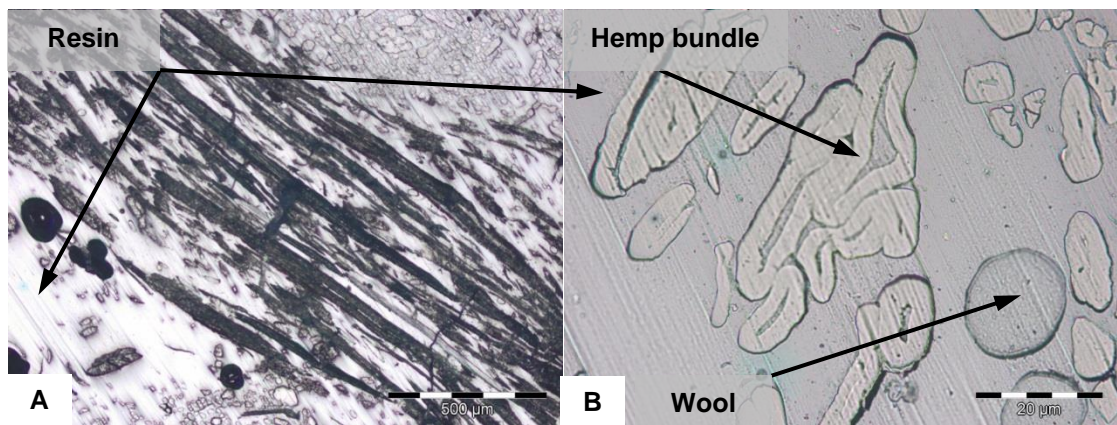


Figure 94 (A) A longitudinal cross section through the hemp-wool yarn laminate (B) A transverse cross section through the hemp-wool reinforced laminate

5.6 Comparison with Other Composite Materials

How does the developed Palapreg-eco hemp and flax laminate flexural properties compare with other flax reinforced laminates? Table 18 presents a review of the flexural strength and modulus of hemp and flax NFCs, together with the volume fraction and processing methods. The volume fraction of reinforcement used ranges from 10% to 70%, the flexural modulus is between 0.8GPa and 25GPa and the flexural strength is in the range 31 - 219MPa. The large variation reported in the results from the literature is due to NFC properties having a dependency on multiple factors, namely fibre aspect ratio, fibre type, surface morphology, fibre treatment, structure, arrangement, resin type and processing route. Recently, knitted fabric reinforced flax composites were revisited by Sawpan et al. (2012), who evaluated the flexural properties of epoxy matrix composites processed by the lay-up technique. The research used a variety of stacking sequences. The specific flexural properties reported were low in comparison with the findings of Goutianos (2006) for the same lay-up processing technique. Mechanical processing such as hot pressing, filament winding and pultrusion allow for higher fibre orientation precision and increased volume fractions. Hackled and aligned fibres were used by Van Der Oever [163] for a thermoplastic matrix. Bledzki [166] used aligned hemp fibres, which resulted in significant improvement of flexural properties. Sawpan [117] aligned hemp fibres in PLA and unsaturated polyester resin.

Figure 95 and Figure 96 illustrate a comparison of the developed laminates with natural materials, plastic and composites. They present materials flexural modulus and flexural strength maps as a function of density. The green colour corresponds to the family of natural materials, the red colour corresponds to composites and the blue colour represents the family of selected plastics. NFCs are represented with light green oval shape. It is evident that NFCs fill out the position in between glass fibre composites and natural materials in terms of density. The stiffness of NFCs corresponds to the top range of natural materials and synthetic plastics.

Table 18 Flexural properties of the composites reinforced with aligned hemp or flax fibres

<i>Materials</i>	<i>V_f</i> (%)	<i>MOR</i> (MPa)	<i>MOE</i> (GPa)	<i>Processing</i>	<i>Ref.</i>
RandFlax hackled-PP/MAPP	20	70	4.0	HP 200° 40bar	[163]
Rand Flax hackled-PP/MAPP	40	90	7.0	HP 200° 40bar	
Rand Flax scutched-PP/MAPP	40	80	6.0	HP 200° 40bar	
UDHemp Epoxy	35	148-219	5.9-12.4	FW	[166]
UDFlax PP	35	77-149	-	FW	
UD Flax non hackled UP	25	168	19.4	PU(lab.)	[167]
UD Flax hackled UP	25	182	19.5	PU(lab.)	
0/90Fabric Flax UP	31	198	17.0	RTM	
0/90 Fabric Flax EP	28	190	16.0	Hand Lay-Up	
Fabric Flax EP	18-34	*31-106	*0.8-2.9	Hand Lay-Up	[111]
Treated Hemp UP	56	101	10.0	HP 6MPa	[168]
Hemp mat rand UP	10-40	40-110	4.0-7.0	RTM	[169]
Alcali UD Hemp long PLA	10-40	90-68	6.4-5.7	HP 5MPa	[117]
Alcali & Silane UD Hemp UP	10-50	97-88	4.9-6.8	HP 5MPa	[95]

*HP – Hot press, Rand – Random mat reinforcement, MAPP - , PP – polypropylene, FW – Filament winding, UD – unidirectional, PU-pultrusion, EP – epoxy, UP – unsaturated polyester, RTM – Resin transfer moulding, * - values in MPa/g.cm³, STBR-Starch biodegradable resin.*

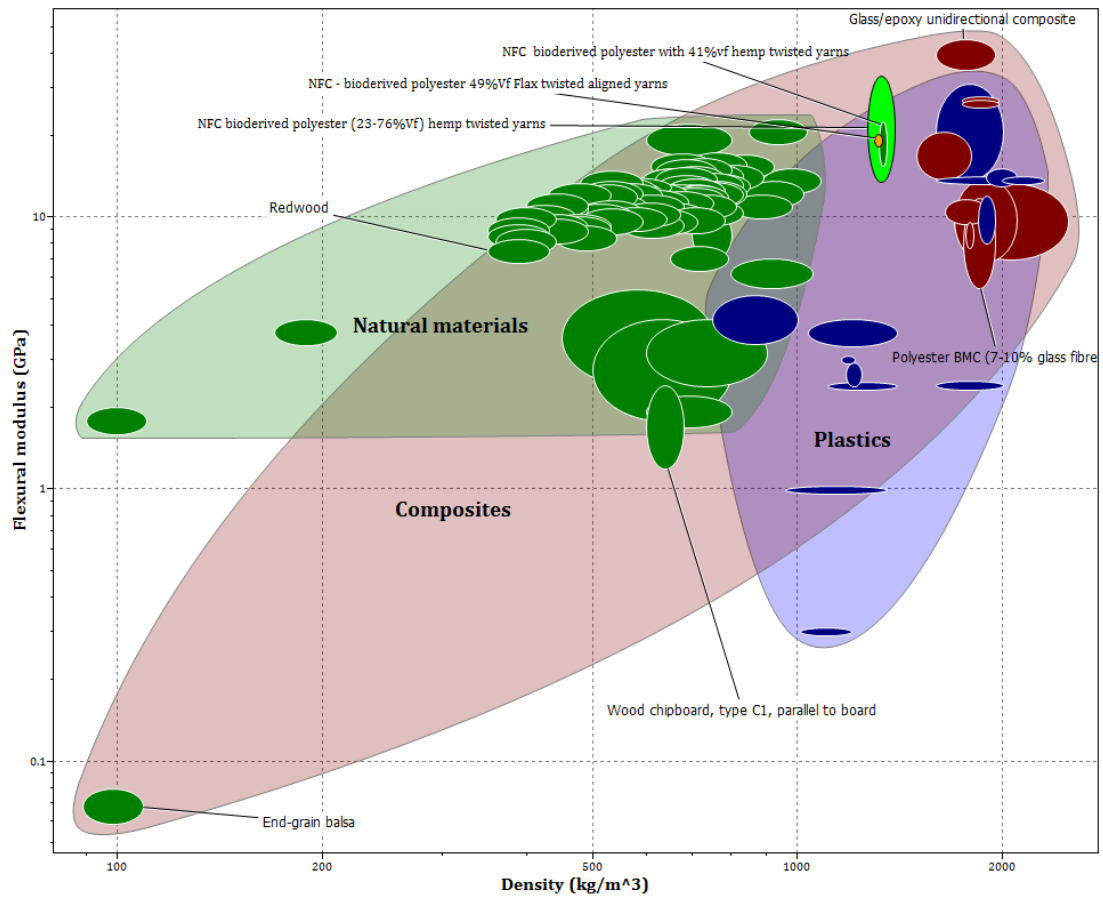


Figure 95 Comparison of flexural modulus properties of developed NFC materials with theoretical values for natural materials plastics and composites (plotted with CES EduPack 2012)

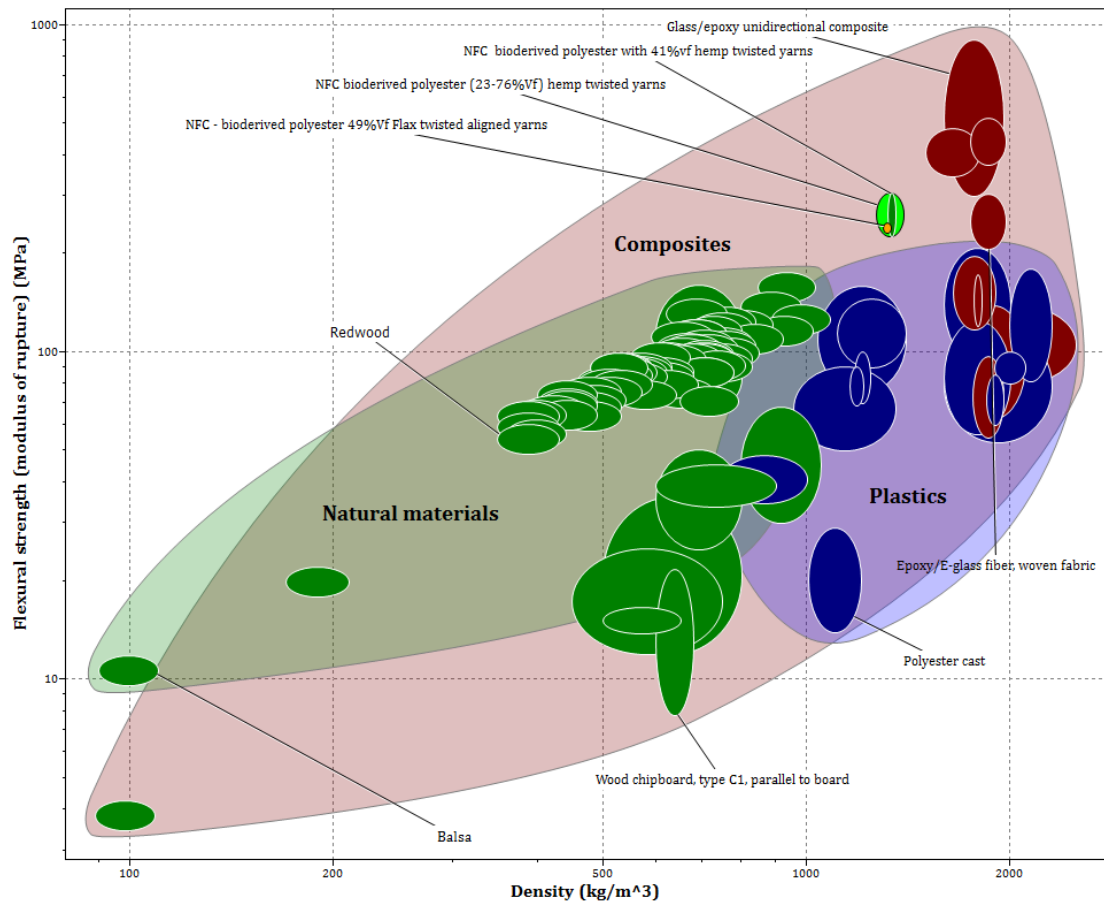


Figure 96 Comparison of flexural strength of the developed NFC with theoretical values for plastics, composites and natural materials against density (plotted with CES EduPack 2012)

5.7 Summary

The flexural behaviour of BFRP was investigated by subsequent analyses of yarn linear density, yarn twist, lamination sequence, fabric waviness and the reinforcement volume fraction. Moreover, the comparison was made with other NFC laminates. The main findings related with tensile properties can be summarised as follows:

- 1) There is a correlation between the hemp yarn linear density and flexural properties. Hemp laminate flexural modulus decreases from 23.2 GPa for the 25Tex yarn reinforcement to 16.0GPa for the 130Tex yarn reinforcement, which is a significant decline of 0.069GPa/Tex. The laminate flexural stress decreases from 304.5MPa

for the 25Tex yarn reinforcement to 226.8MPa for the 130Tex yarn reinforcement, which is a significant decrease of 0.74MPa/Tex.

- 2) Similarly, there is a correlation between the flax yarn linear density and flexural properties. The flexural stiffness was equal to 18.0GPa and 20.2GPa for 240Tex and 590Tex laminates respectively. The tensile stress was equal to 233.0MPa and 246.5MPa for 240Tex and 590Tex flax yarn reinforced laminates.
- 3) The type of the fabric reinforcement has an influence on the flexural properties. The flexural stiffness for hopsack, twill and unidirectional reinforcements are 3.4GPa, 5.0GPa and 7.4GPa respectively. When compared with 3.2GPa of neat matrix flexural strength, only twill and unidirectional reinforcements improved laminate stiffness. The flexural strengths for hopsack, twill and unidirectional reinforcements are 73MPa, 106MPa and 123MPa respectively. Similarly to the stiffness results, only twill and unidirectional reinforcements improve flexural strength when compared with neat resin.
- 4) The relationship between the hemp yarn volume fraction and flexural properties was found to be different from linear. Since the maximum modulus and flexural stress were achieved for the volume fraction of $V_f=76\%$, the optimally performing laminate selected from this assembly would have 34.5GPa stiffness, 326.5MPa flexural strength and 0.018mm/mm strain.
- 5) Similarly, there was an optimal volume fraction selected for the flax yarn reinforcement. The optimal laminate selected from this assembly would have 76% V_f with 20.7GPa flexural stiffness, 188.1MPa flexural strength and 0.017mm/mm flexural strain.

6 Compressive Behaviour of NFC Tubes

Chapter 8 is composed of five sections. In Section 8.1, processed tube structures are presented. Section 8.2 describes yarn properties used for tube processing and resin distribution within the processed samples. Section 8.3 presents the mean strength and stiffness of various NFC tubes. Section 8.4 presents flat and unidirectionally reinforced laminate properties made with the same materials as tubes. Section 8.5 describes observed fracture modes during tube compression tests.

NFCs are not considered as materials withstanding compression and they perform better under tensile loading, which is usually used as a benchmark of a specific composite performance [165, 170, 171], but in order to be applicable in construction industry other properties need to be examined, e.g., weathering [29], fatigue [172] or fire resistance [173]. Moreover, in real life applications, compressive loads are unavoidable, e.g., in tensile-compressive coupling of flexural deformation, unbalanced stacking sequence of a laminate or if residual stresses are present in the composite. Therefore, the performance of NFCs under compressive load was selected to be analysed.

A composite tube, either with round or square profile, is a versatile element in all aspects of engineering and potential applications for a bio-composite tube have been identified, e.g. replacement of wood structure in Hempcrete wall construction, posts, beams, furniture elements or even parts of a bicycle frame. This study focuses on a compressive behaviour of natural fibre composite tubular shells in the elastic region and the post collapse progression, which are considered of importance for energy absorbing structures and safety considerations. A series of tubular hemp composites were processed by filament winding and tested in order to investigate the fracture mechanisms during compressive loading.

6.1 Tube Structures

The NFC tubes were composed of balanced yarn reinforcement layers with the designed wind orientations of 10° , 30° , 45° , 60° and 90° , the actually measured average winding angles of which are $11.1^\circ \pm 0.9$, $\pm 28.9^\circ \pm 1.1$, $45.2^\circ \pm 1.1$, $57.8^\circ \pm 1.4$ and $89.3^\circ \pm 0.4$, being denoted as samples T10, T30, T45, T60 and T90 respectively. The slight variation of the fibre orientation may be caused by the variation in yarn diameter as well as two stages of tubes preparation. Figure 97 presents the examples of four test pieces with different yarn arrangements visible as the surface texture. It can be seen that the developed machine and process are able to formulate the structure of the NFC tubes. The volume fraction of the reinforcement in processed composites was measured by comparing mass of dried reinforcement used and impregnated laminate. The V_f of the processed tubes was equal to 30% (RSD=2%).

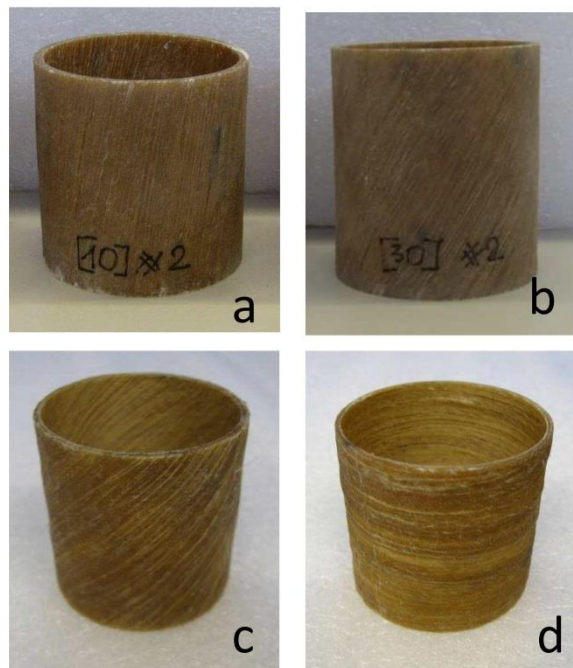


Figure 97 Examples of NFC tubes with four reinforcement arrangements: (a) T10; (b) T30; (c) T45; (d) T90

6.2 Yarn Properties and Resin Distribution

Twisted yarns were used in this study in order to formulate the continuing yarn reinforcement of the discontinuous natural fibres and increase the strength to sustain tension load during filament winding production. The 130 Tex hemp yarn surface is presented in Figure 98A as an example. The image reveals the arrangement of individual technical fibres and the yarn hairiness, which are individual fibres protruding from the main yarn structure. Individual short fibres are held together by the frictional forces induced by the yarn twist, which arranges fibres at an angle to the main yarn direction. The diagram in Figure 98B illustrates the positioning of cross-section images and the direction of the reinforcement angle for the tubes developed.

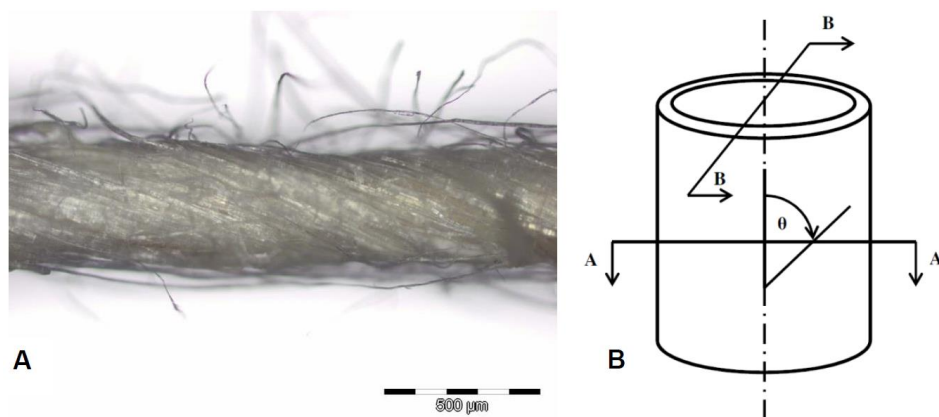


Figure 98 (A) Hemp yarn with 130Tex with visible individual technical fibres arrangement and yarn hairiness (B) A diagram with positioning of cross section images and the angle of the reinforcement

A group of longitudinal and transverse cross sections were prepared in order to illustrate fibre distribution and laminates microstructure (Figure 99). Figure 99A illustrates the cross section microstructure images of the T45 tube wall (in the “A-A” direction – normal to the longitudinal direction of the tube). Figure 99B illustrates the cross section in the “A-A” direction of the tube reinforced with the yarns arranged at 0° (grey region) and 90° (darker region). Figure 99C represents the cross section of the T90 tube wall in the “B-B” direction – perpendicular to the tube direction. Figure 99D illustrates the cross section of the T90 tube wall in the “A-A” direction. The darker regions represent the cross sections of the

yarns in the transverse direction or porosity. It can be seen that the overall impregnation of the technical fibres is visible together with a close packing of individual yarns. The resin penetrated within the yarn and onto the surface of the technical fibres. However, it is evident that there is an uneven distribution of yarns within the tube wall (Figure 99B, Figure 99C), which may be due to the fluctuation of individual yarn diameters leading to uneven individual yarn packing. Uneven compacting (laminating) during the winding formulation can also be observed (Figure 99C, right side); the lighter colour between the yarns shows the concentration of resin. The diameter of the 130 Tex hemp yarn used was $d = 269.3 \pm 39.8\mu\text{m}$ and diameter of the technical fibre composing yarn was equal to $d_f = 14.4 \pm 3.6\mu\text{m}$.

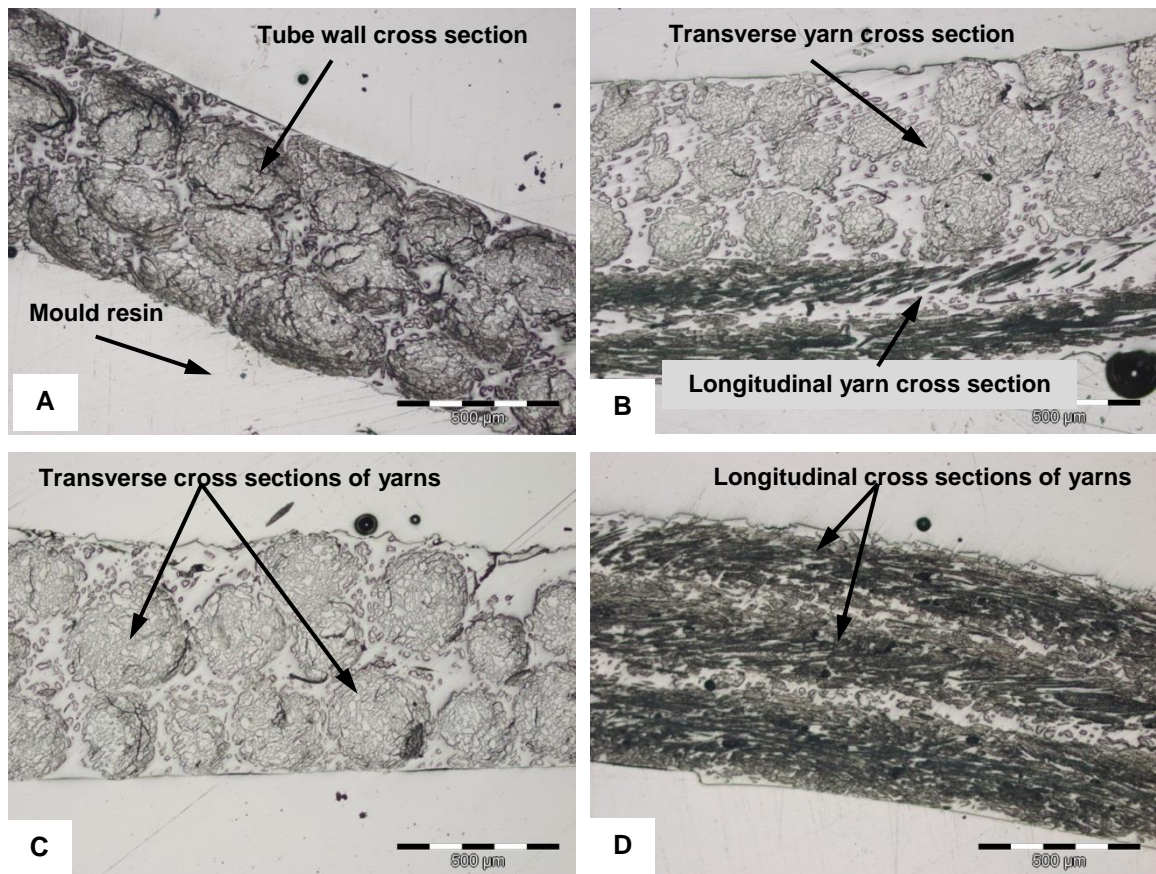


Figure 99 (A) Cross section of the T45 tube in the 'A-A' direction (B) cross section in the 'A-A' direction of the tube with the reinforcement oriented at 90° and 0° (C) the T90 tube in the 'B-B' direction and (D) the T90 tube in the 'A-A' direction

In order to find the allowable load which a yarn can withstand while winding, the yarn tenacity was also measured with 250mm gauge length and 250mm/min crosshead speed in accordance with ISO/DIS 2062. Additionally, samples were also tested with a 4mm gauge. This was selected in order to reduce the possible influence of fibre slipping in comparison with the standard tenacity. The mean load carrying capacity of a yarn tested at 250mm gauge length was $P_{av}=16.8\text{N}$ (RSD=23.7%), while the shorter gauge length resulted in an average load equal to $P_{av}=22.45\text{N}$ (RSD=24.1%). The dispersion of the results is caused by a variation in fibre diameter, fibre length distribution and load distribution across the yarn. Tenacity of a 130 Tex yarn was calculated and equal to 13.6cN/Tex (RSD=16.1%). This result suggests that it is desirable to reduce the length of the yarn transportation path during winding, and the yarn delivery system may influence the integrity of the yarn as well as the NFC properties. A scrutiny of the test results indicated that the impregnation of the individual fibres was complete (Figure 100A), which is represented by filled out small spaces and surface contact, hence processing parameters were suitable for the resin viscosity. However, there may be a weak surface bond between fibre and matrix, which resulted in delamination between the fibre and matrix (Figure 100B), which could be caused by excessive pressure during the polishing process, surface contamination or fibre shrinkage. Figure 100C and Figure 100D also indicate the existence of porosity within the yarn, visible as the darker regions inside the yarn cross sections.

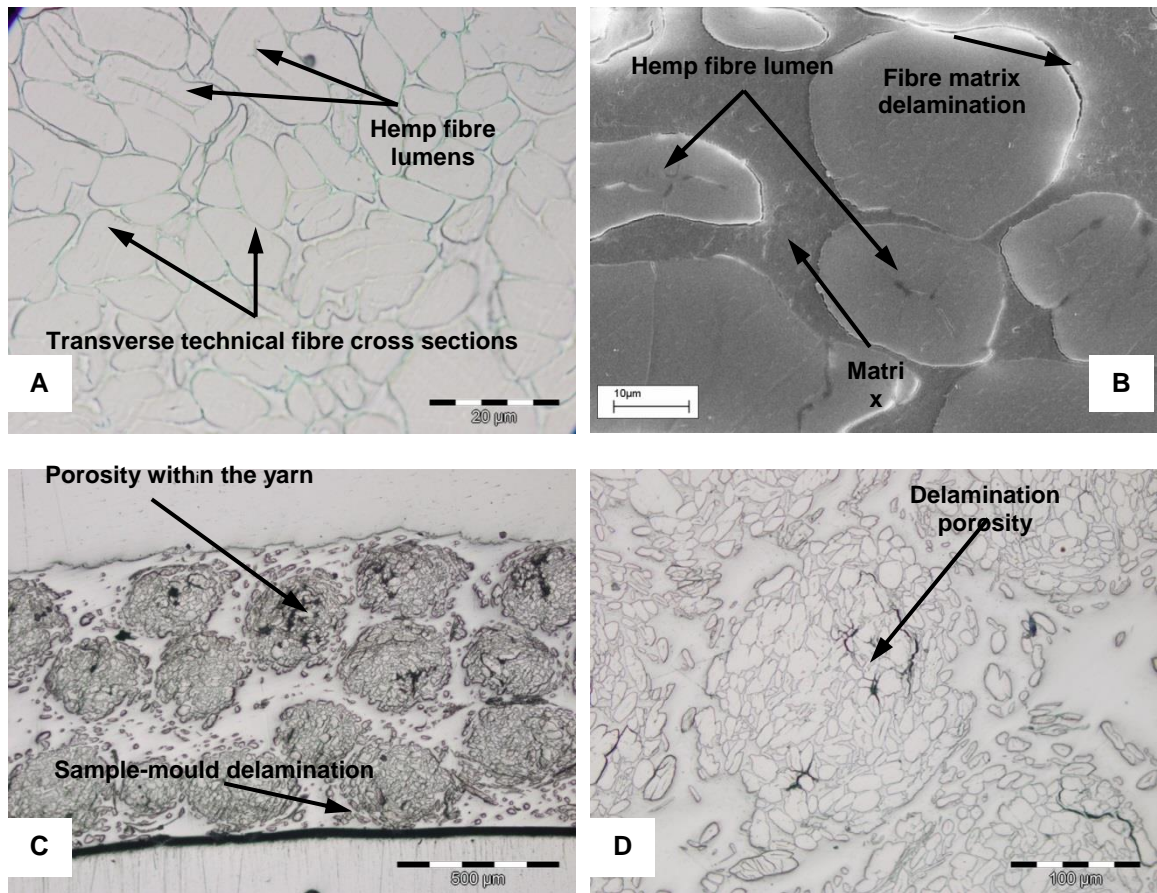


Figure 100 (A) Impregnation of individual technical fibres within the NFC tube (B) interface of hmp-matrix within the NFC tube wall (C) the cross section of the tube wall with porosity within the yarns visible as black areas and (D) optical image of cross section revealing delamination sites within the yarn

6.3 NFC Tubes Compressive Properties

A summarised compression test result for the thin walled tubes with various yarn orientations is presented in Table 19. It can be seen that the modulus and ultimate stress are inversely proportional to the reinforcement orientation angles. The highest stress achieved in NFC hemp tubes is 76MPa with a fibre orientation at 11° , which is about 2.5 times higher than the peak stress observed in tubes with reinforcement aligned at 89° . The highest compression modulus is 5.6GPa achieved for samples with reinforcement at 11° , which is 4 times higher when compared with samples reinforced at 89° . The strain to

failure for the hemp tubes with an angle of 11° is about $2/3$ that of tubes with an angle of 89° . In tubes reinforced at an angle close to the longitudinal direction, the buckling is controlled by fibre effects, such as microbuckling, while loading in the transverse direction has more influence from the matrix when compared with longitudinal loading, and in this case adhesion between fibre and matrix influences the load propagation [174]. A comparison of compressive strength and stiffness of tubes and commercially produced solid rods indicates that the stiffness of both elements is around 5.5 GPa. However, the strength of NFC hemp tubes developed with the fibre orientation of 11° is about $1/3$ higher than that of the commercially produced solid.

Table 19 Influence of the winding angle on compression properties

<i>Sample</i>	σ_{max}	<i>SD</i>	<i>E</i>	<i>SD</i>	<i>Strain at</i>	<i>SD</i>	<i>MoR</i>	<i>SD</i>
<i>wind angle</i>	[MPa]		[GPa]		<i>failure</i>		[MJ/m ³]	
					[mm/mm]			
T90 (89.3°)	30.1	2.4	1.5	0.1	0.036	0.004	0.309	0.033
T60 (57.8°)	33.2	3.4	1.8	0.2	0.032	0.006	0.299	0.056
T45 (45.0°)	53.9	2.1	3.6	0.3	0.032	0.003	0.317	0.039
T30 (28.9°)	63.4	6.1	3.1	0.4	0.031	0.004	0.586	0.091
T10 (11.1°)	76.2	4.2	5.6	0.6	0.024	0.003	0.632	0.190

The relationship between the wind angle and the ultimate compression stress is exponential (Figure 101). The compression strength decreases significantly from 11° to 45° and then both results for samples with 58° and 89° are close to 30MPa. A scrutiny of the compressive strength indicates that the ultimate stress of the developed tubes may increase with a wind angle below 45° , since resin ultimate compression stress is 42MPa. For tubes reinforced at higher wind angles, the compression strength is decreased to below that of resin, because the deteriorating effect of porosity and interface delamination may be higher than the effect of fibre reinforcement.

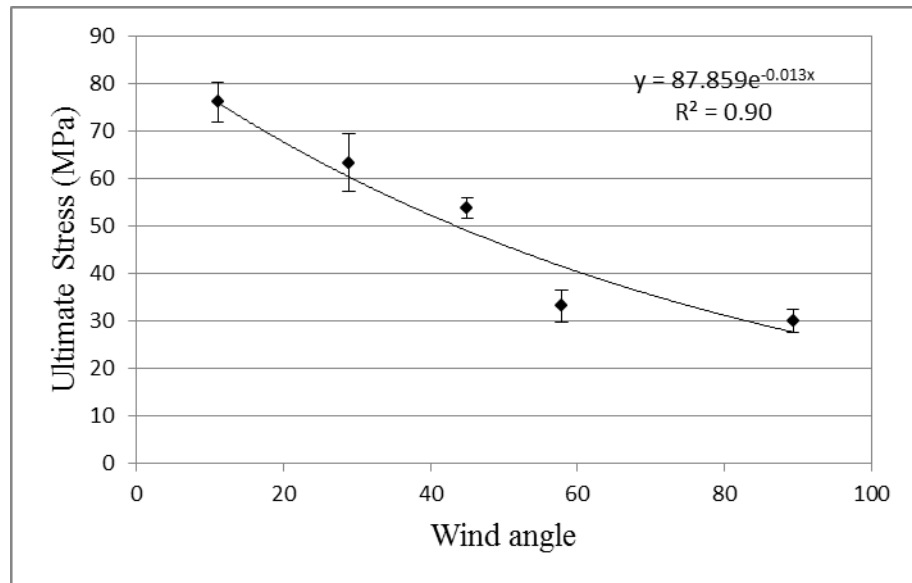


Figure 101 Relationship between the ultimate compression strength of the NFC tubes and the yarn wind angles

A similar relationship is observed between compression modulus and the wind angle (Figure 102). Only the sample with fibres arranged at 11° increases the compression modulus in comparison with pure polyester resin. The rest of samples reinforcement arrangements deteriorate the compressive modulus. This further indicates that the interface strength between matrix and fibres may not be sufficient.

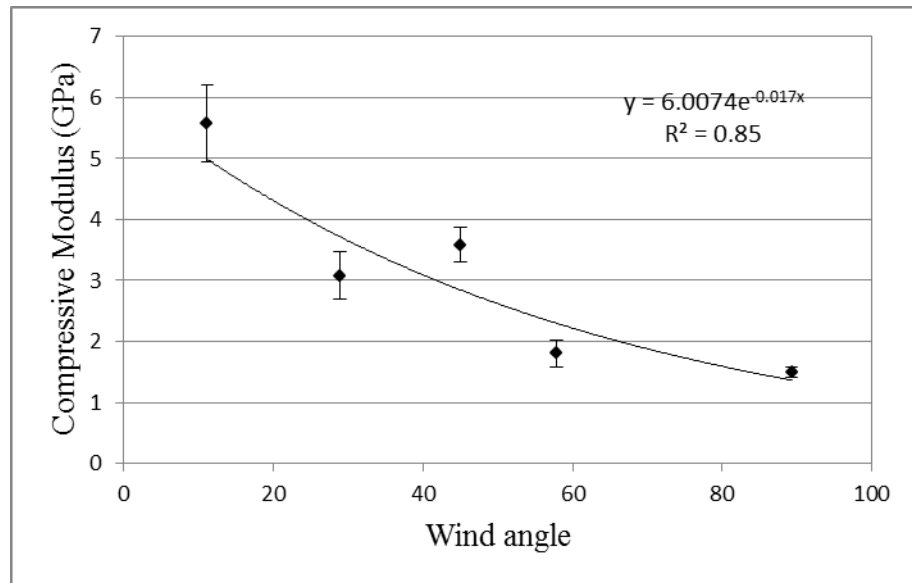


Figure 102 Relationship between the compressive modulus of the NFC tubes and the yarn wind angles

6.4 Laminate Properties

The tensile strength of hemp 130 Tex yarn laminate was evaluated by using rectangular test pieces (Fig. 8B) unidirectionally reinforced with volume fraction $V_f = 30\%$, which was equal to that of the processed tubes. Samples were tensile loaded at 2mm/min until fracture. It was found that the samples have an axial tensile strength of 128.9MPa (RSD=2.5%) and a mean tensile stiffness of 8.9GPa (RSD=7.3%), and the flexural strength and flexural modulus were 165MPa (RSD 5.2%) and 10.2GPa (RSD 4.2%), respectively. An investigation of commercially pultruded hemp reinforced composite rods (Figure 103A) has also been carried out in the research group and outcomes have been published [116]. The summarized results were a compressive strength equal to $\sigma_c=53\text{MPa}$ (SD=0.29), a compressive stiffness equal to $E_c= 3.83\text{GPa}$ (SD=1.09). The reported tensile strength of hemp-polyester composite rods was equal to $\sigma_t=122\text{MPa}$ and a tensile stiffness equal to $E_t= 16.84 \text{ GPa}$. A comparison of the laboratory compression and factory pultruded hemp composites showed that both composites have a very similar tensile strength while the tensile stiffness of the commercially pultruded composites is higher. The difference in the tensile stiffness may be due to the fact that the commercially pultruded samples were made

with hemp fibres arranged at 0° by aligning fibre sliver and then wrapping it with additional polymeric yarn, while the laminates processed in laboratory were made with yarns with twisted architecture (Figure 103A), which inherently changes individual fibres orientation towards the main yarn axis thus decreasing laminate modulus (Figure 103B).

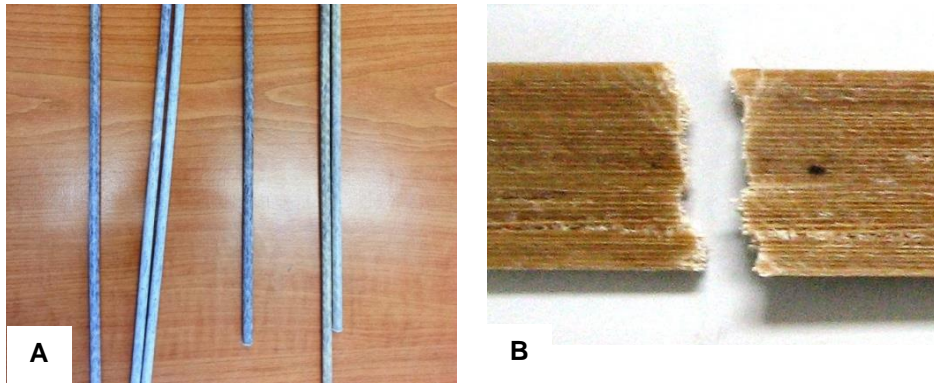


Figure 103 (A) An image of commercially pultruded NFC rods reinforced with hemp yarns (B) a fracture area of the rectangular test piece after tensile test

6.5 Failure Modes

Micromechanical failure theories for unidirectional composites describe that the fracture of fibre reinforced composites consists of one or more mechanisms: microbuckling, kinking, fibre failure, longitudinal cracking or their mixture [143]. Microbuckling starts with a localized single fibre, waviness appears and delamination then follows. Kinking involves the fracture of fibres along the kink bands. Longitudinal cracking appears when cracks are parallel to the fibres [174]. The travelling hinge theory describes post initial fracture behaviour of isotropic thin-walled tubular shells. It was derived from energy relationships, which were based on hinge creation during the collapse of the tube incompressible walls. Tubes buckle in various ways depending on wall elastic properties geometry. It can take the form of annual rings described as concertina shape buckling or diagonal triangular hinges described as diamond shape buckling. Alternatively, composite tubes can collapse through crushing. This is normally observed for thick walled tubes, for which the structure fractures through crumbling on the small scale, as opposed to buckling of the walls. A tubular shell can be designed to crumble under compression load, instead of bending along the hinges.

The crushing consists of the combined work used for microbuckling and micro fragmentation of the material, and it is described through its energy absorption capabilities in respect to volume [175]. The total energy is calculated by integrating the area below the stress–strain axial compression relationship [176, 177].

6.5.1 Microbuckling

The test results show that NFCs can fail through the microbuckling process; an example of NFC microbuckling is given in Figure 104. This fracture mode is characterized as a localized material instability where fibres rotate within the narrow band of about 20 fibre diameters. As reviewed by Schultheisz and Waas [143], microbuckling is controlled by matrix stiffness in shear, which results in sensitivity to time, strain rate and test conditions. Moreover, microbuckling depends on initial processing defects of the composite, such as fibre misalignment or matrix shrinkage induced residual stresses and porosity [174]. This is considered of importance as the hemp yarn may consist of multiple technical fibres, which increase defect content.

Figure 104A depicts the stress-strain response of tube T10 type. The average compressive load for this type of tube was equal to 76.2 MPa (RSD=5.5%). It is evident that the fracture can be characterized by a sudden fracture, followed by force dissipation associated with sliding of the tube walls. Fractures along the fibres are visible as vertical cracks along the surface (Figure 104B). The dotted line indicates one of the test repetitions, showing the consistency of the failure patterns. It is apparent that the microbuckling reduces when the fibre orientation angle increase. A similar observation was made in a previous research on glass fibre reinforced composite tubes [178].

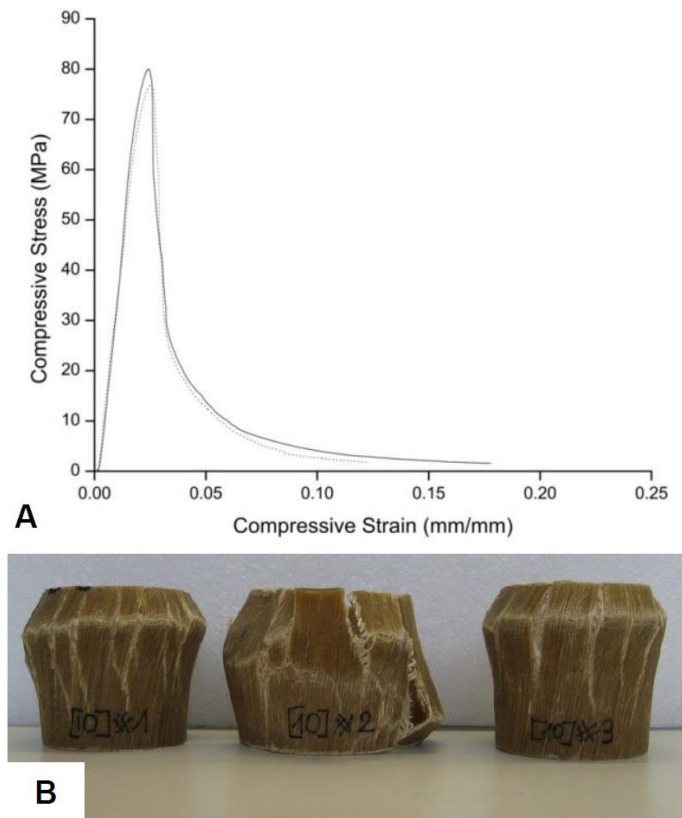


Figure 104 Microbuckling fracture (A) stress-strain response graph (B) Examples of T10 samples fractures in microbuckling

6.5.2 Diamond Shape Buckling

Another type of fracture mode observed in this study for NFC was the diamond shape buckling (Figure 105) as described for travelling hinge buckling. Thin walled tubes, made of plastic isotropic material, can collapse by forming axisymmetric rings or by folding along hinge lines and creating a diamond like pattern after exceeding the buckling initiation stress [179]. The process of the collapse depends upon the geometrical relationship between the tube diameter, wall thickness and tube length. Following an initial peak, which represents a beginning of sample fracture, an oscillation-like pattern emerges, representing the stress concentration-dissipation processes related with subsequent hinges folding (Figure 105A). The initiation load for the samples exhibiting diamond shape buckling is approximately half of the microbuckling initiation load (Figure 104A and Figure 105A). However, in diamond

shape buckling, the load related with the work done on bending of hinges is sustained throughout the collapse.

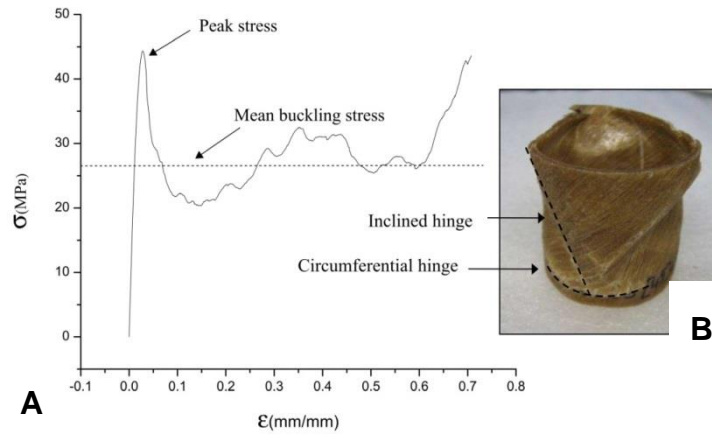


Figure 105 Diamond shape buckling fracture (A) A stress-strain response (dashed line represent mean post buckling load) (B) Diagonal lobes formation in diamond shape buckling collapse

6.5.3 Concertina Shape Buckling

The travelling hinge buckling was also observed in the tests of the NFC, which is the concertina shape buckling. In the T30 samples horizontal symmetrical hinges were created in absence of diagonal lines. This kind of fracture was named concertina buckling mode while observed in isotropic plastic material tubes [179, 180]. Fracture starts from one end and progressively continues until the tube collapses. The process is accompanied with characteristic load oscillations, which relate to the appearance of subsequent lobes as indicated on the graph (Figure 106A). Compression stress-strain graphs for NFCs tubes, in comparison with isotropic plastic tubes, are not smooth. This might be related with the lower tensile strain to break and lower plasticity of the NFCs. The yarn is composed of individual fibres and cracks will progress faster at yarn discontinuity boundaries. During lobe formation, the tube wall is exhibiting flexural deformation, and a crack is created on the extensional side until it stops on the compressed side of the flexed wall.

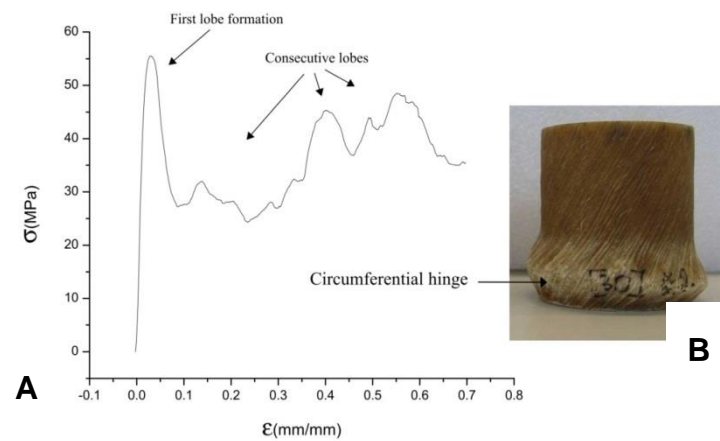


Figure 106 Concertina shape buckling fracture (A) A Stress-strain response (B) Initial stage of concertina shape buckling collapse mode with first circumferential hinge

The main difference between microbuckling (Figure 104), diamond shape buckling (Figure 105) and concertina buckling (Figure 106) is that microbuckling is initiated at higher stress levels. In microbuckling a dramatic load drop follows immediately after fracture initiation, and the tube is not able to sustain additional load. In concertina shape buckling, similar to diamond shape buckling, the post buckling load is sustained until total collapse occurs.

6.5.4 Progressive Crushing

A progressive crushing failure mechanism was observed. The fracture starts from the localized stress concentration at one end and progresses until the whole tube is crumbled. In the plastic tube field, this collapse mechanism was described as the combined work used for micro fragmentation and local interlaminar fracture of the composite wall [176]. Moreover, progressive crushing is also initiated by chamfering the end of the tubular sample, imperfect clamping or voids [181]. Examples of the progressive crushing stress-strain response for two thick walled tubes T30 and T60 are presented in Figure 107A. After reaching a peak load, the graphs start to oscillate around the mean crush propagation stress indicated by dotted lines. Figure 107B illustrates the crushed sample half-way through the test with visible crumbled edges. The crushing is characterized by higher energy absorption in comparison with other fracture mechanisms previously discussed.

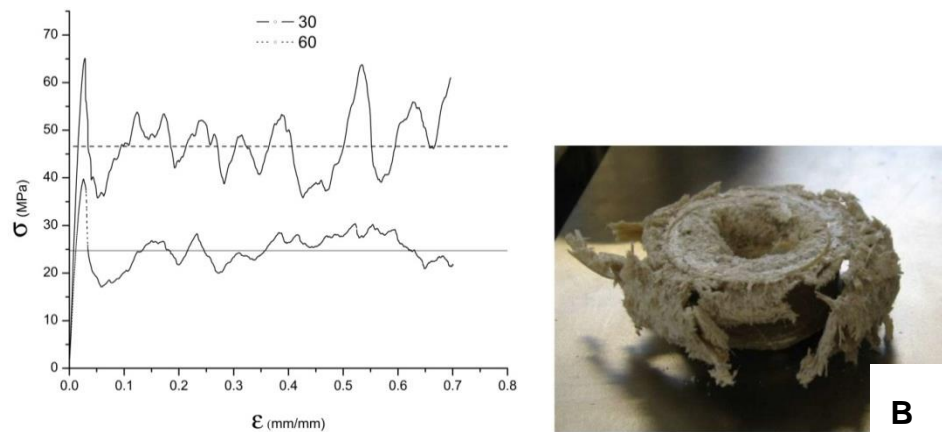


Figure 107 Progressive crushing (A) Examples of stress-stain responses (NFC T30 and T60 tubes with the ratio $t/D > 0.04$. Horizontal straight lines represent mean crushing loads) (B) A crushed sample during the test

The above tests for the BFRP tube compression and compression fracture mechanisms were not performed before on this type of material. There were studies conducted by Harte et al. [182] who studied the collapse and compression failure mechanisms of GFRP.

6.6 Summary

The compressive behaviour of BFRP was investigated with use of filament reinforced tubular shells. The main findings related with compressive properties can be summarised as follows:

- 1) There is a correlation between the hemp yarn reinforcement angle and compressive properties of tubes. The maximum ultimate compressive stress was achieved for shells with reinforcement at 11° angle, i.e. 76MPa.
- 2) Similarly, correlation was observed for compressive stiffness. The maximum compressive modulus was observed for reinforcement at 11° angle, i.e. 5.6GPa.
- 3) Moreover, there were four types of failure modes observed, namely microbuckling, diamond shape buckling, concertina shape buckling and progressive crushing.

7 Weathering Performance of NFCs

Chapter 6 presents analysis of weathering conditions influence on mechanical properties of flax fabric reinforced bio-polyester laminates. It is composed out of three sections. Section 6.1 provides results and discussion about heat ageing. Section 6.2 describes immersion in fluids and environmental weathering influence on BFRPs, and section 6.3 describes water absorption aspects of these laminates.

It is estimated that cellulose is synthesized globally at a rate of 4×10^{10} tonnes/year, which makes it the most abundant plant biomass carbohydrate available [183]. Many organisms and microorganisms use cellulose as a source of energy by breaking it down into glucose during enzymatic processes [184]. Natural fibres (NF) are prone to many types of environmental degradation, i.e. exposition to moisture, UV radiation, bacteria, fungus and termite attack [4]. The natural degradation of cellulose allows for biomass circulation within the eco-system, but at the same time properties of cellulose in man-made materials deteriorate due to the same factors. In order to prevent degradation, treatments, additives and inhibitors are used on matrix systems.

The second form of protecting NF-based materials is sealing-off from a surrounding environment or restricting their use only to indoor applications. In order for a building construction material to meet building standard regulations, a weathering test is performed. Composite materials are evaluated in laboratory weathering tests in controlled environmental conditions or during outdoor environmental weathering. The former test type allows for precise control over influencing factors, but does not take into account a concurrence of multiple outdoor factors. The latter is the closest to reality but cannot be precisely controlled. Moreover, it is specific and sensitive to regional climate changes. Tests are conducted by exposing sample coupons to a deteriorative agent and later measurement of investigated property and comparison against unconditioned material. When measuring

mechanical properties degradation, the flexural test is relatively easy to conduct. As mentioned in Chapter 5, flexure is a compound form of deformation including tension, compression and shear; therefore, it gives information on a compound effect of weathering.

7.1 Heat Ageing

The influence of heat ageing on BFRPs was investigated. The procedure consisted of exposing samples to an elevated temperature, i.e. 110°C, in an air-circulating oven for durations of 30 min and 120 h. After the exposure, coupons were cut into test coupons and tested for ultimate flexural stress, flexural modulus and flexural strain. Figure 108 presents a comparison between flexural modulus results of four types of flax hopsack fabric laminates. The first two laminates were processed by hot pressing technique (Figure 36) with Crystic and Palapreg resins, and are denoted as PE and PP, respectively. The other two laminates were processed with a vacuum bagging technique (Figure 37) with Crystic and Palapreg resins, and are denoted as PEV and PPV, respectively.

There is a difference in flexural modulus values between laminates processed with hot press and vacuum bagging, in both cases, i.e. laminates with Crystic and Palapreg resins. The discrepancy is an outcome of a different processing pressure, which affects laminates fibre volume fraction. These differences between processing techniques were discussed previously in section 4.5, which describes processing influence on laminate tensile properties. Heat ageing had no deteriorative effect on flexural modulus of laminates processed with crystic matrix. Laminates processed with palapreg resin exhibit a visible increase in modulus after 120h exposure, which suggests that the matrix undergoes a post-curing process during heat ageing. This may explain a slight increase in stiffness.

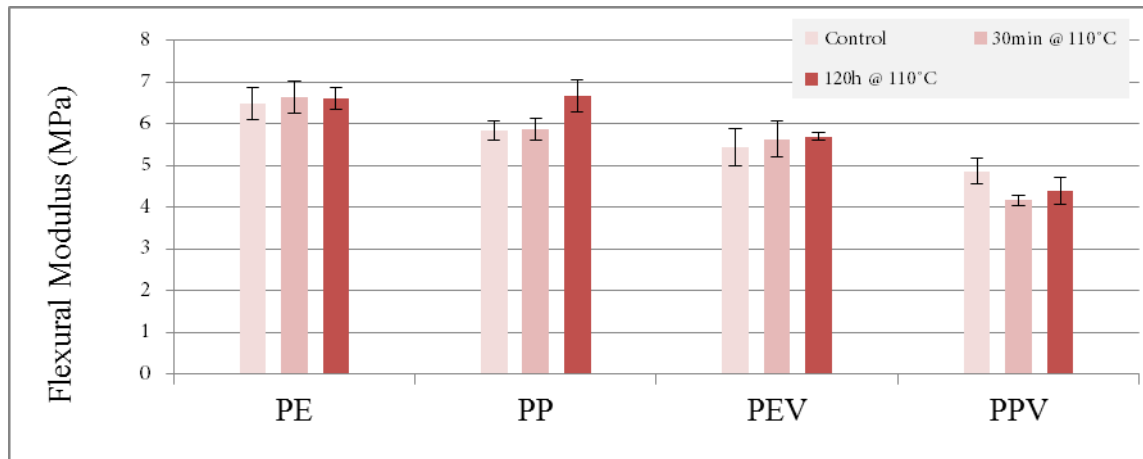


Figure 108 Flexural modulus results for flax non-twisted fibre 250Tex flax yarn hopsack fabric reinforced laminates under heat ageing (compression moulded: PE- Crystic matrix and PP – Palapreg, vacuum bagged: PEV – Crystic and PPV - Palapreg)

Figure 109 presents the flexural stress results for the analysed laminates. The influence of heat ageing on flexural stress is visible for the Crystic matrix after 120h exposure for processing cases. Laminates with Palapreg matrix exhibit no flexural modulus deterioration. This might be explained, similarly to flexural modulus results, with continued post-curing process. It is possible in some composite applications to use slightly under-cured matrix and allowing for natural post-curing to take place, which may extend the life span of the installed part.

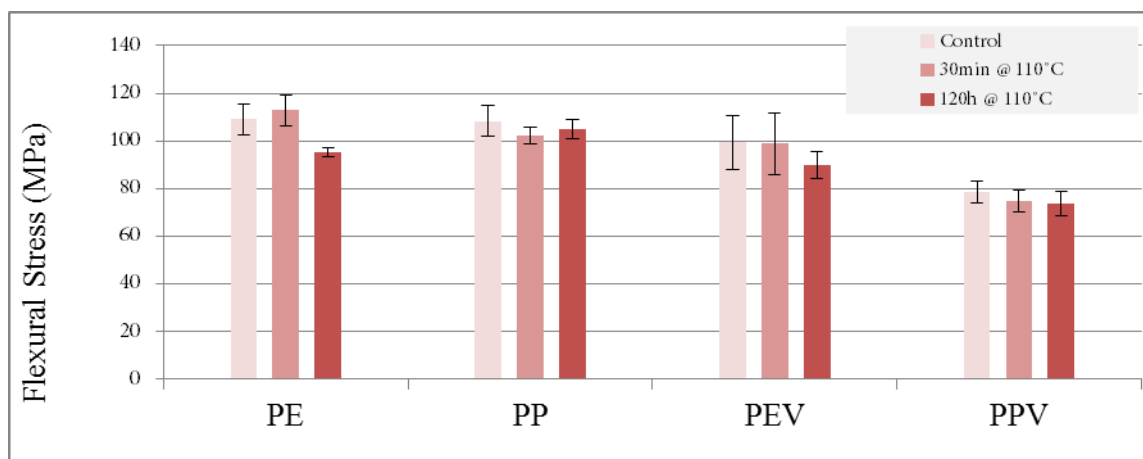


Figure 109 Flexural stress results for flax non-twisted fibre 250Tex flax yarn hopsack fabric reinforced laminates under heat ageing (compression moulded: PE- Crystic matrix and PP – Palapreg, vacuum bagged: PEV – Crystic and PPV - Palapreg)

Figure 110 presents flexural strain results for the analysed laminates. It is visible that heat ageing is reducing average flexural strain to failure for all tested laminates. The strain to

break is reduced with both steps of heat ageing, i.e. for both 30min and 120h exposures. This further suggests that the post-curing process takes place, which leads to an increased cure level and decreased plasticity of the composite. The matrix is becoming more brittle together with an increase of the cure level.

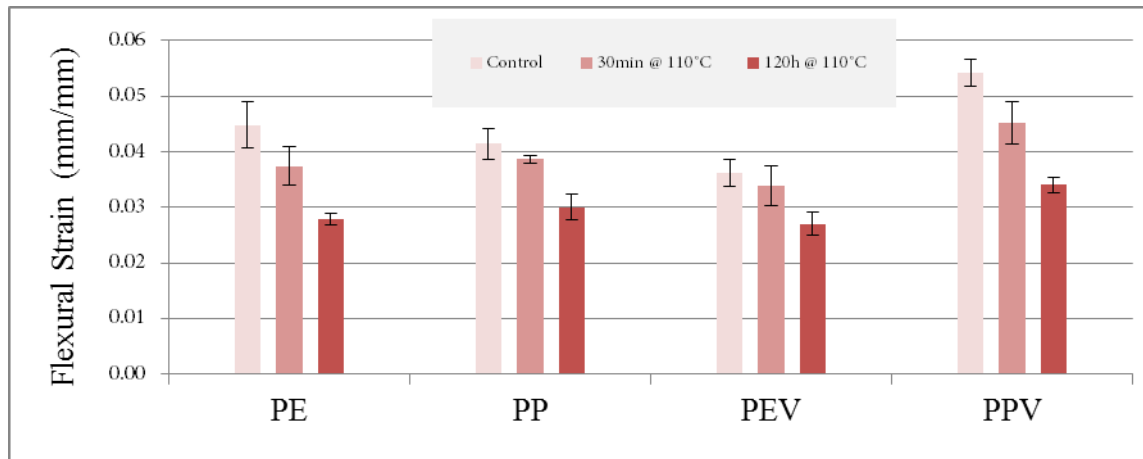


Figure 110 Flexural strain results for flax non-twisted fibre 250Tex flax yarn hopsack fabric reinforced laminates under heat ageing (compression moulded: PE- Crystic matrix and PP – Palapreg, vacuum bagged: PEV – Crystic and PPV - Palapreg)

7.2 Immersion in Fluids and Environmental Weathering

Laminates reinforced with flax fabric were further examined under weathering conditions. Samples were subject to natural environmental weathering in UK climate. Moreover, other groups of samples were subjected to immersion in distilled water and saline solutions for one month. The results were compared against control samples kept in the control indoor environment. Figure 111 presents examples of three control coupons and three coupons after 1 month environmental exposure. There was a change in colour in the treated laminates.

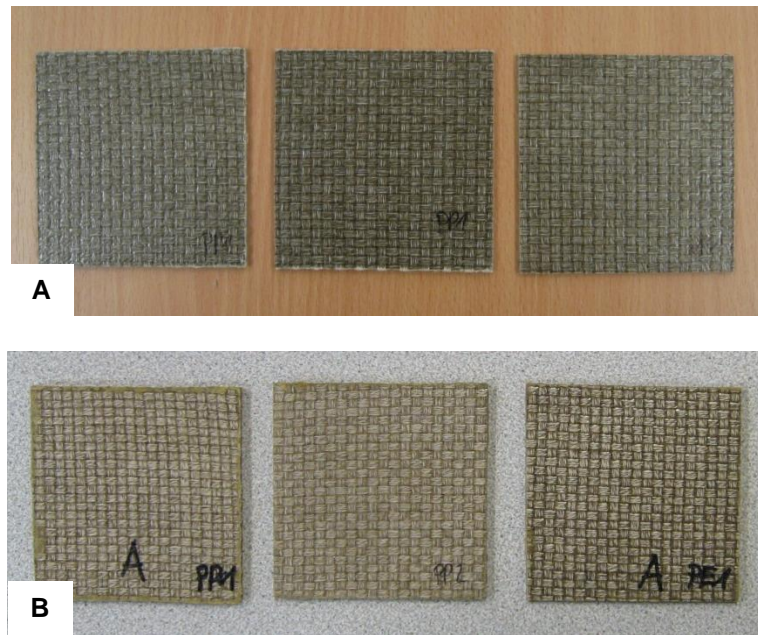


Figure 111 (A) Examples of flax hopsack fabric reinforced PalapregEco matrix laminate coupons. (B) Examples of samples after one month weathering exposure

Figure 112 presents flexural modulus test results for flax laminates after weathering. A reduction of flexural stiffness was observed for all samples after weathering and immersion exposures. For both Crystic and Palapreg matrices, samples exhibited 35% and 40% flexural modulus deterioration, respectively. This is significant material properties deterioration due to the direct exposure and interaction with water.

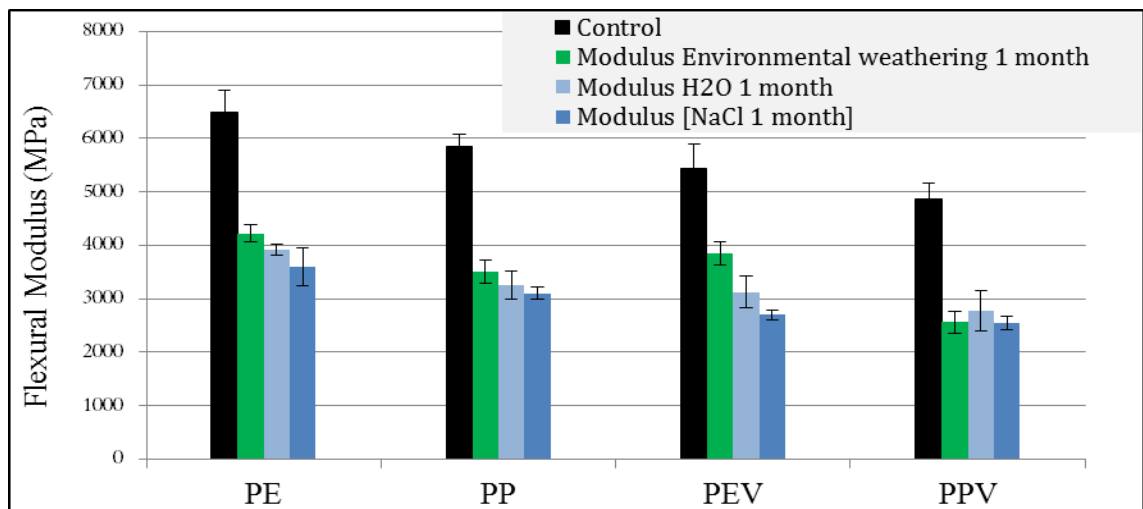


Figure 112 Influence of environmental weathering, immersion in water and saline solution on flexural modulus for flax non-twisted fibre 250Tex flax yarn hopsack fabric reinforced laminates (compression moulded: PE- Crystic matrix and PP – Palapreg, vacuum bagged: PEV – Crystic and PPV - Palapreg)

Figure 113 presents flexural stress test results for flax laminates after weathering. The ultimate flexural stress is reduced after the exposure for all exposed laminates. Saline water had the highest deteriorative influence on flexural strength with up to 19% reduction. For crystic matrix laminates there is a clear gradation of deteriorative influence, from environmental weathering to saline solution causing the biggest reduction. This might be explained with time of exposure to water. In environmental weathering the sample is immersed in water during rainfall and precipitation events.

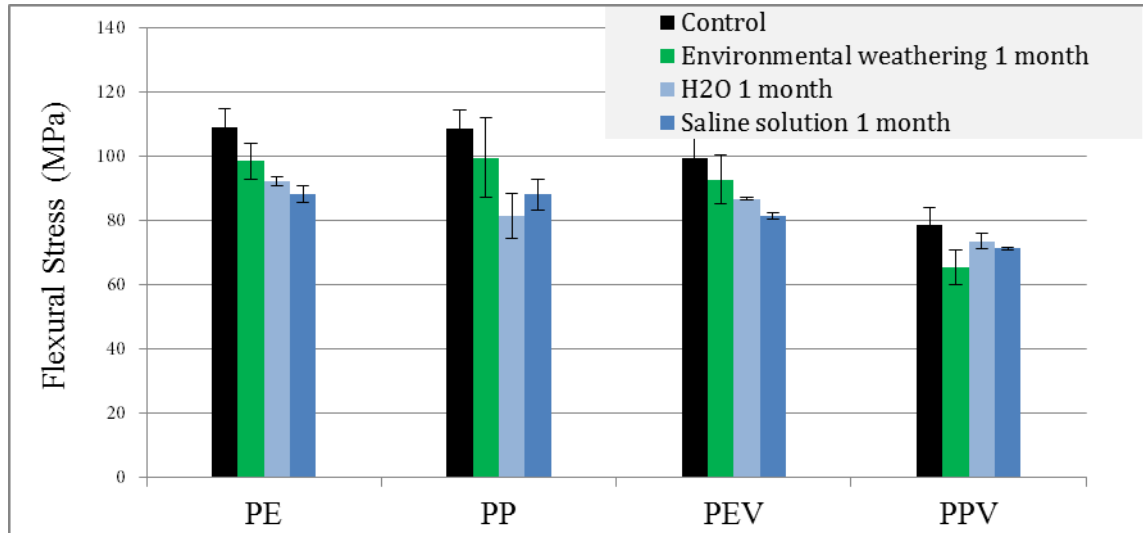


Figure 113 Influence of environmental weathering, immersion in water and saline solution on flexural stress for flax non-twisted fibre 250Tex flax yarn hopsack fabric reinforced laminates (compression moulded: PE- Crystic matrix and PP – Palapreg, vacuum bagged: PEV – Crystic and PPV - Palapreg)

Figure 114 presents flexural strain results for flax laminates after weathering. The flexural strain to break rises for all samples after exposure. This reinforces previous observation and mechanism illustrated in Figure 116, which explains water mechanism deteriorating fibre-matrix interface, thus increasing tensile strain to break.

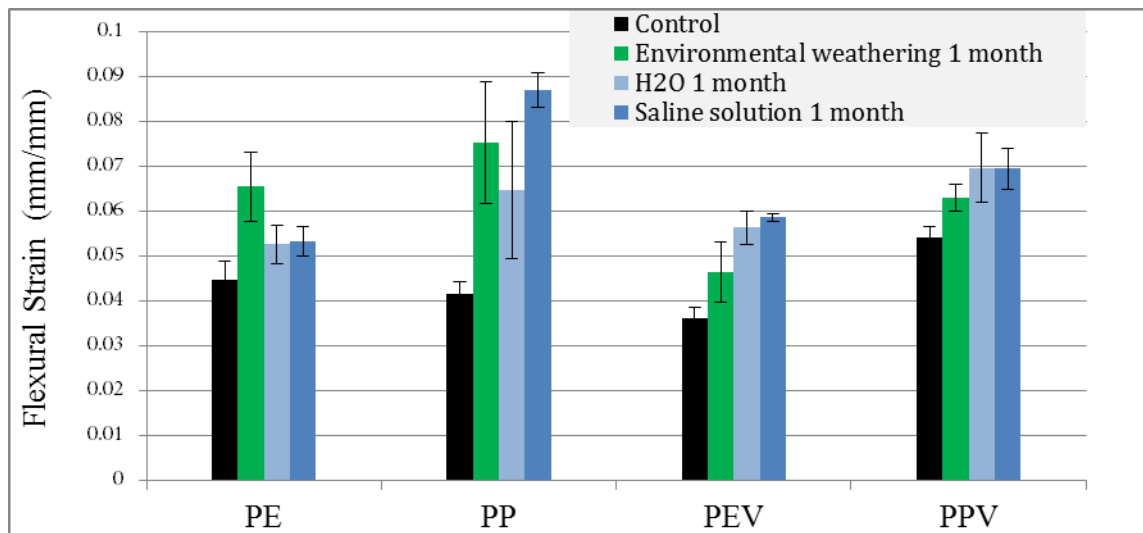


Figure 114 Influence of environmental weathering, immersion in water and saline solution on flexural strain for flax non-twisted fibre 250Tex flax yarn hopsack fabric reinforced laminates (compression moulded: PE- Crystic matrix and PP – Palapreg, vacuum bagged: PEV – Crystic and PPV - Palapreg)

Figure 115 presents the influence of weathering and immersions on the laminate thickness changes. In all cases the thickness of the composites increased. This is due to hydrophilic properties of the bast fibres, which will absorb moisture from air or water when immersed, thus leading to dimensional changes. There was an increase of 3-4% observed after 1m exposure time for Crystic and Palapreg laminates. The water absorption will be discussed further in the next section.

Natural fibre composites with polyester matrix were subject to weathering tests in the past. The aforementioned results confirm the effect of the processing methodology on BFRP sensitiveness to environmental weathering. Other authors' results present the influence of processing and fibre preparation. For instance, the processing methodology described by Mwaikambo and Bisanda [185] makes it possible to conclude that residual moisture was present in their laminate. The authors concluded that weathering did not have an influence on properties, but scrutiny of presented result shows about 20% reduction in ultimate flexural stress. The flexural modulus did not change, but this might be due to aforementioned moisture already present in the composite. This leads to reduced interphase properties between natural fibre and matrix due to steam creation from residual

moisture, hence low initial modulus properties. Therefore, preparation of NF before processing should include removal of contaminants, waxes as well as residual moisture.

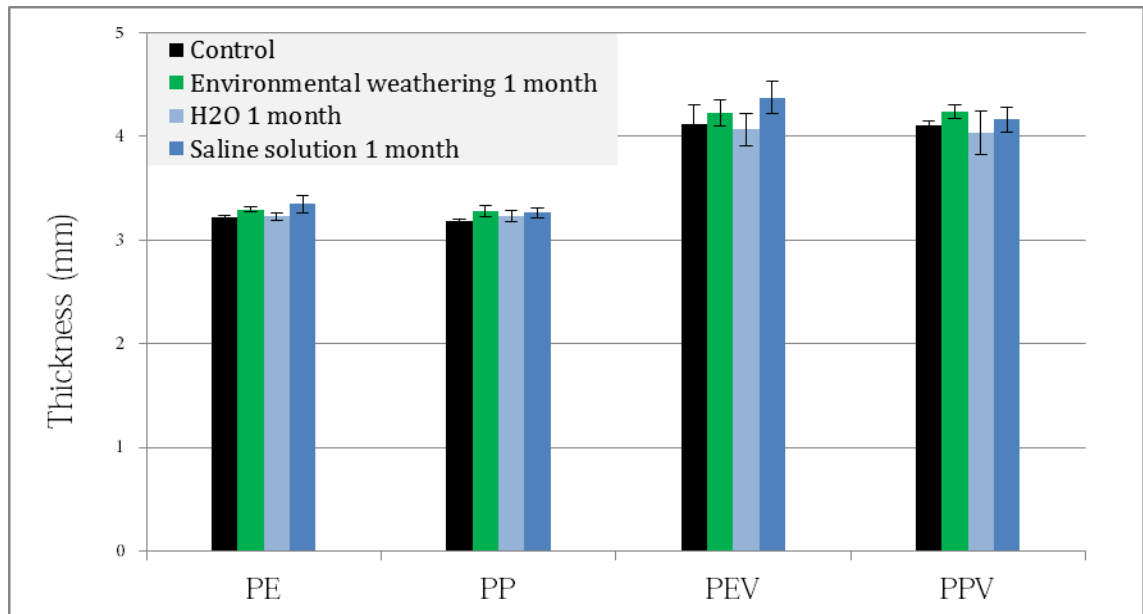


Figure 115 Influence of environmental weathering, immersion in water and saline solution on swelling for flax non-twisted fibre 250Tex flax yarn hopsack fabric reinforced laminates (compression moulded: PE- Crystic matrix and PP – Palapreg, vacuum bagged: PEV – Crystic and PPV - Palapreg)

The decomposition of NF components, i.e. cellulose, hemicellulose, pectin and lignin, is not simultaneous, and individual components differ in sensitivity to deteriorative agents. For instance, lignin is the most prone to photochemical degradation by ultraviolet light. A colour change during natural fibre exposure to ultraviolet light is mostly an effect of the lignin degradation. Therefore, a reduction of the lignin content of NFs by fibre treatment improves their resistance to UV radiation [10]. Gu et al. [186] studied the degradation of polyester films and coatings in alkaline solutions. Before and after the exposure, the surface was examined with an atomic force microscope. It was concluded that the surface does not degrade uniformly and certain regions were more susceptible to hydrolysis, which explained the creation of pits in exposed surfaces. Pothan et al. [187] worked on different aspects of banana–polyester composites with randomly oriented fibre lengths between 20 – 40mm. It was reported that the ultimate tensile stress decreased by 6% for thermally aged laminate. It decreased by 9% for laminate under 6 months of natural weathering and it decreased by 32% for laminate in accelerated water ageing test. Dash et al. [29] conducted

weathering studies on jute alkali treated fibres in unsaturated polyester resin. It was found that flexural stiffness, ultimate tensile strength and Young's modulus, all significantly decreased due to weathering conditions. It was concluded that a high sensitivity to the weathering conditions for polyester matrix natural composites may restrict their applications to dry and low humidity applications. Rodriguez et al. [188] performed analyses of polyester and acrylic matrix composites reinforced with jute fibres. Materials were prepared by vacuum infusion technique and compared by carrying out ignition, thermal degradation and water absorption tests. Composites based on the polyester matrix showed better performance than the acrylic matrix composite. The NFC exhibited a better performance in the water absorption test when compared with GFRP, as expected and did not pass the five second fire ignition tests.

Moisture can induce interface properties deterioration. The schematic mechanism of water induced composite deterioration is presented in Figure 116. The bast fibre embedded in the matrix absorbs water and swells, which create pressure on the interface and fracture. This leads to delamination of the fibres, thus deteriorating mechanical properties.

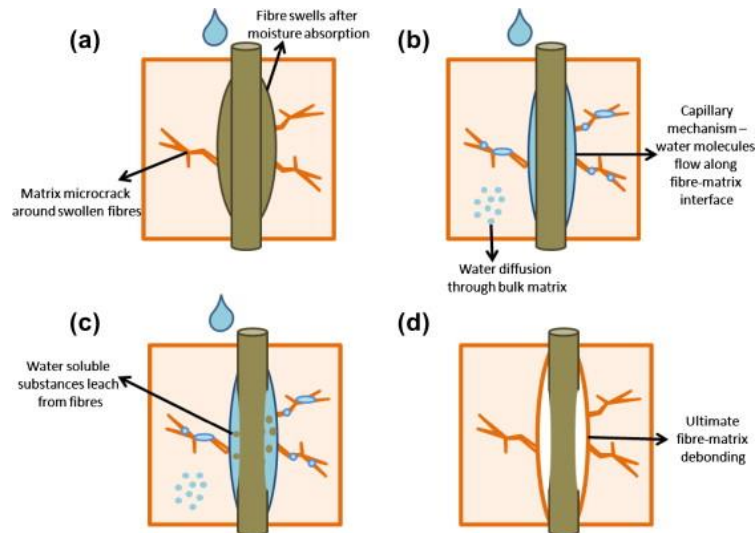


Figure 116 Mechanism of natural fibre debonding due to moisture induced swelling [189]

7.3 Water Absorption

Fick's first and second diffusion laws can be used to calculate the diffusion coefficient [190]. In composite materials, water diffusion can proceed in a Fick and in a non-Fick fashion. Usually, the diffusion of water in composite materials is analysed by comparing it to Fick's law [191-193]. A one-dimensional version of Fick's law is written as:

$$\frac{\partial C}{\partial t} = D \frac{\partial^2 C}{\partial x^2} \quad (22.)$$

where C is the water concentration at given time t and distance x from the surface of the sample and D is the diffusivity (diffusion coefficient). If the behaviour of water absorption can be related to Fick's law, the water content with respect to time can be found as a function of the diffusion coefficient D , expressed in mm^2/s .

$$c(t) = c_s - c_s \frac{8}{\pi^2} \sum_{k=1}^{20} \frac{1}{(2k-1)^2} \exp \left[-\frac{(2k-1)^2 D \pi^2}{d^2} t \right] \quad (23.)$$

where c_s is the water content at the saturation point expressed as a percentage of the total mass, d is the sample thickness expressed in mm and t is the time of exposure expressed in sec. If a correlation with Fick's law is assumed then there is a linear dependency between $\lg(c(t)/c_s)$ and $\lg(D \cdot t)$. Then, the diffusion coefficient in the linear range can be calculated with [191]

$$\sqrt{D} \approx \frac{1}{c_s} \frac{d}{0.52\pi} \frac{c(t)}{\sqrt{t}} \quad (24.)$$

Moisture absorption of polymer composites may lead to their mechanical properties deterioration due to weathering processes. Natural fibres absorb water, thus increasing the potential for deterioration in comparison with reinforcement-like glass fibre. In the previous section, a significant deterioration of flexural properties was observed for water immersed NFC laminates. Table 20 presents moisture absorption of some natural fibres for standard condition moisture and immersion in fluid.

Table 20 Moisture absorption of selected NF [118]

<i>Type of fibre</i>	<i>Absorbency at 65% RH</i>	<i>Transverse swelling in water (%)</i>
Jute	12.5	20–22
Coir	10–12	5–15
Flax	7	20–25
Sisal	10–12	18–20
Ramie	5–6	12–15
Sun hemp	10–11	18–20

Water absorption test results are analysed in a subsequent section. Figure 117 presents results for two types of immersed samples, made by hot pressing technique with unsaturated polyester resin (Crystic) and Palapreg-eco resin with non-twisted fibre flax

250Tex yarn hopsack fabric reinforced laminate. There is only a small difference between both laminate types within the measured timescale, with a visible tendency for lower saturation point in crystic matrix and higher diffusion coefficient in comparison with Palapreg matrix. This gives an indication that crystic matrix composite will absorb water faster, what involves higher stresses creation especially for thicker elements exposed to moisture. Composite based on Palapreg-eco resin will absorb water slower but more water will be absorbed before reaching saturation.

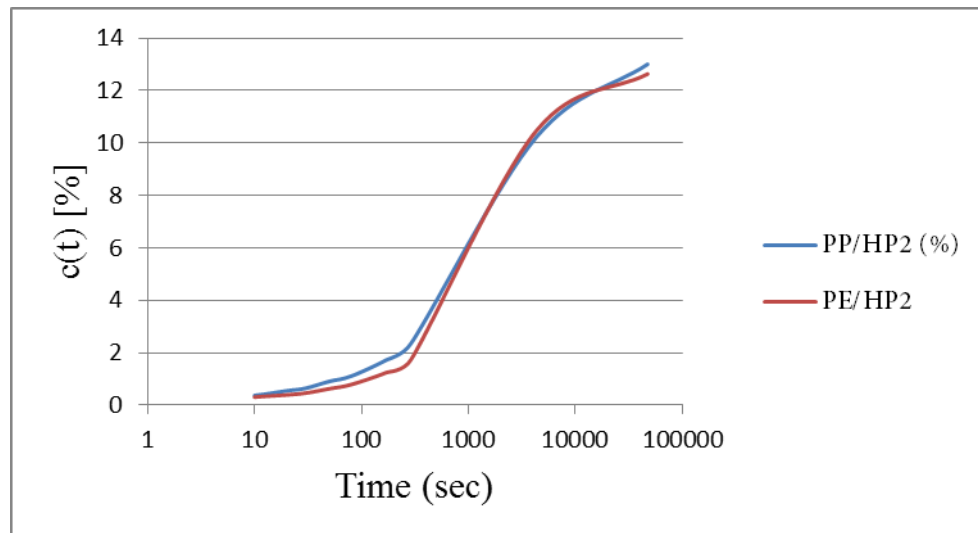


Figure 117 Relationship between time (sec) and water absorption (%) of the total mass. Data compares unsaturated polyester resin (crystic)/flax composite and Palapreg/flax composite

In next section, water absorption data will be compared with Fick's law and the diffusion coefficient will be discussed. Figure 118 presents a relationship between $\lg(D t)$ and c/c_s with results from water absorption test of general grade unsaturated polyester/flax composite. The test data is indicated with black pane symbols. The dotted line represents theoretical Fick's law values. Results were calculated with the method described in the introduction section. The saturation point was calculated at the level of $c_s = 17\%$.

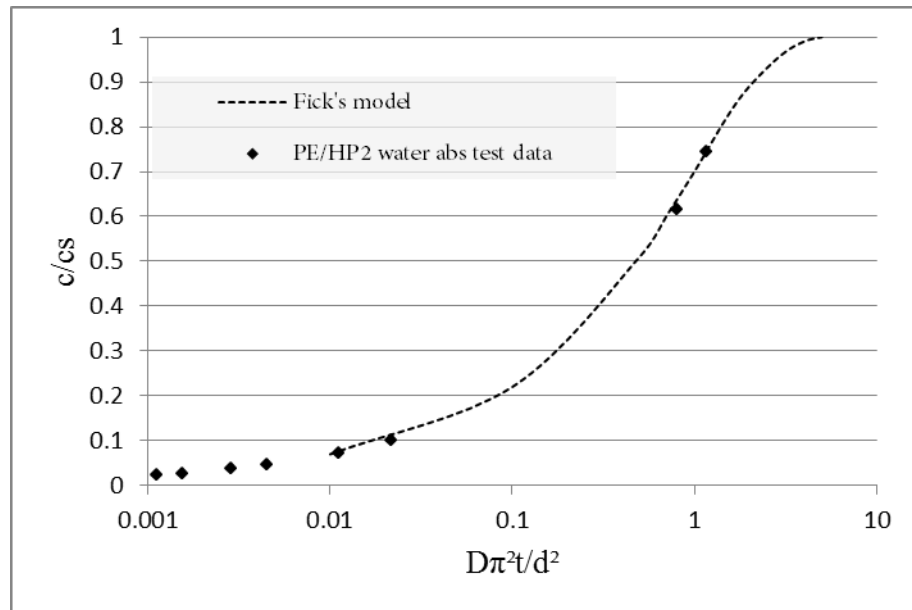


Figure 118 Comparison of flax 4x4 Hoopsack reinforcing unsaturated polyester (Crystic) laminate water absorption data with Fick's model

Figure 119 presents a relationship between $\lg(Dt)$ and c/c_s with results from water absorption test for Palapreg-eco/flax yarn composite. Test result points are indicated with black square symbols and Fick's model theoretical values are represented by the dotted line. The saturation point was calculated at $c_s = 18\%$ (and parameter 0.69). Theoretical saturation points are 17% for Crystic laminate and 18% for Palapreg laminate. The saturation points are theoretical because during the testing period saturation points were not achieved. Kim et al. [194] evaluated the influence of cyclic water sorption on the degradation of epoxy and vinyl ester composites reinforced with sisal fibres. The immersion cycles were 9 days long and were followed by tensile and fracture toughness tests. It was noted that there was a decrease in fracture toughness properties at levels of 50% for epoxy and 60% for vinyl ester composites. The same deterioration levels were observed after continuing the immersion for 400 days. In order to understand the behaviour of NFCs during immersion, Leman et al. [114] investigated the value of the Fickian diffusivity constant, moisture equilibrium and the correction factor. A significant difference was found in the water absorption values for the samples with higher volume fractions of fibres and therefore, number of fibres exposed at the surface. This was concluded as the main reason for the water absorption rate difference. The surface of the NFC needs to be coated or given a gel-coat layer in order to minimise the fibre water

uptake on the surface. In another study of water permeability in NFC materials, jute fabric and its composites were analysed, and it was found that due to fibre swelling, water permeability is reduced [195]. Assarar et al. [30] studied the influence of water immersion on mechanical and acoustic emission tests for epoxy reinforced with flax fibres composites. They concluded that the main mechanism of degradation for samples was caused by the matrix interphase weakening between the flax fibre and the epoxy matrix.

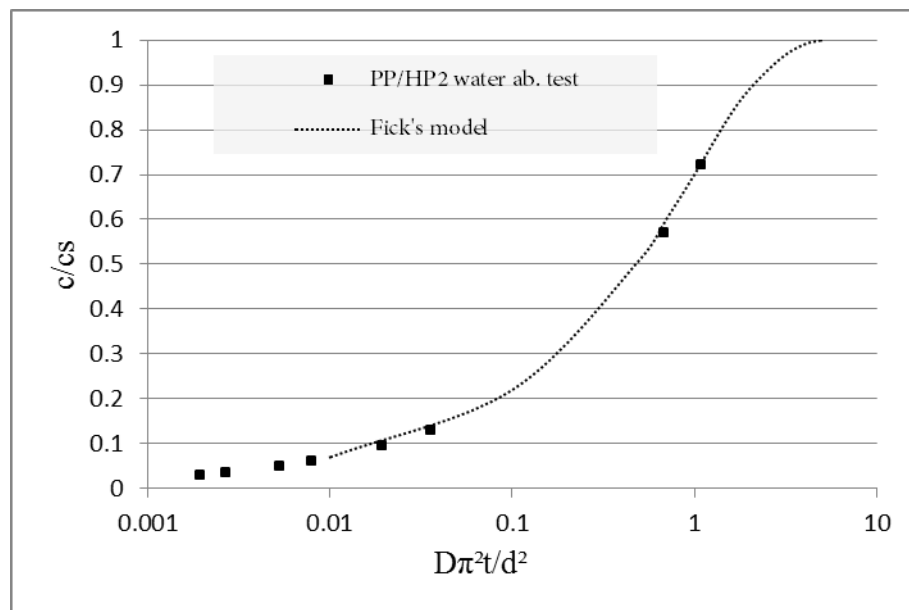


Figure 119 Comparison of flax 4x4 Hoopsack reinforcing PalapregEco laminate water absorption data with Fick's model

7.4 Summary

This chapter discussed weathering of NFCs. The weathering resistance of BFRP was investigated by subjecting flax fabric reinforced laminates to heat ageing, immersion in fluids and environmental weathering. Heat ageing slightly improved ultimate flexural stress and flexural modulus, and simultaneously reduced flexural strain in laminates with PalapregEco matrix. This was attributed to the post-curing process.

During the water immersion test saturation point for the flax laminate was not achieved within the time of the test. Theoretical saturation points were calculated by assuming

Fickian behaviour of the BFRPs. Nevertheless, this needs to be confirmed by performing longer immersion test.

The immersions in fluids and environmental weathering have significant deteriorative effect on the flax BFRP. The mechanical properties deteriorated significantly due to the moisture after one month of exposure. Immersion in the saline solution had the most significant deteriorative influence, reducing flexural modulus even by 50% after 1 month of exposure. It needs to be noted that the tested laminate was without any additives or coatings inhibiting weathering, which could improve the weathering resistance.

8 Inter Laminar Shear Strength of Hemp and Flax Laminates

8.1 Double Notch Shear Test

This chapter describes the interlaminar shear strength test (ILSS) performed on BFRP. It is composed out of three parts, which present results of ILSS tests performed on flax biaxial fabric reinforced composite, flax unidirectional composite and hemp unidirectional composite.

Natural fibre composites were not previously tested for ILSS using double notch shear test (DNST). In this work, ILSS is evaluated for NF yarn and fabric reinforced composites, the applicability of the double notch shear test (DNST) for NFCs is evaluated, as well as the influence of fibre arrangement fibre type and treatment. “Interlaminar shear strength is defined as the shear strength at rupture in which the plane of fracture is located between the layers of reinforcement of a plastic reinforced structure” [196].

ILSS influences the mechanical performance of the laminate. It depends on matrix material and interface properties of the composite. NFCs were previously tested for ILSS with a modified flexural method, which consists of a four point bending test of the thick laminate sample. Ahmed [197] reported interlaminar shear strength from 12MPa – 16MPa for untreated woven jute and flax fabric reinforced polyester hybrid composites tested with flexural test method. Shin et al. [198] reported interlaminar shear strength of 10.5MPa – 16.8 for bamboo fibre reinforced epoxy resin, which were affected by the volume fraction of reinforcement. This type of configuration assures that the laminate will break in the mid plane, at the connection between tensile and compressive deformations.

8.2 Effect of Reinforcement Type

Table 21 presents ILSS strength results for the NFRP laminates reinforced with flax fabric and yarns tested with the DNST method.

Table 21 ILSS compound test results for selected samples reinforced with NF fabrics. Only samples which fractured correctly are included.

<i>Laminate</i>	<i>ILSS</i> (MPa)	<i>RSD</i> %
Flax 250Tex UD	10.36	3.87
Flax 250Tex UD	7.77	2.39
2x2twill [0/90] ₅	6.53	7.56
Flax 590Tex UD	9.13	1.43
4x4hopsack [0/90] ₄	8.84	3.98
4x4[(0/90),(45/45)] ₅	7.72	8.03
4x4hopsack [0/90] ₄ <i>crystic</i>	9.79	6.21

Testing of ILSS in composites is not straight forward, because multiple factors such as matrix cure level, temperature, moisture content, interface strength, impurities and porosity, all affect the results [199]. In order to test the composite correctly, the sample needs to fracture clean between reinforcement layers. Since NFC yarn reinforcements usually have a quite high hairiness, this influences the ILSS test results due to confinement of the energy used for fibre breakage into the ILSS response. During the test multiple samples had to be discarded, after examination, and the test repeated. Table 22 presents the results for the hemp reinforced Palapreg-Eco resin samples with changing volume fraction of the fibres. It was observed that, for most of the samples ILSS is at the level of 10MPa. With an increase in the volume fraction of the fibres, and possible over compaction ($V_f=76$ and $V_f=89$), ILSS starts to drop to 7.77MPa and finally 4.26MPa. This may be explained with the interface deterioration and the increasing influence of the dry spots at the touching points between the fibres. Due to an increase in V_f , fibres start to touch each other without bonding what contributes to the lowered ILSS performance.

8.3 Flax and Hemp Unidirectional Laminates

Table 22 ILSS test results for the flax unidirectional laminate samples.

<i>Laminate</i>	<i>ILSS</i> (MPa)	<i>SD</i>
Flax UD V_f 23	9.85	1.93
Flax UD V_f 30	10.36	0.40
Flax UD V_f 51	10.53	1.20
Flax UD V_f 56	10.89	2.05
Flax UD V_f 76	7.77	0.19
Flax UD V_f 89	4.26	1.06

Table 23 represents ILSS results for the hemp yarn reinforcing Palapreg-Eco matrix. Samples were processed with various volume fractions. For the first three samples made out of fine yarns, the ILSS is the highest at around 16MPa. For the samples made out of hemp yarns with the highest tex value, results achieved are approximately at 13MPa level and the same for the medium range Tex value yarns in this setting. It is apparent that for hemp yarn reinforced unidirectional composites, the increase in volume fraction of fibres has no deteriorative effect on the ILSS. It is possible that the saturation point was not achieved for those samples as for flax reinforced composite.

Table 23 ILSS test results for the unidirectional hemp composites

<i>Laminate</i>	<i>ILSS</i> (MPa)	<i>SD</i>	<i>V_f</i> %
Hemp yarn 25Tex P1	16.77	0.13	
Hemp yarn 25Tex P2	16.25	0.34	
Hemp yarn 25Tex P3	15.60	0.29	
Hemp yarn 130Tex	12.51	0.67	41
Hemp yarn 130Tex	13.46	0.69	51
Hemp yarn 130Tex	13.08	0.34	76
Hemp yarn 39Tex	12.38	0.84	23

Hemp yarn 39Tex	14.42	1.78	32
Hemp yarn 39Tex	13.24	0.18	41
Hemp yarn 39Tex	13.28	0.37	51
Hemp yarn 39Tex	12.37	0.40	76

8.4 Summary

Results indicate that the highest interlaminar properties are for laminates reinforced with hemp fibres. This is in line with the tensile properties results, which were also superior for hemp yarn composites. It suggests that the interface properties of twisted hemp yarn composites and PalapregEco resin are higher than for flax reinforced composites. This can be attributed to an effect of improved matrix-fibre interface. Nevertheless, testing of the BFRPs with DNST method is new and it would be useful to compare results with other methods. This could exclude potential influence of yarn hairiness on the test result.

9 Final Conclusions

The main aim of this research was to develop and characterise Natural Fibre Composites (NFC) based on hemp and flax. This work was undertaken in order to achieve an improved understanding of processing, performance and applicability of NFCs for civil engineering applications. At present, NFCs are being used in non-structural or semi structural applications. The existing solutions are not sufficient for civil engineering practices. There is a perception of low mechanical properties, dimensional stability and moisture resistance related with NFCs, because of lack of understanding of this group of materials. It was stated in the research hypothesis that the existing natural fibre composites (NFCs) are not suitable for building applications due to their poor mechanical performance, and that it can be improved through optimisation of reinforcement and processing parameters. This would allow for the development of NFCs with sufficient mechanical properties to be used as sandwich panels or tubes for civil engineering applications. The hypothesis was confirmed through experimental studies and subsequent analysis, which led to the development of a series of NFC laminates, including flat panels and tubular composites, and production technologies. It was shown that the mechanical properties of NFCs, e.g. tensile and flexural modulus, could be improved by using selected natural fibre yarn reinforcements. The development of processing route, bio-sourced matrix characterisation, reinforcement selection and characterisation and weathering tests, allowed a better understanding of NFCs and hence optimum processing of NFC panels and tubes.

Some specific conclusions can be summarised as follows:

- 1) The yarn with twisted architecture was more suitable for composite processing routes compared to non-twisted or non-woven mats, which rely on tensioning of the reinforcement during processing i.e. pulltrusion, pullwinding or winding.
- 2) The developed processing procedure consisting of filament winding and hot-pressing proved to be suitable to create repeatable laminates and allowed for the control over volume fraction and architecture for various reinforcements made of flax, hemp and blended hemp and wool fibres.

3) The highest modulus and ultimate tensile strength were achieved for laminates based on twisted hemp yarns, above 14GPa and 400MPa respectively, and similarly, high flexural modulus and strength above 34GPa and 320MPa respectively. Non-twisted yarns were developed in order to create laminates with individual single fibres arranged in the same direction, an improved arrangement of which should improve the tensile stiffness and tensile stress of laminates. However, this advantage was not observed due to the dislocations of fibres caused by tension during the winding procedure.

4) Laminates reinforced with hemp-wool fibre reinforcement showed significantly lower mechanical properties than flax or pure hemp yarn reinforced laminates. This may be attributed to several factors, i.e. low self-strength of wool fibre, incompatibility of wool with selected resin system and inconsistent distribution of wool fibres. The lower mechanical performance, in comparison, discounted the foreseen benefits from inclusion of another type of bio-fibres and possible improvement of insulation properties. Therefore, a conclusion is not to recommend use of this reinforcement with matrix and processing procedure used.

5) The new Palapreg ECO® resin system used, which is partially (55%) derived from raw renewable resources, proved to create laminates with similar or higher mechanical properties than synthetic Crystic polyester resin. In a long perspective, the use of fully renewable composites, i.e. where matrix and reinforcement are from renewable resources, is seen as a future of NFCs.

6) NFC tubes were developed and analysed. NFC tubes could be processed with repeatable properties. However, how the reinforcements were arranged within the tube affected the compressive strength and stiffness. The highest compressive strength achieved was 76MPa. A composite tube, either with round or square profile, is a versatile element in all aspects of engineering. Potential applications for a bio-composite tube have been identified, e.g. replacement of wood structure in Hempcrete wall construction, posts, beams, furniture elements or even parts of a bicycle frame.

Weathering of the developed NFCs presented the biggest concerns. Flax laminates were analysed under natural and controlled weathering conditions. The mechanical properties deteriorated significantly due to the moisture after one month of exposure. It needs to be noted that the tested laminate was without any additives or coatings inhibiting weathering, which could improve the weathering resistance.

10 Recommendations for Future Work

1) Flax reinforced NFCs performed poorly in the weathering environment, therefore, it is recommended to investigate the possibilities of improving the weathering resistance. The influence of matrix additives in the form of inhibitors could be analysed. Another way to improve the weathering performance could be changes in the fibre-matrix interphase, e.g. by use of coupling agents or fibre coatings. Alternatively, an influence of different laminate surface coatings can be analysed.

2) The hemp based laminates and tubes were not placed under weathering analysis due to the time constraint. Further investigation with the control over moisture and UV radiation levels would be highly important. Tubes were developed, but the subject was not even partially exhausted. An influence of other reinforcement arrangements, volume fraction and optimisation of the impregnation procedure could be performed. An improvement of the compression properties could be done by using foam filled tubes. Different types of foams could be used in order to assess the key mechanical properties in order to improve the properties.

3) Tube elements need to be connected, which is an important issue in composite materials. The investigation of the suitable connection system could be performed.

4) A compatibility analysis of the NFC with Hemcrete could be performed. Hemcrete is a specific insulation material, which relies on vapour permeability and usually wood is used as reinforcement for single standing wall. The analysis of wood reinforcement replacement with NFC tube could be an important subject.

5) Another issue with NFC is their fire resistance. Up until now, research in this area has been limited. It would be valuable to investigate the inclusion of fire retardant inhibitors within the matrix or in the form of coatings on the surface of the laminate.

11 References

- [1] A. D. La Rosa, G. Recca, J. Summerscales, A. Latteri, G. Cozzo and G. Cicala, "Bio-based versus traditional polymer composites. A life cycle assessment perspective," *J. Clean. Prod.*, vol. 74, pp. 135-144, 7/1, 2014.
- [2] J. C. Gilson, "Asbestos cancer: past and future hazards," *Proc. R. Soc. Med.*, vol. 66, pp. 395-403, Apr, 1973.
- [3] M. A. Silverstein, L. S. Welch and R. Lemen, "Developments in asbestos cancer risk assessment," *Am. J. Ind. Med.*, vol. 15, pp. 850-858, 2009.
- [4] R. Wool and X. S. Sun, *Bio-Based Polymers and Composites*. Academic Press, 2011.
- [5] D. V. Rosato, M. G. Rosato and D. V. Rosato, *Concise Encyclopedia of Plastics*. Springer, 2000.
- [6] B. Norman, "Some Developments in the Manufacture and Use of Synthetic Materials for Aircraft Construction," *Flight - the Aircraft Engineer*, vol. a-c, 12th January. 1939.
- [7] L. Yan, N. Chouw and K. Jayaraman, "Flax fibre and its composites – A review," *Composites Part B: Engineering*, vol. 56, pp. 296-317, 1, 2014.
- [8] G. Koronis, A. Silva and M. Fontul, "Green composites: A review of adequate materials for automotive applications," *Composites Part B: Engineering*, vol. 44, pp. 120-127, 1, 2013.
- [9] D. B. Dittenber and H. V. S. GangaRao, "Critical review of recent publications on use of natural composites in infrastructure," *Composites Part A: Applied Science and Manufacturing*, vol. 43, pp. 1419-1429, 8, 2012.

- [10] A. Shahzad, "Hemp fiber and its composites—a review," *J. Composite Mater.*, vol. 46, pp. 973-986, 2012.
- [11] M. J. John and S. Thomas, "Biofibres and biocomposites," *Carbohydr. Polym.*, vol. 71, pp. 343-364, 2/8, 2008.
- [12] P. Malnati, "ECO Elise concept: Lean, speedy and green," *Composites Technology*, vol. 8, pp. 46-48, 2009.
- [13] N. De Bruyne, "Aero Research Technical Notes," *Bulletin*, 1956.
- [14] G. Marsh, "Next step for automotive materials," *Materials Today*, vol. 6, pp. 36-43, 4, 2003.
- [15] M. H. Dato, "Mechanics of fibrous composites," *Elsevier Science Publishers Ltd.(UK)*, 1991, pp. 636, 1991.
- [16] M. Fan, "Sustainable fibre-reinforced polymer composites in construction," in *Management, Recycling and Reuse of Waste Composites*, 1st ed., V. Goodship, Ed. Cambridge: Woodhead Publishing, 2009, pp. 518.
- [17] *Isolatie - Duurzame Jeugdwerkinfrastructuur - Technische fiche.*
- [18] *BUND-Jahrbuch 2013 – Ökologisch Bauen und Renovieren mit den Themenbereichen Planung, Musterhäuser, Gebäudehülle, Haustechnik, Innenraum.*
- [19] International Organization for Standardization, "14040: Environmental management—life cycle assessment—principles and framework," *London: British Standards Institution*, 2006.
- [20] EU-European Commission, "International Reference Life Cycle Data System (ILCD) handbook e general guide for Life Cycle Assessment e detailed guidance," *Institute for Environment and Sustainability*, 2010.
- [21] P. BSi, "2050: 2011 Specification for the assessment of the life cycle greenhouse gas emissions of goods and services," *British Standards Institute: London, UK*, 2011.

- [22] K. Ip and A. Miller, "Life cycle greenhouse gas emissions of hemp–lime wall constructions in the UK," *Resour. Conserv. Recycling*, vol. 69, pp. 1-9, 12, 2012.
- [23] D. G. Hepworth, R. N. Hobson, D. M. Bruce and J. W. Farrent, "The use of unretted hemp fibre in composite manufacture," *Composites Part A: Applied Science and Manufacturing*, vol. 31, pp. 1279-1283, 11, 2000.
- [24] F. Cherubini, N. D. Bird, A. Cowie, G. Jungmeier, B. Schlamadinger and S. Woess-Gallasch, "Energy- and greenhouse gas-based LCA of biofuel and bioenergy systems: Key issues, ranges and recommendations," *Resour. Conserv. Recycling*, vol. 53, pp. 434-447, 2009.
- [25] S. V. Joshi, L. T. Drzal, A. K. Mohanty and S. Arora, "Are natural fiber composites environmentally superior to glass fiber reinforced composites?" *Composites Part A: Applied Science and Manufacturing*, vol. 35, pp. 371-376, 3, 2004.
- [26] A. D. La Rosa, A. Recca, A. Gagliano, J. Summerscales, A. Latteri, G. Cozzo and G. Cicala, "Environmental impacts and thermal insulation performance of innovative composite solutions for building applications," *Constr. Build. Mater.*, vol. 55, pp. 406-414, 3/31, 2014.
- [27] Saskatchewan Ministry of Agriculture, "Hemp production in Saskatchewan," pp. 13/11/2012, 2009.
- [28] P. C. Struik, S. Amaducci, M. J. Bullard, N. C. Stutterheim, G. Venturi and H. T. H. Cromack, "Agronomy of fibre hemp (*Cannabis sativa* L.) in Europe," *Industrial Crops and Products*, vol. 11, pp. 107-118, 3, 2000.
- [29] B. N. Dash, A. K. Rana, H. K. Mishra, S. K. Nayak and S. S. Tripathy, "Novel low-cost jute polyester composites. III. Weathering and thermal behavior," *J. Appl. Polym. Sci.*, vol. 78, pp. 1671-1679, 2000.
- [30] M. Assarar, D. Scida, A. El Mahi, C. Poilâne and R. Ayad, "Influence of water ageing on mechanical properties and damage events of two reinforced composite materials: Flax–fibres and glass–fibres," *Mater Des*, vol. 32, pp. 788-795, 2, 2011.

- [31] E. Kvavadze, O. Bar-Yosef, A. Belfer-Cohen, E. Boaretto, N. Jakeli, Z. Matskevich and T. Meshveliani, "30,000-Year-Old Wild Flax Fibers," *Science*, vol. 325, pp. 1359-1359, September 11, 2009.
- [32] C. Bergfjord, S. Karg, A. Rast-Eicher, M. -. Nosch, U. Mannering, R. G. Allaby, B. M. Murphy and B. Holst, "Comment on "30,000-Year-Old Wild Flax Fibers"," *Science*, vol. 328, pp. 1634-1634, June 25, 2010.
- [33] E. Kvavadze, O. Bar-Yosef, A. Belfer-Cohen, E. Boaretto, N. Jakeli, Z. Matskevich and T. Meshveliani, "Response to Comment on "30,000-Year-Old Wild Flax Fibers"," *Science*, vol. 328, pp. 1634-1634, June 25, 2010.
- [34] N. R. Hollen and J. Saddler, "Textiles," 1968.
- [35] M. L. Joseph, "Introductory Textile Science 1986," *Holt, Rinehart and Winston, New York*, .
- [36] G. H. Johnson, "Textile fabrics: their selection and care from the standpoint of use, wear, and launderability," 1927.
- [37] M. Athar and S. M. Nasir, "Taxonomic perspective of plant species yielding vegetable oils used in cosmetics and skin care products," *African Journal of Biotechnology*, vol. 4, pp. 36-44, 2005.
- [38] M. Gorree, J. Guinee, G. Huppel and L. Oers, "Environmental life cycle assessment of linoleum," *The International Journal of Life Cycle Assessment*, vol. 7, pp. 158-166, 05/01, 2002.
- [39] J. Carter, "Potential of flaxseed and flaxseed oil in baked goods and other products in human nutrition," *Cereal Foods World (USA)*, 1993.
- [40] S. C. Cunnane, S. Ganguli, C. Menard, A. C. Liedtke, M. J. Hamadeh, Z. Chen, T. Wolever and D. J. Jenkins, "High α -linolenic acid flaxseed (*Linum usitatissimum*): some nutritional properties in humans," *Br. J. Nutr.*, vol. 69, pp. 443-453, 1993.

- [41] S. C. Cunnane, M. J. Hamadeh, A. C. Liede, L. U. Thompson, T. M. Wolever and D. J. Jenkins, "Nutritional attributes of traditional flaxseed in healthy young adults." *The American Journal of Clinical Nutrition*, vol. 61, pp. 62-68, January 01, 1995.
- [42] M. Mosiewicki, J. Borrajo and M. Aranguren, "Mechanical properties of woodflour/linseed oil resin composites," *Polym. Int.*, vol. 54, pp. 829-836, 2005.
- [43] A. Motawie, E. Hassan, A. Manieh, M. Aboul-Fetouh and A. F. El-Din, "Some epoxidized polyurethane and polyester resins based on linseed oil," *J Appl Polym Sci*, vol. 55, pp. 1725-1732, 1995.
- [44] F. Rasti and G. Scott, "The effects of some common pigments on the photo-oxidation of linseed oil-based paint media," *Studies in Conservation*, vol. 25, pp. 145-156, 1980.
- [45] A. Demirbas, "Production of biodiesel fuels from linseed oil using methanol and ethanol in non-catalytic SCF conditions," *Biomass Bioenergy*, vol. 33, pp. 113-118, 2009.
- [46] A. Demirbaş, "Biodiesel fuels from vegetable oils via catalytic and non-catalytic supercritical alcohol transesterifications and other methods: a survey," *Energy Conversion and Management*, vol. 44, pp. 2093-2109, 2003.
- [47] E. Hallier, D. v Schlechtendal, L. Langethal, E. Schenk and W. Müller, *Flora Von Deutschland*. Fr. Eugen Köhler, 1886.
- [48] F. P. Yearbook, "FAO," *Rome, Italy ISBN*, pp. 978-992, 2012.
- [49] G. H. Lawrence, "Taxonomy of vascular plants," *New York*, vol. 9, 1951.
- [50] C. Sourrouille, B. Marshall, D. LiÃ©nard and L. Faye, "From neanderthal to nanobiotech: From plant potions to pharming with plant factories," in , L. Faye and V. Gomord, Eds. Humana Press, 2009, pp. 1-23.
- [51] K. Wade, "Anglo-Saxon and medieval (rural)," *Research and Archaeology: A Framework for the Eastern Counties*, vol. 2, 2000.

- [52] G. A. Lower, "Flax and hemp: From the seed to the loom," *YMechanical Engineering, Feb*, vol. 26, 1937.
- [53] P. Mechanics, "New billion-dollar crop," *Popular Mechanics Feb*, pp. 238-238, 1938.
- [54] J. Summerscales, N. P. J. Dissanayake, A. S. Virk and W. Hall, "A review of bast fibres and their composites. Part 1 – Fibres as reinforcements," *Composites Part A: Applied Science and Manufacturing*, vol. 41, pp. 1329-1335, 10, 2010.
- [55] W. Brandt, M. Gürke, G. Schellenberg and M. Vogtherr, *Köhler's Medicinal-Plflanzen in Naturgetreuen Abbildungen Mit Kurz Erläuterndem Texte: Atlas Zur Pharmacopoea Germanica, Austriaca, Belgica, Danica, Helvetica, Hungarica, Rossica, Suecica, Neerlandica, British Pharmacopoeia, Zum Codex Medicamentarius, Sowie Zur Pharmacopoeia of the United States of America*. FE Köhler, 1887.
- [56] Nova-Institut, "Biowerkstoff - Report on bio based plastics and composites," *RENEVABLE-RESOURCES*, vol. Issue 7, 2010.
- [57] D. F. Musto, "The 1937 Marijuana Tax Act," *Arch. Gen. Psychiatry*, vol. 26, pp. 101-108, 1972.
- [58] K. Esau, "Anatomy of Seed Plants. 2 da ed," *New York*, 1977.
- [59] W. Commons, "Wikimedia Commons," *Retrieved June*, vol. 2, 2012.
- [60] T. Schäfer and B. Honermeier, "Effect of sowing date and plant density on the cell morphology of hemp (*Cannabis sativa* L.)," *Industrial Crops and Products*, vol. 23, pp. 88-98, 2006.
- [61] M. Hughes, "Defects in natural fibres: their origin, characteristics and implications for natural fibre-reinforced composites," *J. Mater. Sci.*, vol. 47, pp. 599-609, 01/01, 2012.
- [62] V. Goodship, *Management, Recycling and Reuse of Waste Composites*. Elsevier, 2009.

- [63] A. K. Bledzki and J. Gassan, "Composites reinforced with cellulose based fibres," *Progress in Polymer Science*, vol. 24, pp. 221-274, 5, 1999.
- [64] H. Krassig, "Structure of cellulose and its relation to properties of cellulose fibers," *Cellulose and its Derivatives: Chemistry, Biochemistry and Applications/Editors, JF Kennedy...[Et AL.]*, 1985.
- [65] D. Dai and M. Fan, "Investigation of the dislocation of natural fibres by Fourier-transform infrared spectroscopy," *Vibrational Spectroscopy*, vol. 55, pp. 300-306, 3, 2011.
- [66] J. Gassan, A. Chate and A. Bledzki, "Calculation of elastic properties of natural fibers," *J. Mater. Sci.*, vol. 36, pp. 3715-3720, 08/01, 2001.
- [67] K. Charlet, C. Baley, C. Morvan, J. P. Jernot, M. Gomina and J. Bréard, "Characteristics of Hermès flax fibres as a function of their location in the stem and properties of the derived unidirectional composites," *Composites Part A: Applied Science and Manufacturing*, vol. 38, pp. 1912-1921, 2007.
- [68] J. Gratton and Y. Chen, "Development of a field-going unit to separate fiber from hemp (*Cannabis sativa*) stalk." *Appl. Eng. Agric.*, vol. 20, pp. 139-145, 2004.
- [69] Y. Chen, J. L. Gratton and J. Liu, "Power Requirements of Hemp Cutting and Conditioning," *Biosystems Engineering*, vol. 87, pp. 417-424, 4, 2004.
- [70] D. Catling and J. Grayson, *Identification of Vegetable Fibers*. Chapman and Hall in assoc. with Methuen. Inc., 1982.
- [71] H. L. Bos, D. O. Van and O. C. J. J. Peters, "Tensile and compressive properties of flax fibres for natural fibre reinforced composites," *J. Mater. Sci.*, vol. 37, pp. 1683-1692, 04/01, 2002.
- [72] H. L. Bos and A. M. Donald, "In situ ESEM study of the deformation of elementary flax fibres," *J. Mater. Sci.*, vol. 34, pp. 3029-3034, 07/01, 1999.

- [73] S. S. Munawar, K. Umemura and S. Kawai, "Characterization of the morphological, physical, and mechanical properties of seven nonwood plant fiber bundles," *Journal of Wood Science*, vol. 53, pp. 108-113, 2007.
- [74] V. Placet, "Characterization of the thermo-mechanical behaviour of Hemp fibres intended for the manufacturing of high performance composites," *Composites Part A: Applied Science and Manufacturing*, vol. 40, pp. 1111-1118, 2009.
- [75] N. Zafeiropoulos and C. Baillie, "A study of the effect of surface treatments on the tensile strength of flax fibres: Part II. Application of Weibull statistics," *Composites Part A: Applied Science and Manufacturing*, vol. 38, pp. 629-638, 2007.
- [76] A. K. Bledzki and J. Gassan, "Composites reinforced with cellulose based fibres." *Prog. in Poly. Sci.*, vol. 24, pp. 221-274, 1999.
- [77] W. E. Morton and J. W. Hearle, *Physical Properties of Textile Fibres*. Textile Institute, 1993.
- [78] P. Hagstrand and K. Oksman, "Mechanical properties and morphology of flax fiber reinforced melamine-formaldehyde composites," *Polymer Composites*, vol. 22, pp. 568-578, 2001.
- [79] D. H. Mueller and A. Krobjilowski, "New discovery in the properties of composites reinforced with natural fibers," *Journal of Industrial Textiles*, vol. 33, pp. 111-130, 2003.
- [80] K. L. Pickering, *Properties and Performance of Natural-Fibre Composites*. Woodhead Pub., 2008.
- [81] A. K. Mohanty, M. Misra and L. T. Drzal, *Natural Fibres, Biopolymers, and Biocomposites*. CRC Press, 2005.
- [82] D. G. Hepworth, R. N. Hobson, D. M. Bruce and J. W. Farrent, "The use of unretted hemp fibre in composite manufacture." *Comp. Part A*, vol. 31, pp. 1279-1283, May, 2000.

- [83] H. Wang, R. Postle, R. Kessler and W. Kessler, "Removing pectin and lignin during chemical processing of hemp for textile applications," *Text. Res. J.*, vol. 73, pp. 664-669, 2003.
- [84] D. E. Akin, J. A. Foulk, R. B. Dodd and D. D. McAlister III, "Enzyme-retting of flax and characterization of processed fibers," *J. Biotechnol.*, vol. 89, pp. 193-203, 2001.
- [85] Y. Li, K. Pickering and R. Farrell, "Analysis of green hemp fibre reinforced composites using bag retting and white rot fungal treatments," *Industrial Crops and Products*, vol. 29, pp. 420-426, 2009.
- [86] B. Wielage, T. Lampke, G. Marx, K. Nestler and D. Starke, "Thermogravimetric and differential scanning calorimetric analysis of natural fibres and polypropylene," *Thermochimica Acta*, vol. 337, pp. 169-177, 1999.
- [87] D. Dupeyre and M. Vignon, "Fibres from semi-retted hemp bundles by steam explosion treatment," *Biomass Bioenergy*, vol. 14, pp. 251-260, 1998.
- [88] H. S. Sharma, "Chemical retting of flax using chelating compounds," *Ann. Appl. Biol.*, vol. 113, pp. 159-165, 1988.
- [89] F. Munder, C. Furll and H. Hempel, "Processing of bast fiber plants for industrial application," *Natural Fibers, Biopolymers and Biocomposites*, pp. 109-140, 2005.
- [90] I. Van de Weyenberg, J. Ivens, A. De Coster, B. Kino, E. Baetens and I. Verpoest, "Influence of processing and chemical treatment of flax fibres on their composites," *Composites Sci. Technol.*, vol. 63, pp. 1241-1246, 2003.
- [91] V. Tserki, N. Zafeiropoulos, F. Simon and C. Panayiotou, "A study of the effect of acetylation and propionylation surface treatments on natural fibres," *Composites Part A: Applied Science and Manufacturing*, vol. 36, pp. 1110-1118, 2005.
- [92] P. Khristova, J. Tomkinson and G. Lloyd Jones, "Multistage peroxide bleaching of French hemp," *Industrial Crops and Products*, vol. 18, pp. 101-110, 2003.

- [93] S. Ouajai, A. Hodzic and R. Shanks, "Morphological and grafting modification of natural cellulose fibers," *J Appl Polym Sci*, vol. 94, pp. 2456-2465, 2004.
- [94] H. Wang, R. Postle, R. Kessler and W. Kessler, "Removing pectin and lignin during chemical processing of hemp for textile applications," *Text. Res. J.*, vol. 73, pp. 664-669, 2003.
- [95] M. A. Sawpan, K. L. Pickering and A. Fernyhough, "Effect of fibre treatments on interfacial shear strength of hemp fibre reinforced polylactide and unsaturated polyester composites," *Composites Part A: Applied Science and Manufacturing*, vol. 42, pp. 1189-1196, 9, 2011.
- [96] R. Umer, S. Bickerton and A. Fernyhough, "Characterising wood fibre mats as reinforcements for liquid composite moulding processes," *Composites Part A: Applied Science and Manufacturing*, vol. 38, pp. 434-448, 2, 2007.
- [97] M. Acar and J. F. Harper, "Textile composites from hydro-entangled non-woven fabrics," *Comput. Struct.*, vol. 76, pp. 105-114, 6, 2000.
- [98] E. Ghassemieh, M. Acar and H. K. Versteeg, "Improvement of the efficiency of energy transfer in the hydro-entanglement process," *Composites Sci. Technol.*, vol. 61, pp. 1681-1694, 9, 2001.
- [99] HempFlax, "*Hemp and flax mats*," pp. 30/04/2013, 2013.
- [100] H. L. Needles, *Textile Fibers, Dyes, Finishes, and Processes: A Concise Guide*. Noyes Publications, 1986.
- [101] N. Pan, T. Hua and Y. Qiu, "Relationship Between Fiber and Yarn Strength," *Textile Research Journal*, vol. 71, pp. 960-964, 2001.
- [102] H. B. Tang, B. G. Xu, X. M. Tao and J. Feng, "Mathematical modeling and numerical simulation of yarn behavior in a modified ring spinning system," *Appl. Math. Model.*, vol. 35, pp. 139-151, 1, 2011.

- [103] F. K. Ko, "From textile to geotextiles," in *Seminar in Honour of Professor Robert Koerner*, 2004, .
- [104] K. Buet-Gautier and P. Boisse, "Experimental analysis and modeling of biaxial mechanical behavior of woven composite reinforcements," *Exp. Mech.*, vol. 41, pp. 260-269, 09/01, 2001.
- [105] B. N. Cox and G. Flanagan, *Handbook of Analytical Methods for Textile Composites*. National Aeronautics and Space Administration, 1997.
- [106] J. Raquez, M. Deléglise, M. Lacrampe and P. Krawczak, "Thermosetting (bio) materials derived from renewable resources: a critical review," *Progress in Polymer Science*, vol. 35, pp. 487-509, 2010.
- [107] E. Zini and M. Scandola, "Green composites: An overview," *Polymer Composites*, vol. 32, pp. 1905-1915, 2011.
- [108] L. Pupure, N. Doroudgarian and R. Joffe, "Moisture uptake and resulting mechanical response of biobased composites. I. constituents," *Polymer Composites*, vol. 35, pp. 1150-1159, 2014.
- [109] K. Adekunle, D. Åkesson and M. Skrifvars, "Biobased composites prepared by compression molding with a novel thermoset resin from soybean oil and a natural-fiber reinforcement," *J Appl. Polym. Sci.*, vol. 116, pp. 1759-1765, 2010.
- [110] A. Hodzic, R. Coakley, R. Curro, C. C. Berndt and R. A. Shanks, "Design and Optimisation of Biopolyester Bagasse Fiber Composites." *Bio. Mat and Bioenergy*, vol. 1, pp. 46-55, 2007.
- [111] B. Muralidhar, V. Giridev and K. Raghunathan, "Flexural and impact properties of flax woven, knitted and sequentially stacked knitted/woven preform reinforced epoxy composites," *Journal of Reinforced Plastics and Composites*, vol. 31, pp. 379-388, 2012.

- [112] C. Santulli, F. Sarasini, J. Tirillò, T. Valente, M. Valente, A. P. Caruso, M. Infantino, E. Nisini and G. Minak, "Mechanical behaviour of jute cloth/wool felts hybrid laminates," *Mater Des*, vol. 50, pp. 309-321, 9, 2013.
- [113] B. Masseteau, F. Michaud, M. Irle, A. Roy and G. Alise, "An evaluation of the effects of moisture content on the modulus of elasticity of a unidirectional flax fiber composite," *Composites Part A: Applied Science and Manufacturing*, vol. 60, pp. 32-37, 5, 2014.
- [114] Z. Leman, S. M. Sapuan, A. M. Saifol, M. A. Maleque and M. M. H. M. Ahmad, "Moisture absorption behavior of sugar palm fiber reinforced epoxy composites," *Mater Des*, vol. 29, pp. 1666-1670, 2008.
- [115] L. Conzatti, F. Giunco, P. Stagnaro, M. Capobianco, M. Castellano and E. Marsano, "Polyester-based biocomposites containing wool fibres," *Composites Part A: Applied Science and Manufacturing*, vol. 43, pp. 1113-1119, 7, 2012.
- [116] X. Peng, M. Fan, J. Hartley and M. Al-Zubaidy, "Properties of natural fiber composites made by pultrusion process," *Journal of Composite Materials*, vol. 46, pp. 237-246, January 01, 2012.
- [117] M. A. Sawpan, K. L. Pickering and A. Fernyhough, "Flexural properties of hemp fibre reinforced polylactide and unsaturated polyester composites," *Composites Part A: Applied Science and Manufacturing*, vol. 43, pp. 519-526, 2012.
- [118] M. Thiruchitrambalam, A. Athijayamani, S. Sathiyamurthy and A. S. Thaheer, "A Review on the Natural Fiber-Reinforced Polymer Composites for the Development of Roselle Fiber-Reinforced Polyester Composite," *Journal of Natural Fibers*, vol. 7, pp. 307-323, 11/30; 2014/09, 2010.
- [119] S. Waigaonkar, B. Babu and A. Rajput, "Curing studies of unsaturated polyester resin used in FRP products," *Indian J. Eng. Mater. Sci.*, vol. 18, pp. 31-39, 2011.
- [120] Y. Yang and L. J. Lee, "Microstructure formation in the cure of unsaturated polyester resins," *Polymer*, vol. 29, pp. 1793-1800, 1988.

- [121] M. Ton-That, K. C. Cole, C. Jen and D. R. França, "Polyester cure monitoring by means of different techniques," *Polymer Composites*, vol. 21, pp. 605-618, 2000.
- [122] D. Gay, S. V. Hoa and S. W. Tsai, *Composite Materials: Design and Applications*. CRC press, 2002.
- [123] M. Biron, *Thermoplastics and Thermoplastic Composites*. William Andrew, 2012.
- [124] P. A. Sreekumar, K. Joseph, G. Unnikrishnan and S. Thomas, "A comparative study on mechanical properties of sisal-leaf fibre-reinforced polyester composites prepared by resin transfer and compression moulding techniques," *Composites Sci. Technol.*, vol. 67, pp. 453-461, 3, 2007.
- [125] P. Yu, A. Huang, W. Lo, H. Chua and G. Chen, "Conversion of food industrial wastes into bioplastics," in *Biotechnology for Fuels and Chemicals* Anonymous Springer, 1998, pp. 603-614.
- [126] S. Domenek, P. Feuilleley, J. Gratraud, M. Morel and S. Guilbert, "Biodegradability of wheat gluten based bioplastics," *Chemosphere*, vol. 54, pp. 551-559, 2004.
- [127] B. Witholt and B. Kessler, "Perspectives of medium chain length poly (hydroxyalkanoates), a versatile set of bacterial bioplastics," *Curr. Opin. Biotechnol.*, vol. 10, pp. 279-285, 1999.
- [128] J. M. Luengo, B. García, A. Sandoval, G. Naharro and E. R. Olivera, "Bioplastics from microorganisms," *Curr. Opin. Microbiol.*, vol. 6, pp. 251-260, 2003.
- [129] G. Mehta, A. K. Mohanty, M. Misra and L. T. Drzal, "Effect of novel sizing on the mechanical and morphological characteristics of natural fiber reinforced unsaturated polyester resin based bio-composites," *J. Mater. Sci.*, vol. 39, pp. 2961-2964, 04/01, 2004.
- [130] J. J. van Soest, S. Hulleman, D. De Wit and J. Vliegthart, "Crystallinity in starch bioplastics," *Industrial Crops and Products*, vol. 5, pp. 11-22, 1996.

- [131] O. Shoseyov, A. Heyman, S. Lapidot, S. Meirovitch, Y. Nevo and T. Gustafsson, *Cellulose-Based Composite Materials*, 2011.
- [132] M. Mironescu and V. Mironescu, "New concept for the obtention of biopolymers-based food biofilms," *Journal of Agroalimentary Processes and Technologies*, vol. 12, pp. 219-216, 2006.
- [133] H. Kakita, H. Kamishima, M. Ohno and A. Chirapart, "Marine biopolymers from the red algae, *Gracilaria* spp," *Recent Advances in Marine Biotechnology*, vol. 9, pp. 79-109, 2003.
- [134] M. Carus, S. Karst, A. Kauffmann, J. Hobson and S. Bertucelli, "The European Hemp Industry: Cultivation, processing and applications for fibres, shivs and seeds," *European Industrial Hemp Association (EIHA), Hürth (Germany)*, 2013.
- [135] N. K. Gupta and R. Velmurugan, "Analysis of polyester and epoxy composite shells subjected to axial crushing." 2000.
- [136] M. A. Dweib, B. Hu, A. O'Donnell, H. W. Shenton and R. P. Wool, "All natural composite sandwich beams for structural applications," *Composite Structures*, vol. 63, pp. 147-157, 2, 2004.
- [137] International Organization for Standardization, "3597-3: 2003, Textile-glass-reinforced plastics," *Determination of Mechanical Properties on Rods made of Roving-Reinforced Resin. Determination of Compressive Strength*, .
- [138] International Organization for Standardization, "ISO 1183-2:2004 - Plastics - Methods for determining the density of non-cellular plastics -- Part 2: Density gradient column method," 2004.
- [139] International Organization for Standardization., "BS EN ISO 62:2008 - Plastics. Determination of water absorption," .
- [140] International Organization for Standardization., "ISO 2062:2009- Textiles -- Yarns from packages -- Determination of single-end breaking force and elongation at break using constant rate of extension (CRE) tester," .

- [141] International Organization for Standardization, *Fibre-Reinforced Plastic Composites : Determination of Flexural Properties*. Geneve: International Organization for Standardization, 1998.
- [142] International Organization for Standardization, *Fibre-Reinforced Plastic Composites : Determination of Flexural Properties*. Geneve: International Organization for Standardization, 1998.
- [143] C. R. Schultheisz and A. M. Waas, "Compressive failure of composites, part I: Testing and micromechanical theories," *Prog. Aerospace Sci.*, vol. 32, pp. 1-42, 1996.
- [144] British Standards Institution., *BS PL 4: 2005 - Properties of Unsaturated Polyester Resins for Low Pressure Laminating of High Strength Fibre Reinforced Composites — Specification*. Geneve: British Standards Institution, 2005.
- [145] B. ISO, "527-5: 1997 BS 2782-3: Method 326G: 1997 Plastics—Determination of tensile properties—Part 5: Test conditions for unidirectional fibre-reinforced plastic composites," *British Standards Institute, UK*, 1997.
- [146] M. Ho, H. Wang, J. Lee, C. Ho, K. Lau, J. Leng and D. Hui, "Critical factors on manufacturing processes of natural fibre composites," *Composites Part B: Engineering*, vol. 43, pp. 3549-3562, 12, 2012.
- [147] D. Zygoyiannis, "Sheep production in the world and in Greece," *Small Ruminant Research*, vol. 62, pp. 143-147, 3, 2006.
- [148] C. Gorse, D. Johnston and M. Pritchard, *A Dictionary of Construction, Surveying, and Civil Engineering*. Oxford University Press, 2012.
- [149] D. U. Shah, P. J. Schubel and M. J. Clifford, "Modelling the effect of yarn twist on the tensile strength of unidirectional plant fibre yarn composites," *Journal of Composite Materials*, vol. 47, pp. 425-436, February 01, 2013.
- [150] J. W. Hearle, P. Grosberg and S. Backer, "Structural mechanics of fibers, yarns, and fabrics," 1969.

- [151] B. Madsen, P. Hoffmeyer, A. B. Thomsen and H. Lilholt, "Hemp yarn reinforced composites – I. Yarn characteristics," *Composites Part A: Applied Science and Manufacturing*, vol. 38, pp. 2194-2203, 10, 2007.
- [152] D. U. Shah, P. J. Schubel and M. J. Clifford, "Modelling the effect of yarn twist on the tensile strength of unidirectional plant fibre yarn composites," *Journal of Composite Materials*, March 13, 2012.
- [153] M. Miwa and I. Endo, "Critical fibre length and tensile strength for carbon fibre-epoxy composites," *J. Mater. Sci.*, vol. 29, pp. 1174-1178, 1994.
- [154] F. Awaja, M. Gilbert, G. Kelly, B. Fox and P. J. Pigram, "Adhesion of polymers," *Progress in Polymer Science*, vol. 34, pp. 948-968, 2009.
- [155] Y. Luo and I. Verpoest, "Biaxial tension and ultimate deformation of knitted fabric reinforcements," *Composites Part A: Applied Science and Manufacturing*, vol. 33, pp. 197-203, 2, 2002.
- [156] G. Hivet and P. Boisse, "Consistent mesoscopic mechanical behaviour model for woven composite reinforcements in biaxial tension," *Composites Part B: Engineering*, vol. 39, pp. 345-361, 3, 2008.
- [157] H. Rouette, "Encyclopedia of Textile Finishing," 2001.
- [158] A. Kelly and a. W. Tyson, "Tensile properties of fibre-reinforced metals: copper/tungsten and copper/molybdenum," *J. Mech. Phys. Solids*, vol. 13, pp. 329-350, 1965.
- [159] N. Pan, "Theoretical determination of the optimal fiber volume fraction and fiber-matrix property compatibility of short fiber composites," *Polymer Composites*, vol. 14, pp. 85-93, 1993.
- [160] H. Cox, "The elasticity and strength of paper and other fibrous materials," *British Journal of Applied Physics*, vol. 3, pp. 72, 1952.

- [161] H. Krenchel, *Fibre Reinforcement*. Alademisk forlag, 1964.
- [162] J. L. Thomason and M. A. Vlugs, "Influence of fibre length and concentration on the properties of glass fibre-reinforced polypropylene: 1. Tensile and flexural modulus," *Composites Part A: Applied Science and Manufacturing*, vol. 27, pp. 477-484, 1996.
- [163] M. Van den Oever, H. Bos and M. Van Kemenade, "Influence of the physical structure of flax fibres on the mechanical properties of flax fibre reinforced polypropylene composites," *Applied Composite Materials*, vol. 7, pp. 387-402, 2000.
- [164] A. Kelly and W. R. Tyson, "Tensile properties of fibre-reinforced metals: Copper/tungsten and copper/molybdenum," *J. Mech. Phys. Solids*, vol. 13, pp. 329-350, 12, 1965.
- [165] B. Madsen, P. Hoffmeyer and H. Lilholt, "Hemp yarn reinforced composites – II. Tensile properties," *Composites Part A: Applied Science and Manufacturing*, vol. 38, pp. 2204-2215, 10, 2007.
- [166] A. Bledzki, H. Fink and K. Specht, "Unidirectional hemp and flax EP-and PP-composites: Influence of defined fiber treatments," *J Appl Polym Sci*, vol. 93, pp. 2150-2156, 2004.
- [167] S. Goutianos, T. Peijs, B. Nystrom and M. Skrifvars, "Development of Flax Fibre based Textile Reinforcements for Composite Applications", *J Applied Composite Materials*, vol. 13, 2006.
- [168] S. H. Aziz and M. P. Ansell, "The effect of alkalization and fibre alignment on the mechanical and thermal properties of kenaf and hemp bast fibre composites: Part 1 – polyester resin matrix," *Composites Sci. Technol.*, vol. 64, pp. 1219-1230, 7, 2004.
- [169] G. Sabe, N. Cetin, C. S. Hill and M. Hughes, "RTM Hemp Fibre-Reinforced Polyester Composites," *Applied Composite Materials*, vol. 7, pp. 341-349, 11/01, 2000.

- [170] G. W. Beckermann and K. L. Pickering, "Engineering and evaluation of hemp fibre reinforced polypropylene composites: Micro-mechanics and strength prediction modelling," *Composites Part A: Applied Science and Manufacturing*, vol. 40, pp. 210-217, 2, 2009.
- [171] F. X. Espinach, F. Julian, N. Verdaguer, L. Torres, M. A. Pelach, F. Vilaseca and P. Mutje, "Analysis of tensile and flexural modulus in hemp strands/polypropylene composites," *Composites Part B: Engineering*, vol. 47, pp. 339-343, 4, 2013.
- [172] T. Yuanjian and D. H. Isaac, "Impact and fatigue behaviour of hemp fibre composites," *Composites Sci. Technol.*, vol. 67, pp. 3300-3307, 12, 2007.
- [173] A. Naughton, M. Fan and J. Bregulla, "Fire resistance characterisation of hemp fibre reinforced polyester composites for use in the construction industry," *Composites Part B: Engineering*, vol. 60, pp. 546-554, 4, 2014.
- [174] A. M. Waas and C. R. Schultheisz, "Compressive failure of composites, part II: Experimental studies," *Prog. Aerospace Sci.*, vol. 32, pp. 43-78, 1996.
- [175] D. Hull, "A unified approach to progressive crushing of fibre-reinforced composite tubes," *Composites Sci. Technol.*, vol. 40, pp. 377-421, 1991.
- [176] G. L. Farley and R. M. Jones, "Crushing Characteristics of Continuous Fiber-Reinforced Composite Tubes," *Journal of Composite Materials*, vol. 26, pp. 37-50, January 01, 1992.
- [177] Y. Liu and X. Gong, "Compressive behavior and energy absorption of metal porous polymer composite with interpenetrating network structure," *Transactions of Nonferrous Metals Society of China*, vol. 16, Supplement 2, pp. s439-s443, 6, 2006.
- [178] A. Harte, N. A. Fleck and M. F. Ashby, "Energy absorption of foam-filled circular tubes with braided composite walls," *European Journal of Mechanics - A/Solids*, vol. 19, pp. 31-50, 1, 2000.

- [179] W. Johnson, P. D. Soden and S. T. S. Al-Hassani, "Inextensional collapse of thin-walled tubes under axial compression," *The Journal of Strain Analysis for Engineering Design*, vol. 12, pp. 317-330, October 01, 1977.
- [180] A. Pugsley, "The large-scale crumpling of thin cylindrical columns," *The Quarterly Journal of Mechanics and Applied Mathematics*, vol. 13, pp. 1-9, 1960.
- [181] H. G. S. J. Thuis and V. H. Metz, "The influence of trigger configurations and laminate lay-up on the failure mode of composite crush cylinders," *Composite Structures*, vol. 28, pp. 131-137, 1994.
- [182] A. Harte and N. A. Fleck, "Deformation and failure mechanisms of braided composite tubes in compression and torsion," *Acta Materialia*, vol. 48, pp. 1259-1271, 4/2, 2000.
- [183] M. P. Coughlan, "The properties of fungal and bacterial cellulases with comment on their production and application," *Biotechnology and Genetic Engineering Reviews*, vol. 3, pp. 39-110, 1985.
- [184] P. Beguin, "Molecular Biology of Cellulose Degradation," *Annu. Rev. Microbiol.*, vol. 44, pp. 219-248, 10/01; 2014/09, 1990.
- [185] L. Y. Mwaikambo and E. T. N. Bisanda, "The performance of cotton–kapok fabric–polyester composites," *Polym. Test.*, vol. 18, pp. 181-198, 6, 1999.
- [186] X. Gu, D. Raghavan, T. Nguyen, M. R. VanLandingham and D. Yebassa, "Characterization of polyester degradation using tapping mode atomic force microscopy: exposure to alkaline solution at room temperature," *Polym. Degrad. Stab.*, vol. 74, pp. 139-149, 2001.
- [187] L. A. Pothan, S. Thomas and N. R. Neelakantan, "Short Banana Fiber Reinforced Polyester Composites: Mechanical, Failure and Aging Characteristics," *Journal of Reinforced Plastics and Composites*, vol. 16, pp. 744-765, May 01, 1997.

- [188] E. Rodríguez, R. Petrucci, D. Puglia, J. M. Kenny and A. Vázquez, "Characterization of Composites Based on Natural and Glass Fibers Obtained by Vacuum Infusion," *Journal of Composite Materials*, vol. 39, pp. 265-282, February 01, 2005.
- [189] Z. N. Azwa, B. F. Yousif, A. C. Manalo and W. Karunasena, "A review on the degradability of polymeric composites based on natural fibres," *Mater Des*, vol. 47, pp. 424-442, 5, 2013.
- [190] A. Fick, "On liquid diffusion," *J. Membr. Sci.*, vol. 100, pp. 33-38, 3/31, 1995.
- [191] P. Bonniau and A. R. Bunsell, "A Comparative Study of Water Absorption Theories Applied to Glass Epoxy Composites," *Journal of Composite Materials*, vol. 15, pp. 272-293, May 01, 1981.
- [192] L. Cai and Y. Weitsman, "Non-Fickian Moisture Diffusion in Polymeric Composites," *Journal of Composite Materials*, vol. 28, pp. 130-154, January 01, 1994.
- [193] A. Espert, F. Vilaplana and S. Karlsson, "Comparison of water absorption in natural cellulosic fibres from wood and one-year crops in polypropylene composites and its influence on their mechanical properties," *Composites Part A: Applied Science and Manufacturing*, vol. 35, pp. 1267-1276, 11, 2004.
- [194] H. J. Kim and D. W. Seo, "Effect of water absorption fatigue on mechanical properties of sisal textile-reinforced composites," *Int. J. Fatigue*, vol. 28, pp. 1307-1314, 10, 2006.
- [195] G. Francucci, E. S. Rodríguez and A. Vázquez, "Study of saturated and unsaturated permeability in natural fiber fabrics," *Composites Part A: Applied Science and Manufacturing*, vol. 41, pp. 16-21, 1, 2010.
- [196] M. Shokrieh and L. Lessard, "An Assessment of the Double-Notch Shear Test for Interlaminar Shear Characterization of a Unidirectional Graphite/Epoxy under Static and Fatigue Loading," *Applied Composite Materials*, vol. 5, pp. 49-64, 01/01, 1998.

- [197] K. S. Ahmed and S. Vijayarangan, "Tensile, flexural and interlaminar shear properties of woven jute and jute-glass fabric reinforced polyester composites," *J. Mater. Process. Technol.*, vol. 207, pp. 330-335, 2008.
- [198] F. Shin, X. Xian, W. Zheng and M. Yipp, "Analyses of the mechanical properties and microstructure of bamboo-epoxy composites," *J. Mater. Sci.*, vol. 24, pp. 3483-3490, 1989.
- [199] T. Kant and K. Swaminathan, "Estimation of transverse/interlaminar stresses in laminated composites—a selective review and survey of current developments," *Composite Structures*, vol. 49, pp. 65-75, 2000.